Fitted Numerical Schemes for a Class of Singularly Perturbed Differential-Difference Equations

Ababi Hailu Ejere

A Dissertation Submitted to the Department of Applied Mathematics, School of Applied Natural Science

Presented in Partial Fulfillment of the Requirement for the Degree of Doctor of Philosophy in Mathematics (Numerical Analysis)

Office of Graduate Studies
Adama Science and Technology University

June, 2023
Adama, Ethiopia

Fitted Numerical Schemes for a Class of Singularly Perturbed Differential-Difference Equations

Ababi Hailu Ejere

Supervisor: Gemechis File Duressa (Ph.D, Prof.)
Co-Supervisors: Tekle Gemechu Dinka (Ph.D)
Mesfin Mekuria Woldaregay (Ph.D)

A Dissertation Submitted to the Department of Applied Mathematics, School of Applied Natural Science

Presented in Partial Fulfillment of the Requirement for the Degree of Doctor of Philosophy in Mathematics (Numerical Analysis)

Office of Graduate Studies
Adama Science and Technology University

June, 2023
Adama, Ethiopia

DECLARATION AND RECOMMENDATION

Declaration

I hereby declare that this dissertation entitled " **Fitted Numerical Schemes for a Class of Singularly Perturbed Differential-Difference Equations** " is my original work. That is, it has not been submitted for the award of any academic degree, diploma or certificate in any other university. All sources of materials used for this dissertation have been duly acknowledged through appropriate citations.

Name of student	Signature	Date

Recommendation

We, the supervisors of this dissertation, hereby certify that we have read and revised the dissertation entitled "**Fitted Numerical Schemes for a Class of Singularly Perturbed Differential-Difference Equations**" prepared under our guidance by **Ababi Hailu Ejere** submitted in partial fulfillment of the requirements for the degree of Doctor of Philosophy in Mathematics (Numerical Analysis). Therefore, we recommend the submission of the dissertation to the department for further review and defense.

Major Supervisor	Signature	Date
Co-supervisor 1	Signature	Date
Co-supervisor 2	Signature	Date

APPROVAL PAGE

We hereby certify that the recommendations and suggestions made by the board of examiners are appropriately incorporated into the final version of the dissertation entitled " **Fitted Numerical Schemes for a Class of Singularly Perturbed Differential-Difference Equations** " by **Ababi Hailu Ejere**.

Major Supervisor	Signature	Date
Co-supervisor 1	Signature	Date
Co-supervisor 2	Signature	Date

We, the undersigned, members of the Board of Examiners of the dissertation open defense by **Ababi Hailu Ejere** have read and evaluated the dissertation entitled " **Fitted Numerical Schemes for a Class of Singularly Perturbed Differential-Difference Equations** " and examined the candidate during open defense. This is, therefore, to certify that the dissertation is accepted for partial fulfillment of the requirement of the degree of Doctor of Philosophy in Mathematics (Numerical Analysis).

Chairperson	Signature	Date
Internal Examiner 1	Signature	Date
Internal Examiner 2	Signature	Date
External Examiner 1	Signature	Date
External Examiner 2	Signature	Date

Finally, approval and acceptance of the dissertation is contingent upon submission of its final copy to the Office of Postgraduate Studies (OPGS) through the candidate's Department Graduate Council (DGC) and School Graduate Committee (SGC).

Department Head	Signature	Date
School Dean	Signature	Date
Office of Postgraduate Studies, Dean	Signature	Date

ACKNOWLEDGMENT

First of all, thanks to the Almighty God for helping me in all situations. Next, I would like to convey my profound gratitude to my supervisors, Prof. Gemechis, Dr. Mesfin, and Dr. Tekle, for their unwavering support during this research project. I greatly appreciate their ongoing assistance, inspiration, counsel, and perceptive remarks. This dissertation could not have been finished without their direction.

I would like to thank all doctoral committee members for their constructive criticism in the progress reports. I owe gratitude to Editors and Reviewers for their valuable feedback on the manuscripts submitted to journals for publication. In addition, I express my acknowledgment to the Examiners for their insightful comments and suggestions in finalizing this dissertation. It made a significant contribution for the advancement of this work. Also, I would like to thank my fellow postgraduate students for their encouragement and support.

I would like to express my gratitude to Adama Science and Technology University for providing me financial support in this dissertation, as well as Ethiopian Defence University for sponsoring this Ph.D fellowship. Also, thanks to all staff members of Applied Mathematics in the two institutions for their cooperation, support and encouragement.

I express my gratitude to my parents and families. This dissertation would have not been possible without their unwavering faith and moral support. The daily faith of my mother kept me healthy and pleasant throughout my works. She has been a source of inspiration in my life and I dedicate this dissertation to her. I owe my gratitude to my sisters, Shibire and Lishan, for their unfailing support in my career. Special thanks to my sister-in law, Selam, who greatly helped me, not only in this research work, but also in supporting my families, while I spent the majority of my time working on it.

Last but not least, I want to express my gratitude to my beloved wife, Hirut, who shares a portion of my soul and has been with me in every steps of this journey and beyond.

TABLE OF CONTENTS

LIST OF TABLES **viii**
LIST OF FIGURES **x**
LIST OF ACRONYMS AND ABBREVIATIONS **xii**
ABSTRACT **xiii**
CHAPTER ONE: INTRODUCTION **1**
1.1 Singular perturbation problems 1
1.2 Singularly perturbed differential-difference equations 3
1.3 Fitted numerical schemes for singularly perturbed differential-difference equations 4
1.4 Statement of the problem 6
1.5 Objectives of the study 7
1.5.1 General objective 7
1.5.2 Specific objectives 8
1.6 Significance of the study 8
1.7 Scopes of the study 8
1.8 Mathematical preliminaries 10
1.9 Organization of the study 12
CHAPTER TWO: LITERATURE REVIEW **13**
CHAPTER THREE: RESEARCH METHODOLOGY **23**
3.1 Study area and period 23
3.2 Study design 23
3.3 Source of information 23
3.4 Methods of scheme formulation 23
3.5 Study procedures 24
CHAPTER FOUR: AN EXPONENTIALLY FITTED OPERATOR METHOD VIA DOMAIN DECOMPOSITION FOR SINGULARLY PERTURBED ORDINARY DIFFERENTIAL EQUATIONS WITH LARGE NEGATIVE SHIFT **25**
4.1 The governing problem 25
4.2 Properties of the continuous solution 26
4.3 The numerical method 28
4.4 Numerical results and discussions 36
4.5 Summary 44

CHAPTER FIVE: A FITTED MESH FINITE DIFFERENCE METHOD FOR SINGULARLY PERTURBED PARABOLIC DIFFERENTIAL EQUATIONS WITH NEGATIVE SHIFT **45**

5.1 The governing problem 45
5.2 Properties of the continuous solution 46
5.3 The numerical method 50
5.3.1 Temporal discretization 50
5.3.2 Spatial discretization 55
5.4 Numerical results and discussions 60
5.5 Summary 68

CHAPTER SIX: A UNIFORMLY CONVERGENT FITTED MESH METHOD FOR SINGULARLY PERTURBED PARTIAL DIFFERENTIAL EQUATIONS WITH LARGE NEGATIVE SHIFT **69**

6.1 The governing problem 69
6.2 Properties of the continuous solution 70
6.3 The numerical method 73
6.3.1 Temporal discretization 73
6.3.2 Spatial discretization 80
6.4 Numerical results and discussions 87
6.5 Summary 91

CHAPTER SEVEN: A NONSTANDARD FINITE DIFFERENCE METHOD FOR SINGULARLY PERTURBED PARTIAL DIFFERENTIAL EQUATIONS WITH LARGE NEGATIVE SHIFT **93**

7.1 The governing problem 93
7.2 Properties of the continuous solution 94
7.3 The numerical method 97
7.3.1 Temporal discretization 97
7.3.2 Spatial discretization 101
7.4 Numerical results and discussions 106
7.5 Summary 114

CHAPTER EIGHT: A TENSION SPLINE FITTED METHOD FOR SINGULARLY PERTURBED PARTIAL DIFFERENTIAL EQUATIONS WITH LARGE NEGATIVE SHIFT **115**

8.1 The governing problem 115
8.2 Properties of the continuous solution 117

8.3 The numerical method . . . 118
8.3.1 Temporal semi-discretization . . . 118
8.3.2 Spatial discretization . . . 121
8.4 Numerical results and discussions . . . 129
8.5 Summary . . . 137
CHAPTER NINE: A NONSTANDARD FINITE DIFFERENCE SCHEME FOR SINGULARLY PERTURBED PARTIAL DIFFERENTIAL EQUATIONS WITH SPATIO-TEMPORAL DELAYS **138**
9.1 The governing problem . . . 138
9.2 Properties of the continuous solution . . . 140
9.3 The numerical method . . . 142
9.3.1 Temporal discretization . . . 143
9.3.2 Spatial discretization . . . 145
9.4 Numerical results and discussions . . . 149
9.5 Summary . . . 156
CONCLUSIONS AND RECOMMENDATIONS **157**
REFERENCES **168**

LIST OF TABLES

4.1 Maximum absolute errors and rate of convergence of Example 4.4.1 for different values of ε and N. 38
4.2 Maximum absolute errors and rate of convergence of Example 4.4.2 for different values of ε and N. 39
4.3 Maximum absolute errors and rate of convergence of Example 4.4.3 for different values of ε and N. 40
4.4 Comparison of the present scheme with other published works in literature. . . 41

5.1 Maximum absolute errors and convergence rates of Example 5.4.1 for $\delta = 0.1$. 61
5.2 Maximum absolute errors and convergence rates of Example 5.4.2 for $\delta = 0.1$. 62
5.3 Maximum absolute error and convergence rates of Example 5.4.3 for $\delta = 0.1$. . 64

6.1 Maximum absolute errors and convergence rate for Example 6.4.1 taking $\beta = 1$ and $\theta = 0.5$. 88
6.2 Maximum absolute errors and convergence rate for Example 6.4.2, taking $\beta = 1.5$ and $\theta = 0.5$ 89
6.3 Comparisons of the present method with other results in literature. 90

7.1 Maximum absolute error and rate of convergence for Example 7.4.1. 107
7.2 Maximum absolute error and rate of convergence for Example 7.4.2. 108
7.3 Maximum absolute error and rate of convergence for Example 7.4.3. 109
7.4 Comparison of the proposed method with other published results in the literature. 110

8.1 Maximum errors and corresponding convergence rate of Example 8.4.1. 131
8.2 Maximum errors and corresponding convergence rates of Example 8.4.2. 132
8.3 Comparison of the proposed scheme and other results in literature. 133
8.4 Comparison of the proposed fitted mesh, nonstandard finite difference and tension spline fitted methods 134

9.1 Maximum absolute errors and convergence rates for Example 9.4.1, taking $\tau = \frac{\varepsilon}{4}$. 150
9.2 Maximum absolute errors and convergence rates for Example 9.4.2 taking $\tau = \frac{\varepsilon}{4}$. 151
9.3 Maximum absolute errors and convergence rates for Example 9.4.3 taking $\tau = \frac{\varepsilon}{4}$. 152

LIST OF FIGURES

4.1 Numerical solutions of Example 4.4.1 for $N = 2^8$ and different values of ε. . . 42
4.2 Numerical solutions of Example 4.4.2 for $N = 2^8$ and different values of ε. . . 42
4.3 Log-log plots of maximum absolute errors versus N for (a) Example 4.4.1 and (b) Example 4.4.2 43

5.1 Effect of the negative shift on the solution for (a) Example 5.4.1 and (b) Example 5.4.3 for $\varepsilon = 2^{-10}$. 63
5.2 Effect of the perturbation parameter in resolving the boundary layers for (a) Example 5.4.1 and (b) Example 5.4.3 for $\delta = 0.1$. 63
5.3 Effect of δ on the surface plots of the solution for Example 5.4.1 taking $\varepsilon = 2^{-10}$. 65
5.4 Effect of ε on the surface plots of the solution for Example 5.4.1 taking $\delta = 0.1$. 65
5.5 Effect of δ on the surface plots of the solution for Example 5.4.3 taking $\varepsilon = 2^{-12}$. 66
5.6 Effect of ε on the surface plots of the solution for Example 5.4.3 taking $\delta = 0.1$. 66
5.7 Log-log plots of maximum absolute errors versus N for (a) Example 5.4.1 and (b) Example 5.4.3 67

6.1 Simulations of the numerical solution of Example 6.4.1, taking θ=0.5, β=1 and N=72 and M=72 at four different time levels (line plots). 91
6.2 Simulations of the numerical solution of Example 6.4.1, taking θ=0.5, β=1 and N=72 and M=72 at four different time levels (Surface plots). 91
6.3 Simulations of the numerical solution of Example 6.4.2, taking θ=0.5, β=1 and N=64 and M=32 at four different time levels (line plots). 92
6.4 Simulations of the numerical solution of Example 6.4.2, taking θ=0.5, β=1 and N=64 and M=32 at four different time levels (Surface plots). 92

7.1 Line plots for the numerical solution of Example 7.4.2 for $N = 72$ and $M = 72$ at different time levels. 111
7.2 Surface plots for the numerical solution of Example 7.4.2 for $N = 72$ and $M = 72$. 111
7.3 Line plots for the numerical solution of Example 7.4.3 for $N = 128$ and $M = 64$. 112
7.4 Surface plots for the numerical solution of Example 7.4.3 for $N = 128$ and $M = 64$. 112

7.5 Log-log plots of maximum absolute error versus N for (a) Example 7.4.2 and (b) Example 7.4.3. 113

8.1 Line plots for the solution of Example 8.4.1 for $N = 128$ at different time levels. 130
8.2 Surface plots for the solution of Example 8.4.1 for $N = 128$ and $M = 64$. . . . 130
8.3 Line plots for the solution of Example 8.4.2 taking $N = 288$ at different time levels. 135
8.4 Surface plots for the solution of Example 8.4.2 taking $N = 72$ and $M = 72$. . . 135
8.5 The log-log graphs of the maximum absolute errors versus mesh numbers for Example 8.4.1 in (a) and for Example 8.4.2 in (b). 136

9.1 Effect of the perturbation parameter in boundary layers resolving for (a) Example 9.4.2 and (b) Example 9.4.3 when $\tau = \frac{\varepsilon}{4}$. 153
9.2 Surface plot simulations of Example 9.4.2, for various values of ε at $\tau = \frac{\varepsilon}{4}$. . . 154
9.3 Surface plot simulations of Example 9.4.3, for various values of ε at $\tau = \frac{\varepsilon}{4}$. . . 154
9.4 The log-log plots of maximum absolute errors versus N for (a) Example 9.4.2 and (b) Example 9.4.3. 155

LIST OF ACRONYMS AND ABBREVIATIONS

Δt and h	Temporal and spatial uniform meshes, respectively
Γ and $\bar{\Gamma}$	Open and closed domain in the spatial direction, respectively
Λ and $\bar{\Lambda}$	Open and closed domain in the temporal direction, respectively
$\mathcal{L}_\varepsilon^N$, $\mathcal{L}_\varepsilon^{N,M}$	Difference operators
$\mathcal{L}_\varepsilon$	Differential operator
$\lvert . \rvert$	Absolute value
$\lVert . \rVert$ or $\lVert . \rVert_\Omega$	Maximum norm over the domain Ω
Ω and $\bar{\Omega}$	Open and cloesd domain of a continuous problem, respectively
Ω^M and $\Omega^{N,M}$	Time semi-discrete and fully-discrete domain, respectively
$\partial\Omega$	Boundary of the domain Ω
σ	Fitting factor
τ	Transition parameter of a piece-wise uniform meshes
τ and δ	Temporal and spatial delays, respectively
ε	Perturbation parameter
C	Generaric positive constant independent of ε
$C^{(k)}(\Omega)$, $C^{(k)}\bar{\Omega}$	k times continuously differentiable functions in the respective domain
D^+, D^- and D^+D^-	Forward, backward and central difference operators
$e^{N,M}$, $e_\varepsilon^{N,M}$	Maximum absolute errors
h_i, h_{i+1}	Mesh widths of a piece-wise uniform mesh

M and N	Temporal and spatial mesh numbers, respectively
$r^{N,M}$, $r_{\varepsilon}^{N,M}$	Rates of convergence
t, x, x_i, x_{i+1}	Independent variables
$u(x)$, $u(x,t)$	Solution of the continuous problem
U_i^N, $U_i^{N,M}$	Solutions of the discrete problem
V, V_i^{j+1}	Smooth component of the solution of a fitted mesh numerical scheme
W, $W_{L,i}^{j+1}$, $W_{R,i}^{j+1}$	Singular component of the solution of a fitted mesh numerical scheme
FMFDM	Fitted Mesh Finite Difference Method
FOFDM	Fitted Operator Finite Difference Method
NSFDM	Nonstandard Finite Difference Method
RPP	Regular Perturbation Problem
SPDDE	Singularly Perturbed Differential-Difference Equation
SPP	Singular Perturbation Problem

ABSTRACT

Singularly perturbation problem is a problem involving small positive parameter, which causes a large effect on the problem. A class of delay differential equations that would be obtained by maintaining the small parameter multiplying the highest order derivative is said to be a singularly perturbed differential-difference equation. Due to the effect of the small parameter, narrow regions (boundary layers) frequently adjoin the boundaries of the domain are exhibited in the solution, and the delay term give rise to an interior layer. In the layer regions, the solution changes rapidly with changing values of the perturbation parameter. This rapid changing behavior of the layer region makes it difficult to solve the problem analytically. Standard numerical methods, on the other hand, do not give satisfactory results as they do not consider the layer behaviors. As a result, formulating parameter-uniform numerical schemes for a singularly perturbed problems has become a popular research topic. The main aim of this dissertation is to formulate and analyze fitted numerical schemes that converge independent of the perturbation parameter for a class of singularly perturbed differential-difference equations in which the diffusion term is dominated by the reaction term. The numerical schemes are either fitted operator finite difference method or fitted mesh finite difference method. Construction of a fitted operator parameter-uniform numerical scheme involves replacing the standard finite difference operator by an operator which reflects the singularly perturbed nature of the differential operator on a uniform mesh. The other successful approach of formulating a parameter-uniform numerical scheme involves the use of standard finite difference operators on a special piecewise uniform meshes condensed around the layer regions. Formulating such form of numerical schemes for a class of singularly perturbed differential-difference equation yields a uniformly convergent numerical results, that overcomes the limitations of the standard numerical methods. In this dissertation, six uniformly convergent numerical schemes are formulated. The stability estimate of each scheme is established and the parameter-uniform convergence of the schemes are investigated and proved. To demonstrate the validity and applicability of the formulated numerical schemes, various numerical experiments are performed and confirmed with the theoretical findings. The theoretical and numerical results confirm that the formulated schemes are more accurate and uniformly convergent as compared to other previous research works in the literature.

Keywords: *Singular perturbation problem, Differential-difference equations, Fitted numerical scheme, Uniform convergence, Boundary layers, Interior layer.*

CHAPTER ONE

INTRODUCTION

1.1 Singular perturbation problems

The history of singular perturbation problems (SPPs) dates back to the early 20^{th} century, with the pioneering work of mathematicians such as Prandtl, Friedrichs, and Wasow. At the 3^{rd} International Congress of Mathematicians held in Heidelberg in 1904, Prandtl introduced the concept of boundary layers, which are thin layers of fluid near a solid boundary where the velocity and other properties of the fluid change rapidly. This led to the development of boundary layer theory, which relied heavily on singular perturbation methods (O'Malley, 2014). However, until the 1950s, the field did not begin to flourish with the development of new mathematical techniques and tools for analyzing these problems. It was first used in the works of Friedrichs & Wasow (1946) on non-linear vibrational problems. Despite its long history, singular perturbation problems are still in a state of irrepressible development in various scientific discoveries (Duressa et al., 2023).

Nowadays, SPPs are widely used in various areas of science and engineering. For instance, in control theory, singular perturbation problem is used in modeling the systems with fast and slow dynamics and develop new control techniques (Zhang et al., 2014). In chemical kinetics, singular perturbation problem is used to develop a simplified models that accurately capture the behavior of chemical reactions that occur on different time scales (Zhao & Lam, 2019). In the study of population dynamics, singular perturbation techniques are used to study the behavior of populations in situations where there are multiple time scales, such as in the predator-prey dynamics of ecosystems (Campillo & Lobry, 2012). In neuroscience singular perturbation theory is used to study the behavior of neural networks in situations where there are multiple time scales, such as in the dynamics of action potentials in neurons (Coombes, 2008). Apart from these, SPPs are used in robotics, material science, biophysics, aerospace engineering, power systems, climate modeling, and others.

In differential equations, singular perturbation problem occurs when the small parameter (ε), $0 < \varepsilon \ll 1$, multiplies the term with highest order derivatives. Thus, naively taking ε to be zero changes the very nature of the problem (Kumar et al., 2011). For instance, in fluid dynamics one of a well known singularly perturbed partial differential equation is the Navier-Stoke equation

$$\frac{\partial(\eta u)}{\partial t}+\frac{\partial(\eta u^2+p)}{\partial x}+\frac{\partial(\eta vu)}{\partial y}-\frac{1}{Re}\left(\frac{\partial u_{xx}}{\partial x}+\frac{\partial u_{xy}}{\partial y}\right)=0, \tag{1.1}$$

with appropriate initial and boundary conditions, where u and v are the components of its velocity, η is the density of the fluid and p is the pressure. The parameter Re is known as Reynolds number, which is proportional to the length scale, velocity scale and inversely proportional to the kinematic viscosity of the fluid. If Re is sufficiently large, then (1.1) is a singularly perturbed differential equation, and the corresponding small parameter, $\frac{1}{Re}$, is a perturbation parameter. Taking the perturbation parameter equal to zero, reduce (1.1) to the Euler equation

$$\frac{\partial(\eta u)}{\partial t}+\frac{\partial(\eta u^2+p)}{\partial x}+\frac{\partial(\eta vu)}{\partial y}=0, \tag{1.2}$$

which is different from the Navier-stoke equation. Thus, ignoring the perturbation parameter removes the essential nature of the problem and leads to incorrect results and can mask important features of the solution (Kokotović et al., 1999).

Depending on the effect of ε, perturbation problems can be categorized as regular and singular perturbation problems. A regular perturbation problem (RPP) is the one in which the perturbed problem for small and nonzero values of the perturbation parameter is qualitatively the same as the unperturbed problem for $\varepsilon = 0$. One can obtain a convergent expansion of the solution with respect to ε, consisting of the unperturbed solution and higher order corrections. On the other hand, a singular perturbation problem (SPP) is the one for which the perturbed problem is qualitatively different from the unperturbed problem. One can obtain an asymptotic, but possibly divergent expansion of the solution, that depends on the parameter ε (Hunter, 2004).

In singular perturbation problems, the perturbation parameter causes boundary layer(s), thin region near the boundary of the domain where the solution changes rapidly. This occurs when there is a large disparity between two scales in the problem, such as in the case of a small parameter ε multiplying the term with highest order derivatives. The boundary layer arises when ε is very small, causing the solution to change rapidly near the boundary (Naidu, 2002). The boundary layer can be visualized as a thin layer of thickness $O(\varepsilon)$. Inside the layer, the solution varies rapidly and outside the layer, the solution varies slowly. The behavior of the solution in the layer region is different from that of outside the layer region, and so it is important to study singular perturbation problems in these regions, separately.

Boundary layers are observed in various physical situations. For instance, in fluid mechanics the effects of viscosity is significant in forming a layer of fluid in the immediate vicinity of a bounding surface for large Reynold's number (Landau & Lifshitz, 2013). In water-pipe problem, boundary layers are formed for cellular flows at high Péclet numbers (Novikov et al., 2005). On aircraft wings, viscous force distort the surrounding non-viscous flow and forms a boundary layer on the part of the flow close to the wing (Duan et al., 2013). In the Earth's atmosphere, the atmospheric boundary layer is the air layer near the ground affected by diurnal heat, moisture, or momentum transfer to or from the surface (Chen et al., 1997). In these types of phenomena, perturbations are operative over a very narrow region across which the dependent variable undergoes very rapid change. These narrow regions frequently adjoin the boundaries or some interior point of the domain of interest, owing to the fact that the small parameter multiplies the highest derivative. Therefore, the problems exhibit boundary and/or interior layers, i.e., there are thin regions where the solution of the problem changes abruptly.

The locations and behaviors of the layers of SPP may depend on ε and the nature of the perturbation problem. One common approach to identify the location of the boundary layers is to use asymptotic analysis, which involves expanding the solution in a series of terms that capture the dominant behavior at different length scales. By matching these terms across the boundary or interfacing regions, one can determine the location and thickness of the boundary layer. Another approach is to use numerical methods, such as finite difference techniques, to solve the problem and then examine the behavior of the solution near the boundary or interfacing regions. In particular, one can look for regions where the solution changes rapidly or exhibits oscillations, which may indicate the presence of a boundary layer. Ultimately, the best approach will depend on the specific problem at hand and the available tools and techniques for the computation and analysis.

In a second order singularly perturbed differential equations, if ε multiplies the term with highest order derivative and the first order derivative term is the dominant term, then the solution of the problem exhibits a boundary layer either on the left or the right end of the domain depending on the sign of the coefficient of the first order derivative term. Such type of problems are said to be convection diffusion problem. On the other hand, if the reaction term is the dominant term, then the differential equation is known as a reaction-diffusion problem whose solution exhibits two boundary layers, one on the right and the other on the left side of the domain.

1.2 Singularly perturbed differential-difference equations

A class of delay differential equations in which ε multiplies the term with highest order derivative and involves at least one shift argument is said to be a singularly perturbed differential-difference equation (SPDDE). Such types of differential equations are frequently observed in the mathematical models of various scientific phenomena, such as in the modeling of biological mathematics (Rihan, 2021), the study of bistable devices (Derstine et al., 1982), variational problems in control theory (Glizer, 2003), in the modeling human pupil-light reflex modeling (Longtin & Milton, 1989), in the modeling of neuronal variability (Stein, 1965), for modeling the optimal control of telecommunication systems Erfani et al. (2018), in the modeling of HIV infection (Culshaw & Ruan, 2000), in the modeling of COVID-19 pandemic and spread (Shayak et al., 2020; Guglielmi et al., 2022), and others.

The difference between the non-delay and delay singularly perturbed problems is that sometimes delay problems exhibit extra interior layers in the solution of the problems. The shifting arguments may be less or greater than the singular perturbation parameter. If the perturbation parameter is greater than the delay argument, then the problem is known as a singularly perturbed problem with small shift and if the perturbation parameter is less than the delay argument, then the problem is known as a singularly perturbed problem with large shift. Such type of variations in the problem brings significant effect in the solution and hence treated differently (Rao & Chakravarthy, 2014).

1.3 Fitted numerical schemes for singularly perturbed differential-difference equations

Due to the rapidly changing behaviors of the layer regions, it is tedious to solve SPPs analytically. On the other hand, standard computational methods, such as finite difference method, finite element method, finite volume method and spectral methods are also known to be inadequate to solve SPPs as they require a huge number of mesh points to give a satisfactory solution (Roos et al., 2008). In this context, careful numerical tests reveal that the standard computational methods fail to minimize the maximum point-wise error as the mesh size is refined, until it is equal to the perturbation parameter in its order of magnitude. Also, they fail to be robust as the perturbation parameter decreases and closer to a critical value (Farrell et al., 2000). Such methods are unfit and their results are contrary to the natural expectation of error analysis in an acceptable computational methods. These drawbacks motivated researchers to develop ε–uniform fitted numerical schemes for SPPs, in which the error constant and the order of convergence are free from the effect of the perturbation parameter.

It is also known that a finite difference method has two major components, such as the finite difference operator $\mathcal{L}_{\varepsilon}^{N,M}$ that is used to approximate the differential operator $\mathcal{L}_{\varepsilon}$ and the mesh $\Omega^{N,M}$ that replaces the continuous domain Ω. By the standard finite difference methods is meant that almost all of the finite difference methods have been applied successfully to the problems that are not singularly perturbed. Generally, these methods are stable and accurate, and hence their solutions converge to the exact solution, as N increases infinitely. However, none of these methods are ε-uniform, so that a new attribute is required.

The development of ε-uniform numerical schemes can be categorized into two classes, such as fitted operator finite difference method (FOFDM) and fitted mesh finite difference method (FMFDM). The methods are said to be fitted, because they are designed in such a way that they handle the abruptly varying behavior of a solution in the layers and the numerical instabilities created by the presence of the perturbation parameter. These methods use the small parameter, ε, to control the size of the numerical grid near the boundary, allowing for a more precise representation of the boundary layer. By using this technique, ε-uniform methods can provide more accurate predictions of the solution in the layers where the perturbation parameter is a critical factor.

The first approach substitutes the differential operator corresponding to the continuous problem by a fitted finite difference operator, which captures the layer behaviors of the singularly perturbed problem on a uniform mesh. The method is first suggested by Allen & Southwell (1955) in solving the problem of the flow of a viscous fluid past a fixed cylinder. And the first successful numerical analysis of ε-uniform finite difference methods was given by Il'in (1969) for a linear boundary value problem. In most cases the fitted finite difference operator is used at all points of the mesh. But, Farrell (1987) has proved that in some cases the fitted finite difference operator is required only in a neighborhood of the layers, while a standard finite difference operator can be used on the mesh points in the rest of the domain. The development of FOFDM employs an appropriate choice of the difference coefficients, in such a way that some or all of the exponential functions are in the null space of the differential operator, or part of it, are also in the null space of the finite difference operator (Mohapatra & Natesan, 2011; Das & Natesan, 2013). In such procedures, the finite difference operator is referred to as an exponentially fitted finite difference operator. The corresponding numerical scheme is obtained by applying the finite difference operator to obtain a system of equations on a uniform mesh.

The usual techniques to develop a fitted operator methods require a fitting factor to be incorporated in the standard finite difference scheme and then it is derived by assuming that the method converges to the exact solution uniformly. The other technique, which categorized under the class of fitted operator finite difference methods is the nonstandard finite difference methods (NSFDMs), by which the dispersive or dissipative nature of the solution of the problem is captured in the scheme by a systematical construction of suitable denominator functions for the discrete derivative (Lubuma & Patidar, 2007). Such method is constructed applying the nonstandard modeling rules of (Mickens, 1994). It is well known that, these rules allow one to incorporate the essential physical properties of the differential equations in the numerical schemes so that they provide reliable numerical results.

The other well recognized approach for developing ε-uniform numerical scheme is known as fitted mesh finite difference method (FMFDM), which involves the use of a suitable mesh that is adapted to the singular perturbation problem. These methods have extra advantage over the fitted operator methods due to their implementation on the standard finite difference operators and their extensions to solve higher dimensional and nonlinear problems with complicated domain structure. By the fitted or adapted mesh finite difference method, a piece-wise uniform mesh is formed with specially chosen transition points, which separate the coarse and the fine meshes. These piece-wise uniform fitted or adapted meshes were first introduced by Shishkin (1988) and improved to be ε-uniform in a series of different research works. What distinguishes a Shishkin mesh from any other piece-wise uniform mesh is the choice of the transition parameter. Usually more condensed meshes are formed in the layers, where we observe a significant effect of the perturbation parameter and coarse meshes are formed outside of the layers. Thus, to formulate a fitted mesh method, it requires apriori knowledge of the width and location of the regions, where the solution shows fast variation. Such knowledge is then applied to generate an appropriate mesh on the domain of the problem.

For fitted mesh finite difference methods, if sufficient apriori information about the solution is available, then appropriate meshes can be constructed where the accuracy of the solution depends only on the number of meshes and is free from the influence of the perturbation parameter. The meshes formed in this case is globally piece-wise uniform rather than uniform, because the sub-intervals in a neighborhood of the end points of the domain are small. Then, for a transition parameter (say τ) approaching to zero, the meshes are said to be condensing near the boundary point. It can be noticed that, whatever the value of the transition parameter, all of the sub-intervals consist of N meshes and consequently the mesh points x_i are the endpoints of these N meshes. Also, there are various approaches of adapting the meshes, involving complicated redistribution of the mesh points have been considered by different authors. For instance, the research works of Bakhvalov (1969), Gartland (1988), Liseıkin (1983) and Vulanovic (1986) are some layer adapted methods which have no simple piece-wise uniform fitted meshes.

1.4 Statement of the problem

In the real world, various phenomena are described by singularly perturbed differential-difference equations, a type of delay differential equations that maintains a small perturbation parameter in the diffusion term causing a rapidly fluctuating solutions. Such rapid variation of the solution forms boundary layers in the vicinity of the body, the widths of which depend on the perturbation parameter. In addition, these problems involve shifting arguments (delays), which may give rise to interior layers. Because of these complicated factors, it is difficult to determine the analytical solutions of these problems. As a result, numerical methods are of fundamental requirement in obtaining some useful insights on the solutions of the problems. However, standard numerical methods such as the finite difference method, finite element method, finite volume method, and spectral methods produce large errors, rendering them unsuitable for practical use. The standard methods do not consider the behavior of layers, unless an extremely large number of mesh points are considered, which need a massive computational cost or it may fail to give the targeted results. It is therefore of great research interest to formulate a sound mathematical theory and precise computational approaches for singularly perturbed differential-difference equations and related problems emerging in the real-world applications.

Few research works have been available in the recent years with various numerical approaches and results. For instance, Swamy et al. (2015), Sirisha & Reddy (2017b), Debela et al. (2020) and Tirfesa et al. (2022) have devised different approaches for singularly perturbed ordinary differential equation with small delay. Subburayan & Ramanujam (2013), Nicaise & Xenophontos (2013), Manikandan et al. (2014), Chakravarthy & Kumar (2021) formulated different numerical schemes for a singularly perturbed ordinary differential equations with large delay. Bansal & Sharma (2018) and Kumari & Kumar (2020) treated singularly perturbed partial differential equations with large delay by formulating different numerical schemes. The accuracy and rate of convergence of these numerical schemes are not accurate enough.

However, in recent trends in the development of numerical methods for singularly perturbed problems, if the order of ε-uniform numerical scheme is low, the scheme is inefficient for practical use. So, developing ε-uniform numerical schemes with a high order of convergence is an important research work (Shishkin & Shishkina, 2008). Motivated by this recommendation, accurate and ε-uniformly convergent numerical schemes are formulated for a class of SPDDEs in this dissertation.

1.5 Objectives of the study

1.5.1 General objective

The general objective of this dissertation is to formulate numerical schemes for a class of singularly perturbed differential-difference equations.

1.5.2 Specific objectives

The specific objectives of this study are:

1. formulating fitted operator numerical methods.
2. formulating fitted mesh numerical methods.
3. establishing the stability estimate of the formulated numerical methods.
4. investigating the convergence of the formulated numerical methods.

1.6 Significance of the study

This dissertation provides fitted numerical schemes, which are accurate and uniformly convergent for a class of singularly perturbed differential-difference equations. The methods allow are important to simulate and study the behavior of systems that exhibit small parameter, which cause large effect on the system. They enable to capture the rapidly changing behaviors of the layer regions, where the solution varies abruptly. They also provide valuable insights for other researchers in the area to realize the mathematical theory and computational methods of singularly perturbed problems, and may be helpful in the demonstration of scientific models involving applications of SPDDEs. Moreover, the analyses and results presented in this study will convey valuable information to enhance and extend the knowledge in the area for future research works.

1.7 Scopes of the study

There are various forms of SPDDEs. However, this dissertation focuses on developing and analyzing fitted numerical methods for the following governing problems.

Governing problem I

For a differential operator $\mathcal{L}_\varepsilon$, a singularly perturbed ordinary differential equation with large negative shift is considered as

$$\begin{cases} \mathcal{L}_\varepsilon u(x) = -\varepsilon u''(x) + a(x)u(x) + b(x)u(x-1) = f(x), \quad x \in (0,2), \\ u(x) = \phi(x), \; x \in [-1,0], \\ u(2) = \alpha, \end{cases} \tag{1.3}$$

where $0 < \varepsilon \ll 1$. The numerical formulation and analysis of this model problem is presented in Chapter Four. The proposed method to solve this problem is also published in the Journal of Mathematics and available on https://doi.org/10.1155/2022/7974134.

Governing problem II

For a differential operator $\mathcal{L}_\varepsilon$, a singularly perturbed delay partial differential equation is considered as

$$\begin{cases} \mathcal{L}_\varepsilon u(x,t) = u_t(x,t) - \varepsilon u_{xx}(x,t) + a(x)u(x,t) + b(x)u(x-\delta,t) = f(x,t),\ (x,t) \in \Omega, \\ u(x,0) = u_0(x),\ \ x \in \bar{\Gamma} = [0,L], \\ u(x,t) = \phi(x,t),\ \ (x,t) \in \mathit{\Omega}^-, \\ u(L,t) = \alpha(t),\ \ (L,t) \in \mathit{\Omega}^+, \end{cases} \tag{1.4}$$

where $0 < \varepsilon \ll 1$, $\mathit{\Omega}^- = \{(x,t) : x \in [-\delta, 0]\ ,\ t \in \bar{\mathit{\Lambda}} = [0,T]\}$, $\mathit{\Omega}^+ = \{(L,t) : t \in \bar{\mathit{\Lambda}}\}$ for the shift argument δ, finite time T and space L. For $\delta \in (0,1)$, the solution involves weak interior layer, and its detail discussion is presented in Chapter Five. For $\delta = 1$, interior layer exhibited in the solution at $x = 1$. In Chapter Six, fitted mesh numerical method is formulated to solve the problem, and the obtained method is published in the journal of SN Applied Sciences and available on https://doi.org/10.1007/s42452-022-05203-9. In Chapter Seven, non-standard finite difference method is proposed to solve the problem, and the developed method is published in the International Journal of Mathematics and Mathematical Sciences and available on https://doi.org/10.1155/2023/7215106. In Chapter Eight, a tension spline fitted numerical method is developed and analyzed for the problem the problem, and the numerical method is published in the journal of BMC Research Notes and available https://doi.org/10.1186/s13104-023-06361-8.

Governing problem III

A singularly perturbed partial differential equation involving spatial and temporal delays is considered as

$$\begin{cases} \mathcal{L}_\varepsilon u(x,t) = u_t(x,t) - \varepsilon u_{xx}(x,t) + a(x)u(x,t) + b(x)u(x-\delta,t-\tau) = f(x,t),\ (x,t) \in \Omega, \\ u(x,t) = u_0(x,t),\ \ (x,t) \in \{(x,t) : x \in [0,2], t \in [-\tau, 0]\}, \\ u(x,t) = \phi(x,t),\ \ (x,t) \in \mathit{\Omega}^-, \\ u(2,t) = \alpha(t),\ \ (2,t) \in \mathit{\Omega}^+, \end{cases} \tag{1.5}$$

where $0 < \varepsilon \ll 1$, $0 < \delta \leq 1$, $0 < \tau \leq 1$, $\mathit{\Omega}^- = \{(x,t) : x \in [-\delta, 0],\ t \in [0,T]$, $\mathit{\Omega}^+ = \{(2,t) : t \in [0,T]\}$ a finite time T. For $\delta = 1$ and τ is of $o(\varepsilon)$, the solution involves interior layer, and the detail work is presented in Chapter Nine. The formulated scheme is also published in the journal of Frontiers in Applied Mathematics and Statistics, Numerical Analysis and Scientific Computation, and available on https://doi.org/10.3389/fams.2023.1125347.

1.8 Mathematical preliminaries

In this section, some definitions and discussions of terms and phrases that are widely used in the dissertation are provided.

Definition 1.8.1 Boundary layer is a narrow region near the end points of the domain, where the solution of the problem varies rapidly for small values of the perturbation parameter. Interior layer is a narrow region in the internal parts of the domain that may arise due to the shift argument. The width of the layers depends on the value of ε.

Finite difference approximation: Finite difference equation is an equation obtained by discretizing the domain and replacing the exact derivatives by the finite difference operators to obtain the finite difference approximation of the differential equation. The common finite difference operators, derived using the Taylor's series expansion for any mesh function u_i at a mesh points x_i with $h = x_{i+1} - x_i$ are denoted as follows.

$$
\begin{aligned}
D^+u_i &= \frac{u_{i+1} - u_i}{h} + O(h) \\
D^-u_i &= \frac{u_i - u_{i-1}}{h} + O(h) \\
D^0u_i &= \frac{u_{i+1} - u_{i-1}}{2h} + O(h^2) \\
\delta^2 u_i &= D^+D^-u_i = \frac{u_{i+1} - 2u_i + u_{i-1}}{h^2} + O(h^2)
\end{aligned}
$$

Definition 1.8.2 Standard or classical numerical methods are computational methods, such as standard finite difference, finite element, finite volume and spectral methods that do not consider the behavior of the solutions in the layer regions. In solving singular perturbation problems, these methods fail to produce satisfactory results as ε approaches to zero (Farrell et al., 2000).

Definition 1.8.3 Local truncation error is the difference between the analytical solution and the numerical approximation at a mesh point, and global truncation error is the accumulation of the local truncation errors up to a given mesh point.

Definition 1.8.4 (Miller et al., 2012). Consider a family of mathematical problems parameterized by a singular perturbation parameter ε, where $\varepsilon \in (0, 1]$. Suppose that each problem in the family has a unique solution, denoted by u_ε and let U_ε be a numerical approximation of u_ε, defined on the mesh $\bar{\Omega}^N$ and obtained by a numerical method with in N mesh numbers. Then, the numerical solutions U_ε are said to converge ε-uniformly or robust to the exact solution u_ε, if there exist a positive integer N_0, and positive numbers C and P, where all are independent of of N and ε, such that, for all $N \geq N_0$,

$$\sup_{0<\varepsilon\leq 1} \|U_\varepsilon - u_\varepsilon\| \leq CN^{-P}. \tag{1.6}$$

Here P is called the ε-uniform rate of convergence and C is called the ε-uniform error constant.

By this definition, if a numerical method is ε-uniformly convergent, then for all values of $\varepsilon \in (0, 1]$, no matter how small, the point-wise error at the mesh points is never greater than CN^{-P}, for all values of $N \geq N_0$. And, since C, P and N_0 are independent of ε, it implies that the upper bound on the error is independent of ε. This dissertation is focused on the development and implementation of ε-uniformly convergent numerical schemes in the context of Definition 1.8.4 for solving SPDDEs.

It is know that the convergence of the standard finite difference methods involves the concepts of consistency and stability. That is, when the rate of convergence is required, consistency is replaced by a more stringent condition of accuracy of degree P, where P is some positive number. Then, the theoretical results are consistency and stability, which imply convergence and similarly accuracy of degree P and stability imply convergence of rate P. Such results of standard finite difference methods can be applied immediately to ε-uniform finite difference methods, provided that the conditions of accuracy and stability are also ε-uniform. This is rarely the case, which needs more careful analysis. Moreover, in many cases, it is not easy to determine that a given finite difference method has ε-uniform accuracy of some order $P > 0$, where P and the local truncation error constant are independent of ε. In such cases an alternative method of proof of the ε-uniform convergence may also be necessary. Such problems are briefly discussed by Gartland Jr (1989).

Numerical and asymptotic analyses: In solving singularly perturbed problems, there are two principal approaches. One is the numerical analysis, which deals with providing quantitative information about a particular problem and the second one is asymptotic analysis, which deals with the qualitative behaviors, such as the location and width of the layers in the solution and semi-quantitative information about a particular problem assuming ε goes to zero. Broad class of problems are treated by numerical analysis, while comparatively a restricted class of problems are solved using the asymptotic methods (Kadalbajoo & Reddy, 1989).

M-Matrices (Linß, 2009). M-matrices are the discrete counterparts of inverse-monotone differential operators, which have importance in the convergence analysis of finite difference methods and when studying systems of differential equations. A matrix $P \in R^{N\times N}$ is said to be

- an L_0-matrix if $a_{ij} \leq 0, \forall i, j = 1, 2, ..., N$ with $i \neq j$.
- inverse monotone if for any two vectors $v, w \in R$, $Pv \leq Pw$ implies that $v \leq w$.
- an M-matrix if it is an inverse monotone L_0-matrix.

The inverse monotonicity of a matrix P can also be characterized by $P^{-1} \geq 0$, where it is implicitly assumed that P^{-1} exists.

Lemma 1.8.1 *(M-Criterion). Suppose $P \in R^{N\times N}$ be an L_0-matrix. Then, P is an M-matrix if and only if there exist a vector $e \in R^N$ with $e \geq 0$ and $Pe \geq 0$. Moreover,*

$$\|P^{-1}\| \leq \frac{\|e\|}{\min_i |(Pe)_i|} \tag{1.7}$$

1.9 Organization of the study

This study consists of nine chapters. **Chapter 1** deals with the introduction of singularly perturbation problems. Research problems, objectives of the study, significance of the study, scope of the study and some mathematical preliminaries, which are used widely in this research work are incorporated in this chapter.

In **Chapter 2**, some related recent works on various forms of singularly perturbed differential-difference equations are reviewed. The considered problems, methods formulated to treat the problems and results obtained are briefly surveyed. Research gaps in the area that have received little attention and require further study are identified in this chapter.

Chapter 3 deals with the methodology of the study. The study design, sources of information, the methods applied and general procedures of this study are described in this chapter.

Chapters 4-9 covers the main works of the dissertation. It is organized in three parts. An exponentially fitted operator method via domain decomposition for the SPDDE given in (1.3) is presented in Chapter 4. Four different numerical schemes are proposed and analyzed for the SPDDE considered in (1.4) in Chapters 5-8. In Chapter 9, a nonstandard finite difference method is formulated and analyzed for the SPDDE considered in (1.5).

CHAPTER TWO

LITERATURE REVIEW

The theory and numerical study of singularly perturbed problems began towards the end of the nineteenth century, when approximate solutions were constructed from asymptotic expansions. However, the systematic study of numerical approaches for solving singular perturbation problems began in the late 1970s (Roos et al., 2008). The research frontier has steadily expanded since then, and the presentation of new developments in the analysis has become a rigorous research in applied sciences and engineering, where various works have been published. Numerous books or monographs have appeared in this area which either dealt with asymptotic approach or the numerical approaches. Some of the familiar monographs include Van Dyke (1975), O'Malley (1991), Farrell et al. (2000), Holmes (2007), Nayfeh (2008), Roos et al. (2008), Shishkin & Shishkina (2008), Linß (2009), Miller et al. (2012), and so on. Some surveys are also published, which deal with the review of different form of singular perturbation problems and the methods developed to treat the problems. For instance, Kadalbajoo & Reddy (1989), Kumar et al. (2007), Kadalbajoo & Gupta (2010), Roos (2012), Sharma et al. (2013), Kurina et al. (2017) and Duressa et al. (2023) are some survey articles of reviewing numerical schemes for singularly perturbed problems. In this chapter, various published research works on recently formulated uniformly convergent numerical methods for singularly perturbed differential-difference equations are briefly reviewed.

Manikandan et al. (2014) solved a singularly perturbed reaction-diffusion type with large delay as

$$\varepsilon u''(x) + a(x)u(x) + b(x)u(x-1) = f(x),\ x \in (0,2), \tag{2.1}$$

subject to $u(x) = \phi(x),\ -1 \leq x \leq 0,\ u(2) = \varphi$ with $0 < \varepsilon \ll 1$. The authors suggested a numerical scheme using a classical finite difference method on a piece-wise uniform Shishkin mesh. Stability estimate and convergence analysis of the method is investigated and proved, which showed that the method is almost first order convergent in the maximum norm.

Swamy et al. (2015) treated a linear singularly perturbed delay reaction-diffusion equation of the form

$$\varepsilon u''(x) + a(x)u(x-\delta) + b(x)u(x) = f(x),\ x \in (0,1), \tag{2.2}$$

subject to $u(x) = \phi(x),\ -\delta \leq x \leq 0,\ u(1) = \varphi$ with $0 < \varepsilon \ll 1$ and δ is a small delay of $o(\varepsilon)$. They constructed a computational method for this problem by replacing the original singularly perturbed delay differential equation by the first order neutral type delay differential equation and then employed the Trapezoidal rule. Applying linear interpolation, they obtained a uniformly convergent finite difference scheme.

Selvi & Ramanujam (2016) also presented a numerical method to solve (2.1) based on an iterative scheme, so that the solution is obtained as the limit of the solutions to a sequence of the non-delay problems. The numerical solutions of the non-delay problems are obtained by applying existing finite difference schemes and finite element method for the non- delay singularly perturbed equations. Error estimates are investigated in the supreme norm. Numerical results illustrating the theory are also included. An extensive amount of computational works have been carried out to demonstrate the applicability of the proposed methods. In this techniques, it is observed that the order of convergent is increased depending on the number of iteration.

Subburayan (2016) suggested a hybrid initial value method on Shishkin mesh to treat a singularly perturbed problem

$$\varepsilon u''(x) + a(x)u'(x) + b(x)u(x) + c(x)u(x-1) = f(x)\ x \in (0, 2), \tag{2.3}$$

subject to the interval and boundary conditions $u(x) = \phi(x),\ -1 \leq x \leq 0,\ u(2) = \varphi$ with $0 < \varepsilon \ll 1$. By this technique, they obtained a second order uniformly convergent result. In the work of Chakravarthy et al. (2017a), this problem is treated by constructing an exponentially fitted operator scheme to overcome the drawbacks of the corresponding classical counter parts. They established stability estimate and convergence analysis, and obtained that the scheme is a second order uniformly convergent method.

Sirisha & Reddy (2017a) treated a convection type singularly perturbed problem of the form

$$\varepsilon u''(x) + a(x)u'(x-\delta) + b(x)u(x) = f(x) \text{ on } (0, 1), \tag{2.4}$$

with $u(x) = \phi(x),\ -\delta \leq x \leq 0,\ u(1) = \beta$ with $0 < \varepsilon \ll 1$ and δ is a small delay of $o(\varepsilon)$. They proposed a numerical integration technique. The shift argument is handled using Taylor's series expansion, and consequently the second order delay differential equation is replaced by an asymptotically equivalent first order neutral type delay differential equation. Then, an exponential integrating factor is introduced to the resulted first order delay equation. The trapezoidal rule of integration along with linear interpolation is employed to get a numerical scheme. Venkata & Palli (2017) proposed an exponentially fitted spline method for such problem and obtained that the scheme provides a second order convergence and free from the perturbation parameter.

Devendra (2018) solved a singularly perturbed problem involving small negative shift and turning interior point as

$$\varepsilon u''(x) + a(x)u'(x-\delta) + b(x)u(x) = f(x),\ x \in (-1,1), \tag{2.5}$$

with the conditions $u(x) = \phi(x),\ -1-\delta \leq x \leq 0,\ u(1) = \beta$ with $0 < \varepsilon \ll 1$ and δ is small delay of $o(\varepsilon)$. The author used cubic B-spline functions and handled the shift term by the first two terms of Taylor series approximation. Then, to obtain an approximate solution, a B-spline collocation method based on Shishkin mesh is proposed. The convergence analysis of the proposed method is discussed and the scheme is uniformly convergent of almost order two.

Chakravarthy & Kumar (2018) proposed an adaptive mesh scheme for a singularly perturbed partial differential equation

$$u_t - \varepsilon u_{xx}(x,t) + a(x)u_x(x,t) + b(x)u(x,t) + c(x)u(x-\delta,t) + d(x)u(x+\eta,t) = f(x,t),\ x \in (0,2), \tag{2.6}$$

with the initial and internal boundary conditions $u(x,0) = \phi_0(x),\ x \in [0,1]$, $u(x,t) = \phi_l(x,t),\ (x,t) \in \{(x,t) : x \in [-\delta,0],\ t \in [0,T]\}$, $u(x,t) = \phi_r(x,t),\ (x,t) \in \{(x,t) : x \in [-\delta,0]\}$, where $0 < \varepsilon \ll 1$. To formulate the method, the authors used backward Euler scheme for the time variable and the concept of entropy function is used for the spatial variable using the central difference operator. To overcome the effects of the shift and advance parameters, they defined a special mesh, so that the terms containing the shifts lie on the mesh point after discretization. It is observed that in such method prior information of the width and position of the layers are not required. And the obtained method converges uniformly with respect to the perturbation parameter.

Govindarao & Mohapatra (2018) proposed a scheme for the singularly perturbed problem of the form

$$\begin{aligned}
&\left(u_t - \varepsilon u_{xx} + a(x)u_x + b(x)u\right)(x,t) = c(x)u(x,t-\tau) + f(x,t),\\
&u(x,t) = \phi_l(t),\ (x,t) \in \{(x,t):\ x = 0, 0 \leq t \leq T\},\\
&u(x,t) = \phi_r(t),\ (x,t) \in \{(x,t):\ x = 1, 0 \leq t \leq T\},\\
&u(x,t) = \phi_c(t),\ (x,t) \in \{(x,t):\ x \in [0,1], -\tau \leq t \leq 0\},
\end{aligned} \tag{2.7}$$

where $0 < \varepsilon \ll 1$ and τ is a time delay. To obtain a global second order accuracy, the authors proposed a hybrid scheme, which is a combination of the midpoint upwind method and central difference method in the spatial direction and an implicit-trapezoidal method in the temporal direction. The standard Shishkin mesh was extended to the hybrid of standard Shishkin mesh and Bakhvalov-Shishkin mesh and the method is parameter-uniformly convergent of second order in time and space.

Bansal & Sharma (2018) considered a singularly perturbed reaction-diffusion of the form

$$u_t(x,t) - \varepsilon u_{xx}(x,t) + a(x)u(x,t) + b(x)u(x-1,t) = f(x,t), \tag{2.8}$$

with the conditions

$$\begin{aligned} &u(x,0) = u_0(x),\ x \in [0,2],\\ &u(x,t) = \phi(x,t),\ (x,t) \in \{(x,t) : -1 \le x \le 0,\ 0 \le t \le T\},\\ &u(2,t) = \beta(2,t),\ (2,t) \in \{(2,t) :\ 0 \le t \le T\}, \end{aligned}$$

where $0 < \varepsilon \ll 1$ and T is a finite time. They proposed a numerical scheme to treat the problem by approximating the derivative term with respect to time using the implicit Euler scheme on a uniform meshes and in the spatial direction, they used the central difference operator on a piecewise uniform Shishkin meshes. They investigated the stability estimate and convergence result of the proposed method. By this method, it is observed that the scheme is uniformly convergent of order one in time and almost of order two in the spatial direction.

Sahihi et al. (2019) constructed a computational method using reproducing kernel Hilbert space method based on collocation scheme for (2.4). The approach is based on the division of the problem's domain into two sub-intervals, one with boundary layer and the other without a boundary layer, and then they applied the reproducing kernel Hilbert space method in each sub-intervals. From this study, it is observed that the method is with less computational work, fast convergence and high precision.

Adilaxmi et al. (2019) treated a singularly perturbed problem involving mixed shifts as

$$\varepsilon u''(x) + a(x)u'(x) + b(x)u(x-\delta) + c(x)u(x+\eta) = f(x),\ x \in (0,1) \tag{2.9}$$

subject to $u(x) = \phi(x),\ -\delta \le x \le 0,\ u(x) = \varphi(x),\ x \in [1, 1+\eta]$ with $0 < \varepsilon \ll 1$, δ and η be shift parameters of $o(\varepsilon)$. They simplified the shift terms using the Taylor's series approximation and replaced the original second order differential equation by an asymptotically equivalent singularly perturbed problem. Then, the resulted first order problem was solved using the nonstandard finite difference method.

Woldaregay & Duressa (2019) solved singularly perturbed parabolic differential-difference equation given by

$$u_t - \varepsilon^2 u_{xx}(x,t) + a(x)u_x(x,t) + b(x)u(x,t) + c(x)u(x-\delta,t) + d(x)u(x+\eta,t) = f(x,t),\ x \in (0,2) \tag{2.10}$$

with the initial and internal boundary conditions $u(x,0) = \phi_0(x),\ \ x \in [0,1],\ u(x,t) = \phi_l(x,t),\ \ (x,t) \in \{(x,t) : -\delta \leq x \leq 0 \leq t \leq T\},\ u(x,t) = \phi_r(x,t),\ \ (x,t) \in \{(x,t) : -\delta \leq x \leq 0\}$, where $0 < \varepsilon \ll 1$. To overcome the the effect of the shift parameters, they used Taylor's series approximation and to overcome the influence of ε, they formulated an ε-uniform scheme based on the method of line using the NSFDM in the spatial direction and the implicit Runge-Kutta method in the temporal direction. The method is obtained to be ε-uniformly convergent of second order in time and one in space.

Sekar & Tamilselvan (2019) treated a singularly perturbed problem with non-local boundary condition given as

$$\begin{aligned}
&-\varepsilon u''(x) + a(x)u'(x) + b(x)u(x) + c(x)u(x-1) = f(x),\ x \in (0,2),\\
&u(x) = \phi(x),\ x \in [-1,0],\\
&\kappa u(2) = u(2) - \varepsilon \int_0^2 g(x)u(x)dx = l,
\end{aligned} \tag{2.11}$$

where $0 < \varepsilon \ll 1$ and $\int_0^2 g(x)dx < 1$. The authors suggested a finite difference scheme with an appropriate piece-wise uniform Shishkin type mesh. They established the stability estimate and investigated the convergence of the method, so that the scheme is uniformly convergent almost of second order. Debela & Duressa (2020) also treated (2.11) by developing a fitted operator method on a uniform mesh. The non-local integral is handled using the Simpson's rule of integration. They accelerated the rate of convergence to second order using the Richardson extrapolation.

Woldaregay & Duressa (2020) solved the problem in (2.9) by constructing an exponentially fitted finite difference scheme. The numerical analysis and experiment show that the method converges uniformly with linear order before Richardson extrapolation and quadratic order after Richardson extrapolation. Musharary (2020) also constructed a hybrid numerical scheme for such problem. Using the cubic spline difference scheme in the fine mesh, and the modified upwind scheme in the coarse mesh, they formulated a hybrid scheme. They established a theoretical uniform bound in the discrete maximum norm and demonstrated that the formulated scheme is uniformly convergent.

Mbroh et al. (2020) solved the problem in (2.7) by proposing a numerical method via a step by step discretization. First, the spatial derivatives were discretized using a finite difference method, and then Crank-Nicolson method was applied to the resulted initial value scheme on a uniform meshes. The proposed method is then analyzed for its convergence and accelerated the accuracy by using the Richardson extrapolation. From the results obtained, it was concluded that the obtained method is uniformly convergent of first order in space and second order in time.

Kumari & Kumar (2020) solved a singularly perturbed differential equation in (2.8) by formulating a uniformly convergent scheme. The scheme is constructed applying the Crank-Nicolson method on the temporal uniform mesh and the standard central operator is used on a piece-wise uniform spatial meshes. From the theoretical and numerical experiments carried out, the obtained scheme is uniformly convergent of order two in time and almost order one in space.

Melesse et al. (2020) solved the problem in (2.5) by constructing a hybrid numerical scheme. They constructed a numerical method applying the mid-point upwind technique in the outer region and the central difference approach in the layer regions on piece-wise uniform Shishkin meshes. They established the stability estimate and investigated the convergence analysis of the numerical scheme. They obtained that the proposed hybrid scheme is ε-uniformly convergent of almost second order in the maximum norm.

Sathya & Rao (2020) presented a stabilized central difference method with exponential fitting factor for the problem in (2.3). The method is developed by re-approximating the error terms in the central difference approximation of the given boundary value problem, leading to a stabilizing effect and a second order convergent method is obtained. An error analysis of the method is investigated so that the scheme is uniformly convergent of second order.

A singularly perturbed ordinary differential equation with small negative shift in the convection and reaction terms of the form

$$\varepsilon u''(x) + a(x)u'(x-\delta) + b(x)u(x-\delta) + c(x)u(x) = f(x) \ x \in (0,1), \tag{2.12}$$

subject to $u(x) = \phi(x),\ -\delta \leq x \leq 0,\ u(1) = \varphi(1)$ with $0 < \varepsilon \ll 1$ and δ be a small delay parameter of $o(\varepsilon)$, is solved in by Angasu et al. (2021) and Woldaregay & Duressa (2021). In both articles, Taylor's series approximation was used to handle the delay terms. In the former article, the authors developed an exponentially fitted numerical scheme and obtained that the scheme is accurate and convergent. In the later article, the problem is solved using the technique of nonstandard finite difference method.

Chakravarthy & Kumar (2021) solved the problem in (2.1), and improved the results by constructing a fitted operator scheme on a uniform meshes. To handle the abruptly varying behavior of the layer regions, the authors introduced a fitting factor and derive it using the Numerov's method. They solved numerical examples and concluded that the method is convergent uniformly in the perturbation parameter.

Elango et al. (2021) focused on the study of a singularly perturbed partial differential equation with delay and having an integral boundary condition as

$$\begin{aligned}
&u_t(x,t) - \varepsilon u_{xx}(x,t) + a(x)u(x,t) + b(x)u(x-1,t) = f(x,t),\\
&u(x,t) = \phi_l(x,t),\ \phi_l(x,t) \in \{(x,t) : -1 \le x \le 0,\ 0 \le t \le T\},\\
&\kappa u(x,t) = u(2,t) - \varepsilon \int_0^2 g(x)u(x,t)dx = \phi_r(x,t),\ \phi_r(x,t) \in \{(2,t) : 0 \le t \le T\}\\
&u(x,t) = \phi_b(x,t),\ \phi_b(x,t) \in \{(x,0) :\ 0 \le x \le 2\},
\end{aligned} \tag{2.13}$$

They constructed a numerical scheme applying the standard central difference for the second order space derivative and backward difference for the first order time derivative. They simplified the integral boundary condition using the trapezoidal rule and constructed a numerical method on a piece-wise uniform spatial meshes. From the analyses of the method, they concluded that the method is convergent of first order in time and almost of second order in space.

Duressa & Bullo (2021) modified the studies and results in solving (2.2) by proposing a high order numerical method. In this method, the delay term is expanded using the Taylor's series expansion and as a result the problem is transformed to a convention-diffusion form. Then using the finite difference methods, they obtained a three-term recurrence relation finite difference approximation. To accelerate the convergence result, they used Richardson extrapolation technique and obtained an improved order of convergence. Tirfesa et al. (2022) improved it more by developing a non-polynomial cubic spline method. In this method, the singularly perturbed delay reaction-diffusion equation is transformed into an asymptotically equivalent two-point boundary value problem using Taylor series expansion. Then, a non-polynomial cubic spline approximation is developed into a three-term recurrence relation and obtained that it is accurate and convergent of order four.

Babu et al. (2022) also treated (2.7). In this method, based on the harmonic mesh, which are nonuniform and fine in the vicinity of the layer region, the authors constructed a parameter-uniform numerical scheme using backward Euler scheme to discretize the time derivative and the upwind finite difference scheme to discretize space derivative of the equation. The temporal delay was handled by choosing a positive integer times the time mesh yielding the delay parameter. From the theoretical and numerical experiments, it was proved that the proposed scheme is computationally more efficient as compared to other meshes like Bakvalov and Shishkin meshes.

Prasad et al. (2022) presented a computational method based on an exponential spline method for solving problem (2.4). To control the oscillations in the solution, the authors included a parameter, which is based on the exponential spline function and a special type of mesh is developed. To enhance the effectiveness of the scheme, a fitting factor is introduced, which is determined using the theory of singular perturbation.

A singularly perturbed parabolic equation of the form

$$\varepsilon u_{xx}(x,t) + a(x)u_x(x,t) - b(x)u(x-1,t) - c(x)u(x,t) - u_t(x,t) = f(x,t), \tag{2.14}$$

with initial and interval boundary conditions $u(x,0) = u_0(x),\ x \in [0,2]$, $u(x,t) = \phi(x,t),\ (x,t) \in \{(x,t) : -1 \le x \le 0,\ 0 \le t \le T\}$, $u(2,t) = \beta(2,t),\ (2,t) \in \{(2,t) :\ 0 \le t \le T\}$, where $0 < \varepsilon \ll 1$ and T is a finite time, is solved by Daba & Duressa (2022). Due to the presence of discontinuity and large delay, interior layers appear in the solution. To solve the problem, they formulated a numerical scheme using implicit Euler technique in the temporal direction and used a cubic spline in compression on a uniform spatial meshes. The method is obtained to be uniformly convergent of first order in time and second order in space.

Ayele et al. (2022) also solved (2.14) by constructing a numerical method applying the Crank-Nicolson in the temporal direction and NSFDM in the spatial direction. The authors described that the interior layer is caused by the delay term and the weak boundary layers are exhibited by the discontinuity of the convection coefficient and source functions. However, the occurrence of weak layers due to coefficient and source functions is not clearly described.

Gobena & Duressa (2022) treated problem (2.13) and improved its accuracy by formulating a fitted numerical scheme. To formulate the scheme, they used the Crank-Nicolson technique on the temporal mesh and an exponentially fitted operator method on a uniform spatial mesh. It is obtained that the scheme is uniformly convergent of second order in both time and spatial direction.

Elango & Unyong (2023) treated a singularly perturbed problem given as

$$\begin{aligned} &-\varepsilon u''(x) + a(x)u(x) + b(x)u(x-1) + c(x)u(x+1) = f(x)\ x \in (0,3), \\ &u(x) = \phi(x),\ x \in [-1,0],\ u(x) = \varphi(x),\ x \in [3,4] \end{aligned} \tag{2.15}$$

for $0 < \varepsilon \ll 1$. They solved the problem by constructing two non-uniform meshes used as part of the finite difference method. And they obtained that scheme is convergent of almost first order for the Shishkin mesh and it is convergent of first order for the Bakhvalov–Shishkin mesh formation.

A singularly perturbed problem with a non-local boundary condition of the form

$$\begin{aligned} & -\varepsilon u''(x) + a(x)u(x) + b(x)u(x-1) = f(x),\ x \in (0,2) \\ & u(x) = \phi(x),\ x \in [-1,0], \\ & \kappa u(2) = u(2) - \varepsilon \int_0^2 g(x)u(x)dx = l, \end{aligned} \tag{2.16}$$

where $0 < \varepsilon \ll 1$ and $\int_0^2 g(x)dx < \beta$ is solved by Elango (2023). The authors suggested a finite difference scheme with an appropriate piece-wise Shishkin type mesh. Using the discrete norm, the error estimate is analyzed , and obtained that the method is almost of first order. However, the solution of reaction-diffusion problems are expected to be of second order, and hence the result obtained by Elango (2023) contradicts this assumption

Brdar et al. (2023) considered a singularly perturbed time-dependent problem of the form

$$\begin{aligned} & u_t(x,t) - \varepsilon^2 u_{xx}(x,t) + a(x)u(x,t) + b(x)u(x-1,t) = f(x,t), \\ & u(x,0) = u_0(x),\ x \in [0,2], \\ & u(x,t) = \phi(x,t),\ (x,t) \in \{(x,t) : -1 \le x \le 0,\ 0 \le t \le T\}, \\ & u(2,t) = \beta(2,t),\ (2,t) \in \{(2,t) :\ 0 \le t \le T\}, \end{aligned} \tag{2.17}$$

where $0 < \varepsilon \ll 1$ and T is a finite time. The authors treated the problem using the finite element technique in the spatial direction and a discontinuous Galerkin technique in the temporal direction. They investigated the uniform error estimate and obtained that the scheme is convergent of second order in time and space. Tiruneh et al. (2023) treated the problem in (2.17) by constructing a nonstandard finite difference method on a uniform spatial mesh, and then using the Crank-Nicolson method on a uniform time mesh. The error analysis shows that the scheme is uniformly convergent of second order in time and space.

Hailu & Duressa (2023) considered a singularly perturbed problem with integral boundary conditions as

$$\begin{aligned} & u_t(x,t) - \varepsilon u_{xx}(x,t) + a(x)u_x(x,t) + b(x)u(x,t) + c(x)u(x-1,t) = f(x,t), \\ & u(x,t) = \phi_b(x,t),\ \phi_b(x,t) \in \{(x,0) :\ 0 \le x \le 2\}, \\ & u(x,t) = \phi_l(x,t),\ \phi_l(x,t) \in \{(x,t) : -1 \le x \le 0,\ 0 \le t \le T\}, \\ & \kappa u(x,t) = u(2,t) - \varepsilon \int_0^2 g(x)u(x,t)dx = \phi_r(x,t),\ \phi_r(x,t) \in \{(2,t) : 0 \le t \le T\}, \end{aligned} \tag{2.18}$$

for the singular perturbation $0 < \varepsilon \ll 1$. To treat the problem, the authors formulated a numerical method applying implicit Euler technique in the time direction and an exponentially fitted difference method in the spatial direction. They used Simpson's rule of integration for the integral boundary conditions, and the first order of convergence is accelerated to order two applying the Richardson extrapolation.

From the various research works reviewed above, it is observed that a significant amount of research has been done on different forms of SPDDEs in terms of designing and analyzing the numerical methods. Most of the works are focused on the problems involving small shift arguments. Different fitted finite difference methods have been developed, analyzed and validated to be implemented for practical purposes. However, singularly perturbed differential equations with large negative shifts, that arise in various fields of science and engineering, have received relatively very little attention from the research community. This observation suggests that there is still much to be explored in the area, and more research is needed to formulate new and more efficient numerical methods that can handle the problems and to explore their applications in various fields. This dissertation is mostly focused on formulating and analyzing numerical methods for singularly perturbed differential equations involving large negative shift.

CHAPTER THREE

RESEARCH METHODOLOGY

3.1 Study area and period

This study is conducted in Applied Mathematics focusing on a class of singularly perturbed differential-difference equations. These problems are considered in this study, because they require parameter-independent numerical methods, which yield accurate, stable and convergent results. The study is mainly focused on formulating, analyzing and validating fitted numerical schemes for the problems under consideration. And this dissertation is conducted from September 2019 to June 2023.

3.2 Study design

The dissertation is designed to employ documentary review of various singularly perturbed differential equations, description of the continuous solution, mathematical derivation of the numerical methods and numerical experiments on a singularly perturbed differential-difference equations.

3.3 Source of information

The relevant sources of information for this dissertation include various books, previously published articles and related studies available on google scholar, and the experimental results are obtained by writing and implementing computer programs for the developed numerical schemes on a Matlab software package.

3.4 Methods of scheme formulation

In this dissertation, to formulate fitted numerical schemes for a class of singularly perturbed differential-difference equations, finite difference methods are used either on a uniform or piece-wise uniform meshes. On a uniform meshes, fitted operator finite difference methods, which involve replacing the standard finite difference operator by one which captures the layer behavior of the problem are formulated. And on a piece-wise uniform meshes, fitted mesh finite difference methods are formulated by modifying the meshes that adapt to the singular perturbation problems.

3.5 Study procedures

To achieve the stated objectives, the following general procedures are employed

1) Describing the model problem.
2) Describing the properties of the continuous solution.
3) Discretizing the solution domain.
4) Formulating fitted numerical method on the discretized domains.
5) Establishing the stability estimate of the formulated numerical methods.
6) Investigating the convergence of the formulated numerical methods.
7) Confirming the theoretical findings by numerical experiments.
8) Comparing the formulated schemes with others in the literature.
9) Conclusion on the proposed methods.

CHAPTER FOUR

AN EXPONENTIALLY FITTED OPERATOR METHOD VIA DOMAIN DECOMPOSITION FOR SINGULARLY PERTURBED ORDINARY DIFFERENTIAL EQUATIONS WITH LARGE NEGATIVE SHIFT

This chapter deals with the formulation and analysis of an exponentially fitted operator scheme for solving a singularly perturbed ordinary differential equations involving large negative shift on a decomposed solution domain. Such problem arises frequently in the mathematical modeling of various physical and biological phenomena. The studies of these problems have shown that the behavior of the layers can change its character with the changes of the perturbation parameter, and this makes it difficult to solve the problem analytically. Few works are available in literature with various forms of numerical schemes. However, most of the formulated schemes are not accurate enough and have low parameter-uniform convergence rate. In this chapter, a numerical scheme is formulated by decomposing the domain into six subdomains, four inner regions and two outer regions. For each inner regions, an exponentially fitted finite difference scheme is proposed and combining all with the reduced schemes of the outer regions, an accurate and convergent numerical scheme is obtained.

4.1 The governing problem

Consider a second order singularly perturbed delay differential equation is considered as

$$\mathcal{L}_\varepsilon u(x) = -\varepsilon u''(x) + a(x)u(x) + b(x)u(x-1) = f(x),\ x \in (0,2), \tag{4.1}$$

with the interval and boundary conditions given as

$$\begin{cases} u(x) = \phi(x),\ x \in [-1,0], \\ u(2) = \alpha, \end{cases} \tag{4.2}$$

where $u(x) \in C(\bar{\Gamma}) = C^0[0,2] \cap C^2((0,1) \cup (1,2))$ and the functions $a(x)$, $b(x)$ and $f(x)$ are assumed to be sufficiently smooth, bounded and independent of ε on $[0,2]$. Moreover, for arbitrary constant λ, the coefficient functions satisfy the conditions

$$a(x) + b(x) \geq 2\lambda > 0 \text{ for and } b(x) < 0,\ x \in [0,2] \tag{4.3}$$

Also, $\phi(x)$ is a smooth function on $[-1, 0]$ and α is a given constant, which are independent of ε. Problems (4.1)-(4.2) can be rewritten as

$$\mathcal{L}_{\varepsilon,1}u(x) = -\varepsilon u''(x) + a(x)u(x) = f(x) - b(x)\phi(x-1),\ x \in (0, 1], \tag{4.4a}$$

$$\mathcal{L}_{\varepsilon,2}u(x) = -\varepsilon u''(x) + a(x)u(x) + b(x)u(x-1) = f(x),\ x \in (1, 2) \tag{4.4b}$$

with $u(x) = \phi(x)$ on $[-1, 0]$, $u(1^-) = u(1^+)$, $u'(1^-) = u'(1^+)$ and $u(2) = \alpha$, where 1^- and 1^+ represent the left and right side limit of u at $x = 1$, respectively. Due to the influence of the perturbation parameter, the solution $u(x)$ of the boundary value problem (4.1)-(4.2) exhibits strong boundary layers at $x = 0$ and $x = 2$ (Natesan & Bawa, 2007), and due to the large negative shift, interior (interfacing) layers occur on left and right sides of $x = 1$ (Subburayan, 2016). Such type of problem has a unique solution (Eloe et al., 2005).

4.2 Properties of the continuous solution

Lemma 4.2.1 *(Dinesh et al., 2017). For the smooth functions $a(x)$ and $b(x)$ satisfying (4.3), let $\psi(x) \in C(\bar{\Gamma})$, such that $\psi(0) \geq 0$, $\psi(2) \geq 0$ and $\mathcal{L}_\varepsilon \psi(x) \geq 0$ on $(0, 2)$. Then, $\psi(x) \geq 0$ on* $[0, 2]$.

Proof. Let x^* be given such that $\psi(x^*) = \min_{x\in[0,2]}\psi(x)$ and for the contrary, suppose $\psi(x^*) < 0$. By the given conditions, $x^* \notin \{0, 2\}$ and from the extreme value theorem, it follows that $\psi'(x^*) = 0$ and $\psi''(x^*) \geq 0$. Consequently,

$$\begin{aligned} \mathcal{L}_{\varepsilon,1}\psi(x^*) &= -\varepsilon\psi''(x^*) + a(x^*)\psi(x^*) < 0,\ x^* \in (0, 1], \\ \text{and}\quad \mathcal{L}_{\varepsilon,2}\psi(x^*) &= -\varepsilon\psi''(x^*) + a(x^*)\psi(x^*) + b(x^*)\psi(x^* - 1) \\ &\leq -\varepsilon\psi''(x^*) + [a(x^*) + b(x^*)]\psi(x^*) < 0,\ x^* \in (1, 2), \end{aligned}$$

which is a contradiction to the given hypothesis, so that the assumption is wrong. This implies that $\psi(x^*) \geq 0$ and $\psi(x) \geq 0$, for all $x \in [0, 2]$. ■

Lemma 4.2.2 *(Dinesh et al., 2017). Let the conditions in (4.3) hold true and $u(x)$ be any function on Γ. Then, for all $x \in [0, 2]$, $|u(x)| \leq \frac{1}{2\lambda}\|\mathcal{L}_\varepsilon u\| + \max\{|u(0)|, |u(2)|\}$.*

Proof. Define two functions as $\varphi^{\pm}(x) = \frac{1}{\lambda}\|\mathcal{L}_\varepsilon u\| + \max\{|u(0)|, |u(2)|\} \pm u(x)$. By these functions, one can have

$$\begin{aligned} &\text{At } x = 0,\ \varphi^{\pm}(0) = \frac{1}{\lambda}\|\mathcal{L}_\varepsilon u\| + \max\{|u(0)|, |u(2)|\} \pm u(0) \geq \frac{1}{\lambda}\|\mathcal{L}_\varepsilon u\| \geq 0, \\ &\text{At } x = 2,\ \varphi^{\pm}(2) = \frac{1}{\lambda}\|\mathcal{L}_\varepsilon u\| + \max\{|u(0)|, |u(2)|\} \pm u(2) \geq \frac{1}{\lambda}\|\mathcal{L}_\varepsilon u\| \geq 0. \end{aligned}$$

And by (4.4) for all $x \in (0,2)$,

$$\begin{aligned}
\mathcal{L}_{\varepsilon,1}\varphi^{\pm}(x) =& -\varepsilon\varphi''_{\pm} + a(x)\varphi^{\pm}(x)\\
=& \mp\varepsilon\varphi''_{\pm} + \frac{a(x)}{\lambda}\|\mathcal{L}_{\varepsilon,1}u\| + a(x)\max\{|u(0)|,|u(2)|\} \pm a(x)u(x)\\
=& \pm[a(x) - b(x)\psi(x-1)] + \frac{a(x)}{\lambda}\|f(x) - b(x)\psi(x-1)\| + a(x)\max\{|u(0)|,|u(2)|\}\\
\geq& a(x)\max\{|u(0)|,|u(2)|\} \geq 0,\ x \in (0,1].
\end{aligned}$$

$$\begin{aligned}
\mathcal{L}_{\varepsilon,2}\phi^{\pm}(x) =& -\varepsilon\varphi''_{\pm} + a(x)\varphi^{\pm}(x) + b(x)\varphi^{\pm}(x-1)\\
=& \mp\varepsilon\varphi''_{\pm} + \frac{a(x)}{\lambda}\|\mathcal{L}_{\varepsilon,2}u(x)\| + \frac{b(x)}{\lambda}\|\mathcal{L}_{\varepsilon,2}u(x-1)\| + [a(x)+b(x)]\max\{|u(0)|,|u(2)|\}\\
&\pm a(x)u(x) \pm b(x)u(x-1)\\
=& \pm f(x) + \frac{b(x)}{\lambda}\|\mathcal{L}_{\varepsilon,2}u(x)\| + \frac{b(x)}{\lambda}\|\mathcal{L}_{\varepsilon,2}u(x-1)|| + [a(x)+b(x)]\max\{|u(0)|,|u(2)|\}\\
\geq& [a(x)+b(x)]\max\{|u(0)|,|u(2)|\} \geq 2\alpha\max\{|u(0)|,|u(2)|\} \geq 0,\ x \in (1,2).
\end{aligned}$$

Applying Lemma 4.2.1, we obtain $\varphi^{\pm}(x) \geq 0$, for all $x \in [0,2]$, and hence $|u(x)| \leq \frac{1}{\beta}\|\mathcal{L}_{\varepsilon}u\| + \max\{|u(0)|,|u(2)|\}$, for all $x \in [0,2]$. ■

Lemma 4.2.3 *(Manikandan et al., 2014). Let the conditions in (4.2) hold true and $u(x)$ be the solution of (4.1)-(4.2). Then, the k^{th} derivatives of $u(x)$ are estimated as*

$$\begin{aligned}
&|u^{(k)}(x)| \leq C\varepsilon^{-\frac{k}{2}}(\|u\| + \|f\|),\ \text{if } k = 0,1,\\
&|u^{(k)}(x)| \leq C\varepsilon^{-\frac{k}{2}}(\|u\| + \|f\| + \|f^{(k-2)}\|\varepsilon^{\frac{k-2}{2}}),\ \text{if } k = 2,3,4.
\end{aligned}$$

Proof. The case for $k = 0$ holds true by Lemma 4.2.2. For the case $k = 1$, let $x \in (0,1)$ and construct an associated neighborhood $N_x = (\iota, \iota + \sqrt{\varepsilon})$, such that $x \in N_x$ and $N_x \subset [0,1]$. By the Mean Value Theorem for some $s \in \bar{N}_x$, it follows that

$$|u'(s)| = \left|\frac{u(\iota+\sqrt{\varepsilon}) - u(\iota)}{(\iota+\sqrt{\varepsilon}) - \iota}\right| = \varepsilon^{-\frac{1}{2}}|u(\iota+\sqrt{\varepsilon}) - u(\iota)| \leq 2\varepsilon^{-\frac{1}{2}}\|u\|.$$

Then, for $x \in N_x$,

$$\begin{aligned}
|u'(x)| =& |u'(s) + u'(x) - u'(s)| = |u'(s) + \int_s^x u''(t)dt|\\
=& |u'(s) + \frac{1}{\varepsilon}\int_s^x [-f(t) + a(t)u(t) + b(t)\psi(t-1)]dt|,\ t \in (a,x)\\
\leq& |u'(s)| + \frac{1}{\varepsilon}[\|f\| + a\|u\| + b\|\phi\|]\sqrt{\varepsilon}\\
\leq& C\varepsilon^{-\frac{1}{2}}(\|u\| + \|f\|).
\end{aligned}$$

By a similar procedure, for $x \in (1,2)$, construct a neighborhood $N_x = (\iota, \iota + \sqrt{\varepsilon}) \subset (1,2)$. Then, by the Mean Value Theorem as above, it becomes $|u'(x)| \leq C\varepsilon^{-\frac{1}{2}}(\|u\| + \|f\|)$.
The case for $k = 2$, follows rearranging terms in (4.1) as

$$u''(x) = \varepsilon^{-1}[a(x)u(x) + b(x)u(x-1) - f(x)]. \tag{4.5}$$

From this, $|u''(x)| \leq C\varepsilon^{-1}(\|u\| + \|f\|)$. Differentiating both sides of (4.5) once and twice yields

$$\begin{aligned}
|u'''(x)| =& \varepsilon^{-1}|a'(x)u(x) + a(x)u'(x) + b'(x)u(x-1) + b(x)u'(x-1) - f'(x)| \\
\leq& \varepsilon^{-1}(C + C\varepsilon^{-\frac{1}{2}}(\|u\| + \|f\|) + \|f'\|) \leq C\varepsilon^{-\frac{3}{2}}(\|u\| + \|f\| + \|f'\|\varepsilon^{\frac{1}{2}}). \\
|u^{(4)}(x)| =& \varepsilon^{-1}|(a'(x)u(x))' + (a(x)u'(x))' + (b'(x)u(x-1))' + (b(x)u'(x-1))' - f''(x)| \\
\leq& C\varepsilon^{-2}(\|u\| + \|f\| + \|f''\|\varepsilon),
\end{aligned}$$

which completes the proof of the required estimate. ■

4.3 The numerical method

In this section, the asymptotic techniques and derivation of the numerical methods are discussed in detail. To handle the essential behavior of the solution, the locations of the two boundary layers and the interfacing layers are described, and the mathematical derivation of the numerical method is described.

Description of the numerical method

Since the solution of (4.1) exhibits two boundary layers and interior (interfacing) layers, the domain is divided into six sub-domains, such as two boundary layers, two interior layers (left and right side of $x = 1$) and two outer regions. Let the asymptotically expanded solution of (4.1)-(4.2) be given as

$$u(x,\varepsilon) = \sum_{i=0}^{\infty}(u_{i1}(x) + v_{i1}(\gamma_1) + v_{i2}(\gamma_2))\varepsilon^i, \ x \in (0,1], \tag{4.6a}$$

$$u(x,\varepsilon) = \sum_{i=0}^{\infty}(u_{i2}(x) + v_{i3}(\gamma_3) + v_{i4}(\gamma_4))\varepsilon^i, \ x \in (1,2), \tag{4.6b}$$

where $\gamma_1 = \frac{x}{\sqrt{\varepsilon}}$, $\gamma_2 = \frac{1-x}{\sqrt{\varepsilon}}$, $\gamma_3 = \frac{x-1}{\sqrt{\varepsilon}}$ and $\gamma_4 = \frac{2-x}{\sqrt{\varepsilon}}$. Then, the corresponding zeros order asymptotic expansions of (4.6a)-(4.6b) are given by

$$u(x) = u_{01}(x) + v_{01}(\gamma_1) + v_{02}(\gamma_2), \ x \in (0,1], \tag{4.7a}$$

$$u(x) = u_{02}(x) + v_{03}(\gamma_3) + v_{04}(\gamma_4), \ x \in (1,2), \tag{4.7b}$$

where $u_{01}(x) = \frac{f(x)-b(x)\phi(x-1)}{a(x)}$ and $u_{02}(x) = \frac{f(x)-b(x)u_0(x-1)}{a(x)}$ are the asymptotic solutions of the reduced problem on $(0,1]$ and $(1,2)$ respectively, which do not satisfy the conditions in (4.2).

From the solution of the reduced problem, the value of $u(x=1)=\beta$ (say) can be obtained. In (4.7a)-(4.7b), v_{01} is the left boundary layer function, v_{02} is the left side of $x=1$ interior layer function, v_{03} is the right side of $x=1$ interior layer function and v_{04} is the right boundary layer function.

The functions v_{01}, v_{02}, v_{03} and v_{04} satisfy respectively, the following transformed homogeneous differential equations.

$$-\frac{d^2v_{01}(\gamma_1)}{d\gamma_1^2}+a(0)v_{01}(\gamma_1)=0;\ \gamma_1\in(0.\infty), \tag{4.8a}$$
$$-\frac{d^2v_{02}(\gamma_2)}{d\gamma_2^2}+a(1)v_{02}(\gamma_2)=0;\ \gamma_2\in(0.\infty), \tag{4.8b}$$
$$-\frac{d^2v_{03}(\gamma_3)}{d\gamma_3^2}+a(1)v_{03}(\gamma_3)=0;\ \gamma_3\in(0.\infty), \tag{4.8c}$$
$$-\frac{d^2v_{04}(\gamma_4)}{d\gamma_4^2}+a(2)v_{04}(\gamma_4)=0;\ \gamma_4\in(0.\infty). \tag{4.8d}$$

Solving each sub-equations in (4.8) at the corresponding terminal points and by (4.7a)-(4.7b) yields the zeros order solution of (4.1)-(4.2) as

$$u(x)=u_{01}(x)+\lambda_1e^{-\sqrt{\frac{a(0)}{\varepsilon}}x}+\lambda_2e^{-\sqrt{\frac{a(1)}{\varepsilon}}(1-x)},\ x\in(0,1], \tag{4.9a}$$
$$u(x)=u_{02}(x)+\lambda_3e^{-\sqrt{\frac{a(1)}{\varepsilon}}(x-1)}+\lambda_4e^{-\sqrt{\frac{a(2)}{\varepsilon}}(2-x)},\ x\in(1,2), \tag{4.9b}$$

where λ_1, λ_2, λ_3 and λ_4 can be obtained using the interval and boundary conditions as

$$\lambda_1=\frac{[\phi(0)-u_{01}(0)]-[\beta-u_{01}(1)]e^{-\sqrt{\frac{a(1)}{\varepsilon}}}}{1-e^{-\left(\sqrt{\frac{a(0)}{\varepsilon}}+\sqrt{\frac{a(1)}{\varepsilon}}\right)}}, \tag{4.10a}$$
$$\lambda_2=\frac{[\beta-u_{01}(1)]-[\phi(0)-u_{01}(0)]e^{-\sqrt{\frac{a(0)}{\varepsilon}}}}{1-e^{-\left(\sqrt{\frac{a(0)}{\varepsilon}}+\sqrt{\frac{a(1)}{\varepsilon}}\right)}} \tag{4.10b}$$
$$\lambda_3=\frac{[\beta-u_{02}(1)]-[\beta-u_{02}(2)]e^{-\sqrt{\frac{a(2)}{\varepsilon}}}}{1-e^{-\left(\sqrt{\frac{a(1)}{\varepsilon}}+\sqrt{\frac{a(2)}{\varepsilon}}\right)}} \tag{4.10c}$$
$$\lambda_4=\frac{[\alpha-u_{02}(2)]-[\beta-u_{02}(1)]e^{-\sqrt{\frac{a(1)}{\varepsilon}}}}{1-e^{-\left(\sqrt{\frac{a(1)}{\varepsilon}}+\sqrt{\frac{a(2)}{\varepsilon}}\right)}} \tag{4.10d}$$

Derivation of the numerical method

The domain $[0,2]$ is divided into N equal parts with a uniform mesh length h. Suppose $0=x_0,x_1,x_2,...,x_{\frac{N}{2}}=1,x_{\frac{N}{2}+1},x_{\frac{N}{2}+2},...,x_N=2$ be the mesh points. Then, $x_i=ih;\ i=$

$0, 1, 2, ..., N$. Choosing the terminal points as $x_{n_1} = \sqrt{\varepsilon}$, $x_{n_2} = 1 - \sqrt{\varepsilon}$, $x_{n_3} = 1 + \sqrt{\varepsilon}$ and $x_{n_4} = 2 - \sqrt{\varepsilon}$, suppose that the left boundary layer is in the interval $[0, \sqrt{\varepsilon}]$, the right boundary layer is in the interval $[2 - \sqrt{\varepsilon}, 2]$, the left interior layer is in the interval $[1 - \sqrt{\varepsilon}, 1]$, the right interior layer is in the interval $[1, 1 + \sqrt{\varepsilon}]$, the left outer region is in the interval $[\sqrt{\varepsilon}, 1 - \sqrt{\varepsilon}]$ and the right outer region is in the interval $[1 + \sqrt{\varepsilon}, 2 - \sqrt{\varepsilon}]$.

Now, at $x = x_i$, (4.1) can be written as $-\varepsilon u''(x_i) + a(x_i)u(x_i) + b(x_i)u(x_i - 1) = f(x_i)$. Let U_i be the approximate solution of $u(x_i)$. Then by the central finite difference method, $u''(x_i) = \delta_x^2 U_i - \frac{h^2}{12}U_i^{(4)} + R$, where $R = \frac{-h^4}{360}U^{(6)}(t)$, $t \in [x_i - h, x_i + h]$. Introducing a fitting factor σ to obtain an ε-independently convergent scheme,

$$\begin{aligned}\mathcal{L}_\varepsilon^N U_i = &- \frac{\varepsilon\sigma}{h^2}U_{i-1} + \left(\frac{2\varepsilon\sigma}{h^2} + a_i\right)U_i - \frac{\varepsilon\sigma}{h^2}U_{i+1} + \frac{\varepsilon\sigma h^2}{12}U_i^{(4)} \\ &- \varepsilon\sigma R + b_i U(x_i - 1) = f(x_i),\ i = 1, 2, ..., N-1,\end{aligned} \tag{4.11}$$

which leads to

$$\mathcal{L}_{\varepsilon,1}^N U_i = A_i U_{i-1} + B_i U_i + A_i U_{i+1} = D_i + T_i,\ i = 1, 2, ..., \frac{N}{2}, \tag{4.12a}$$

$$\mathcal{L}_{\varepsilon,2}^N U_i = A_i U_{i-1} + B_i U_i + A_i U_{i+1} = E_i + T_i,\ i = \frac{N}{2} + 1, \frac{N}{2} + 2, ..., N-1, \tag{4.12b}$$

where $A_i = -\frac{\varepsilon\sigma}{h^2}$, $B_i = \frac{2\varepsilon\sigma}{h^2} + a_i$, $D_i = f_i - b_i\phi_{i-\frac{N}{2}}$, $E_i = f_i - b_i U_{i-N/2}$ and $T_i = -\frac{\varepsilon\sigma h^2}{12}U^{(4)}(t) + \varepsilon\sigma O(h^4)$ for $t \in [x_i - h, x_i + h]$.

To handle the abruptly changing behaviors of solutions in the layers, an exponential fitting factor is introduced in each layers as follows.

Case 1: Left boundary layer

On the interval $[0, \sqrt{\varepsilon}]$, we introduce a fitting factor σ in (4.11) as

$$-\varepsilon\sigma_1\left(\frac{U_{i-1} - 2U_i + U_{i+1}}{h^2}\right) + a_i U_i = D_i + T_i \text{ for } i = 1, 2, ..., \frac{N}{8}. \tag{4.13}$$

To determine the fitting factor σ_1 on the left boundary layer, the left boundary layer asymptotic solution is used with the left outer solution given by

$$U_i = U_{01}(x_i) + \lambda_1 e^{-\sqrt{\frac{a(0)}{\varepsilon}}x_i}. \tag{4.14}$$

Assuming that the solution converges uniformly to the solution of (4.1)-(4.2), from (4.13), $-\frac{\sigma_1}{\rho^2}(U_{i-1} - 2U_i + U_{i+1}) = D_i + T_i - a_i U_i$, where $\rho = \frac{h}{\sqrt{\varepsilon}}$. Taking the limit as $h \to 0$, yields

$$-\lim_{h\to 0}\frac{\sigma_1}{\rho^2}(U_{i-1} - 2U_i + U_{i+1}) = \lim_{h\to 0}(D_i + T_i - a_i U_i). \tag{4.15}$$

From the asymptotic solution (4.14), it follows that $U_{i-1} = U_{01}(x_{i-1}) + \lambda_1 e^{-\sqrt{\frac{a(0)}{\varepsilon}}x_i} e^{\sqrt{a(0)}\rho}$ and $U_{i+1} = U_{01}(x_{i+1}) + \lambda_1 e^{-\sqrt{\frac{a(0)}{\varepsilon}}x_i} e^{-\sqrt{a(0)}\rho}$. Inserting these in (4.15) and simplifying gives

$$\sigma_1 = \left(\frac{\sqrt{a(0)}\rho/2}{\sinh(\sqrt{a(0)}\rho/2)} \right)^2, \tag{4.16}$$

which is the fitting factor in the interval $[0, \sqrt{\varepsilon}]$. Having this fitting factor in (4.13),

$$-\frac{\varepsilon\sigma_1}{h^2}U_{i-1} + \left(\frac{2\varepsilon\sigma_1}{h^2} + a_i\right)U_i - \frac{\varepsilon\sigma_1}{h^2}U_{i+1} = D_i + T_i, \text{ for } i = 1, 2, \ldots \frac{N}{8}. \tag{4.17}$$

Case 2: Left outer region

On the interval $[\sqrt{\varepsilon}, 1 - \sqrt{\varepsilon}]$, setting $\varepsilon = 0$, (4.11) becomes

$$a_i U_i = D_i, \text{ for } i = \frac{N}{8} + 1, \frac{N}{8} + 2, \ldots, \frac{3N}{8}, \tag{4.18}$$

which is the scheme in the left outer region.

Case 3: Left side interior layer

On the interval $[1 - \sqrt{\varepsilon}, 1]$, introducing a fitting factor σ_2 in (4.11) yields

$$-\varepsilon\sigma_2 \left(\frac{U_{i-1} - 2U_i + U_{i+1}}{h^2}\right) + a_i U_i = D_i + T_i \text{ for } i = \frac{3N}{8} + 1, \frac{3N}{8} + 2, \ldots, \frac{N}{2}. \tag{4.19}$$

To determine the fitting factor σ_2, the corresponding interior layer asymptotic solution is used with the left outer region solution given as

$$U_i = U_{01}(x_i) + \lambda_2 e^{-\sqrt{\frac{a(1)}{\varepsilon}}(1-x_i)}. \tag{4.20}$$

Assuming that the solution converges uniformly to the solution of (4.1)-(4.2), from (4.19), one cane obtain that

$$-\lim_{h\to 0} \frac{\sigma_2}{\rho^2}(U_{i-1} - 2U_i + U_{i+1}) = \lim_{h\to 0}(D_i + T_i - a_i U_i), \tag{4.21}$$

where $\rho = \frac{h}{\sqrt{\varepsilon}}$. From (4.20), $U_{i-1} = U_{01}(x_{i-1}) + \lambda_2 e^{-\sqrt{\frac{a(1)}{\varepsilon}}(1-x_i)} e^{-\sqrt{a(1)}\rho}$ and $U_{i+1} = U_{01}(x_{i+1}) + \lambda_2 e^{-\sqrt{\frac{a(1)}{\varepsilon}}(1-x_i)} e^{\sqrt{a(1)}\rho}$. Substituting these into (4.21) and simplification gives a fitting factor in the interior layer on the left side of $x = 1$ as

$$\sigma_2 = \left(\frac{\sqrt{a(0)}\rho/2}{\sinh(\sqrt{a(1)}\rho/2)} \right)^2. \tag{4.22}$$

And with this fitting factor, it is possible to obtain

$$-\frac{\varepsilon\sigma_2}{h^2}U_{i-1}+\left(\frac{2\varepsilon\sigma_2}{h^2}+a_i\right)U_i-\frac{\varepsilon\sigma_2}{h^2}U_{i+1}=D_i+T_i,\ \text{for } i=\frac{3N}{8}+1,\frac{3N}{8}+2,...,\frac{N}{2}. \quad (4.23)$$

Case 4: Right side interior layer

On the interval $[1,1+\sqrt{\varepsilon}]$, introducing a fitting factor σ_3 in (4.11) gives

$$-\varepsilon\sigma_3\left(\frac{U_{i-1}-2U_i+U_{i+1}}{h^2}\right)+a_iU(x_i=E_i+T_i,\ \text{for } i=\frac{N}{2}+1,\frac{N}{2}+2,...,\frac{5N}{8}. \quad (4.24)$$

To determine σ_3, the right side interior layer asymptotic solution is used with the right outer solution given by

$$U_i=U_{02}(x_i)+\lambda_3 e^{-\sqrt{\frac{a(1)}{\varepsilon}}(x_i-1)}. \quad (4.25)$$

Again, assuming that the solution converges uniformly to the solution of (4.1)-(4.2), from (4.24), one can find that

$$-\lim_{h\to 0}\frac{\sigma_3}{\rho^2}(U_{i-1}-2U_i+U_{i+1})=\lim_{h\to 0}(E_i+T_i-a_iU_i), \quad (4.26)$$

where $\rho=\frac{h}{\sqrt{\varepsilon}}$. Using (4.25), it follows that $U_{i-1}=U_{02}(x_{i-1})+\lambda_3 e^{-\sqrt{\frac{r(1)}{\varepsilon}}(x_i-1)}e^{\sqrt{a(1)}\rho}$ and $U_{i+1}=U_{02}(x_{i+1})+\lambda_3 e^{-\sqrt{\frac{a(1)}{\varepsilon}}(x_i-1)}e^{-\sqrt{a(1)}\rho}$. Putting these in (4.26) and simplifying gives the fitting factor σ_3 in the right side interior layer as

$$\sigma_3=\left(\frac{\sqrt{a(0)}\rho/2}{\sinh(\sqrt{a(1)}\rho/2)}\right)^2. \quad (4.27)$$

Having this fitting factor, (4.24) becomes

$$-\frac{\varepsilon\sigma_3}{h^2}U_{i-1}+\left(\frac{2\varepsilon\sigma_3}{h^2}+a_i\right)U_i-\frac{\varepsilon\sigma_3}{h^2}U_{i+1}=E_i+T_i\ \text{for } i=\frac{N}{2}+1,\frac{N}{2}+2,...,\frac{5N}{8}. \quad (4.28)$$

Case 5: Right outer region

On the right outer region $[1+\sqrt{\varepsilon},2-\sqrt{\varepsilon}]$, setting $\varepsilon=0$, (4.12b) is reduced to

$$a_iU_i=E_i,\ \text{for } i=\frac{5N}{8}+1,\frac{5N}{8}+2,...,\frac{7N}{8}, \quad (4.29)$$

which is the right outer region scheme.

Case 6: Right boundary layer

On the interval $[2-\sqrt{\varepsilon},2]$, introducing a fitting factor σ_4 in (4.11) gives

$$-\varepsilon\sigma_4\left(\frac{U_{i-1}-2U_i+U_{i+1}}{h^2}\right)+a_iU_i=E_i+T_i,\ \text{for } i=\frac{7N}{8}+1,\frac{7N}{8}+2,...,N. \quad (4.30)$$

To determine σ_4, the right boundary layer asymptotic solution is used with right outer solution, which is given by

$$U_i = U_{02}(x_i) + \lambda_4 e^{-\sqrt{\frac{a(2)}{\varepsilon}}(2-x_i)}. \tag{4.31}$$

Assuming that the solution converges uniformly to the solution of (4.1)-(4.2), it follows that

$$-\lim_{h\to 0}\frac{\sigma_4}{\rho^2}(U_{i-1} - 2U_i + U_{i+1}) = \lim_{h\to 0}(E_i + T_i - a_i U_i), \tag{4.32}$$

where $\rho = \frac{h}{\sqrt{\varepsilon}}$. From ((4.31)), $U_{i-1} = U_{02}(x_{i-1}) + \lambda_4 e^{-\sqrt{\frac{r(2)}{\varepsilon}}(2-x_i)} e^{\sqrt{a(2)}\rho}$ and $U_{i+1} = U_{02}(x_{i+1}) + \lambda_4 e^{-\sqrt{\frac{a(2)}{\varepsilon}}(2-x_i)} e^{-\sqrt{a(2)}\rho}$, and putting these into (4.32) and simplifying, the fitting factor is obtained as

$$\sigma_4 = \left(\frac{\sqrt{a(0)}\rho/2}{\sinh(\sqrt{a(2)}\rho/2)}\right)^2. \tag{4.33}$$

With this fitting factor, the numerical scheme in right boundary layer is given as

$$-\frac{\varepsilon\sigma_4}{h^2}U_{i-1} + \left(\frac{2\varepsilon\sigma_4}{h^2} + a_i\right)U_i - \frac{\varepsilon\sigma_4}{h^2}U_{i+1} = E_i + T_i \text{ for } i = \frac{7N}{8}+1, \frac{7N}{8}+2, ..., N. \tag{4.34}$$

Thus, the solution of the considered singularly perturbed differential equation with large negative shift can be obtained by solving the recurrence relations in (4.17), (4.23), (4.28) and (4.34) together with the outer layer schemes (4.18) and (4.29).

Discrete stability estimate

To establish the computational stability of the proposed numerical scheme, the approaches of Tiruneh & Reddy (2007) and Smith et al. (1985) is used as follow. From (4.12a), consider the recurrence relation

$$A_i U_{i-1} + B_i U_i + A_i U_{i+1} = D_i, \; i = 1, 2, ..., \frac{N}{2}, \tag{4.35}$$

where $A_i = -\frac{\varepsilon\sigma}{h^2}$ and $B_i = \frac{2\varepsilon\sigma}{h^2} + a_i$ with σ as in (4.16) or (4.22) and subject to the boundary conditions $U_0 = \phi(0)$ and $U_{\frac{N}{2}} = U(x_{\frac{N}{2}})$. Now, set

$$U_i = P_i U_{i+1} + Q_i, \text{ for } i = N-1, N-2, ..., 2, 1, \tag{4.36}$$

where $P_i = P(x_i)$ and $Q_i = Q(x_i)$ are determined as follows. From (4.36), $U_{i-1} = P_{i-1}U_i + Q_{i-1}$ and substituting in (4.35) gives

$$U_i = \frac{-A_i}{A_i P_{i-1} + B_i}U_{i+1} + \frac{D_i - A_i Q_{i-1}}{A_i P_{i-1} + B_i}. \tag{4.37}$$

From (4.36) and (4.37),

$$P_i = \frac{-A_i}{A_i P_{i-1} + B_i} \tag{4.38a}$$

$$Q_i = \frac{D_i - A_i Q_{i-1}}{A_i P_{i-1} + B_i}. \tag{4.38b}$$

Using the initial condition $U_0 = \psi(0) = P_0 U_1 + Q_0$, we can solve (4.38a) and (4.38b). Choose $P_0 = 0$, it follows that $Q_0 = U_0$. Using this and $U_{\frac{N}{2}} = U(x_{\frac{N}{2}})$, compute P_i and Q_i for all $i = 1, 2, ..., \frac{N}{2}$. Suppose that in computing P_i from (4.38a), a small error e_i be committed. Then, $P_i^* = P_i + e_i$ and $P_{i-1}^* = P_{i-1} + e_{i-1}$. But, it is to compute $P_i^* = \frac{-A_i}{A_i P_{i-1}^* + B_i}$. So,

$$e_i = P_i^* - P_i = \frac{-A_i}{A_i P_{i-1}^* + B_i} + \frac{A_i}{A_i P_{i-1} + B_i} = -\frac{A_i P_i}{A_i P_{i-1} + A_i e_{i-1} + B_i} e_{i-1}.$$

From the assumption in (4.3), $a(x) > 0$ and since $A_i = -\frac{\varepsilon\sigma}{h^2}$ and $B_i = \frac{2\varepsilon\sigma}{h^2} + a_i$, it follows that $|B_i| > |2A_i|$, for $i = 1, 2, ..., N-1$. Then, from (4.38a), $P_1 = \frac{-A_1}{A_1 P_0 + B_1} < 1$, $P_2 = \frac{-A_2}{A_2 P_1 + B_2} < \frac{-A_2}{A_2 + B_2} < 1$ as $P_1 < 1$ and successively, continuing in this manner yields $|P_i| < 1$ for $i = 0, 1, 2, ..., N-1$. Thus, under the assumption that there is small initial error, $|e_i| = \left| -\frac{A_i P_i}{A_i P_{i-1} + A_i e_{i-1} + B_i} \right| |e_{i-1}|$, which implies that $|e_i| < |e_{i-1}|$. This implies that (4.38a) is stable. In a similar procedure, it is possible to show that (4.38b) is also stable and following the same procedure for the numerical scheme (4.12b), a similar result can be obtained. This shows that the formulated finite difference scheme is stable.

Error analysis

To provide the error analysis of the proposed numerical scheme, the approach in Duressa (2021); Sathya & Rao (2020) is used. From (4.12a), a system of equations can be written as

$$-\frac{\varepsilon\sigma}{h^2} U_{i-1} + \left(\frac{2\varepsilon\sigma}{h^2} + a_i \right) U_i - \frac{\varepsilon\sigma}{h^2} U_{i+1} + g_i + T_i = 0, \ \forall i = 1, 2, ..., \frac{N}{2}, \tag{4.39}$$

where σ is as in (4.16) or (4.22), $g_i = -f_i + b_i \phi_{i-\frac{N}{2}}$ and $T_i = \frac{\varepsilon\sigma h^2}{12} u_i^{(4)}(t),\ t \in [x_i - h, x_i + h]$. Incorporating the conditions $U(0) = \phi(0)$ and $U(1) = U(x_{\frac{N}{2}})$ in (4.39), a system of equations in matrix form is given as

$$(G + H)U + M + T(h) = 0, \tag{4.40}$$

where $G = \frac{\varepsilon\sigma}{h^2}\begin{pmatrix} 2 & -1 & 0 & \dots & 0 \\ -1 & 2 & -1 & \dots & 0 \\ \vdots & \vdots & \vdots & \dots & \vdots \\ \vdots & \vdots & \vdots & \dots & -1 \\ 0 & 0 & \dots & -1 & 2 \end{pmatrix}$ is a tri-diagonal matrix of order $\frac{N}{2}-1$

and $H = \begin{pmatrix} a_1 & 0 & 0 & \dots & 0 \\ 0 & a_2 & 0 & \dots & 0 \\ \vdots & \vdots & \vdots & \dots & \vdots \\ \vdots & \vdots & \vdots & \dots & 0 \\ 0 & 0 & \dots & 0 & a_{1-\frac{N}{2}} \end{pmatrix}$ is a diagonal matrix of order $\frac{N}{2}-1$.

And the associated vectors of (4.40) are $M = \left(g_1 - \frac{\varepsilon\sigma\phi(0)}{h^2}, g_2, ..., g_{\frac{N}{2}2}, g_{\frac{N}{2}-1} - \frac{\varepsilon\sigma}{h^2}\beta\right)^t$, $T(h) = \left(T_1, T_2, ..., T_{\frac{N}{2}-1}\right)^t$. Now, let U^* be the approximation of U satisfying the system of equations

$$(G+H)\,U^* + M = 0 \tag{4.41}$$

and suppose that the i^{th} truncation error be $e_i = U_i^* - U_i$, $i = 1, 2, ..., \frac{N}{2}-1$, such that $E = \left(e_1, e_2, ..., e_{\frac{N}{2}}\right)^t = U^* - U$. Taking the difference between (4.40) and (4.41) yields

$$(G+H)\,E = T(h). \tag{4.42}$$

Let $a_i \leq K,\ \forall i = 1, 2, ..., N/2-1$, for arbitrary constant K and let $H_{i,i}$ be the $(i,i)^{th}$ entry of matrix H. Then since $a_i > 0$, for a sufficiently small h, we have $H_{i,i} \neq 0$ and $\frac{2\varepsilon\sigma}{h^2} + H_{i,i} \neq 0$ for $i = 1, 2, ..., \frac{N}{2}-1$. These show that $(G+H)$ is an irreducible matrix.

In matrix $(G+H)$, if S_i be the sum of entries on the i^{th} row, then $S_i = \frac{\varepsilon\sigma}{h^2} + a_i,\ i = 1, \frac{N}{2}-1$ and $S_i = a_i,\ i = 2, 3, ..., \frac{N}{2}-2$. Let's define $K_1 = \min_{1\leq i\leq \frac{N}{2}} a_i$ and $K_2 = \max_{1\leq i\leq \frac{N}{2}} a_i$, which imply that $0 < K_1 \leq K \leq K_2$. Thus, for a sufficiently small value of h, $(G+H)$ is monotone, so that it is non-singular and $(G+H)^{-1} \geq 0$. From (4.42),

$$\|E\| \leq \|\,(G+H)^{-1}\,\|\|T(h)\| \tag{4.43}$$

and in each row of $(G+H)$, it is true that

$$S_i \geq h^2\left(\frac{\varepsilon\sigma}{h^2} + a_i\right),\ i = 1, \frac{N}{2} - 1 \text{ and } S_i \geq h^2 a_i,\ i = 2, 3, ..., \frac{N}{2} - 2.$$

Suppose that $(G+H)^{-1}_{(i,j)}$ be the $(i,j)^{th}$ entry of $(G+H)^{-1}$ and define that

$$\|\,(G+H)^{-1}\,\| = \max_{1\leq i\leq \frac{N}{2}-1} \sum_{j=1}^{\frac{N}{2}-1} \left|(G+H)^{-1}_{i,j}\right| \text{ and } \|T(h)\| = \max_{1\leq i\leq \frac{N}{2}-1} |T_i|.$$

Since

$$\sum_{j=1}^{\frac{N}{2}-1}(G+H)^{-1}_{i.j}\,S_j = 1,\ i=1,2,...,\frac{N}{2}-1 \text{ and } (G+H)^{-1}\geq 0,$$

it follows that

$$(G+H)^{-1}_{i,j}\leq\frac{1}{S_j}<\frac{1}{h^2(\frac{\varepsilon\sigma}{h^2}+a_i)},\ j=1,\frac{N}{2}-1,$$

and

$$\sum_{j=2}^{N/2-2}(G+H)^{-1}_{i,j}\leq\frac{1}{\min\limits_j S_j}\leq\frac{1}{h^2a_i},\ i=1,2,...,\frac{N}{2}-2.$$

From (4.43), using the i^{th} row sum,

$$\begin{aligned}\|E\|\leq\|\,(G+H)^{-1}\,\|\|T(h)\| &= \max_{1\leq i\leq\frac{N}{2}-1}\sum_{j=1}^{\frac{N}{2}-1}|\,(G+H)^{-1}_{i,j}\,|\times\max_{1\leq i\leq\frac{N}{2}-1}|T_i| \\ &\leq\frac{1}{h^2}\left|\frac{1}{\frac{\varepsilon\sigma}{h^2}+a_i}+\frac{1}{a_i}+\frac{1}{\frac{\varepsilon\sigma}{h^2}+a_i}\right|\times\frac{\varepsilon\sigma|u^{(4)}(\xi_i)|}{12}h^2,\ \xi_i\in(x_i,x_{i+1}).\end{aligned}$$

Since σ is given as in (4.16) or (4.22) for the corresponding sub-regions, assuming sufficiently small h, we obtain $\|E\|\leq Ch^2$. Thus, for sufficiently chosen large value of C, this result shows the second order convergence of the proposed scheme on $(0,1]$, and by a similar analysis, the convergence of the numerical scheme can be investigated on $(1,2)$.

4.4 Numerical results and discussions

In this section, the numerical experiments are presented to test the applicability of the derived numerical scheme. If the exact solution is given or can be determined, the maximum point-wise error is computed as $e^N_\varepsilon=\max\limits_{i=0,1,...,N}|u(x_i)-U^N_i|$. And if the exact solution of a problem is not known, then the double mesh principle (Doolan et al., 1980) is used to determine the maximum absolute error and corresponding convergence rate of the proposed numerical scheme. That is, for a mesh function U_i, the maximum absolute error is computed as

$$e^N_\varepsilon=\max_i|U^N_i-U^{2N}_i|,\tag{4.44}$$

where U^{2N}_i is the approximate solution obtained by taking $2N$ mesh points. The uniform absolute error is then determined by

$$e^N=\max_\varepsilon(e^N_\varepsilon).\tag{4.45}$$

The corresponding convergence rate is computed by

$$r^N_\varepsilon=\frac{\log(e^N_\varepsilon/e^{2N}_\varepsilon)}{\log 2}\tag{4.46}$$

and the uniform convergence rate is obtained as

$$r^N = \max_{\varepsilon}(r_\varepsilon^N). \tag{4.47}$$

Example 4.4.1 *(Selvi & Ramanujam, 2016). Consider a constant coefficient boundary value problem* $-\varepsilon u''(x) + 5u(x) - u(x-1) = 1,\ u(x) = 1,\ x \in [-1, 0],\ u(2) = 2.$

Example 4.4.2 *(Dinesh et al., 2017). Consider a variable coefficient boundary value problem* $-\varepsilon u''(x) + (x+5)u(x) - u(x-1) = 1,\ \ u(x) = 1,\ x \in [-1, 0],\ u(2) = 2.$

Example 4.4.3 *(Manikandan et al., 2014). Consider a constant coefficient boundary value problem* $-\varepsilon u''(x) + 2u(x) - u(x-1) = 0,\ u(x) = 1,\ x \in [-1, 0],\ u(2) = 1.$

To elucidate the stability, uniform convergence and accuracy of the finite difference scheme developed in this chapter, maximum absolute errors and corresponding convergence rates are computed for each examples. Since the exact solutions are not given for the considered examples, the techniques in (4.44)-(4.47) are used to show the maximum absolute error and convergence rate. As it is shown in Tables 4.1, 4.2 and 4.3, the maximum absolute errors and convergence rates of Examples 4.4.1, 4.4.2 and 4.4.3 are given, respectively by taking various values of ε and N. From these tables, one can observe that the maximum point-wise error decreases when the mesh number increases. This confirms with the desired numerical results that increasing the mesh numbers increases the accuracy of the result. On the other hand, for each mesh number, decreasing the value of the perturbation parameter yields stable and uniform maximum absolute error, which confirms with the theoretical results. As shown in Table 4.4, the results obtained applying the formulated scheme are compared with some other published results in the literature. From this table, one can see that the numerical schemes developed in this chapter is accurate and uniformly convergent to solve the considered problem.

The numerical solutions of examples 4.4.1 and 4.4.2 are simulated graphically in Figures 4.1 and 4.2, respectively for various values of ε. In these figures, one can observe that minimizing the perturbation parameter decreases the width of the boundary layers and the interior layer, and characterized by steep gradients. The convergence result of the formulated method is also simulated by plotting the log-log graph of the maximum absolute errors versus mesh numbers as shown in Figure 4.3. From the log-log plots, one can visualize that increasing the mesh numbers (i.e decreasing the mesh sizes) decreases the maximum absolute error, and decreasing the value of the perturbation parameter yields stable maximum absolute errors.

Table 4.1: Maximum absolute errors and rate of convergence of Example 4.4.1 for different values of ε and N.

$\downarrow \varepsilon$ | $N \rightarrow$	512	1024	2048	4096	8192
2^{0}	1.8437e-04	4.6688e-05	1.1747e-05	2.9463e-06	7.3777e-07
	1.9815	1.9908	1.9953	1.9977	
2^{-2}	1.3535e-04	3.4390e-05	8.6676e-06	2.1757e-06	5.4704e-07
	1.9766	1.9883	1.9942	1.9918	
2^{-4}	4.3100e-05	1.1071e-05	2.8057e-06	7.0623e-07	1.8821e-07
	1.9609	1.9804	1.9902	1.9078	
2^{-6}	1.1424e-05	2.9831e-06	7.6189e-07	1.9250e-07	4.8824e-08
	1.9372	1.9692	1.9847	1.9792	
2^{-8}	4.8890e-05	1.3402e-05	3.5042e-06	8.9565e-07	2.2639e-07
	1.8671	1.9353	1.9681	1.9841	
2^{-10}	1.6110e-04	4.8891e-05	1.3402e-05	3.5042e-06	8.9566e-07
	1.7203	1.8671	1.9353	1.9681	
2^{-12}	4.2044e-04	1.0110e-04	4.8891e-05	1.3402e-05	3.5042e-06
	1.3839	1.7203	1.8671	1.9353	
2^{-14}	6.0346e-04	4.2044e-04	1.6110e-04	4.8891e-05	1.3402e-05
	0.5214	1.3839	1.7203	1.8671	
2^{-16}	5.9842e-04	3.9522e-04	1.7203e-04	5.0582e-05	1.3516e-05
	0.5985	1.2000	1.7660	1.9040	
2^{-18}	5.9840e-04	4.0946e-04	1.7380e-04	5.0619e-05	1.3520e-05
	0.5474	1.2363	1.7797	1.9046	
2^{-20}	5.9841e-04	4.0943e-04	1.7408e-04	5.0620e-05	1.3530e-05
	0.5475	1.2339	1.7820	1.9035	
e^{N}	6.0346e-04	4.2044e-04	1.7408e-04	5.0620e-05	1.3530e-05
r^{N}	0.5214	1.2721	1.7820	1.9035	

Table 4.2: Maximum absolute errors and rate of convergence of Example 4.4.2 for different values of ε and N.

$\downarrow \varepsilon \mid N \rightarrow$	512	1024	2048	4096	8192
2^{0}	1.8665e-04	4.7283e-05	1.1900e-05	2.9948e-06	7.4744e-07
	1.9809	1.9904	1.9953	1.9976	
2^{-2}	1.2319e-04	3.1343e-05	7.9051e-06	1.9850e-06	4.9735e-07
	1.9747	1.9873	1.9936	1.9968	
2^{-4}	2.7505e-05	7.0856e-06	1.7983e-06	4.5299e-07	1.1368e-07
	1.9567	1.9783	1.9891	1.9945	
2^{-6}	1.0979e-05	2.9195e-06	7.5245e-07	1.9099e-07	4.8108e-08
	1.9110	1.9561	1.9781	1.9891	
2^{-8}	4.1803e-05	1.1706e-05	3.1648e-06	7.9473e-07	2.0141e-07
	1.8364	1.8871	1.9936	1.9803	
2^{-10}	1.3501e-04	4.2281e-05	1.2033e-05	3.0998e-06	7.9521e-07
	1.6750	1.8130	1.9567	1.9628	
2^{-12}	3.3699e-04	1.3657e-04	4.3426e-05	1.1798e-05	3.1031e-06
	1.3031	1.6530	1.8800	1.9268	
2^{-14}	4.3315e-04	1.3802e-04	5.7230e-05	2.1108e-05	6.9812e-06
	1.6500	1.2700	1.4390	1.5962	
2^{-16}	4.3226e-04	1.4013e-04	5.6930e-05	1.9876e-05	6.8120e-06
	1.6251	1.2995	1.5182	1.5449	
2^{-18}	4.3218e-04	1.4109e-04	5.7004e-05	2.0812e-05	6.8120e-06
	1.6115	1.3075	1.4536	1.6113	
2^{-20}	4.3221e-04	1.4113e-04	5.6816e-05	2.1200e-05	6.8091e-06
	1.6147	1.3127	1.4222	1.6385	
e^{N}	4.3315e-04	1.4113e-04	5.7230e-05	2.1200e-05	6.9812e-06
r^{N}	1.6178	1.3022	1.4327	1.6025	

Table 4.3: Maximum absolute errors and rate of convergence of Example 4.4.3 for different values of ε and N.

$\downarrow \varepsilon$ | $N \rightarrow$	512	1024	2048	4096	8192
2^{0}	8.5338e-05	2.1595e-05	5.4317e-06	1.3621e-06	3.4114e-07
	1.9985	1.9912	1.9956	1.9974	
2^{-2}	7.4882e-05	1.8975e-05	4.7761e-06	1.1981e-06	3.0003e-07
	1.9805	1.9902	1.9951	1.9976	
2^{-4}	5.0149e-05	1.2755e-05	3.2163e-06	8.0754e-07	2.0261e-07
	1.9752	1.9876	1.9938	1.9948	
2^{-6}	3.7180e-05	9.4821e-06	2.3941e-06	6.0149e-07	1.5058e-07
	1.9712	1.9857	1.9929	1.9980	
2^{-8}	1.1403e-04	2.9523e-05	7.5077e-06	1.8928e-06	4.7517e-07
	1.9495	1.9754	1.9878	1.9940	
2^{-10}	4.2339e-04	1.1395e-04	2.9504e-05	7.5028e-06	1.8915e-06
	1.8936	1.9494	1.9754	1.9879	
2^{-12}	1.4397e-03	4.2339e-04	1.1395e-04	2.9504e-05	7.5028e-06
	1.7657	1.8936	1.9494	1.9754	
2^{-14}	3.9298e-03	1.4397e-03	4.2339e-04	1.1395e-04	2.9504e-05
	1.4487	1.7657	1.8936	1.9494	
2^{-16}	5.9127e-03	3.9298e-03	1.4397e-03	4.2339e-04	1.1395e.04
	0.5894	1.4486	1.7657	1.8936	
2^{-18}	5.6718e-03	3.4217e-03	1.2628e-03	4.0845e-04	1.2004e.04
	0.7291	1.4381	1.6284	1.7666	
2^{-20}	5.6293e-03	3.4020e-03	1.2708e-03	4.1240e-04	1.1820e.04
	0.7266	1.4206	1.6236	1.8028	
e^{N}	5.9127e-03	3.9298e-03	1.4397e-03	4.2339e-04	1.2004e-04
r^{N}	0.5894	1.4487	1.7657	1.8185	

Table 4.4: Comparison of the present scheme with other published works in literature.

$N \rightarrow$	1024	2048	4096	8192
Example 4.4.1				
Present scheme				
e^N	4.2044e-04	1.7408e-04	5.0620e-05	1.3530e-05
r^N	1.2721	1.7820	1.9035	-
Selvi & Ramanujam (2016)				
e^N	4.7371e-04	1.6440e-04	5.5672e-05	-
r^N	1.5268	1.5622	-	-
Example 4.4.2				
Present scheme				
e^N	1.4113e-04	5.7230e-05	2.1200e-05	6.9812e-06
r^N	1.3027	1.4327	1.6025	1.6852
Dinesh et al. (2017)				
e^N	9.7137e-04	4.0988e-04	1.8682e-04	8.8062e-05
r^N	1.0430	1.0217	1.0109	1.0056
Example 4.4.3				
$N \rightarrow$	128	256	512	1024
Present scheme				
e^N	3.9298e-03	1.4397e-03	4.2339e-04	1.1395e-04
r^N	1.4486	1.7657	1.8936	1.8974
Manikandan et al. (2014)				
e^N	0.5770e-02	0.3410e-02	0.2010e-02	0.1140e-03
r^N	0.6100	0.7320	0.7920	0.8170

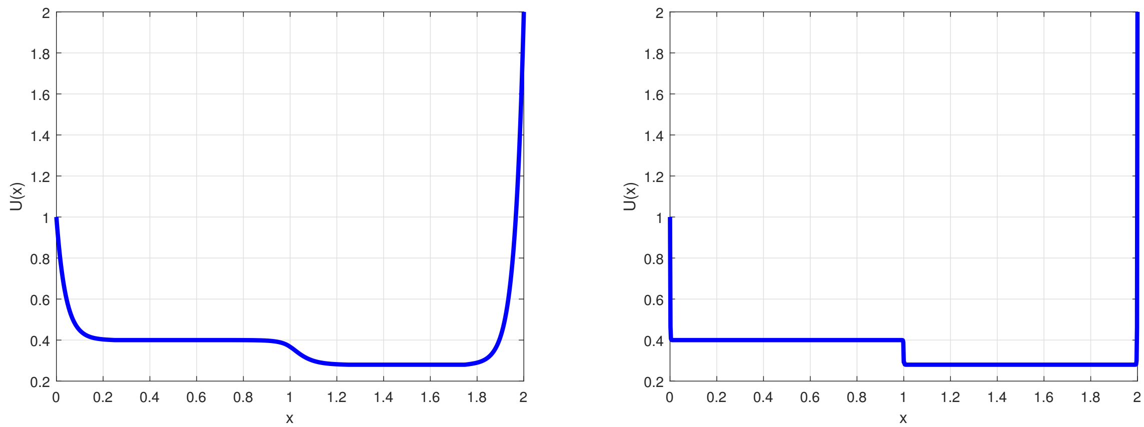

(a) $\varepsilon = 2^{-6}$ (b) $\varepsilon = 2^{-14}$

Figure 4.1: Numerical solutions of Example 4.4.1 for $N = 2^8$ and different values of ε.

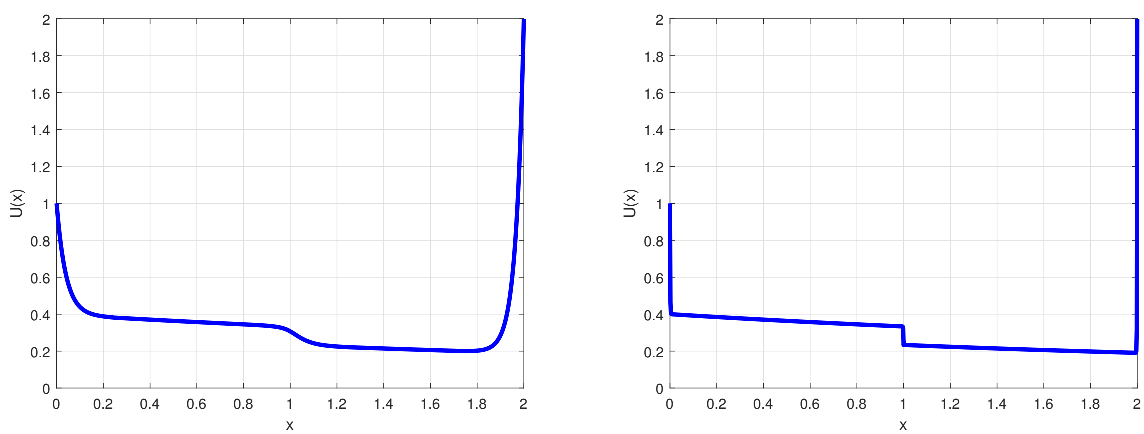

(a) $\varepsilon = 2^{-6}$ (b) $\varepsilon = 2^{-14}$

Figure 4.2: Numerical solutions of Example 4.4.2 for $N = 2^8$ and different values of ε.

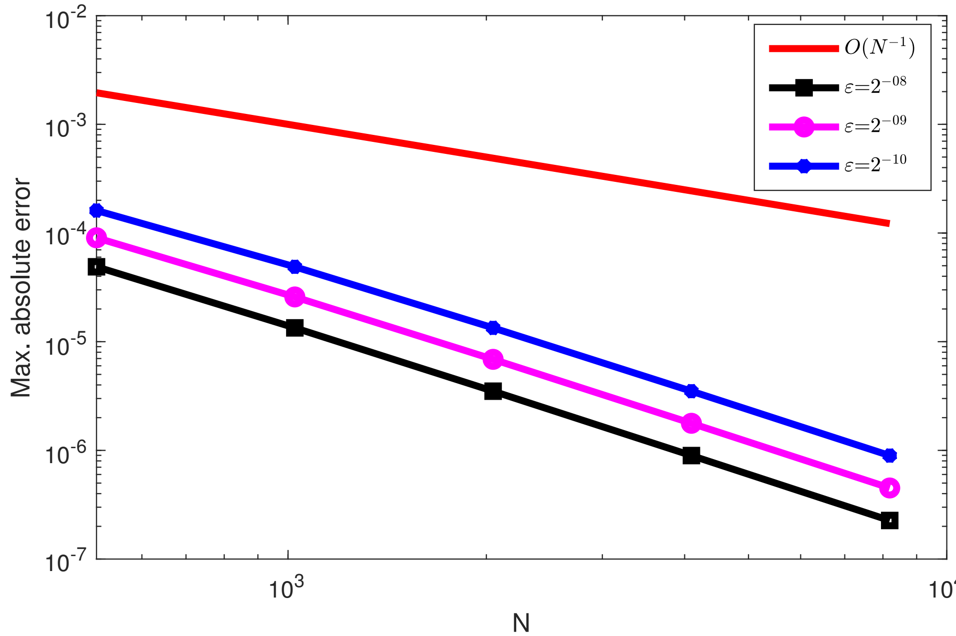

(a)

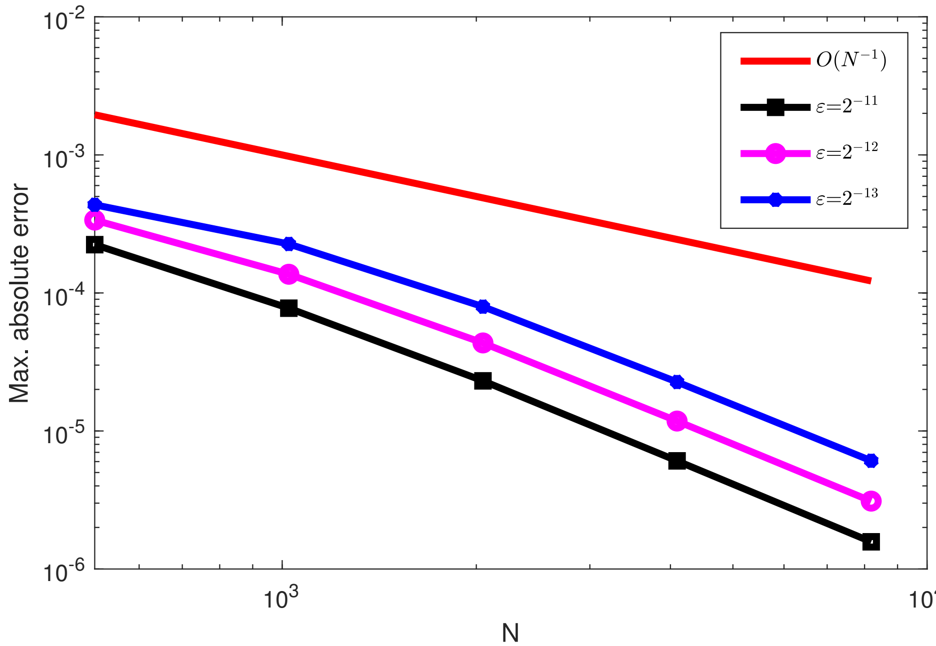

(b)

Figure 4.3: Log-log plots of maximum absolute errors versus N for (a) Example 4.4.1 and (b) Example 4.4.2

4.5 Summary

In this chapter, a second order singularly perturbed ordinary differential equation involving large negative shift is considered. The differential equation is transformed to difference equations by decomposing the domain into its boundary, interior and outer regions. In each boundary and interior layer sub-domains, the problem is discretized and exponentially fitted numerical schemes are formulated. And in each outer layer regions, reduced problems are obtained by setting $\varepsilon = 0$. Combining these schemes, a second order ε-uniformly convergent numerical method is derived. To validate the formulated method, three numerical examples are considered and solved. The numerical results of the examples are confirmed with the theoretical analysis of the proposed numerical scheme, and hence the proposed method is convergent independent of the perturbation parameter. The main findings of the chapter are summarized as follow:

1. A second order uniformly convergent numerical scheme is obtained for singularly perturbed ordinary differential equations involving large negative shifts.
2. The width of the layers decrease by decreasing the value of ε, but its steepness become more sharp.
3. The maximum absolute errors decrease by decreasing the mesh sizes.
4. Decreasing the value of ε yields stable and maximum absolute errors.
5. The global error estimate is obtained to be of order two.
6. The accuracy of the present numerical scheme is better than other compared methods in the literature.

CHAPTER FIVE

A FITTED MESH FINITE DIFFERENCE METHOD FOR SINGULARLY PERTURBED PARABOLIC DIFFERENTIAL EQUATIONS WITH NEGATIVE SHIFT

This chapter deals with the study of singularly perturbed partial differential equations involving negative shift argument. A fitted mesh finite difference scheme is formulated and its analysis is investigated when the delay parameter $\delta \in (0,1)$. The solution exhibits two boundary layers due to the influence of the perturbation parameter, and a weak interior layer due to the presence of the shift argument. To solve the problem, the time domain is discretized into uniform meshes and the spatial domain is discretized into piece-wise uniform Shishkin meshes. On the temporal uniform mesh, the Crank-Nicolson method is applied and on the spatial piece-wise uniform meshes, the central difference method is applied to transform the problem into a fully discrete scheme. The formulated finite difference method is shown to be uniformly convergent.

5.1 The governing problem

A SPDDE is considered on $\Omega = \Gamma \times \Lambda = (0,1) \times (0,T]$ and $\partial\Omega = \{(x,0) \cup (0,t) \cup (1,t) : x \in \bar{\Gamma}, t \in \bar{\Lambda}\}$ for a fixed time T as

$$u_t(x,t) - \varepsilon u_{xx}(x,t) + a(x)u(x,t) + b(x)u(x-\delta,t) = f(x,t), \tag{5.1}$$

subject to the initial and boundary conditions

$$\begin{cases} u(x,0) = u_0(x),\ x \in \bar{\Gamma} = [0,1], \\ u(x,t) = \phi(x,t),\ (x,t) \in \Omega^-, \\ u(1,t) = \alpha(t),\ (1,t) \in \Omega^+, \end{cases} \tag{5.2}$$

where $\Omega^- = \{(x,t) : x \in [-\delta, 0]\ ,\ t \in \bar{\Lambda}\}$, $\Omega^+ = \{(1,t) : t \in \bar{\Lambda}\}$, $0 < \varepsilon \ll 1$ and $0 < \delta < 1$. The considered functions $a(x)$, $b(x)$, $f(x,t)$, $u_0(x)$, $\phi(x,t)$ and $\alpha(t)$ are assumed to be sufficiently smooth, bounded and independent of the perturbation parameter.

Using the differential operator $\mathcal{L}_\varepsilon$, (5.1) can be written as

$$\mathcal{L}_\varepsilon u(x,t) = G(x,t), \tag{5.3}$$

where

$$\mathcal{L}_{\varepsilon}u(x,t)=\begin{cases}u_t(x,t)-\varepsilon u_{xx}(x,t(x,t))+a(x)u(x,t),\ (x,t)\in(0,\delta]\times\Lambda,\\ u_t(x,t)-\varepsilon u_{xx}(x,t)+a(x)u(x,t)+b(x)u(x-\delta,t),\ (x,t)\in(\delta,1)\times\Lambda\end{cases}\tag{5.4}$$

and

$$G(x,t)=\begin{cases}f(x,t)-b(x)\phi(x-\delta,t),\ (x,t)\in(0,\delta]\times\Lambda,\\ f(x,t),\ (x,t)\in(\delta,1)\times\Lambda.\end{cases}\tag{5.5}$$

Moreover, for arbitrary positive constant λ, the coefficient functions $a(x)$ and $b(x)$ satisfy the conditions

$$a(x)+b(x)\geq 2\lambda>0 \text{ and } b(x)<0,\ x\in\bar{\Gamma}.\tag{5.6}$$

For the model problem (5.1)–(5.2), the existence and uniqueness of the solution are guaranteed by the Holder continuity of the functions involved in the problem and imposing compatibility conditions at the corner points as

$$\begin{cases}u_0(0,0)=\phi(0,0),\\ u_0(1,0)=\alpha(1,0)\end{cases}\tag{5.7}$$

and

$$\begin{cases}\phi_t(0,0)-\varepsilon(u_t)_{xx}(0,0)+a(0)u_0(0,0)+b(0)u_0(-\delta,0)=f(0,0),\\ \alpha_t(1,0)-\varepsilon(u_0)_{xx}(1,0)+a(1)u_0(1,0)+b(1)u_0(1-\delta,0)=f(1,0).\end{cases}\tag{5.8}$$

Since the solution of the problem under consideration has boundary layers on both ends of the domain, by (5.7) and (5.8), it is guaranteed that there exist a constant C independent of the perturbation parameter Roos et al. (2008). Thus, for $(x,t)\in\bar{\Omega}$,

$$|u(x,t)-u_0(x)|\leq Ct.\tag{5.9}$$

Remark 5.1.1 *Since twin boundary layers are exhibited near* $\{(0,t):t\in[0,T]\}$ *and* $\{(1,t):t\in[0,T]\}$ *of* $\bar{\Omega}$*, there is no constant* C *independent of* ε *satisfying*

$$|u(x,t)-\phi(0,t)|\leq Cx \text{ and } |u(x,t)-\alpha(t)|\leq C(1-x).$$

5.2 Properties of the continuous solution

Assuming the above basic assumptions, the following properties of the continuous solution of (5.1)-(5.2) hold true.

Lemma 5.2.1 *The solution $u(x,t)$ of the continuous problem (5.1)-(5.2) is bounded as*

$$|u(x,t)| \leq C,\ (x,t) \in \bar{\Omega}.$$

Proof. From (5.9), since $|u(x,t)| - |u_0(x)| \leq |u(x,t) - u_0(x)| \leq Ct$, it gives $|u(x,t)| \leq Ct + |u_0(x)|$. For a fixed time T, since $t \in (0,T]$ and $u_0(x) \in C^2(\bar{\Omega})$, it implies that $Ct + |u_0(x)|$ is bounded, so that $|u(x,t)| \leq C$, $(x,t) \in \bar{\Omega}$. ■

Lemma 5.2.2 *(Kumari & Kumar, 2020). For a function $\vartheta(x,t) \in C^{2,1}(\bar{\Omega})$, let $\vartheta(x,t) \geq 0, (x,t) \in \partial\Omega$ and $\mathcal{L}_\varepsilon\vartheta(x,t) \geq 0,\ (x,t) \in \Omega$. Then, we have $\vartheta(x,t) \geq 0,\ (x,t) \in \bar{\Omega}$.*

Proof. Let $(\xi,\eta) \in \bar{\Omega}$ and assume that $\vartheta(\xi,\eta) = \min_{\bar{\Omega}}\vartheta(x,t) < 0$. From the given condition $(\xi,\eta) \notin \partial\Omega$. By the assumption and extreme values, it follows that $\vartheta_t(\xi,\eta) = 0,\ \vartheta_x(\xi,\eta) = 0$ and $\vartheta_{xx}(\xi,\eta) > 0$. Then,
Case 1: For $x \in (0,\delta]$, $\mathcal{L}_\varepsilon\vartheta(\iota,\eta) = \vartheta_t(\iota,\eta) - \varepsilon\vartheta_{xx}(\iota,\eta) + a(\iota)\vartheta(\iota,\eta) < 0$.
Case 2: For $x \in (\delta,1)$, $\mathcal{L}_\varepsilon\vartheta(\xi,\eta) = \vartheta_t(\xi,\eta) - \varepsilon\vartheta_{xx}(\xi,\eta) + a(\xi)\vartheta(\xi,\eta) + b(x)u(x-\delta,t) = \vartheta_t(\xi,\eta) - \varepsilon\vartheta_{xx}(\xi,\eta) + [a(\xi) + b(\xi)]\vartheta(\xi,\eta) + b(\xi)[\vartheta(\xi-\delta,\eta) - \vartheta(\xi,\eta)] < 0$.
From the two cases, $\mathcal{L}_\varepsilon\vartheta(\xi,\eta) < 0$, which is a contradiction to the given hypothesis. Thus, the assumption fails and hence $\vartheta(\xi,\eta) \geq 0$, which implies that $\vartheta(x,t) \geq 0$, $(x,t) \in \bar{\Omega}$. ■

Lemma 5.2.3 *(Swaminathan et al., 2016). The solution $u(x,t)$ of the continuous problem (5.1)–(5.2) is estimated as*

$$|u(x,t)| \leq \frac{\|f\|}{2\lambda} + \max\{|u_0(0)|, |\phi(0,t)|, |\alpha(t)|\}.$$

Proof. Defining barrier functions as $\pi^{\pm}(x,t) = \frac{\|f\|}{2\lambda} + \max\{|u_0(0)|, |\phi(0,t)|, |\alpha(t)|\} \pm u(x,t)$, one can find that

$$\pi^{\pm}(x,0) = \frac{\|f\|}{2\lambda} + \max\{|u_0(0)|, |\phi(0,t)|, |\alpha(t)|\} \pm u_0(x) \geq 0,$$
$$\pi^{\pm}(0,t) = \frac{\|f\|}{2\lambda} + \max\{|u_0(0)|, |\phi(0,t)|, |\alpha(t)|\} \pm \phi_0(t) \geq 0,$$
$$\pi^{\pm}(1,t) = \frac{\|f\|}{2\lambda} + \max\{|u_0(0)|, |\phi(0,t)|, |\alpha(t)|\} \pm \alpha(t) \geq 0.$$

For $x \in (0,\delta],\ t \in (0,T]$, one can have

$$\begin{aligned}\mathcal{L}_\varepsilon\pi^{\pm}(x,t) =& \pi_t^{\pm}(x,t) - \varepsilon\pi_{xx}^{\pm}(x,t) + a(x)\pi^{\pm}(x,t)\\ =& a(x)\left(\frac{\|f\|}{2\lambda} + \max\{|u_0(0)|, |\phi(0,t)|, |\alpha(t)|\}\right) \pm f(x,t) \geq 0.\end{aligned}$$

For $x \in (\delta, 1),\ t \in (0, T]$, one can obtain

$$\begin{aligned}\mathcal{L}_\varepsilon \pi^{\pm}(x,t) =& \pi_t^{\pm}(x,t) - \varepsilon \pi_{xx}^{\pm}(x,t) + a(x)\pi^{\pm}(x,t) + b(x)\pi^{\pm}(x-\delta,t)\\ =& [a(x)+b(x)]\left(\frac{\|f\|}{2\lambda} + \max\{|u_0(0)|, |\phi(0,t)|, |\alpha(t)|\}\right) \pm f(x,t) \geq 0.\end{aligned}$$

Hence, $\mathcal{L}_\varepsilon \pi^{\pm}(x,t) \geq 0$ and by the maximum principle, $\pi^{\pm}(x,t) \geq 0$, $(x,t) \in \bar{\Omega}$, which implies the required stability estimate. ■

Lemma 5.2.4 *(Kumari & Kumar, 2020). The derivatives of the solution $u(x,t)$ of (5.1)-(5.2) are bounded as*

$$\left|u^{(k,m)}(x,t)\right| \leq \begin{cases} C\left(1 + \varepsilon^{\frac{-k}{2}} B_{\varepsilon,1}\right), & (x,t) \in (0,\delta],\ t \in \Lambda,\\ C\left(1 + \varepsilon^{\frac{-k}{2}} B_{\varepsilon,2}\right), & (x,t) \in (\delta,1),\ t \in \Lambda \end{cases}$$

for all non-negative integers k and m such that $0 \leq k + 2m \leq 4$, where the functions $B_{\varepsilon,}$ and $B_{\varepsilon,}$ are given by $B_{\varepsilon,1} = \exp(-\sqrt{\lambda/\varepsilon}x) + \exp(-\sqrt{\lambda/\varepsilon}(\delta - x)$ and $B_{\varepsilon,2} = \exp(-\sqrt{\lambda/\varepsilon}(x - \delta)) + \exp(-\sqrt{\lambda/\varepsilon}(1-x)$.

Proof. Consider the case when $k = 0$ for $(x,t) \in \bar{\Omega}$, which provides the derivatives of $u(x,t)$ with respect to t. For $m = 0$, the result holds by Lemma 5.2.1. For the case $m = 1$, equation (5.1) becomes

$$u_t(x,t) = \varepsilon u_{xx}(x,t) - a(x)u(x,t) - b(x)u(x-\delta,t) + f(x,t). \tag{5.10}$$

On the side $t = 0$, (5.10) becomes

$$u_t(x,0) = \varepsilon u_{xx}(x,0) - a(x)u(x,0) - b(x)u(x-\delta,0) + f(x,0). \tag{5.11}$$

Without loss of generality, assume that $u(x,0) = u_0 = 0$, $u(x,t) = \phi(x,t) = 0$, $u(1,t) = 0$. Then, along the sides $x = 0$ and $x = 1$, it follows that $u(x,t) = 0$, which implies that $u_t(x,t) = 0$ and along $t = 0$, $u(x,0) = 0$, which implies that $u_{xx}(x,0) = 0$. On $(0,\delta]$, $u(x-\delta,0) = u_0(x-\delta,0) = \phi(x-\delta,0) = 0$ and on $(\delta,1)$, $u_0(x-\delta,0) = 0$. Combining these results gives $u(x-\delta,0) = 0$ and hence (5.11) becomes $u_t(x,0) = f(x,0)$. Since f is smooth function, $|u(x,0)| \leq C$ on $\partial\Omega$, so that

$$|u_t(x,t)| \leq C \quad \text{on } \bar{\Omega}. \tag{5.12}$$

Similarly for $m = 2$, differentiating (5.1) with respect to t gives

$$u_{tt}(x,t) - \varepsilon u_{txx}(x,t) + a(x)u_t(x,t) + b(x)u_t(x-\delta,t) = ft(x,t)$$

and along $t = 0$, it becomes

$$u_{tt}(x,0) - \varepsilon u_{txx}(x,0) + a(x)u_t(x,0) + b(x)u_t(x-\delta,0) = ft(x,0). \tag{5.13}$$

Since $u_t(x,0) = f(x,0)$, $u_{txx}(x,0) = fxx(x,0)$ and $u_t(x-\delta,0) = 0$, so that (5.13) becomes $u_{tt}(x,0) = \varepsilon f_{xx}(x,0) - a(x)f(x,0) + f_t(x,0)$. Hence, $|u_{tt}(x,0)| \leq C$ on $\partial\Omega$ and since f is smooth function, $|u_{tt}(x,t)| \leq C$, $(x,t) \in \Omega$. Thus, for sufficiently large choice of C, $|u_{tt}(x,t)| \leq C$ on $\bar{\Omega}$.

In a similar procedure, to bound the derivatives of the solution $u(x,t)$ with respect to the spatial variable, consider the cases for $k = 0, 1, 2, 3, 4$. For $k = 0$, it implies Lemma 5.2.1. For the case $k = 1$, let $x \in \Omega$ and consider a neighborhood of $I = (e, e+\sqrt{\varepsilon})$, $\forall x \in I$. For some $\zeta \in \bar{I}$ and $t \in (0,T]$ by the mean value theorem, it becomes

$$|u_x(\zeta,t)| = \left|\frac{u(e+\sqrt{\varepsilon},t) - u(e,t)}{\sqrt{\varepsilon}}\right| = \varepsilon^{\frac{-1}{2}}|u(e+\sqrt{\varepsilon},t) - u(e,t)| \leq 2\varepsilon^{\frac{-1}{2}}\|u\|. \tag{5.14}$$

For $x \in \bar{I}$,

$$\begin{aligned}
u_x(x,t) &= u_x(\zeta,t) + u_x(x,t) - u_x(\zeta,t) \\
&= u_x(\zeta,t) + \int_\zeta^x u_{xx}(s,t)ds \\
&= \ u_x(\zeta,t) + \varepsilon^{-1}\int_\zeta^x \left(u_t(s,t) + a(s)u(s,t) + b(s)u(s-\delta,t) - f(s,t)\right)ds. \\
\Rightarrow \quad |u_x(x,t)| &\leq |u_x(\zeta,t)| + C\varepsilon^{-1}\int_\zeta^x \left(\|u\| + \|f\|\right)ds \\
&= |u_x(\zeta,t)| + C\varepsilon^{-1}\left(\|u\| + \|f\|\right)\varepsilon^{\frac{1}{2}}.
\end{aligned}$$

Inserting (5.14) into the above result gives $|u_x(x,t)| \leq C\varepsilon^{\frac{-1}{2}}$, $(x,t) \in \bar{\Omega}$. Rearranging (5.1) implies

$$u_{xx}(x,t) = \varepsilon^{-1}\left(u_t(x,t) + a(x)u(x,t) + b(x)u(x-\delta,t) - f(x,t)\right). \tag{5.15}$$

For a fixed time $t \in [0,T]$ and for $x \in [0,1]$, since $|u| \leq C$, $|u_t| \leq C$ and f is smooth function, $|u_{xx}(x,t)| \leq C\varepsilon^{-1}$. Differentiating both sides of (5.15) with respect to t becomes

$$u_{txx}(x,t) = \varepsilon^{-1}\left(u_{tt}(x,t) + a(x)u_t(x,t) + b(x)u_t(x-\delta,t) - ft(x,t)\right).$$

Since $|u_t| \leq C$, $|u_{tt}| \leq C$ and $|f_t(x,t)| \leq C$, it follows that $|u_{txx}(x,t)| \leq C\varepsilon^{-1}$. Similar procedure holds for the remaining values of k and m satisfying $0 \leq k + 2m \leq 4$, so that the bounds on the derivatives of the solution can be easily determined. ■

5.3 The numerical method

To derive a fitted numerical scheme, the temporal and spatial domains are discretized. Then, the semi-discrete scheme is derived in the temporal direction, and a fully-discrete scheme is constructed in the spatial directions as follows.

5.3.1 Temporal discretization

Consider M uniform meshes on the time domain $[0,T]$ with mesh size Δt as $\bar{\Lambda}_t^M = \{\Delta t = T/M,\ t_j = j\Delta t,\ j = 0,1,2,...,M\}$. Let $U^{j+1}(x)$ is the approximate solution of (5.1)-(5.2) at the $(j+1)^{th}$ time level. Using the Crank-Nicolson method on, the temporal semi-discrete scheme of (5.1) becomes

$$\begin{aligned}
&-\varepsilon U_{xx}^{j+1}(x) + \left(\frac{2}{\Delta t} + a(x)\right) U^{j+1}(x) + b(x)U^{j+1}(x-\delta) \\
&= \varepsilon U_{xx}^{j}(x) + \left(\frac{2}{\Delta t} - a(x)\right) U^{j}(x) - b(x)U^{j}(x-\delta) + f^{j+1}(x) + f^{j}(x),
\end{aligned} \tag{5.16}$$

which can be written as

$$\mathcal{L}_\varepsilon^M U^{j+1}(x) = \pi^{j+1}(x),\ j+1 = 1,2,...,M \tag{5.17}$$

with the initial and boundary conditions

$$\begin{cases} U^0(x,0) = u_0(x),\ x \in \bar{\Gamma} = [0,1], \\ U^{j+1}(x) = \phi^{j+1}(x),\ x \in [-\delta, 0], \\ U^{j+1}(1) = \alpha(t_{j+1}),\ t_{j+1} \in [0,T], \end{cases} \tag{5.18}$$

where

$$\pi^{j+1}(x) = \begin{cases} \varepsilon U_{xx}^{j}(x) + \left(\frac{2}{\Delta t} - a(x)\right) U^{j}(x) - b(x)\phi^{j}(x-\delta) + f^{j+1}(x) + f^{j}(x),\ x \in (0,\delta], \\ \varepsilon U_{xx}^{j}(x) + \left(\frac{2}{\Delta t} - a(x)\right) U^{j}(x) - b(x)U^{j}(x-\delta) + f^{j+1}(x) + f^{j}(x),\ x \in (\delta,1), \end{cases}$$

$$\mathcal{L}_\varepsilon^M U^{j+1}(x) = \begin{cases} -\varepsilon U_{xx}^{j+1}(x) + \left(\frac{2}{\Delta t} + a(x)\right) U^{j+1}(x) + b(x)\phi^{j+1}(x-\delta),\ x \in (0,\delta], \\ -\varepsilon U_{xx}^{j+1}(x) + \left(\frac{2}{\Delta t} + a(x)\right) U^{j+1}(x) + b(x)U^{j+1}(x-\delta),\ x \in (\delta,1). \end{cases}$$

Lemma 5.3.1 *For a smooth function $\vartheta^{j+1}(x)$, suppose that $\vartheta^{j+1}(x) \geq 0$, $x \in \partial\Gamma$ and $\mathcal{L}_\varepsilon^M \vartheta^{j+1}(x) \geq 0$, $x \in \Gamma$. Then, $\vartheta^{j+1}(x) \geq 0$, $x \in \bar{\Gamma}$.*

Proof. Let s be given in $\bar{\Gamma}$, such that $\vartheta^{j+1}(s) = \min_{\bar{\Gamma}} \vartheta^{j+1}(x)$ and suppose that $\vartheta^{j+1}(s) < 0$. From the given hypothesis, $s \notin \partial\Gamma$ and by the assumption and extreme value properties, it follows that $\vartheta_x^{j+1}(s) = 0$ and $\vartheta_{xx}^{j+1}(s) > 0$. Then, consider following cases two cases.

Case 1: For $s \in (0, \delta]$, $\mathcal{L}_\varepsilon^M \vartheta^{j+1}(s) = -\varepsilon \vartheta_{xx}^{j+1} + \left(\frac{2}{\Delta t} + a(s)\right) \vartheta^{j+1}(s) < 0$.
Case 2: For $s \in (\delta, 1)$, $\mathcal{L}_\varepsilon^M \vartheta^{j+1}(s) = -\varepsilon \vartheta_{xx}^{j+1} + \left(\frac{2}{\Delta t} + a(s)\right) \vartheta^{j+1}(s) + b(s)\vartheta^{j+1}(s-\delta) < -\varepsilon \vartheta_{xx}^{j+1} + [\frac{2}{\Delta t} + a(s) + b(s)]\vartheta^{j+1}(s) < 0$.
The two cases contradict the given hypothesis. Thus, the assumption fails, and hence $\vartheta^{j+1}(s) \geq 0$, implying $\vartheta^{j+1}(x) \geq 0$, $x \in \bar{\Gamma}$. Thus, the semi-discrete maximum principle is satisfied by the operator $\mathcal{L}_\varepsilon^M$ and as a result,

$$\|(\mathcal{L}_\varepsilon^M)^{-1}\| \leq (1 + 2\lambda \Delta t)^{-1}. \tag{5.19}$$

■

Lemma 5.3.2 *(Bansal & Sharma, 2018) Let $U^{j+1}(x)$ be the solution of (5.16)-(5.17). Then, it can be estimated as*

$$|U^{j+1}(x)| \leq \frac{\Delta t \|\mathcal{L}_\varepsilon^M U\|}{1 + 2\lambda \Delta t} + \max\{|U^{j+1}(0)|, |U^{j+1}(1)|\}, x \in \bar{\Gamma}$$

Proof. Define barrier functions as

$$\vartheta_\pm^{j+1}(x) = \frac{\Delta t \|\mathcal{L}_\varepsilon^M U\|}{1 + 2\lambda \Delta t} + \max\{|U^{j+1}(0)|, |U^{j+1}(1)|\} \pm U^{j+1}(x).$$

Then, it is easy to see that $\vartheta_\pm^{j+1}(0) \geq 0$ and $\vartheta_\pm^{j+1}(1) \geq 0$. And
Case 1: For $0 < x \leq \delta$,

$$\begin{aligned}
\mathcal{L}_\varepsilon^M \vartheta_\pm^{j+1}(x) &= -\varepsilon(\vartheta_{xx}^{j+1})_\pm + \left(\frac{2}{\Delta t} + a(x)\right) \vartheta_\pm^{j+1}(x) \\
&= \pm \pi^{j+1}(x) + \left(\frac{2}{\Delta t} + a(x)\right) [\frac{\Delta t \|\mathcal{L}_\varepsilon^M U\|}{1 + 2\lambda \Delta t} + \max\{|U^{j+1}(0)|, |U^{j+1}(1)\}] \\
&\geq \left(\frac{2}{\Delta t} + a(x)\right) [\max\{|U^{j+1}(0)|, |U^{j+1}(1)\}] \geq 0.
\end{aligned}$$

Case 2: For $\delta < x < 1$,

$$\begin{aligned}
\mathcal{L}_\varepsilon^M \vartheta_\pm^{j+1}(x) &= -\varepsilon(\vartheta_{xx}^{j+1})_\pm + \left(\frac{2}{\Delta t} + a(x)\right) \vartheta_\pm^{j+1}(x) + b(x)\vartheta_\pm^{j+1}(x-\delta) \\
&\geq -\varepsilon(\vartheta_\pm^{j+1})_{xx} + \left(\frac{2}{\Delta t} + a(x)\right) \vartheta_\pm^{j+1}(x) + b(x)\vartheta_\pm^{j+1}(x) \\
&= \pm \omega^{j+1}(x) + \left(\frac{2}{\Delta t} + a(x) + b(x)\right) [\frac{\Delta t \|\mathcal{L}_\varepsilon^M U\|}{1 + 2\lambda \Delta t} + \max\{|U^{j+1}(0)|, |U^{j+1}(1)\}] \\
&\geq \left(\frac{2}{\Delta t} + a(x) + b(x)\right) [\max\{|U^{j+1}(0)|, |U^{j+1}(1)\}] \geq 0.
\end{aligned}$$

Thus, applying Lemma 5.3.1, one can obtain that $\vartheta_\pm^{j+1}(x) \geq 0$, $x \in \bar{\Gamma}$, which implies the required estimation. ■

Lemma 5.3.3 *Given that* $|\frac{\partial^k u(x,t)}{\partial t^k}| \leq C$ *for* $(x,t) \in \bar{\Omega}$ *and* $k = 0,\ 1,\ 2$, *the local truncation error is estimated as* $\|e^{j+1}\| \leq C(\Delta t)^3$, $j+1$=1, 2, ..., M. *And with this condition, the global error is estimated as* $\|E^{j+1}\| \leq C(\Delta t)^2,\ j+1$=1, 2, ..., M.

Proof. Choose the center point $(x, t_{j+1/2})$ of the temporal mesh as a convenient base point where the Taylor series is expanded. Then $U(x, t_{j+1})$ and $U(x, t_j)$ can be expanded as

$$U^{j+1}(x) = U^{j+1/2}(x) + \frac{\Delta t}{2} U_t^{j+1/2} + \frac{(\Delta t)^2}{8} U_{tt}^{j+1/2} + O((\Delta t)^3), \tag{5.20a}$$

$$U^j(x) = U^{j+1/2}(x) - \frac{\Delta t}{2} U^{j+1/2} + \frac{(\Delta t)^2}{8} U^{j+1/2} + O((\Delta t)^3). \tag{5.20b}$$

Now, subtracting (5.20b) from (5.20a) gives

$$\frac{U^{j+1}(x) - U^j(x)}{\Delta t} = U_t^{j+1/2}(x) + O((\Delta t)^3). \tag{5.21}$$

Using (5.1) into (5.21) at $(x, t_{j+1/2})$ gives

$$\begin{aligned} \frac{U^{j+1}(x) - U^j(x)}{\Delta t} =& \varepsilon U_{xx}^{j+1/2}(x) - a(x)U^{j+1/2}(x) - b(x)U^{j+1/2}(x-\delta) \\ &+ f(x, t_{j+1/2}) + O((\Delta t)^3). \end{aligned} \tag{5.22}$$

Putting (5.22) into the time semi-discrete problem (5.16) gives

$$\begin{aligned} &\varepsilon U_{xx}^{j+1/2}(x) - a(x)U^{j+1/2}(x) - b(x)U^{j+1/2}(x-\delta) + f(x, t_{j+1/2}) + O((\Delta t)^3) \\ &- \frac{\varepsilon}{2}\left(U_{xx}^{j+1}(x) + U_{xx}^j(x)\right) + \frac{a(x)}{2}\left(U^{j+1}(x) + U^j(x)\right) \\ &+ \frac{b(x)}{2}\left(U^{j+1}(x-\delta) + U^j(x-\delta)\right) = \frac{1}{2}\left(f^{j+1}(x) + f^j(x)\right), \end{aligned}$$

which can be written equivalently as

$$\mathcal{L}_{\varepsilon,x}^{M}\left(U(x, t_{j+1}) - U^{j+1}(x)\right) = O((\Delta t)^3). \tag{5.23}$$

Using (5.19) into (5.23), a boundary value problem of the form $\mathcal{L}^{M_\varepsilon} e^{j+1}(x) = O((\Delta t)^3)$ with $e^{j+1}(0, t_{j+1}) = 0$ and $e^{j+1}(1) = 0$. Applying Lemma 5.3.1, the local truncation error is estimated as $\|e^{j+1}\| \leq C((\Delta t)^3)$.

Using the estimation of the local truncation error up to $(j+1)^{th}$ time level,

$$\begin{aligned} \|E^{j+1}\| =& \left\| \sum_{\zeta=1}^{j} e^{\zeta} \right\|, \ \ j \leq T/\Delta t \\ =& \|e^1 + e^2 + ... + e^j\| \\ \leq& \|e^1\| + \|e^2\| + ... + \|e^{j+1}\| \\ \leq& C'T(\Delta t)^2 \leq C(\Delta t)^2, \ j = 0, 1, 2, ..., M. \end{aligned}$$

Thus, the temporal semi-discrete scheme is convergent of order two. ■

Remark 5.3.1 The Shishkin decomposition of the solution $U^{j+1}(x)$ of the semi-discrete problem (5.17) is $U^{j+1}(x) = V^{j+1}(x) + W^{j+1}(x)$, where the regular component $V^{j+1}(x)$ is the solution of the problem

$$\begin{aligned}
\mathcal{L}^M_{\varepsilon,1}V^{j+1}(x) =&\pi(x,t_{j+1}),\ x\in(0,\delta],\ V^{j+1}(0)=u_0(0,t_{j+1}),\\
&V^{j+1}(\delta^-)=(l(\delta))^{-1}[\pi(\delta,t_{j+1})+\pi(\delta,t_j)+m(\delta)U^j(\delta)-b(\delta)\phi(0,t_{j+1})],\\
\mathcal{L}^M_{\varepsilon,2}V^{j+1}(x) =&\pi(x,t_{j+1}),\ x\in(\delta,1),\ V^{j+1}(1)=u_0(1,t_{j+1}),\\
&V^{j+1}(\delta^+)=(a(\delta))^{-1}[\pi(\delta,t_{j+1})+\pi(\delta,t_j)+b(\delta)U^j(\delta)-b(\delta)V^{j+1}_0(0)],
\end{aligned}$$

where $l(x) = \frac{2}{\Delta t} + a(x)$ and $m(x) = \frac{2}{\Delta t} - a(x)$. The singular component $W^{j+1}(x)$ is the solution of the problem

$$\begin{aligned}
&\mathcal{L}^M_{\varepsilon,1}W^{j+1}(x)=0,\ x\in(0,\delta]\ \text{ and }\ \mathcal{L}^M_{\varepsilon,2}W^{j+1}(x)=0,\ x\in(\delta,1),\\
&W^{j+1}(0)=U^{j+1}(0)-V^{j+1}(0),\ W^{j+1}(1)=U^{j+1}(1)-V^{j+1}(1),\\
&V^{j+1}(\delta^-)+W^{j+1}(\delta^-)=V^{j+1}(\delta^+)+W^{j+1}(\delta^+).
\end{aligned}$$

Since the problem under consideration involves two boundary layers, the singular component can be further decomposed as $W^{j+1}(x) = W_L^{j+1}(x) + W_R^{j+1}(x)$, where

$$W_L^{j+1}(x)=W^{j+1}(0)W_{L,1}^{j+1}(x)+\gamma_1 W_{L,2}^{j+1}(x)\ \text{ and }\ W_R^{j+1}(x)=\gamma_2 W_{R,1}^{j+1}(x)+W^{j+1}(1)W_{R,2}^{j+1}(x),$$

where the constants γ_1 and γ_2 are arbitrarily chosen constants in such a way that the weak interior layer conditions at $x = \delta$ are satisfied. The sub-divisions of the singular component satisfy the following problems.

$$\begin{aligned}
\mathcal{L}^M_{\varepsilon,1}W^{j+1}_{L,1}(x)&=0,\ x\in(0,\delta], \qquad (5.24)\\
W^{j+1}_{L,1}(0)=&W^{j+1}(0),\ W^{j+1}_{L,1}(0)=0 \text{ and } W^{j+1}_{L,1}(x)=0,\ x\in[\delta,1].\\
\mathcal{L}^M_{\varepsilon,1}W^{j+1}_{L,2}(x)&=0,\ x\in(0,\delta], \qquad (5.25)\\
W^{j+1}_{L,2}(0)=&0,\ W^{j+1}_{L,2}(\delta)=0 \text{ and } W^{j+1}_{L,2}(x)=0,\ x\in[\delta,1].
\end{aligned}$$

$$\begin{aligned}
\mathcal{L}^M_{\varepsilon,2}W^{j+1}_{R,1}(x)&=0,\ x\in[\delta,1], \qquad (5.26)\\
W^{j+1}_{R,1}(\delta)=&0,\ W^{j+1}_{R,1}(1)=0 \text{ and } W^{j+1}_{R,1}(x)=0,\ x\in(0,\delta].\\
\mathcal{L}^M_{\varepsilon,2}W^{j+1}_{R,2}(x)&=0,\ x\in(\delta,1], \qquad (5.27)\\
W^{j+1}_{R,2}(\delta)=&0,\ W^{j+1}_{R,2}(1)=W^{j+1}(1) \text{ and } W^{j+1}_{R,2}(x)=0,\ x\in[0,\delta].
\end{aligned}$$

Lemma 5.3.4 *The derivatives of the solution $U^{j+1}(x)$ and its components can be estimated as follows.*

$$\left|\frac{d^kU^{j+1}(x)}{dx^k}\right| \leq \begin{cases} C(1+\varepsilon^{\frac{-k}{2}}d_1(x)),\ x\in[0,\delta], \\ C(1+\varepsilon^{\frac{-k}{2}}d_2(x)),\ x\in[\delta,1], \end{cases}$$

$$\left|\frac{d^kV^{j+1}(x)}{dx^k}\right| \leq \begin{cases} C(1+\varepsilon^{\frac{-(k-2)}{2}}d_1(x)),\ x\in[0,\delta], \\ C(1+\varepsilon^{\frac{-(k-2)}{2}}d_2(x)),\ x\in[\delta,1], \end{cases}$$

$$\left|\frac{d^kW^{j+1}(x)}{dx^k}\right| \leq \begin{cases} C\varepsilon^{\frac{-k}{2}}d_1(x),\ x\in[0,\delta], \\ C\varepsilon^{\frac{-k}{2}-k/2}d_2(x),\ x\in[\delta,1], \end{cases}$$

where $k=0,\,1,\,2,\,3,\ d_1(x)=e^{-\sqrt{\frac{\lambda}{\varepsilon}}x}+e^{-\sqrt{\frac{\lambda}{\varepsilon}}(\delta-x)}$ *and* $d_2(x)=e^{-\sqrt{\frac{\lambda}{\varepsilon}}(x-\delta)}+e^{-\sqrt{\frac{\lambda}{\varepsilon}}(1-x)}$.

Proof. The estimation for $k=0$ implies Lemma 5.3.2. For $k=1$, construct a neighborhood of $I_x=(s,s+\sqrt{\varepsilon})$, such that $x\in\bar{I}_x$ and $I_x\in(0,\delta]$. For some $\eta\in\bar{I}_x$, one can obtain that

$$|U_x^{j+1}(\eta)|=\varepsilon^{\frac{-1}{2}}|U^{j+1}(s+\sqrt{\varepsilon})-U^{j+1}(s)|\leq 2\varepsilon^{\frac{-1}{2}}\|U^{j+1}\|.$$

Then, for any $x\in\bar{I}_[x]$, it is possible to get

$$\begin{aligned}|U_x^{j+1}(x)|=&|U_x^{j+1}(\eta)+\varepsilon^{-1}\int_\eta^x\left[(\frac{2}{\Delta t}+a(x))U^{j+1}(s)-\pi(s,t_{j+1})\right]ds|\\ \leq&|U_x^{j+1}(\eta)|+C\varepsilon^{-1}(\|U^{j+1}\|+\|\pi\|)\\ \leq&C\varepsilon^{\frac{-1}{2}}\leq C\left[1+\varepsilon^{\frac{-1}{2}}(e^{-\sqrt{\frac{\lambda}{\varepsilon}}x}+e^{-\sqrt{\frac{\lambda}{\varepsilon}}(\delta-x)})\right],\ x\in(0,\delta].\end{aligned}$$

For $m\in\{2,3,4\}$, the estimates can be verified easily using the bounds of $U^{j+1}(x)$ and $U_x^{j+1}(x)$. The estimate for the smooth component follows the decomposition provided in Remark 5.3.1. Since $V^{j+1}(x)=V_0^{j+1}(x)+\varepsilon V_1^{j+1}(x)$, where $V_1^{j+1}(x)$ is the solution of a scheme similar to (5.17), it is possible to obtain

$$\left|\frac{d^kV^{j+1}(x)}{dx^k}\right|\leq C(1+\varepsilon^{\frac{-(k-)}{2}})\leq C(1+\varepsilon^{\frac{-(k-1)}{2}}(e^{-\sqrt{\frac{\lambda}{\varepsilon}}x}+e^{-\sqrt{\frac{\lambda}{\varepsilon}}(\delta-x)}),\ x\in(0,\delta],\ k=0,1,2,3.$$

And the singular component is estimated as

$$\left|\frac{d^kW^{j+1}(x)}{dx^k}\right|\leq C\varepsilon^{\frac{-k}{2}}\leq C\varepsilon^{\frac{-k}{2}}(e^{-\sqrt{\frac{\lambda}{\varepsilon}}x}+e^{-\sqrt{\frac{\lambda}{\varepsilon}}(\delta-x)}),\ x\in(0,\delta],\ k=0,1,2,3.$$

By similar procedures, the estimates for $x\in(\delta,1)$ can be easily verified. ■

5.3.2 Spatial discretization

Consider a piece-wise uniform mesh $\bar{\Gamma}_x^N$ with N mesh numbers on the spatial domain $[0,1]$. Let's sub-divide it as $[0,1]=[0,\tau]\cup(\tau,1-\tau]\cup(1-\tau,1]$, where τ is a transition parameter, which separates the non-uniform meshes and given by

$$\tau=\min\left\{\frac{1}{4},2\sqrt{\frac{\varepsilon}{\lambda}}\ln N\right\}.$$

To get a piece-wise uniform mesh, consider $\frac{N}{4}$ meshes on each of the fine mesh regions $[0,\tau]$ and $(1-\tau,1)$ and $\frac{N}{2}$ meshes on the coarse region $(\tau,1-\tau]$. The mesh points are $x_i=x_{i-1}+h_i$, $i=1,2,...,N$, where the mesh size h_i's are given as

$$h_i=\begin{cases}\frac{4\tau}{N},\ i=1,2,...,\frac{N}{4},\\ \frac{2-4\tau}{N},\ i=\frac{N}{4}+1,\frac{N}{4}+2,...,\frac{3N}{4},\\ \frac{4\tau}{N},\ i=\frac{3N}{N}+1,\frac{3N}{N}+2,...,N.\end{cases}$$

To handle the influence of the delay term a special mesh is considered, so that the term containing the shift argument lies on the mesh point after discretization. Now, define the finite difference operators as

$$\begin{aligned}D^+U(x_i)&=\frac{U(x_i)-U(x_{i-1})}{h_{i+1}},\quad D^-U(x_i)=\frac{U(x_i)-U(x_{i-1})}{h_i},\\ D^+D^-U(x_i)&=\frac{2}{h_{i+1}+h_i}(D^+-D^-)U(x_i),\ i=0,1,...,N.\end{aligned}$$

Using the finite difference operators in (5.16), we obtain a fully discrete scheme as

$$\mathcal{L}_\varepsilon^{N,M}U_i^{j+1}=\pi_i^{j+1},\ j=0,1,2,...,M-1, \tag{5.28}$$

with the conditions $U_i^0=u_0(x_i)$, $x_i\in[0,1]$, $U^{j+1}(x_i)=\phi^{j+1}(x_i)$, $x_i\in(0,\delta]$ and $U^{j+1}(x_N)=\alpha(t_{j+1})$, $x_i\in(\delta,1)$, where

$$\mathcal{L}_\varepsilon^{N,M}U_i^{j+1}=\begin{cases}-\varepsilon D^+D^-U_i^{j+1}+\left(\frac{2}{\Delta t}+a_i\right)U_i^{j+1}+b_i\phi_{i-r}^{j+1},\ i=1,2,...,r,\\ -\varepsilon D^+D^-U_i^{j+1}+\left(\frac{2}{\Delta t}+a_i\right)U_i^{j+1}+b_iU_{i-r}^{j+1},\ i=r+1,r+2,...,N-1,\end{cases}$$

and $$\pi_i^{j+1}=\begin{cases}\varepsilon D^+D^-U_i^j+\left(\frac{2}{\Delta t}-a_i\right)U_i^j-b_i\phi_{i-r}^j+f_i^{j+1}+f_i^j,\ i=1,2,...,r,\\ \varepsilon D^+D^-U_i^j+\left(\frac{2}{\Delta t}-a_i\right)U_i^j-b_iU_{i-r}^j+f_i^{j+1}+f_i^j,\ i=r+1,r+2,...,N-1\end{cases}$$

for $r=\delta N,$ so that $r\in\{1,2,...,N-1\}$.

On simplification of (5.28), it gives the system of equations of the form

$$A_iU_{i+1}^{j+1}+B_iU_i^{j+1}+C_iU_{i-1}^{j+1}=D_iU_{i+1}^j+E_iU_i^j+F_iU_{i-1}^j+H_{i,j}, \tag{5.29}$$

where

$$A_i = \frac{-2\varepsilon}{h_{i+1}(h_i+h_{i+1})},\ \ B_i = \frac{2\varepsilon}{h_i+h_{i+1}}\left(\frac{2\varepsilon}{h_{i+1}}+\frac{2\varepsilon}{h_i}\right)+\frac{2}{\Delta t}+a_{i+1},\ C_i = \frac{-2\varepsilon}{h_i(h_i+h_{i+1})},$$
$$D_i = \frac{2\varepsilon}{h_{i+1}(h_i+h_{i+1})},\ \ E_i = \frac{-2\varepsilon}{h_i+h_{i+1}}\left(\frac{2\varepsilon}{h_{i+1}}+\frac{2\varepsilon}{h_i}\right)+\frac{2}{\Delta t}-a_i,\ F_i = \frac{2\varepsilon}{h_i(h_i+h_{i+1})}$$
$$H_{i,j} = \begin{cases} f_i^{j+1}+f_i^j - b_{i+1}\phi_{i-r}^{j+1} - b_i\phi_{i-r}^j,\ i=1,2,...,r,\ j=0,1,2,...,M-1,\\ f_i^{j+1}+f_i^j - b_{i+1}U_{i-r}^{j+1} - b_iU_{i-r}^j,\ i=r+1,...,N-1,\ j=0,1,2,...,M-1.\end{cases}$$

Lemma 5.3.5 *(Discrete maximum principle). Let ϑ_i^{j+1} be a given mesh function satisfying $\vartheta_0^{j+1}\geq 0$ and $\vartheta_N^{j+1}\geq 0$. If $\mathcal{L}_\varepsilon^{N,M}\vartheta_i^{j+1}\geq 0$, $i=1, 2, ..., N-1$, then $\vartheta_i^{j+1}\geq 0$, $i=0, 1, 2, ..., N$.*

Proof. For some $k\in\{0,1,2,...,N\}$, suppose that $\vartheta_k^{j+1} = \min\limits_{i=0(1)N}\vartheta_i^{j+1} < 0$. Then,

$$\begin{aligned}
\mathcal{L}_{\varepsilon,1}^{N,M}\vartheta_k^{j+1} &= -\,\varepsilon D^+D^-\vartheta_k^{j+1} + \left(\frac{2}{\Delta t}+a_k\right)\vartheta_k^{j+1} + b_k\phi_{k-r}^{j+1} < 0,\ k=1,2,...,r,\\
\mathcal{L}_{\varepsilon,2}^{N,M}\vartheta_k^{j+1} &= -\,\varepsilon D^+D^-\vartheta_k^{j+1} + \left(\frac{2}{\Delta t}+a_k\right)\vartheta_k^{j+1} + b_k\vartheta_{k-r}^{j+1}\\
&\leq -\,\varepsilon D^+D^-\vartheta_k^{j+1} + \left(\frac{2}{\Delta t}+a_k+b_k\right)\vartheta_k^{j+1} < 0,\ k=r+1,r+2,...,N-1,
\end{aligned}$$

which is a contradiction to the hypothesis. Hence, the assumption fails, and hence $\vartheta_i^{j+1}\geq 0$, i=0, 1, 2, ..., N. ∎

Lemma 5.3.6 *(Kumari & Kumar, 2020). If U_i^{j+1} is the solution of (5.28), then it can be estimated as*

$$|U_i^{j+1}| \leq \frac{\Delta t\|\pi\|}{1+2\lambda\Delta t} + \max\{|U^{j+1}(0)|,\ |U^{j+1}(1)|\},\ i=0,1,...,N.$$

Proof. Define two barrier functions as

$$\varphi_{i,j+1}^{\pm} = \frac{\Delta t\|\pi\|}{1+2\lambda\Delta t} + \max\{|U^{j+1}(0)|,\ |U^{j+1}(1)|\} \pm U_i^{j+1},$$

for which the following results hold true.

$$\varphi_{0,j+1}^{\pm} = \frac{\Delta t\|\pi\|}{1+2\lambda\Delta t} + \max\{|U^{j+1}(0)|,\ |U^{j+1}(1)| \pm U_0^{j+1}\} \geq \frac{\Delta t\|\pi\|}{1+2\lambda\Delta t} \geq 0$$
$$\varphi_{N,j+1}^{\pm} = \frac{\Delta t\|\pi\|}{1+2\lambda\Delta t} + \max\{|U^{j+1}(0)|,\ |U^{j+1}(1)| \pm U_N^{j+1}\} \geq \frac{\Delta t\|\pi\|}{1+2\lambda\Delta t} \geq 0.$$

Case 1: For $i = 1, 2, ..., r$,

$$\begin{aligned}\mathcal{L}_{\varepsilon,1}^{N,M}\varphi_{i,j+1}^{\pm} &= -\varepsilon D^{+}D^{-}\varphi_{i,j+1}^{\pm} + \left(\frac{2}{\Delta t} + a_i\right)\varphi_{i,j+1}^{\pm}\\ &= \left(\frac{2}{\Delta t} + a_i\right)\left(\frac{\Delta t\|\pi\|}{1+2\lambda\Delta t} + \max\{|U^{j+1}(0)|,\ |U^{j+1}(1)|\}\right) \pm \pi_i^{j+1}\\ &\geq \left(\frac{2}{\Delta t} + a_i\right)\left(\max\{|U^{j+1}(0)|,\ |U^{j+1}(1)|\}\right) \geq 0.\end{aligned}$$

Case 2: For $i = r+1, r+2, ..., N-1$,

$$\begin{aligned}\mathcal{L}_{\varepsilon,2}^{N,M}\varphi_{i,j+1}^{\pm} &= -\varepsilon D^{+}D^{-}\varphi_{i,j+1}^{\pm} + \left(\frac{2}{\Delta t} + a_i\right)\varphi_{i,j+1}^{\pm} + b_i\varphi_{i-r,j+1}^{\pm}\\ &= \left(\frac{2}{\Delta t} + a_i + b_i\right)\left(\frac{\Delta t\|\pi\|}{1+2\lambda\Delta t} + \max\{|U^{j+1}(0)|,\ |U^{j+1}(1)|\}\right) \pm \pi_i^{j+1}\\ &\geq \left(\frac{2}{\Delta t} + a_i + b_i\right)\left(\max\{|U^{j+1}(0)|,\ |U^{j+1}(1)|\}\right) \geq 0.\end{aligned}$$

Applying Lemma 5.3.6, $\varphi_{i,j+1}^{\pm} \geq 0$, $i = 1, 2, ..., N$, which gives the required estimate. ■

Remark 5.3.2 To obtain an improved error estimate, consider the Shishkin decomposition of U_i^{j+1} as $U_i^{j+1} = V_i^{j+1} + W_i^{j+1}$, where V_i^{j+1} is the smooth component satisfying

$$\begin{aligned}&\mathcal{L}_{\varepsilon}^{N,M}V_i^{j+1} = \pi_i^{j+1},\ i = 0, 1, ..., N,\\ &V^{j+1}(0) = u_0(0),\ \ V^{j+1}(1) = u_0(1),\end{aligned}$$

and W_i^{j+1} is the singular component satisfying

$$\begin{aligned}&\mathcal{L}_{\varepsilon}^{N,M}W_i^{j+1} = 0,\ i = 0, 1, ..., N,\\ &W_0^{j+1} = W^{j+1}(0),\ W_1^{j+1} = W^{j+1}(1).\end{aligned}$$

The singular component W_i^{j+1} is further decomposed as $W_i^{j+1} = W_{L,i}^{j+1} + W_{R,i}^{j+1}$, where the left singular layer $W_{L,i}^{j+1}$ and the right singular layer $W_{R,i}^{j+1}$ are defined as

$$\begin{aligned}&\mathcal{L}_{\varepsilon}^{N,M}W_{L,i}^{j+1} = 0,\ \ W_{L,0}^{j+1} = W_L^{j+1}(0),\ W_{L,1}^{j+1} = 0,\\ &\mathcal{L}_{\varepsilon}^{N,M}W_{R,i}^{j+1} = 0,\ \ W_{R,0}^{j+1} = 0,\ W_{R,1}^{j+1} = W_R^{j+1}(1).\end{aligned}$$

Theorem 5.3.1 *Let $U^{j+1}(x_i)$ be the solution of the scheme (5.17) and U_i^{j+1} be the solution of (5.28). Then, the discrete error estimate in the spatial direction is given as*

$$|U^{j+1}(x_i) - U_i^{j+1}| \leq C(N^{-1}\ln N)^2.$$

Proof. It is well known that the nodal truncation error can be written as

$$U^{j+1}(x_i) - U_i^{j+1} = (V^{j+1}(x_i) - V_i^{j+1}) + (W^{j+1}(x_i) - W_i^{j+1}).$$

As a result, one can estimate the solution's errors separately for the smooth and singular components. The classical argument gives

$$\begin{aligned}\left|\mathcal{L}_\varepsilon^{N,M}(V^{j+1}(x_i) - V_i^{j+1})\right| &= \left|\varepsilon\left(\frac{d^2}{dx^2} - D^+D^-\right)V^{j+1}(x_i)\right| \\ &\leq \begin{cases} C\varepsilon[x_{i+1} - x_{i-1}]|V^{j+1}(x_i)|_3, \ x_i \in [\tau, 1-\tau], \\ C\varepsilon[x_{i+1} - x_{i-1}]^2|V^{j+1}(x_i)|_4, \ \text{otherwise}. \end{cases}\end{aligned}$$

For any piece-wise uniform mesh, since $x_{i+1} - x_{i-1} \leq 2N^{-1}$, we have

$$\left|\mathcal{L}_\varepsilon^{N,M}(V^{j+1}(x_i) - V_i^{j+1})\right| = \begin{cases} CN^{-1}\varepsilon^{\frac{-1}{2}}, \ x_i \in [\tau, 1-\tau] \\ CN^{-2}, \ \text{otherwise}. \end{cases}$$

Now, introduce the function $\varphi(x_i)$ as

$$\varphi(x_i) = CN^{-2} + CN^{-2}\tau\varepsilon^{-1/2}\begin{cases} \frac{x_i}{\tau}, \quad x_i \in [0, \tau], \\ 1, \quad x_i \in [\tau, 1-\tau], \\ \frac{1-x_i}{\tau}, \quad x_i \in [1-\tau, 1]. \end{cases}$$

Then, it follows that $\varphi(x_i) \leq CN^{-2}\ln N$ and

$$\left|\mathcal{L}_\varepsilon^{N,M}\varphi(x_i)\right| \geq \begin{cases} CN^{-1}\varepsilon^{\frac{1}{2}} + N^{-2}, \ x_i \in [\tau, 1-\tau], \\ CN^{-2}, \ \text{otherwise}. \end{cases}$$

Applying the discrete maximum principle, $(V_i^{j+1} - V^{j+1}(x_i)) \leq \varphi(x_i)$, which leads to the bound of the smooth component as

$$|V_i^{j+1} - V^{j+1}(x_i)| \leq CN^{-2}\ln N. \tag{5.30}$$

To obtain the error estimate for the singular component, consider the cases when $\tau = \frac{1}{4}$ and $\tau = 2\sqrt{\frac{\varepsilon}{\lambda}}\ln N < \frac{1}{4}$, separately as follows.

Case 1: When $\tau = \frac{1}{4}$, the mesh is uniform and $\frac{1}{4} \leq 2\sqrt{\frac{\varepsilon}{\lambda}}\ln N$. From this, we have $\varepsilon^{-1/2} \leq C\ln N$ and $x_i - x_{i-1} = \frac{1}{N}$. Using the classical argument, we obtain

$$\begin{aligned}|\mathcal{L}_\varepsilon^{N,M}(W_L^{j+1}(x_i) - W_{L,i}^{j+1})| \leq& C(x_{i+1} - x_{i-1})^2\varepsilon|W_L^{j+1}(x_i)|_4 \\ \leq& C(N^{-1}\ln N)^2\end{aligned}$$

Then, applying Lemma 5.3.5 yields

$$|W_L^{j+1}(x_i) - W_{L,i}^{j+1}| \le C(N^{-1}\ln N)^2. \tag{5.31}$$

Case 2: When $\tau < \frac{1}{4}$, it implies a piece-wise uniform mesh. In this case, consider a nonuniform meshes with mesh sizes $\frac{4\tau}{N}$ in the sub-intervals $[0,\tau]\cup[1-\tau,1]$ and $\frac{2(1-2\tau)}{N}$ in the sub-interval $[\tau, 1-\tau]$. In the sub-intervals $[0,\tau]$ and $[1-\tau,1]$, applying the classical argument gives

$$\begin{aligned}|\mathcal{L}_\varepsilon^{N,M}(W_L^{j+1}(x_i) - W_{L,i}^{j+1})| \le & C(x_{i+1}-x_{i-1})^2\varepsilon|W_L^{j+1}(x_i)|_4\\ \le & CN^{-2}\tau^2\varepsilon^{-1}\\ \le & C(N^{-1}\ln N)^2.\end{aligned}$$

Then, applying the discrete maximum principle gives

$$|W_L^{j+1}(x_i) - W_{L,i}^{j+1}| \le C(N^{-1}\ln N)^2. \tag{5.32}$$

For the case of x_i being in the sub-interval $[\tau, 1-\tau]$, the local truncation error satisfies

$$|\mathcal{L}_\varepsilon(W_L^{j+1}(x_i) - W_{L,i}^{j+1})| \le \varepsilon\left|(D^+D^- - \frac{d^2}{dx^2})W_L^{j+1}(x_i)\right|.$$

But, it is known that $|D^+D^-W_L^{j+1}(x_i)| \le \max\limits_{x_i\in[x_{i-1},x_{i+1}]}\left|\frac{d^2W_L^{j+1}}{dx^2}\right|$, and hence

$$\begin{aligned}|\mathcal{L}_\varepsilon(W_L^{j+1}(x_i) - W_{L,i}^{j+1})| \le & 2\varepsilon\max_{x_i\in[x_{i-1},x_{i+1}]}\left|\frac{d^2W_L^{j+1}}{dx^2}\right|\\ \le & Ce^{-\sqrt{\frac{\mu}{\varepsilon}}x_{i-1}} \le Ce^{-\sqrt{\frac{\lambda}{\varepsilon}}(\tau-\frac{4\tau}{N})} \le CN^{-2}.\end{aligned}$$

Thus, the discrete maximum principle gives that

$$|W_L^{j+1}(x_i) - W_{L,i}^{j+1}| \le CN^{-2},\ x_i\in[\tau,1-\tau]. \tag{5.33}$$

Combination of all error estimates in the sub-intervals $[0,\tau]$, $[\tau,1-\tau]$ and $[1-\tau,1]$ gives

$$|W_L^{j+1}(x_i) - W_{L,i}^{j+1}| \le C(N^{-1}\ln N)^2. \tag{5.34}$$

Thus, from (5.30) and (5.34), one can obtain that

$$|U^{j+1}(x_i) - U_i^{j+1}| \le C(N^{-1}\ln N)^2,\ i = 0,1,...,N,$$

which is the required error estimate in the spatial direction. ■

Theorem 5.3.2 *Suppose that $u(x,t)$ is the solution of the continuous problem (5.1) and U_i^{j+1} is the solution of the discrete problem (5.28). Then, the uniform error is estimated as*

$$\sup_{0<\varepsilon\le 1}\|U_i^{j+1} - u(x_i,t_{j+1})\| \le C((\Delta t)^2 + (N^{-1}\ln N)^2).$$

Proof. Combining Lemma 5.3.3 and Theorem 5.3.1, the uniform error estimate is implied. ■

5.4 Numerical results and discussions

In this section the numerical scheme presented in this chapter and its uniform convergence analyses are validated by solving numerical examples. The examples are taken, which satisfy all the basic assumption considered for the continuous solution, and treated by computing the maximum absolute errors and corresponding convergence rate using the double mesh principles given in (4.44)-(4.47).

Example 5.4.1 *Consider the problem with variable coefficients as* $u_t - \varepsilon u_{xx} + (x+6)u(x,t) - (x^2+1)u(x-\delta,t) = 3$, $u_0(x) = 0$, $x \in \bar{\Gamma}$, $u(x,t) = 0$, $(x,t) \in \Omega^-$, $u(1,t) = 0$, $(1,t) \in \Omega^+$.

Example 5.4.2 *Consider the problem with constant variable coefficient as* $u_t - \varepsilon u_{xx} + 5u(x,t) - 2u(x-\delta,t) = 2$, $u_0(x) = \sin(\pi x)$, $x \in \bar{\Gamma}$, $u(x,t) = 0$, $(x,t) \in \Omega^-$, $u(1,t) = 0$, $(1,t) \in \Omega^+$.

Example 5.4.3 *Consider the problem with negative source function as* $u_t - \varepsilon u_{xx} + 3u(x,t) - u(x-\delta,t) = -1$, $u_0(x) = 0$, $x \in \bar{\Gamma}$, $u(x,t) = 0$, $(x,t) \in \Omega^-$, $u(1,t) = 0$, $(1,t) \in \Omega^+$.

The examples are treated applying the developed numerical scheme in this chapter. Since the exact solutions are not given, the double mesh principle is used to compute the maximum absolute error and corresponding convergence rate. The uniform convergence result is shown by computing the maximum absolute error and rate of convergence as given in Tables 5.1-5.3 for each example, respectively. From the tables, one can visualize that for a given ε, increasing both time and space mesh numbers, decreases the absolute point-wise error. On the other hand, for the mesh numbers, minimizing the perturbation parameter yields stable and uniform point-wise error after certain decrements of ε. This shows the ε-uniform convergence of the proposed numerical schemes.

The numerical solution of the examples are simulated graphically for various values of the perturbation parameter and the shift argument. In Figure 5.1, the effect of the negative shift (δ) is shown for Examples 5.4.1 and 5.4.3. Figure 5.2 shows the effect of ε in layer formation. Surface plots are simulated in Figures 5.3-5.6 to show the physical behaviors of the solutions. In Figures 5.1, 5.3 and 5.5, the effect of the delay on the solution is simulated. That is, by increasing the value of the negative shift parameter, weak interior layers are observed. In Figures 5.2, 5.4 and 5.6, the effect of the perturbation parameter is simulated. This means that if the values of ε is decreasing, then the width of the boundary layers are become narrow. The uniform convergence of the proposed method is shown by plotting log-log figures as given in Figure 5.7. From the log-log plots, it is visualized that increasing the mesh number decreases the maximum absolute errors, and decreasing the value of ε yields stable and uniform convergence.

Table 5.1: Maximum absolute errors and convergence rates of Example 5.4.1 for $\delta = 0.1$.

ε | N $\rightarrow$	40	80	160	320	640
$\downarrow$ | M $\rightarrow$	20	80	320	1280	5120
2^{-2}	8.0154e-03	1.9720e-03	4.9155e-04	1.2279e-04	3.0692e-05
	2.0231	2.0043	2.0012	2.0003	
2^{-4}	8.5644e-03	2.0781e-03	5.1586e-04	1.2874e-04	3.0712e-05
	2.0431	2.0102	2.0025	2.0676	
2^{-6}	3.4637e-03	7.0284e-04	1.6624e-04	4.0983e-05	9.8612e-06
	2.3011	2.0799	2.0202	2.0552	
2^{-8}	6.8511e-03	1.6291e-03	3.6702e-04	9.2345e-05	2.3452e-05
	2.0723	2.1501	1.9908	1.9773	
2^{-10}	1.4758e-02	6.7123e-03	1.6299-03	4.1544e-04	9.9845e-05
	1.1366	2.0420	1.9721	2.0569	
2^{-12}	1.4976e-02	7.9105e-03	2.7148e-03	8.6331e-04	2.2316e-04
	0.9208	1.5429	1.6529	1.9518	
2^{-14}	1.5082e-02	7.9698e-03	2.7344e-03	8.6390e-04	2.4532e-04
	0.9202	1.5433	1.6623	1.8162	
2^{-16}	1.5133e-02	7.9992e-03	2.7439e-03	8.6421e-04	2.4162e-04
	0.9198	1.5436	1.6668	1.8386	
2^{-18}	1.5159e-02	8.0138e-03	2.7486e-03	8.6438e-04	2.4181e-04
	0.9196	1.5438	1.6690	1.8378	
2^{-20}	1.5172e-02	8.0211e-03	2.7510e-03	8.6446e-04	2.4192e-04
	0.9195	1.5438	1.6701	1.8371	
2^{-22}	1.5178e-02	8.0248e-03	2.7522e-03	8.6450e-04	2.5174e-04
	0.9194	1.5439	2.0502	1.7799	
2^{-24}	1.5181e-02	8.0266e-03	2.7528e-03	8.6452e-04	2.6210e-04
	0.9194	1.5439	2.0505	1.7218	
2^{-26}	1.5183e-02	8.0275e-03	2.7530e-03	8.6453e-04	2.6828e-04
	0.9194	1.5439	2.0506	1.1.6882	
2^{-28}	1.5184e-02	8.0280e-03	2.7532e-03	8.6453e-04	2.7320e-04
	0.9194	1.5439	2.0507	1.6620	
$e^{N,M}$	1.5263e-02	7.8572e-03	2.7820e-03	8.6877e-04	2.7195e-04
$r^{N,M}$	0.9580	1.4979	1.6791	1.6756	

Table 5.2: Maximum absolute errors and convergence rates of Example 5.4.2 for $\delta = 0.1$.

ε $\|N \rightarrow$	40	80	160	320	640
$\downarrow$ $\|M \rightarrow$	20	80	320	1280	5120
2^{-2}	6.9631e-03	1.7230e-03	4.2913e-04	1.0717e-04	2.6785e-05
	2.0148	2.0054	2.0015	2.0004	
2^{-4}	7.3952e-03	1.8107e-03	4.5003e-04	1.1234e-04	2.7568e-05
	2.0300	2.0085	2.0022	2.0268	
2^{-6}	2.7981e-03	6.0170e-04	1.4438e-04	3.5722e-05	8.5887e-06
	2.2173	2.0592	2.0150	2.0563	
2^{-8}	5.6017e-03	1.2552e-03	3.2086e-04	8.0622e-05	2.1102e-05
	2.1580	1.9679	1.9927	1.9338	
2^{-10}	1.4354e-02	5.5957e-03	1.4293e-03	3.6312e-04	8.9654e-05
	1.3591	1.9690	1.9768	2.0180	
2^{-12}	1.4232e-02	6.6265e-03	2.1128e-03	6.0819e-04	1.6578e-04
	1.1028	1.6491	1.7966	1.8753	
2^{-14}	1.4165e-02	6.6060e-03	2.0686e-03	6.4561e-04	1.6578e-04
	1.1005	1.6751	1.6799	1.9273	
2^{-16}	1.4130e-02	6.5952e-03	2.0656e-03	6.1392e-04	1.7023e-04
	1.0993	1.6749	1.7504	1.8504	
2^{-18}	1.4113e-02	6.5897e-03	2.0640e-03	5.9802e-04	1.7240e-04
	1.0987	1.6748	1.7872	1.7944	
2^{-20}	1.4104-02	6.5869e-03	2.0632e-03	5.9007e-04	1.7530e-04
	1.0984	1.6747	1.8059	1.7511	
2^{-22}	1.4100e-02	6.5855e-03	2.0628e-03	5.8610e-04	1.7820e-04
	1.0983	1.6748	1.8154	1.7176	
2^{-24}	1.4097e-02	6.5848e-03	2.0625e-03	5.8411e-04	1.8115e-04
	1.0981	1.6747	1.8202	1.6891	
2^{-26}	1.4096e-02	6.5845e-03	2.0626e-03	5.8312e-04	1.8295e-04
	1.0981	1.6747	1.8225	1.6723	
2^{-28}	1.4096e-02	6.5843e-03	2.0625e-03	5.8263e-04	1.8299e-04
	1.0981	1.6747	1.8137	1.6700	
$e^{N,M}$	1.4354e-02	6.5897e-03	2.1128e-03	6.4561e-04	1.8302e-04
$r^{N,M}$	1.1232	1.6411	1.7104	1.8187	

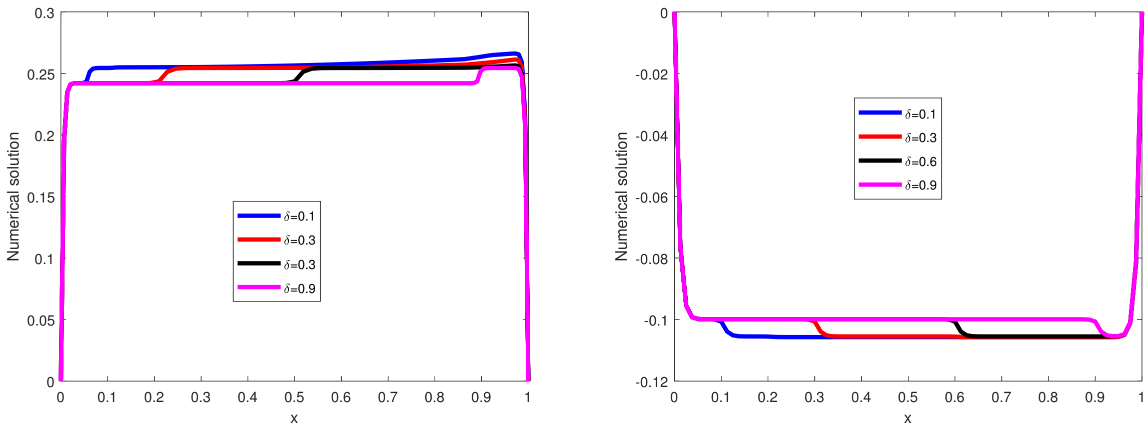

(a) (b)

Figure 5.1: Effect of the negative shift on the solution for (a) Example 5.4.1 and (b) Example 5.4.3 for $\varepsilon = 2^{-10}$.

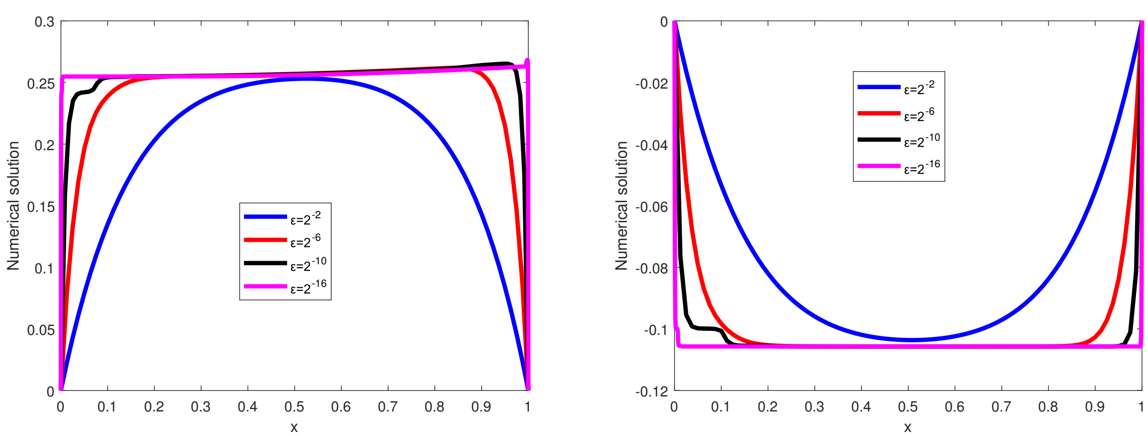

(a) (b)

Figure 5.2: Effect of the perturbation parameter in resolving the boundary layers for (a) Example 5.4.1 and (b) Example 5.4.3 for $\delta = 0.1$.

Table 5.3: Maximum absolute error and convergence rates of Example 5.4.3 for $\delta = 0.1$.

ε $\lvert N \rightarrow$	40	80	160	320	640
$\downarrow$ $\lvert M \rightarrow$	20	80	320	1280	5120
2^{-2}	2.6321e-03	6.5541e-04	1.6373e-04	4.0924e-04	1.0230e-05
	2.0057	2.0011	2.0003	2.0001	
2^{-4}	2.7754e-03	6.8827e-04	1.7168e-04	4.2897e-05	1.1523e-05
	2.0116	2.0033	2.0008	1.8964	
2^{-6}	9.6754e-04	2.2359e-04	5.4764e-05	1.3621-05	3.4215e-06
	2.1135	2.0296	2.0074	1.9931	
2^{-8}	2.3428e-03	4.9001e-04	1.2319e-04	3.0834e-05	8.1623e-06
	2.2573	1.9919	1.9983	1.9175	
2^{-10}	7.3242e-03	2.3684e-03	5.5378e-04	1.3918e-04	3.4213e-05
	1.6288	2.0965	1.9924	2.0243	
2^{-12}	7.3242e-03	2.8810e-03	8.9276e-04	2.9058e-04	9.1453e-04
	1.3461	1.6902	1.6183	1.6678	
2^{-14}	7.3242e-03	2.8810e-03	8.9276e-04	2.9058e-04	9.1427e-04
	1.3461	1.6902	1.6183	1.6682	
2^{-16}	7.3242e-03	2.8810e-03	8.9276e-04	2.9058e-04	9.1423e-04
	1.3461	1.6902	1.6183	1.6683	
2^{-18}	7.3242e-03	2.8810e-03	8.9276e-04	2.9058e-04	9.1419e-04
	1.3461	1.6902	1.6183	1.6684	
2^{-20}	7.3242e-03	2.8810e-03	8.9276e-04	2.9058e-04	9.1419e-04
	1.3461	1.6902	1.6183	1.6684	
2^{-22}	7.3242e-03	2.8810e-03	8.9276e-04	2.9058e-04	9.1419e-04
	1.3461	1.6902	1.6183	1.6684	
2^{-24}	7.3242e-03	2.8810e-03	8.9276e-04	2.9058e-04	9.1419e-04
	1.3461	1.6902	1.6183	1.6684	
2^{-26}	7.3242e-03	2.8810e-03	8.9276e-04	2.9058e-04	9.1419e-04
	1.3461	1.6902	1.6183	1.6684	
2^{-28}	7.3242e-03	2.8810e-03	8.9276e-04	2.9058e-04	9.1419e-04
	1.3461	1.6902	1.6183	1.6684	
$e^{N,M}$	7.3242e-03	2.8810e-03	8.9276e-04	2.9058e-04	9.1453e-04
$r^{N,M}$	1.3461	1.6902	1.6193	1.6678	

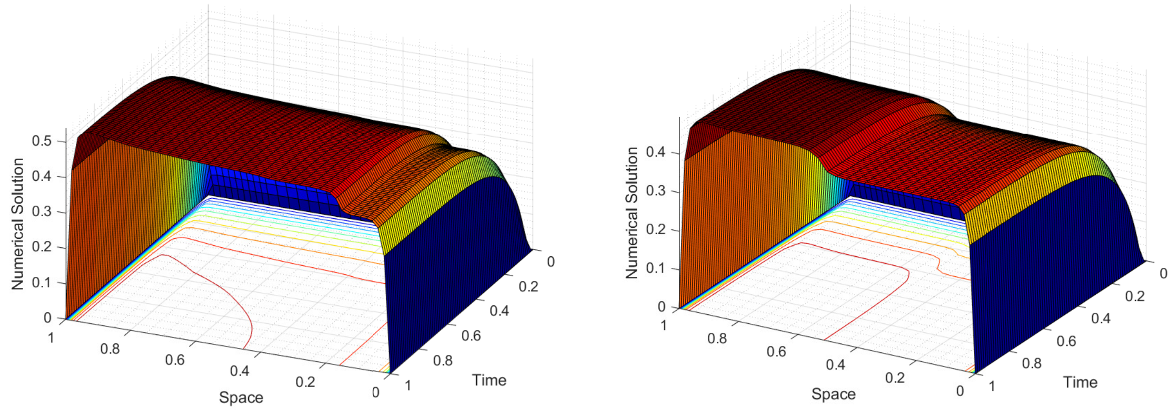

(a) $\delta = 0.2$ (b) $\delta = 0.5$

Figure 5.3: Effect of δ on the surface plots of the solution for Example 5.4.1 taking $\varepsilon = 2^{-10}$.

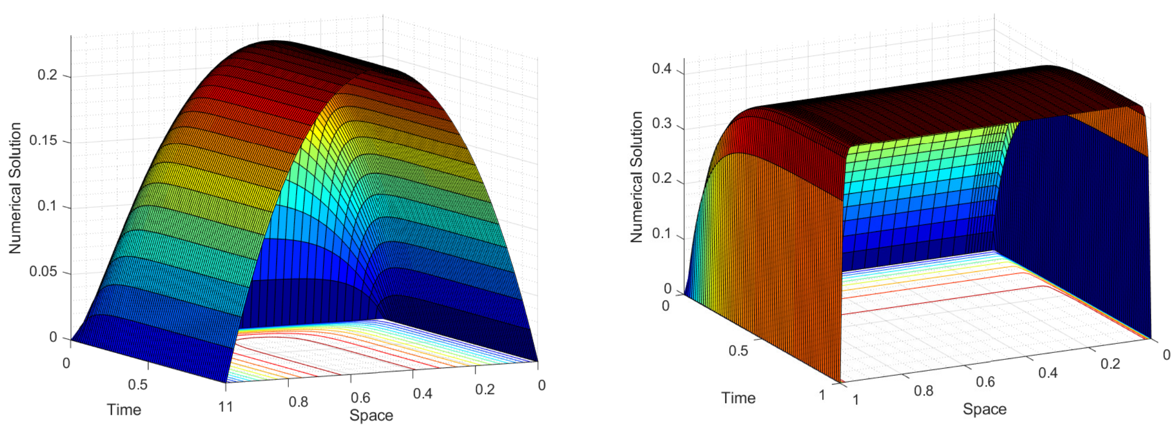

(a) $\varepsilon = 2^{0}$ (b) $\varepsilon = 2^{-12}$

Figure 5.4: Effect of ε on the surface plots of the solution for Example 5.4.1 taking $\delta = 0.1$.

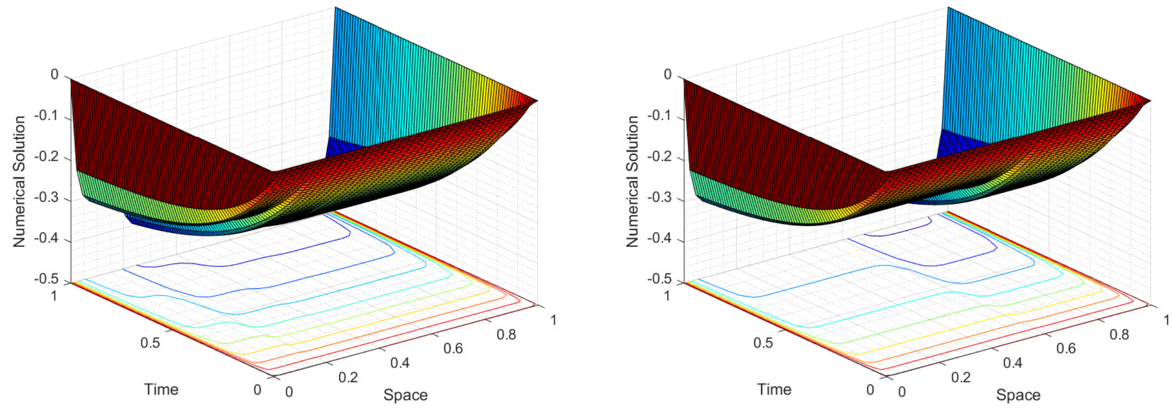

(a) $\delta = 0.2$ (b) $\delta = 0.5$

Figure 5.5: Effect of δ on the surface plots of the solution for Example 5.4.3 taking $\varepsilon = 2^{-12}$.

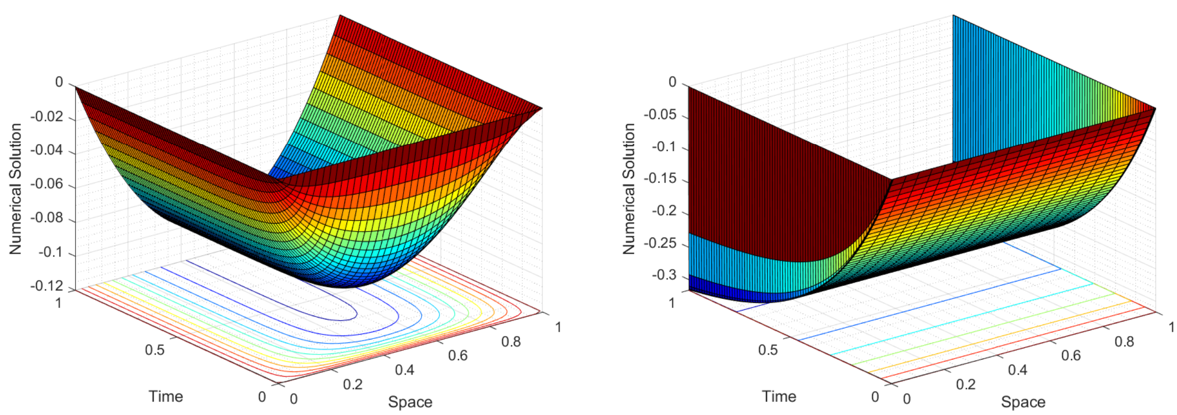

(a) $\varepsilon = 2^0$ (b) $\varepsilon = 2^{-12}$

Figure 5.6: Effect of ε on the surface plots of the solution for Example 5.4.3 taking $\delta = 0.1$.

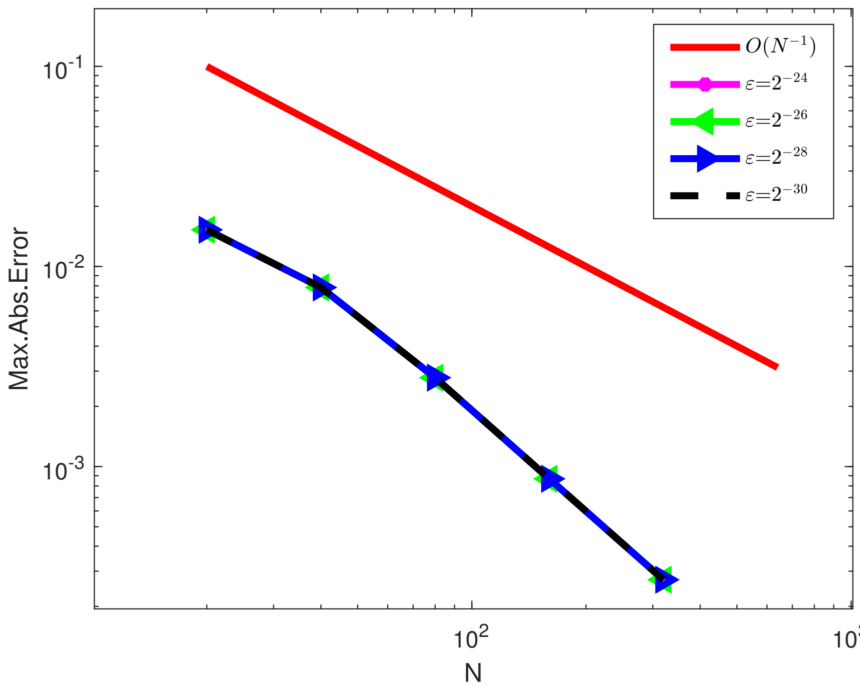

(a)

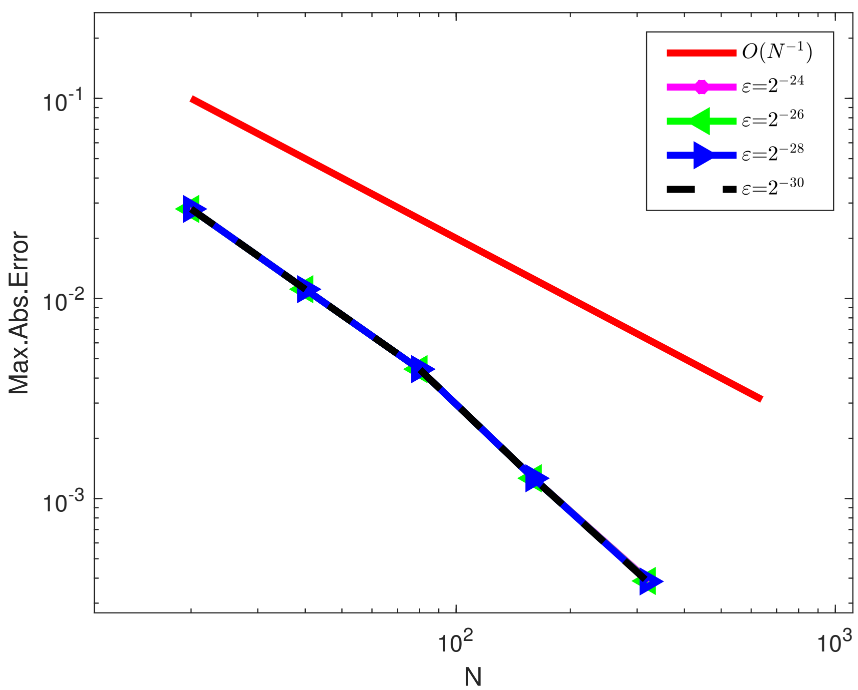

(b)

Figure 5.7: Log-log plots of maximum absolute errors versus N for (a) Example 5.4.1 and (b) Example 5.4.3

.

5.5 Summary

This chapter focuses on formulating and analyzing a convergent numerical method for a singularly perturbed differential equation involving negative shift in the reaction term. To solve the problem, a fitted mesh numerical scheme is formulated on uniform temporal meshes and piecewise uniform spatial meshes. The influence of the negative shift is handled by choosing a special mesh, so that the terms containing the shift lie on the mesh points. The stability estimate is established and its convergence analysis is investigated, which proves that the method is uniformly convergent. Three numerical experiments are solved to test the validity and applicability of the proposed scheme. The solutions of the examples are simulated graphically and the maximum absolute error and order of convergence are computed and given in tabular forms. The effects of the shift and perturbation parameters are also simulated graphically. The convergence analysis of the proposed numerical scheme is shown that the method is uniformly convergent of order two in time and almost of order two in space. Thus, the main results achieved in this chapter can be summarized as follow.

1. A parameter independent fitted mesh numerical scheme is formulated, which is convergent of order two in time and nearly order two in space.
2. Due to ε boundary layers are exhibited in the solution and the negative shift caused extra weak interior layer.
3. Decreasing the value of ε yields stable and uniform maximum absolute error.
4. Increasing the mesh numbers decreases the maximum absolute error.

CHAPTER SIX

A UNIFORMLY CONVERGENT FITTED MESH METHOD FOR SINGULARLY PERTURBED PARTIAL DIFFERENTIAL EQUATIONS WITH LARGE NEGATIVE SHIFT

In this chapter, a time-dependent singularly perturbed partial differential equations involving large delay in the spatial variable is treated. Such types of equations are observed in the modeling of various phenomena, widely in the mathematical modeling of neuronal variability. The effect of the perturbation parameter and the shift term makes it difficult to find the exact solution of the problem. Here, the problem is solved by formulating a fitted mesh finite difference scheme, which yields accurate and uniformly convergent results.

6.1 The governing problem

Consider a time dependent singularly perturbed problem on $\Omega = \Gamma \times \Lambda = (0,2) \times (0,T]$ and $\partial\Omega = \{(x,0) \cup (0,t) \cup (2,t) : x \in \bar{\Gamma} = [0,2], t \in \bar{\Lambda} = [0,T]\}$ for a finite time T as

$$\mathcal{L}_\varepsilon u(x,t) = u_t(x,t) - \varepsilon u_{xx}(x,t) + a(x)u(x,t) + b(x)u(x-1,\ t) = f(x,t), \tag{6.1}$$

subjected to the initial condition and boundary conditions

$$\begin{aligned} &u(x,0) = u_0(x),\ x \in \bar{\Gamma},\\ &u(x,t) = \phi(x,t),\ (x,t) \in \Omega^-,\\ &u(2,t) = \alpha(t),\ (2,t) \in \Omega^+, \end{aligned}$$

where $\Omega^- = \{(x,t) : x \in [-1,0],\ t \in \bar{\Lambda}\}$, $\Omega^+ = \{(2,t) : t \in \bar{\Lambda}\}$ and $0 < \varepsilon \ll 1$.

It is assumed that the functions involved in the continuous problem are all smooth enough and moreover, for arbitrary positive number λ, the functions $a(x)$ and $b(x)$ satisfy the conditions

$$a(x) + b(x) \geq 2\lambda > 0,\ \ b(x) < 0, \quad x \in \bar{\Gamma}. \tag{6.2}$$

Considering the interval boundary conditions, (6.1) can be written as

$$\mathcal{L}_\varepsilon u(x,t) = \begin{cases} u_t(x,t) - \varepsilon u_{xx}(x,t) + a(x)u(x,t) = f(x,t) - b(x)\phi(x-1,\ t),\ (x,t) \in (0,1] \times \Gamma, \\ u_t(x,t) - \varepsilon u_{xx}(x,t) + a(x)u(x,t) + b(x)u(x-1,\ t) = f(x,t),\ (x,t) \in (1,2) \times \Gamma \end{cases} \tag{6.3}$$

with $u(x,0) = u_0(x)$ for $x \in \bar{\Gamma}$, $u(x,t) = \phi(x,t)$ for $(x,t) \in \Omega^-$, $u(2,t) = \alpha(t)$ for $t \in \bar{\Lambda}$, $u(1^-,\ t) = u(1^+,\ t)$ and $u_x(1^-,\ t) = u_x(1^+,\ t)$.
Letting $\varepsilon = 0$, the reduced form of equation (6.3) is given as

$$\mathcal{L}_0 u(x,t) = \begin{cases} (u_0)_t + a(x)u_0(x,t) = f(x) - b(x)\phi(x-1,\ t),\ (x,t) \in (0,1] \times \Gamma, \\ (u_0)_t + a(x)u_0(x,t) + b(x)u_0(x-1,\ t) = f(x),\ (x,t) \in (1,2) \times \Gamma. \end{cases}$$

From the reduced problem, it can be observed that $u_0(x,t)$ does not necessarily satisfy $u_0(0,t) = \phi(0,t)$ and $u_0(2,t) = \alpha(t)$. Hence, the solution involves boundary layers at the end of the domain. At $x = 1$, since $u_0(1^-,t) = \frac{f(1,t)-b(1)\phi(0^-,t)-(u_0)_t(1,t)}{a(1)}$ and $u_0(1^+,t) = \frac{f(1,t)-b(1)u_0(0^+,t)-(u_0)_t(1,t)}{a(1)}$, it is not necessary that $u_0(1^-,t)$ is equal to $u_0(1^+,t)$. Hence, at $x = 1$ the solution involves interior layer. For more information, refer (Manikandan et al., 2014; Kumari & Kumar, 2020). For the guarantee of existence and uniqueness of the solution, compatibility condition is imposed at the corner points as

$$\begin{aligned} &u_0(0,0) = \phi(0,0),\ \ u_0(2,0) = \zeta(0), \\ &\phi_t(0,0) - \varepsilon(u_0)_{xx}(0,0) + a(0)u_0(0,0) + b(0)\phi(-1,0) = f(0,0), \\ &\alpha_t(2,0) - \varepsilon(u_0)_{xx}(2,0) + a(2)u_0(2,0) + b(2)u_0(1,0) = f(2,0). \end{aligned}$$

With the aforementioned conditions and assumptions, the solution of the continuous problem (6.1) can be determined in the given domain. Thus, for $(x,t) \in \bar{\Omega}$, there exist C independent of ε, such that $|u(x,t) - u_0(x)| \le Ct$ (Roos et al., 2008).

6.2 Properties of the continuous solution

In this section, the stability and bound of the continuous solution and its derivatives are discussed, which are important in the analysis of the discrete scheme (Majumdar & Natesan, 2019).

Lemma 6.2.1 *Let ψ be a given sufficiently smooth function on $\bar{\Omega}$. If $\psi(x,t) \ge 0$, $(x,t) \in \partial\Omega$ and $\mathcal{L}_\varepsilon\psi(x,t) \ge 0$, $(x,t) \in \Omega$, then $\psi(x,t) \ge 0$, $(x,t) \in \bar{\Omega}$.*

Proof. Let $(\hat{x},\hat{t}) \in \bar{\Omega}$ be given and assume that $\psi(\hat{x},\hat{t}) = \min_{\bar{\Omega}}\psi(x,t) < 0$. From the hypothesis, $(\hat{x},\hat{t}) \notin \partial\Omega$ and from the derivative tests, $\psi_x(\hat{x},\hat{t}) = 0$ and $\psi_{xx}(\hat{x},\hat{t}) > 0$.
Case 1: On $(0,1]$ by (6.3), $\mathcal{L}_\varepsilon\psi(\hat{x},\hat{t}) = u_t - \varepsilon\psi_{xx} + a(\hat{x})\psi(\hat{x},\hat{t}) <\ 0$.

Case 2: On $(1,2)$ by (6.3), $\mathcal{L}_\varepsilon\psi(\hat{x},\hat{t}) = u_t - \varepsilon\psi_{xx} + a(\hat{x})\psi(\hat{x},\hat{t}) + b(\hat{x})\psi(\hat{x}-1,\hat{t}) \le -\varepsilon\psi_{xx}(\hat{x},\hat{t}) + 2\beta\psi(\hat{x},\hat{t}) < 0$.
The two cases show that $\mathcal{L}_\varepsilon\psi(\hat{x},\hat{t}) < 0$, which contradicts the given hypothesis, so that the assumption fails. As a result, $\psi(\hat{x},\hat{t}) \ge 0$, which gives $\psi(x,t) \ge 0$, $(x,t) \in \bar{\Omega}$. ■

Lemma 6.2.2 *(Swaminathan et al., 2016). Let $u(x,t)$ be the solution of (6.1). Then, it is estimated as*

$$|u(x,t)| \le \max\left\{\|u\|_{\partial\Omega}, \frac{1}{2\lambda}\|\mathcal{L}_\varepsilon u\|\right\},$$

where $\|u\|_{\partial\Omega} = \{|u(x,0)|, |u(0,t)|, |u(2,t)|\}$.

Proof. Define barrier functions as $\omega^{\pm}(x,t) = \max\left\{\|u\|_{\partial\Omega}, \frac{1}{2\lambda}\|\mathcal{L}_\varepsilon u\|\right\} \pm u(x,t)$, which gives

$$\omega^{\pm}(x,0) = \max\left\{\|u\|_{\partial\Omega}, \frac{1}{2\lambda}\|\mathcal{L}_\varepsilon u\|\right\} \pm u(x,0) \ge 0,$$
$$\omega^{\pm}(0,t) = \max\left\{\|u\|_{\partial\Omega}, \frac{1}{2\lambda}\|\mathcal{L}_\varepsilon u\|\right\} \pm u(0,t) \ge 0,$$
$$\omega^{\pm}(2,t) = \max\left\{\|u\|_{\partial\Omega}, \frac{1}{2\lambda}\|\mathcal{L}_\varepsilon u\|\right\} \pm u(2,t) \ge 0.$$

For $x \in (0,1]$,

$$\mathcal{L}_\varepsilon\omega^{\pm}(x,t) = \omega_t^{\pm} - \varepsilon\omega_{xx}^{\pm} + a(x)\omega^{\pm}(x,t) \ge a(x)\max\left\{\|u\|_{\partial\Omega}, \frac{1}{2\lambda}\|f\|\right\} \pm f(x) \ge 0.$$

For $x \in (1,2)$,

$$\begin{aligned}\mathcal{L}_\varepsilon\omega^{\pm}(x,t) =& \omega_t^{\pm} - \varepsilon\omega_{xx}^{\pm} + a(x)\omega^{\pm}(x,t) + b(x)\omega^{\pm}(x-1,t)\\ \ge& 2\beta\max\left\{\|u\|_{\partial\Omega}, \frac{1}{2\lambda}\|f\|\right\} \pm f(x) \ge 0.\end{aligned}$$

Applying Lemma 6.3.1 gives $\omega^{\pm}(x,t) \ge 0$, $(x,t) \in \bar{\Omega}$, which gives the stability estimate. ■

Lemma 6.2.3 *(Swaminathan et al., 2016) For $(x,t) \in \bar{\Omega}$, the derivatives of the solution of equation (6.1) can be estimated as*

$$\left|\frac{\partial^m u(x,t)}{\partial t^m}\right| \le C\left(\|u\|_{\partial\Omega} + \|f\| + \|f_t\| + \|f_{tt}\|\right), \quad m = 0,1,2, \tag{6.4}$$
$$\left|\frac{\partial^m u(x,t)}{\partial x^m}\right| \le C\varepsilon^{\frac{-m}{2}}\left(\|u\|_{\partial\Omega} + \|f\| + \|f_t\|\right), \quad m = 1,2, \tag{6.5}$$
$$\left|\frac{\partial^m u(x,t)}{\partial x^{m-1}\partial t}\right| \le C\varepsilon^{\frac{1-m}{2}}\left(\|u\|_{\partial\Omega} + \|f\| + \|f_t\| + \|f_{tt}\|\right), \quad m = 2,3,4. \tag{6.6}$$

Proof. In (6.4) for $m=0$, $|u(x,t)|\leq C$, which implies Lemma 6.3.2. For $m=1$, rearranging (6.1) gives

$$u_t(x,t)=\varepsilon u_{xx}(x,t)-a(x)u(x,t)-b(x)u(x-1,t)+f(x). \tag{6.7}$$

As described by Kadalbajoo & Awasthi (2011), assume that all of the data considered in (6.1) are zero, which implies that $u(x,0)=u_0=0$, $u(x,t)=\phi(x,t)=0$, $u(2,t)=\alpha(t)=0$. Thus, (6.7) becomes

$$u_t(x,t)=\varepsilon u_{xx}(x,t)-a(x)u(x,0)-b(x)u(x-1,0)+f(x). \tag{6.8}$$

For $(x,t)\in\Omega^-$, $u(x-1,0)=\phi(x-1,0)=0$ and for $(x,t)\in\Omega^+$, $u(x-1,0)=\alpha(0)=0$. Hence, (6.7) can be reduced to $u_t(x,0)=f(x)$, so that the smooth function f yields $|u(x,0)|\leq C$, $x\in\partial\Gamma$, which gives

$$|u_t(x,t)|\leq C\left(\|u\|_{\partial\Omega}+\|f\|+\|f_t\|\right)\quad \text{on } \bar{\Omega}. \tag{6.9}$$

Similarly, for $m=2$, assuming that the initial and boundary values considered in (6.1) are identically zero and differentiating with respect to t gives $u_{tt}-\varepsilon u_{xxt}+a(x)u_t(x,t)+b(x)u_t(x-1,t)=f_t(x)$ and along $t=0$, it becomes

$$u_{tt}(x,0)-\varepsilon u_{xxt}(x,0)+a(x)u_t(x,0)+b(x)u_t(x-1,0)=f_t(x). \tag{6.10}$$

Since $u_{xxt}(x,0)=f_{xx}(x)$ and $u_t(x-1,0)=0$, (6.10) becomes $u_{tt}(x,0)=\varepsilon f_{xx}(x)-a(x)f(x)+f_t(x)$, which implies that $|u_{tt}(x,0)|\leq C$ on $\partial\Omega$ as f is smooth function. Hence,

$$|u_{tt}(x,t)|\leq C\left(\|u\|_{\partial\Omega}+\|f\|+\|f_t\|+\|f_{tt}\|\right)\ \text{ on } \bar{\Omega}.$$

Analogously, the bound of the derivatives of the solution in the spatial variable is obtained easily. That is, for $m=0$, we obtain the stability estimate as in Lemma 6.3.2. For $m=1$, let $x\in\Gamma$ and consider a neighborhood $I=(q,q+\sqrt{\varepsilon})$, $\forall x\in I$. Then, applying the mean value theorem for some $y\in\bar{I}$ and fixed $t\in(0,T]$ gives

$$|u_x(y,t)|=\sqrt{\varepsilon}|u(q+\sqrt{\varepsilon},t)-u(q,t)\sqrt{\varepsilon}|\leq C\varepsilon^{\frac{-1}{2}}\|u\|. \tag{6.11}$$

Now, for any x in $\bar{I}$,

$$\begin{aligned}|u_x(x,t)|=&|u_x(y,t)+\varepsilon^{-1}\int_y^x (u_t(s,t)+a(s)u(s,t)+b(s)u(s-1,t)-f(s))ds|\\ \leq&|u_x(y,t)|+C\varepsilon^{-1}\left(\|u\|_{\partial\Omega}+\|f\|+\|f_t\|\right).\end{aligned}$$

Using (6.11), we can get $|u_x(x,t)| \leq C\varepsilon^{\frac{-1}{2}}\left(\|u\|_{\partial\Omega} + \|f\| + \|f_t\|\right)$. Rearranging the terms in (6.1), we ge $u_{xx}(x,t) = \varepsilon^{-1}\left(u_t + a(x)u(x,t) + b(x)u(x-1,t) - f(x)\right)$. From this result and (6.9), it is possible to write the bound of $u_{xx}(x,t)$ as

$$|u_{xx}(x,t)| \leq C\varepsilon^{-1}\left(\|u\|_{\partial\Omega} + \|f\| + \|f_t\|\right).$$

Similar procedure gives the estimation in (6.6). ■

6.3 The numerical method

In this section, a numerical scheme for the model problem (6.1) is formulated in two stages of discretization, first for the time variable, and then for the spatial variable to obtain a discrete finite difference scheme.

6.3.1 Temporal discretization

For M denoting the number of meshes on $[0,T]$, define a uniform mesh Ω_t^M as $\Omega_t^M = \{t_j = j\Delta t,\ j+1 = 1,2,...,M,\ \Delta t = \frac{T}{M}\}$. Applying the θ-method yields a θ-dependent semidiscrete scheme. For$\theta = 0$, the method yields an explicit scheme, which may not stable. For $\theta = 1/2$, the method become the Crank-Nicolson difference scheme and for $\theta = 1$, it yields an implicit finite difference scheme. In general, the θ-method is numerically stable for $\theta \in [1/2, 1]$ (Woldaregay & Duressa, 2021). Thus, on Ω_t^M, (6.1) is semi-discretized using the θ-method as

$$\begin{aligned}\frac{U^{j+1}(x) - U^{j+1}(x)}{\Delta t} &- \varepsilon\theta U_{xx}^{j+1}(x) - \varepsilon(1-\theta)U_{xx}^{j}(x) + \theta a(x)U^{j+1}(x) + (1-\theta)a(x)U^{j}(x)\\ &+\theta b(x)U^{j+1}(x-1) + (1-\theta)b(x)U^{j}(x-1) = \theta f^{j+1} + (1-\theta)f^{j}(x).\end{aligned}$$

On rearrangement and simplification, it becomes

$$\left(1 + \Delta t\theta\mathcal{L}_\varepsilon^M\right)U^{j+1}(x) = g^{j+1}(x), \tag{6.12}$$

where

$$\left(1 + \Delta t\theta\mathcal{L}_\varepsilon^M\right)U^{j+1}(x) = \begin{cases} -\varepsilon\Delta t\theta U_{xx}^{j+1}(x) + [1 + \theta\Delta t a(x)]U^{j+1}(x), & x \in (0,1],\\ -\varepsilon\Delta t\theta U_{xx}^{j+1}(x) + [1 + \theta\Delta t a(x)]U^{j+1}(x) \\ +\theta\Delta t b(x)U^{j+1}(x-1), & x \in (1,2)\end{cases}$$

and

$$g^{j+1}(x) = \begin{cases} \varepsilon\Delta t(1-\theta)U_{xx}^{j}(x) - [-1 + (1-\theta)\Delta t a(x)]U^{j}(x) + \theta\Delta t f^{j+1}(x) \\ -\theta\Delta t b(x)\phi^{j+1}(x-1) - (1-\theta)\Delta t[b(x)\phi^{j}(x-1) - f^{j}(x)], x \in (0,1],\\ \varepsilon\Delta t(1-\theta)U_{xx}^{j}(x) - [-1 + (1-\theta)\Delta t a(x)]U^{j}(x) + \theta\Delta t f^{j+1}(x) \\ -\theta\Delta t b(x)U^{j}(x-1) + (1-\theta)\Delta t f^{j}(x),\ x \in (1,2)\end{cases}$$

subject to $U^0(x) = u_0(x),\ x \in \bar{\Gamma}$, $U^{j+1}(x) = \phi(x, t_{j+1}),\ x \in [-1, 0],\ j = 0, 1, 2, ..., M-1$ and $U^{j+1}(2, t_{j+1}) = \alpha(t_{j+1}),\ j = 0, 1, 2, ..., M-1$.

Lemma 6.3.1 *(Semi-discrete maximum principle). Let the mesh function $\varphi^{j+1}(x)$, $j = 0, 1, 2, ..., M-1$ satisfies $\varphi^{j+1}(x) \geq 0,\ x \in \partial\Gamma$ and $(1 + \Delta t\theta\mathcal{L}^M_{\varepsilon,x})\varphi^{j+1}(x) \geq 0,\ x \in \Gamma$. Then $\varphi^{j+1}(x) \geq 0$, $x \in \bar{\Gamma}$.*

Proof. For some $\hat{x} \in \Gamma$, assume that $\varphi^{j+1}(\hat{x}) = \min_{x\in\bar{\Gamma}}\varphi^{j+1}(x) < 0$. Then, by the extreme value properties, $\varphi^{j+1}_x(\hat{x}) = 0$ and $\varphi^{j+1}_{xx}(\hat{x}) \geq 0$, and from the given hypothesis, $\hat{x} \notin \{0, 2\}$.
Case 1: For $\hat{x} \in (0, 1]$,

$$(1 + \Delta t\theta\mathcal{L}^M_{\varepsilon,1})\varphi^{j+1}(\hat{x}) = \varphi^{j+1}(\hat{x}) - \varepsilon\theta\Delta t\varphi^{j+1}_{xx}(\hat{x}) + \Delta t\theta a(x)\varphi^{j+1}(\hat{x}) \leq\ 0.$$

Case 2: For $\hat{x} \in (1, 2)$,

$$\begin{aligned}(1 + \Delta t\theta\mathcal{L}^M_{\varepsilon,2})\varphi^{j+1}(\hat{x}) \leq& \varphi^{j+1}(\hat{x}) + \Delta t\theta[-\varepsilon\varphi^{j+1}_{xx}(\hat{x}) + a(\hat{x})\varphi^{j+1}(\hat{x}) + b(\hat{x})\varphi^{j+1}(\hat{x})]\\ \leq& \ \varphi^{j+1}(\hat{x}) - \varepsilon\Delta t\theta\varphi^{j+1}_{xx}(\hat{x}) + 2\beta\Delta t\theta\varphi^{j+1}(\hat{x}) \leq\ 0.\end{aligned}$$

The two cases show that $(1+\Delta t\theta\mathcal{L}^M_{\varepsilon})\varphi^{j+1}(\hat{x}) \leq 0$, for some $\hat{x} \in \Gamma$, which contradicts the given condition. This implies that $\varphi^{j+1}(x) \geq 0$, for all $x \in \bar{\Gamma}$. The maximum principle is satisfied by the operator $1 + \Delta t\theta\mathcal{L}^M_{\varepsilon,x}$, and as a result

$$\| \left(1 + \Delta t\theta\mathcal{L}^M_{\varepsilon,x}\right)^{-1} \| \leq \frac{1}{1 + 2\lambda\theta\Delta t}. \tag{6.13}$$

■

Lemma 6.3.2 *(Woldaregay & Duressa, 2021). Let the solution of the semi-discrete problem (6.12) be $U^{j+1}(x)$, $j = 0, 1, 2, ..., M-1$. Then, it can be estimated as*

$$|U^{j+1}(x)| \leq \frac{\Delta t}{1 + 2\lambda\theta\Delta t}\|g\| + \max\left\{|U^{j+1}(0)|, |U^{j+1}(2)|\right\}. \tag{6.14}$$

Proof. Define two functions as

$$\psi^{j+1}_{\pm}(x) = \frac{\Delta t}{1 + 2\lambda\theta\Delta t}\|g\| + \max\left\{|U^{j+1}(0)|, |U^{j+1}(2)|\right\} \pm U^{j+1}(x).$$

At $x = 0$, $\psi^{j+1}_{\pm}(0) \geq\ \frac{\Delta t}{1+2\lambda\theta\Delta t}\|g\| \geq\ 0$.
At $x = 2$, $\psi^{j+1}_{\pm}(2) \geq\ \frac{\Delta t}{1+2\lambda\theta\Delta t}\|g\| \geq\ 0$.
For $x \in (0, 1]$, from (6.12),

$$\begin{aligned}(1 + \Delta t\theta\mathcal{L}_{\varepsilon,1})\psi^{j+1}_{\pm}(x) =& - \varepsilon\theta\Delta t(\psi_{xx})^{j+1}_{\pm}(x) + [1 + \theta\Delta t a(x)]\psi^{j+1}_{\pm}(x)\\ \geq& [1 + \theta\Delta t a(x)] \max\left\{|U^{j+1}(0)|, |U^{j+1}(2)|\right\} \geq\ 0.\end{aligned}$$

For $x \in (1, 2)$, from (6.12),

$$\begin{aligned}(1 + \Delta t\theta\mathcal{L}_{\varepsilon,2})\psi_{\pm}^{j+1}(x) =& -\varepsilon\theta\Delta t(\psi_{xx})_{\pm}^{j+1}(x) + [1 + \theta\Delta t a(x)]\psi_{\pm}^{j+1}(x)\\ &+ \theta\Delta t b(x)(\psi_{xx})_{\pm}^{j+1}(x-1)\\ \geq& [1 + \theta\Delta t(a(x) + b(x))] \max\left\{|U^{j+1}(0)|, |U^{j+1}(2)|\right\} \geq 0.\end{aligned}$$

As a result, using Lemma 6.3.1, $\psi_{\pm}^{j+1}(x) \geq 0$, which implies the required stability estimate. ■

Lemma 6.3.3 *(Woldaregay & Duressa, 2021). Let* $\left|\frac{\partial^m u(x,t)}{\partial t^m}\right| \leq C$ *for* $(x, t) \in \bar{\Omega}$ *and* $m = 0, 1, 2$*. Then, the local error is estimated as*

$$\|e^{j+1}\| \leq \begin{cases} C(\Delta t)^2, & \text{if } \frac{1}{2} < \theta \leq 1, \\ C(\Delta t)^3, & \text{if } \theta = \frac{1}{2}. \end{cases}$$

Proof. The local truncation error can be determined by selecting an appropriate base point, where the Taylor series is expanded. The convenient base point for a fully implicit method is the point (x_i, t_{j+1}). However, the center point, $(x_i, t_{j+\frac{1}{2}})$ is a convenient base point for any value of $\theta \in [\frac{1}{2}, 1)$ and using this base point, the Taylor series expansion yield

$$\left(1 + \Delta t\theta\mathcal{L}_{\varepsilon,x}^M\right) u^{j+1}(x) = g^{j+1}(x) + (\frac{1}{2} - \theta)O((\Delta t)^2) + O((\Delta t)^3). \tag{6.15}$$

Taking the different between (6.12) and (6.15), yields the local error satisfying

$$\begin{aligned}\left(1 + \Delta t\theta\mathcal{L}_{\varepsilon,x}^M\right) e^{j+1} &= \left(\frac{1}{2} - \theta\right) O((\Delta t)^2) + O((\Delta t)^3),\\ e^{j+1}(0) = 0, \ e^{j+1}(2) &= 0.\end{aligned}$$

Thus, applying Lemma 6.3.1 gives required estimate. ■

Lemma 6.3.4 *Assuming that Lemma 6.3.3 holds true, the global truncation errors* E^{j+1} *can be estimated as*

$$\|E^{j+1}\| \leq \begin{cases} C(\Delta t), & \text{if } \frac{1}{2} < \theta \leq 1, \\ C(\Delta t)^2, & \text{if } \theta = \frac{1}{2}. \end{cases}$$

Proof. By the local error estimate up to the $(j+1)^{th}$ time level for $\frac{1}{2} < \theta \leq 1$,

$$\begin{aligned}\|E^{j+1}\| =& \left\|\sum_{k=1}^{j+1} e^k\right\|, \ j\Delta t \leq T\\ \leq& \|e^1\| + \|e^2\| + ... + \|e^{j+1}\|\\ \leq& C_1((j+1)\Delta t)\Delta t \leq C(\Delta t).\end{aligned}$$

By a similar procedures for $\theta = \frac{1}{2}$,

$$\begin{aligned}\|E^{j+1}\| = &\left\|\sum_{k=1}^{j+1} e^k\right\|, \;\; j\Delta t \leq T\\ \leq&\|e^1\| + \|e^2\| + ... + \|e^{j+1}\| \leq C_1((j+1)\Delta t)(\Delta t)^2 \leq C(\Delta t)^2.\end{aligned}$$

Thus, the constructed semi-discrete scheme is convergent in the temporal direction. ■

Remark 6.3.1 To obtain an improved error estimate, th solution $U^{j+1}(x)$ is decomposed as $U^{j+1}(x) = V^{j+1}(x) + W^{j+1}(x)$, where $V^{j+1}(x)$ is the smooth component satisfying the problem

$$\begin{aligned}\left(1 + \Delta t\theta\mathcal{L}^M_{\varepsilon,1}\right) V^{j+1}(x) =& -\varepsilon\Delta t\theta V^{j+1}_{xx}(x) + [1 + \theta\Delta t a(x)]V^{j+1}(x)\\ =&\varepsilon\Delta t(1-\theta)V^j_{xx}(x) + [1 - (1-\theta)\Delta t a(x)]V^j(x) + \theta\Delta t f^{j+1}(x)\\ &- \theta\Delta t b(x)\phi^{j+1}(x-1) - (1-\theta)\Delta t[b(x)\phi^j(x-1) - f^j(x)], \; x \in (0,1],\\ &V^{j+1}(0) = U^{j+1}_0(0),\\ &V^{j+1}(1) = [1 + \theta\Delta t a(1)]^{-1}([1 - (1-\theta)\Delta t a(1)]V^j(1) + \theta\Delta t f^{j+1}(1)\\ &\quad - \theta\Delta t b(x)\phi^{j+1}(0) - (1-\theta)\Delta t[b(1)\phi^j(0) - f^j(1)]),\end{aligned}$$

$$\begin{aligned}\left(1 + \Delta t\theta\mathcal{L}^M_{\varepsilon,2}\right) V^{j+1}(x) =& -\varepsilon\Delta t\theta V^{j+1}_{xx}(x) + [1 + \theta\Delta t a(x)]V^{j+1}(x) + \theta\Delta t b(x)V^{j+1}(x-1)\\ =&\varepsilon\Delta t(1-\theta)V^j_{xx}(x) + [1 - (1-\theta)\Delta t a(x)]V^j(x) + \theta\Delta t f^{j+1}(x)\\ &- (1-\theta)\Delta t[b(x)V^j(x-1) - f^j(x)], \; x \in (1,2],\\ &V^{j+1}(2) = U^{j+1}_0(2),\\ &V^{j+1}(1) = [1 + \theta\Delta t a(1)]^{-1}([1 - (1-\theta)\Delta t b(1)]V^j(1) + \theta\Delta t f^{j+1}(1)\\ &\quad - (1-\theta)\Delta t[b(1)V^j(0) - f^j(1)]),\end{aligned}$$

and $W^{j+1}(x)$ is the singular component satisfying the problem

$$\begin{aligned}\left(1 + \Delta t\theta\mathcal{L}^M_{\varepsilon,1}\right) W^{j+1}(x) =& -\varepsilon\Delta t\theta W^{j+1}_{xx}(x) + [1 + \theta\Delta t a(x)]W^{j+1}(x) = 0, \; x \in (0,1]\\ \left(1 + \Delta t\theta\mathcal{L}^M_{\varepsilon,2}\right) W^{j+1}(x) =& -\varepsilon\Delta t\theta W^{j+1}_{xx}(x) + [1 + \theta\Delta t a(x)]W^{j+1}(x)\\ &+ \theta\Delta t b(x)W^{j+1}(x-1), \; x \in (1,2),\\ W^{j+1}(0) = U^{j+1}(0) - V^{j+1}(0), \;& W^{j+1}(2) = U^{j+1}(2) - V^{j+1}(2).\end{aligned}$$

The singular component $W^{j+1}(x)$ is further decomposed as

$$W^{j+1}(x) = W^{j+1}_L(x) + W^{j+1}_R(x)$$

where the left singular component is

$$W_L^{j+1}(x) = W^{j+1}(0)W_{L,1}^{j+1}(x) + r_1 W_{L,2}^{j+1}(x)$$

satisfying $\left(1 + \Delta t\theta \mathcal{L}_{\varepsilon,1}^M\right) W_{L,1}^{j+1}(x) = 0$, $x \in (0,1)$ with the conditions

$$W_{L,1}^{j+1}(0) = W^{j+1}(0),\ W_{L,2}^{j+1}(1) = 0,\ W_{L,1}^{j+1}(x) = 0,\ x \in (1,2)$$

and $\left(1 + \Delta t\theta \mathcal{L}_{\varepsilon,1}^M\right) W_{L,2}^{j+1}(x) = 0$, $x \in (0,1)$ with the conditions

$$W_{L,2}^{j+1}(0) = 0,\ W_{L,2}^{j+1}(1) = W_{L,0}^{j+1}(1),\ W_{L,0}^{j+1}(x) = 0,\ x \in (1,2).$$

And the right singular component is

$$W_R^{j+1}(x) = r_2 W_{R,1}^{j+1}(x) + W_{R,0}^{j+1}(2)W_{R,2}^{j+1}(x)$$

satisfying $\left(1 + \Delta t\theta \mathcal{L}_{\varepsilon,2}^M\right) W_{R,1}^{j+1}(x) = 0$, $x \in (1,2)$ with

$$W_{R,1}^{j+1}(1) = W_{R,0}^{j+1}(1),\ W_{R,2}^{j+1}(2) = 0,\ W_{R,1}^{j+1}(x) = 0,\ x \in (0,1).$$

and satisfying $\left(1 + \Delta t\theta \mathcal{L}_{\varepsilon,2}^M\right) W_{R,2}^{j+1}(x) = 0$, $x \in (1,2)$ with

$$W_{R,2}^{j+1}(1) = 0,\ W_{R,2}^{j+1}(2) = W_{R,0}^{j+1}(2),\ W_{R,2}^{j+1}(x) = 0,\ x \in (0,1).$$

In the above singular component conditions, the constants r_1 and r_2 are arbitrarily chosen, so that the jump conditions at $x = 1$ are satisfied.

Lemma 6.3.5 *(Bansal & Sharma, 2018). The derivatives of $U^{j+1}(x),\ j+1 = 1,2,...,M$ and its components can be estimated as*

$$\left|\frac{d^m U^{j+1}(x)}{dx^m}\right| \le \begin{cases} C(1 + \varepsilon^{-\frac{m}{2}}\eta_1(x,\lambda)),\ 0 \le x \le 1, \\ C(1 + \varepsilon^{-\frac{m}{2}}\eta_2(x,\lambda)),\ 1 \le x \le 2, \end{cases}$$

$$\left|\frac{d^m V^{j+1}(x)}{dx^m}\right| \le \begin{cases} C(1 + \varepsilon^{\frac{-(m-2)}{2}}\eta_1(x,\lambda)),\ \ 0 \le x \le 1, \\ C(1 + \varepsilon^{\frac{-(m-2)}{2}}\eta_2(x,\lambda),\ \ 1 \le x \le 2, \end{cases}$$

$$\left|\frac{d^m W^{j+1}(x)}{dx^m}\right| \le \begin{cases} C\varepsilon^{\frac{-m}{2}}\eta_1(x,\lambda),\ 0 \le x \le 1, \\ C\varepsilon^{\frac{-m}{2}}\eta_2(x,\lambda),\ 1 \le x \le 2, \end{cases}$$

where $\eta_1(x,\lambda) = e^{-\sqrt{\frac{\lambda}{\varepsilon}}x} + e^{-\sqrt{\frac{\lambda}{\varepsilon}}(1-x)}$, $\eta_2(x,\lambda) = e^{-\sqrt{\frac{\lambda}{\varepsilon}}(x-1)} + e^{-\sqrt{\frac{\lambda}{\varepsilon}}(2-x)}$ and $m = 0,1,2,3$.

Proof. The proof is done by induction. For $m = 0$, it became Lemma 6.3.2. For $m = 1$, consider $x \in (0, 1]$ and construct an associated neighborhood of $R_x = (q, q + \sqrt{\varepsilon})$, such that $x \in R_x$ and $R_x \in (0, 1]$. Then, by the mean value theorem, for some $y \in \bar{R}_x$,

$$|U_x^{j+1}(y)| = \varepsilon^{-\frac{1}{2}}|U^{j+1}(q + \sqrt{\varepsilon}) - U^{j+1}(q)| \leq 2\varepsilon^{\frac{-1}{2}}\|U^{j+1}\|.$$

Now, for any x in $\bar{R}_x$,

$$\begin{aligned}|U_x^{j+1}(x)| =&|U_x^{j+1}(y) + \varepsilon^{-1}\int_y^x \frac{1}{\theta\Delta t}[(1 + \theta\Delta t a(s))U^{j+1}(s) - g(s, t_{j+1})]ds| \\ \leq&|U_x^{j+1}(y)| + C\varepsilon^{-1}\left(\|U^{j+1}\|_{\partial\Gamma} + \|g\|\right).\end{aligned}$$

Thus, $|U_x^{j+1}(x)| \leq C\varepsilon^{\frac{-1}{2}}$, and Since $\eta_1(x, \lambda) = e^{-\sqrt{\frac{\lambda}{\varepsilon}}x} + e^{-\sqrt{\frac{\lambda}{\varepsilon}}(1-x)}$ is bounded,

$$|U_x^{j+1}(x)| \leq C(1 + \varepsilon^{\frac{-1}{2}}[e^{-\sqrt{\frac{\lambda}{\varepsilon}}x} + e^{-\sqrt{\frac{\lambda}{\varepsilon}}(1-x)}])$$

Using the differential equation and the bounds on U^{j+1} and U_x^{j+1}, the bounds on the higher derivatives can be easily obtained. For the sharper bound of the solution and its derivatives, we considered the decomposition $U^{j+1}(x) = V^{j+1}(x) + W^{J+1}(x)$, so that $V^{j+1}(x) = V_0^{j+1}(x) + \varepsilon V_1^{j+1}(x)$, where V_0^{j+1} is the solution of the reduced problem and $V_1^{j+1}(x)$ satisfies

$$\begin{aligned}(1 + \Delta t\theta\mathcal{L}_{\varepsilon,1}^M)V_1^{j+1}(x) = (V_0^{j+1})_{xx}(x)\\ V^{j+1}(0) = 0 = V_1^{j+1}\end{aligned}$$

Since $V_1^{j+1}(x) = \varepsilon^{-1}(V^{j+1}(x) - V_0^{j+1}(x)) = \varepsilon^{-1}(U^{j+1}(x) - V_0^{j+1}(x) - W^{j+1}(x))$, we have

$$V_1^{j+1}(0) = \varepsilon^{-1}(U^{j+1}(0) - V_0^{j+1}(0) - W^{j+1}(0))$$

and

$$V_1^{j+1}(1) = \varepsilon^{-1}(U^{j+1}(1) - V_0^{j+1}(0) - W^{j+1}(1)).$$

Thus, since $(V_0^{j+1})_{xx}(x)$ is bounded, $V_1^{j+1}(x)$ is the solution of the problem similar to (6.12). This implies that for $m = 0, 1, 2, 3$,

$$\left|\frac{d^m V_1^{j+1}(x)}{dx^m}\right| \leq C(1 + \varepsilon^{\frac{-m}{2}}).$$

Noting that $V^{j+1}(x) = v_0^{j+1}(x) + \varepsilon V_1^{j+1}(x)$, so that the smooth component satisfies

$$\left|\frac{d^m V^{j+1}(x)}{dx^m}\right| \leq C(1 + \varepsilon^{\frac{-(m-2)}{2}}).$$

Therefore, since $\eta_1(x,\lambda) = e^{-\sqrt{\frac{\lambda}{\varepsilon}}x} + e^{-\sqrt{\frac{\lambda}{\varepsilon}}(1-x)}$ is bounded, we have

$$\left|\frac{d^m V^{j+1}(x)}{dx^m}\right| \leq C(1+\varepsilon^{\frac{-(m-2)}{2}}\eta_1(x,\lambda)),\ m=0,1,2,3 \text{ on } [0,1].$$

Next, we construct the bound of the singular component $W^{j+1}(x)$ of the semi-discrete problem. It is well known that $W^{j+1}(x)$ can be further decomposed into left layer and right layer as

$$W^{j+1}(x) = W_L^{j+1}(x) + W_R^{j+1}(x),$$

where the boundary layer functions, $W_L^{j+1}(x)$ and $W_R^{j+1}(x)$ are defined as the solution of the problems

$$(1+\Delta t\theta\mathcal{L}_{\varepsilon,1}^M)W_L^{j+1}(x) = 0,\ W_L^{j+1}(0) = W^{j+1}(0),\ W_L^{j+1}(1) = 0$$

and

$$(1+\Delta t\theta\mathcal{L}_{\varepsilon,2}^M)W_R^{j+1}(x) = 0,\ W_R^{j+1}(1) = 0,\ W_R^{j+1}(2) = W^{j+1}(2).$$

Define barrier functions $\vartheta^{\pm}(x) = C\eta_1(x,\lambda) \pm W_L^{j+1}(x)$, where C is chosen sufficiently large that $\vartheta^{\pm}(0) \geq 0$ and $\vartheta^{\pm}(0) \geq 0$ hold true. Then,

$$\begin{aligned}
\left(1+\Delta t\theta\mathcal{L}_{\varepsilon,1}^M\right)\vartheta^{\pm}(x) =& -\varepsilon\Delta t\theta\vartheta_{xx}^{\pm}(x) + (1+\Delta t\theta a(x))\,\vartheta^{\pm}(x) \\
=& C\left(1+\Delta t\theta(a(x)-\lambda)\right)\eta_1(x,\lambda) \pm \left(-\varepsilon\Delta t\theta W_{L,xx}^{j+1}(x) + (1+\Delta t\theta a(x))W_L^{j+1}\right) \\
=& C\left[1+\Delta t\theta(a(x)-\lambda)\right]\eta_1(x,\lambda) \geq 0,\ \text{as } a(x) \geq \lambda.
\end{aligned}$$

Applying the semi-discrete maximum principle, $\vartheta^{\pm}(x) \geq 0$, which implies that

$$|W_L^{j+1}(x)| \leq C\eta_1(x,\lambda),\ x \in [0,1],$$

which implies that the left boundary layer's solution is bounded. To bound the first derivative $W_L^{j+1}(x)$, the same technique is used as in the proof of the bound of $U_x^{j+1}(x)$ shown above. For each $x \in [0,1]$, there exist $y \in \bar{R}_x = (q, q+\sqrt{\varepsilon})$, such that

$$|(W_L^{j+1})_x(x)| \leq 2\varepsilon^{\frac{-1}{2}}\|W_L^{j+1}\|_{R_x}.$$

Then, it is easily understood that

$$\begin{aligned}
(W_L^{j+1})_x(x) =& (W_L^{j+1})_x(y) + \int_y^x (W_L^{j+1})_{xx}(z)dz \\
=& (W_L^{j+1})_x(y) + \varepsilon^{-1}\int_y^x \frac{1+\Delta t\theta a(z)}{\Delta t\theta}W_L^{j+1}(z)dz.
\end{aligned}$$

From this, one can obtain

$$\begin{aligned}\left|(W_L^{j+1})_x(x)\right| \leq & \|(W_L^{j+1})_x\| + \varepsilon^{-1}\left\|\frac{1+\Delta t\theta a}{\Delta t\theta}\right\|\int_y^x dz\\ \leq & 2\varepsilon^{\frac{-1}{2}}\|W_L^{j+1}\| + \varepsilon^{\frac{-1}{2}}\left\|\frac{1+\Delta t\theta a}{\Delta t\theta}\right\|, \text{ as } x-y\leq\sqrt{\varepsilon}\\ \leq & C\varepsilon^{\frac{-1}{2}}\|W_L^{j+1}\|.\end{aligned}$$

But, $\|W_L^{j+1}\| = \sup_{x\in R_x}|W_L^{j+1}(x)| \leq Ce^{-y\sqrt{\frac{\lambda}{\varepsilon}}}$, which is because of monotonic decrement of $W_L^{j+1}(x)$. Thus,

$$\begin{aligned}\|W_L^{j+1}\| \leq Ce^{-y\sqrt{\frac{\lambda}{\varepsilon}}} = & Ce^{(x-y)\sqrt{\frac{\lambda}{\varepsilon}}}e^{-x\sqrt{\frac{\lambda}{\varepsilon}}}\\ \leq & Ce^{\sqrt{\varepsilon}\sqrt{\frac{\lambda}{\varepsilon}}}e^{-x\sqrt{\frac{\lambda}{\varepsilon}}} \leq Ce^{-x\sqrt{\frac{\lambda}{\varepsilon}}}.\end{aligned}$$

Therefore, $|(W_L^{j+1})_x(x)| \leq C\varepsilon^{\frac{-1}{2}}\eta_1(x,\lambda)$. Using the derivatives on $W_L^{j+1}(x)$, the bounds for $m=2$ and $m=3$ can be easily obtained by similar procedures. The required bounds for $x\in(1,2)$ can be obtained following the above procedures. ■

Remark 6.3.2 Constructing the bound of the solution and its derivatives in Lemma 6.3.5 involved the functions $e^{-\sqrt{\frac{\lambda}{\varepsilon}}x}$, $e^{-\sqrt{\frac{\lambda}{\varepsilon}}(1-x)}$, $e^{-\sqrt{\frac{\lambda}{\varepsilon}}(x-1)}$ and $e^{-\sqrt{\frac{\lambda}{\varepsilon}}(2-x)}$. For these functions, it can be observed that on $(0,1]$, $e^{-\sqrt{\frac{\lambda}{\varepsilon}}x} \geq e^{-\sqrt{\frac{\lambda}{\varepsilon}}(1-x)}$, for all x near 0^- and $e^{-\sqrt{\frac{\lambda}{\varepsilon}}x} \leq e^{-\sqrt{\frac{\lambda}{\varepsilon}}(1-x)}$, for all x near 1^-. On the interval $(1,2)$, $e^{-\sqrt{\frac{\lambda}{\varepsilon}}(x-1)} \geq e^{-\sqrt{\frac{\lambda}{\varepsilon}}(2-x)}$, for all x near x^+ and $e^{-\sqrt{\frac{\lambda}{\varepsilon}}(x-1)} \leq e^{-\sqrt{\frac{\lambda}{\varepsilon}}(2-x)}$, for all x near 2^-. In the left boundary layer in the neighborhood of $x=0$, we have $e^{-\sqrt{\frac{\lambda}{\varepsilon}}x} \gg e^{-\sqrt{\frac{\lambda}{\varepsilon}}(1-x)}$, while in the interior layer in the neighborhood of $x=1^-$, $e^{-\sqrt{\frac{\lambda}{\varepsilon}}x} \ll e^{-\sqrt{\frac{\lambda}{\varepsilon}}(1-x)}$. Similarly, in the interior layer in the neighborhood of $x=1^+$, $e^{-\sqrt{\frac{\lambda}{\varepsilon}}(x-1)} \gg e^{-\sqrt{\frac{\lambda}{\varepsilon}}(2-x)}$, while in the right boundary layer in the neighborhood of $x=2$, $e^{-\sqrt{\frac{\lambda}{\varepsilon}}(x-1)} \ll e^{-\sqrt{\frac{\lambda}{\varepsilon}}(2-x)}$. Based on these results, it may be enough to prove the Lemma that on the part of the mesh corresponding to the left boundary layer with the function $e^{-\sqrt{\frac{\lambda}{\varepsilon}}x}$ and the left side interior layer with the function $e^{-\sqrt{\frac{\lambda}{\varepsilon}}(1-x)}$. Similarly, for the left side interior layer, it may be enough to use the bounding function $e^{-\sqrt{\frac{\lambda}{\varepsilon}}(x-1)}$ and the right boundary layer, it is enough to use the function $e^{-\sqrt{\frac{\lambda}{\varepsilon}}(2-x)}$.

6.3.2 Spatial discretization

Divide the spatial domain $[0,2]$ into two sub-intervals $[0,1]$ and $(1,2]$. For N mesh numbers, consider $\bar{\Omega}_x^N$ as a piece-wise uniform spatial meshes. Then, each sub-intervals can be further divided as $[0,1]=[0,\tau]\cup(\tau,1-\tau]\cup(1-\tau,1]$ and $(1,2]=(1,1+\tau]\cup(1+\tau,2-\tau]\cup(2-\tau,2]$, where τ is a transition parameter, which separates the non-uniform into uniform meshes and given as $\tau = \min\left\{\frac{1}{4}, 2\sqrt{\frac{\varepsilon}{\lambda}}\ln N\right\}$. Consider $\frac{N}{8}$ mesh numbers on each of the fine mesh regions $[0,\tau]$, $(1-\tau,1)$, $(1,1+\tau)$ and $(2-\tau,2)$, and $\frac{N}{4}$ mesh numbers on each of the coarse mesh regions $(\tau,1-\tau]$ and $(1+\tau,2-\tau]$. The nodal mesh points are $x_i = x_{i-1}+h_i,\ i=1,2,...,N$, where the mesh interval h_i's are given by

$$h_i = \begin{cases} \frac{8\tau}{N},\ i=1,2,...,\frac{N}{8},\frac{3N}{8}+1,...,\frac{N}{2},\frac{N}{2}+1,...,\frac{5N}{8},\frac{7N}{8}+1,...,N, \\ \frac{4(1-2\tau)}{N},\ i=\frac{N}{8}+1,...,\frac{3N}{8},\frac{5N}{8}+1,...,\frac{7N}{8}. \end{cases}$$

Now, define the standard finite difference operators as

$$\begin{aligned} D^+U^{j+1}(x_i) &= \frac{U_{i+1}^{j+1}-U_i^{j+1}}{h_{i+1}},\ \ D^-U^{j+1}(x_i) = \frac{U_i^{j+1}-U_{i-1}^{j+1}}{h_i}, \\ D^+D^-U^{j+1}(x_i) &= \frac{2}{h_i+h_{i+1}}\left[D^+U^{j+1}(x_i)-D^-U^{j+1}(x_i)\right]. \end{aligned}$$

Substituting the differential operator in equation (6.12) by the standard finite difference operators gives a discrete scheme as

$$\mathcal{L}_{\varepsilon}^{N,M}U_i^{j+1} = g_i^{j+1},\ j=0,1,2,...,M-1, \tag{6.16}$$

where

$$\mathcal{L}_{\varepsilon}^{N,M}U_i^{j+1} = \begin{cases} -\varepsilon\Delta t\theta D^+D^-U_i^{j+1}+(1+\Delta t\theta a_i)U_i^{j+1},\ \ i=1,2,...,\frac{N}{2}, \\ -\varepsilon\Delta t\theta D^+D^-U_i^{j+1}+(1+\Delta t\theta a_i)U_i^{j+1}+\Delta t\theta b_i U_{N/2-1}^{j+1}, \\ \qquad i=\frac{N}{2}+1,\frac{N}{2}+2,...,N-1, \end{cases}$$

and

$$g_i^{j+1} = \begin{cases} \Delta t(1-\theta)[\varepsilon D^+D^-U_i^j - a_iU_i^j - b_i\phi^j(x_i-1)+f(x_i)] \\ -\theta\Delta t b_i\phi^{j+1}(x_i-1)+\theta\Delta t f(x_i)+U_i^j,\ \ i=1,2,...,\frac{N}{2} \\ \Delta t(1-\theta)[\varepsilon D^+D^-U_i^j - a_iU_i^j - b_iU_{N/2-1}^j+f(x_i)] \\ +U_i^j+\Delta t\theta f(x_i),\ \ i=\frac{N}{2}+1,\frac{N}{2}+2,...,N-1. \end{cases}$$

The scheme in (6.16) can be reduced to a system of equations given by

$$r_i^-U_{i-1}^{j+1}+r_i^0U_i^{j+1}+r_i^+U_{i+1}^{j+1} = G_i,\ \ i=1,2,...,\frac{N}{2},$$

where

$$\begin{aligned} r_i^- &= \frac{-2\varepsilon\theta}{h_i(h_i+h_{i+1})}, \\ r_i^0 &= \frac{2\varepsilon\theta}{h_{i+1}(h_i+h_{i+1})}+\frac{2\varepsilon\theta}{h_i(h_i+h_{i+1})}+\frac{1}{\Delta t}+\theta a_i, \\ r_i^+ &= \frac{-2\varepsilon\theta}{h_{i+1}(h_i+h_{i+1})}, \\ G_i &= (1-\theta)[\varepsilon D_x^+D_x^-U_i^j - a_iU_i^j - b_i\phi^j(x_i-1)+f^j(x_i)] - \theta b_i\phi^{j+1}(x_i-1)+\theta f^{j+1}(x_i)+\frac{1}{\Delta t}U_i^j. \end{aligned}$$

Similarly, one can obtain

$$r_i^- U_{i-1}^{j+1} + r_i^0 U_i^{j+1} + r_i^+ U_{i+1}^{j+1} = G_i^*, \quad i = \frac{N}{2}+1, \frac{N}{2}+2, ..., N,$$

where r_i^-, r_i^0 and r_i^+ are given as above and $G_i^* = (1-\theta)[\varepsilon D^+ D^- U_i^j - a_i U_i^j - b_i U_{\frac{N}{2}-1}^j + f^j(x_i)] + \frac{1}{\Delta t} U_i^j + \theta f^{j+1}(x_i)$.

Lemma 6.3.6 *(Discrete Maximum Principle). Let φ_i^{j+1} be a given mesh function, which satisfies $\varphi_0^{j+1} \geq 0$ and $\varphi_N^{j+1} \geq 0$, $j = 0,1,2,...,M-1$. If $\mathcal{L}_\varepsilon^{N,M} \varphi_i^{j+1} \geq 0$, $i = 1,2,...,N-1$, then $\varphi_i^{j+1} \geq 0$, $i = 0,1,...,N$.*

Proof. Assume that $\varphi_\iota^{j+1} = \min_{i=0,1,...,N} \varphi_i^{j+1} < 0$, for some $\iota \in \{0,1,...,N\}$.

Case 1: For $i = 1,2,...,\frac{N}{2}$,

$$\mathcal{L}_{\varepsilon,1}^N \varphi_\iota^{j+1} = -\varepsilon \Delta t \theta D^+ D^- \varphi^{j+1}(x_\iota) + \left(\frac{1}{\Delta t} + \theta a(x_\iota)\right) \varphi^{j+1}(x_\iota) < 0.$$

Case 2: For $i = \frac{N}{2}+1, \frac{N}{2}+2, ..., N-1$,

$$\begin{aligned}
\mathcal{L}_{\varepsilon,2}^{N,M} \varphi_\iota^{j+1} &= -\varepsilon\theta D^+ D^- \varphi^{j+1}(x_\iota) + \left(\frac{1}{\Delta t} + \theta a(x_\iota)\right) \varphi^{j+1}(x_\iota) + \theta b(x_\iota) \varphi^{j+1}(x_\iota - 1) \\
&\leq -\varepsilon\theta D^+ D^- \varphi^{j+1}(x_\iota) + \left[\frac{1}{\Delta t} + \theta a(x_\iota) + \theta b(x_\iota)\right] \varphi^{j+1}(x_\iota) < 0.
\end{aligned}$$

These two cases contradict the given hypothesis, which implies that $\varphi_i^{j+1} \geq 0$ for all $i = 0,1,...,N$, $j = 0,1,2,...,M-1$. ■

Lemma 6.3.7 *(Bansal & Sharma, 2018). Let U_i^{j+1}, $i = 0,1,...,N$ be a solution of the fully-discrete problem (6.16). Then, it is estimated as*

$$|U_i^{j+1}| \leq \frac{\Delta t \|g\|}{1 + 2\lambda\theta\Delta t} + \max\left\{|U_0^{j+1}|, |U_N^{j+1}|\right\}.$$

Proof. To confirm this estimate, define two barrier functions as

$$(\vartheta_i^{j+1})^\pm = \frac{\Delta t \|g\|}{1 + 2\lambda\theta\Delta t} + \max\left\{|U_0^{j+1}|, |U_N^{j+1}|\right\} \pm U_i^{j+1}.$$

The estimation holds true for $i \in \{0, N\}$, and for other values of i, examine the two cases below.

Case 1: For $i = 1,2,...,\frac{N}{2}$,

$$\begin{aligned}
\mathcal{L}_{\varepsilon,1}^{N,M} (\vartheta_i^{j+1})^\pm &= -\varepsilon\theta D^+ D^- (\vartheta_i^{j+1})^\pm + \left(\frac{1}{\Delta t} + \theta a_i\right) (\vartheta_i^{j+1})^\pm \\
&\geq \left(\frac{1}{\Delta t} + \theta a_i\right) \left(\frac{\Delta t \|g\|}{1 + 2\lambda\theta\Delta t} + \max\left\{|U_0^{j+1}|, |U_N^{j+1}|\right\}\right) \pm g(x_i, t_{j+1}) \\
&\geq (1/\Delta t + \theta a_i) \max\left\{|U_0^{j+1}|, |U_N^{j+1}|\right\} \geq 0.
\end{aligned}$$

Case 2 : For $i = \frac{N}{2}+1, \frac{N}{2}+2, ..., N-1$,

$$\begin{aligned}
\mathcal{L}_2^{N,M}(\vartheta_i^{j+1})^{\pm} =& -\varepsilon\theta D^+D^-(\vartheta_i^{j+1})^{\pm} + \left(\frac{1}{\Delta t}+\theta a(x_i)\right)(\vartheta_i^{j+1})^{\pm} + \theta b(x_i)(\vartheta_{i-\frac{N}{2}}^{j+1})^{\pm}\\
\geq& \left(\frac{1}{\Delta t}+\theta a_i+\theta b_i\right)\left(\frac{\Delta t\|g\|}{1+2\lambda\theta\Delta t}+\max\left\{|U_0^{j+1}|,\ |U_N^{j+1}|\right\}\right) \pm g(x_i,t_{j+1})\\
\geq& \left(\frac{1}{\Delta t}+\theta a_i+\theta b_i\right)\max\left\{|U_0^{j+1}|,\ |U_N^{j+1}|\right\} \geq\ 0.
\end{aligned}$$

So, applying Lemma 6.3.6, the required stability estimate can be obtained. ■

Remark 6.3.3 For the Shishkin's error estimate of the discrete scheme, the solution U_i^{j+1} can be decomposed into its smooth component V_i^{j+1} and singular component W_i^{j+1} as $U_i^{j+1} = V_i^{j+1} + W_i^{j+1}$. The smooth component satisfies the problem

$$\mathcal{L}_\varepsilon^{N,M} V_i^{j+1} = g_i^{j+1},\ j = 0,1,2,...,M-1,$$

where

$$\mathcal{L}_\varepsilon^{N,M} V_i^{j+1} = \begin{cases} -\varepsilon\theta D^+D^-V_i^{j+1} + \left(\frac{1}{\Delta t}+\theta a_i\right)V_i^{j+1},\ i = 1,2,...,\frac{N}{2},\\ -\varepsilon\theta D^+D^-V_i^{j+1} + \left(\frac{1}{\Delta t}+\theta a_i\right)V_i^{j+1} + \theta b(x_i)V_{\frac{N}{2}-1}^{j+1},\\ \qquad i = \frac{N}{2}+1, \frac{N}{2}+2, ..., N-1 \end{cases}$$

$$V_0^{j+1} = V^{j+1}(0),\ V_{\frac{N}{2}-1}^{j+1} = V^{j+1}(1^-),\ V_{\frac{N}{2}+1}^{j+1} = V^{j+1}(1^+),\ V_N^{j+1} = V^{j+1}(2).$$

And the singular component, W_i^{j+1} satisfies the problem

$$\mathcal{L}_\varepsilon^{N,M} W_i^{j+1} = \begin{cases} -\varepsilon\theta D^+D^-W_i^{j+1} + \left(\frac{1}{\Delta t}+\theta a_i\right)W_i^{j+1} = 0,\ i = 1,2,...,\frac{N}{2},\\ -\varepsilon\theta D^+D^-W_i^{j+1} + \left(\frac{1}{\Delta t}+\theta a_i\right)W_i^{j+1} + \theta b_i W_{\frac{N}{2}-1}^{j+1} = 0,\\ \qquad i = \frac{N}{2}+1, \frac{N}{2}+2, ..., N-1, \end{cases}$$

$$W_0^{j+1} = W^{j+1}(0),\ W_N^{j+1} = W^{j+1}(2).$$

Theorem 6.3.1 *Suppose that $U^{j+1}(x_i)$ is the solution of (6.12) and U_i^{j+1} is the solution of (6.16). Then, the truncation error in the spatial direction is estimated as*

$$|U^{j+1}(x_i) - U_i^{j+1}| \leq C(N^{-1}\ln N)^2,\ i = 0,1,2,...,N.$$

Proof. The error at each mesh point (x_i, t_{j+1}) is given as $e_i^{j+1} = U^{j+1}(x_i) - U_i^{j+1}$. So, the error estimates in the regular and singular components can be analyzed separately. Using the classical argument for $i = 1,2,...,\frac{N}{2}-1$, the local error of the regular component is

$$\mathcal{L}_\varepsilon^{N,M}(V^{j+1} - V^{j+1}(x_i)) = -\varepsilon\theta\left(D^+D^- - \frac{d^2}{dx^2}\right)V^{j+1}(x_i).$$

Using the results in chapters 4 and 6 of (Miller et al., 2012), it becomes

$$|\mathcal{L}_\varepsilon^{N,M}(V_i^{j+1}-V^{j+1}(x_i))| \le \begin{cases} C\varepsilon\theta(x_{i+1}-x_{i-1})|V^{j+1}(x_i)|_3, & x_i \in (\tau, 1-\tau), \\ C\varepsilon\theta(x_i-x_{i-1})^2|V^{j+1}(x_i)|_4, & \text{otherwise.} \end{cases} \tag{6.17}$$

And for $m = 0, 1, 2, 3, 4$, the regular component satisfies

$$|V^{(m)}(x_i, t_{j+1})| \le C\left(1+\varepsilon^{\frac{-(m-2)}{2}}\right), \ x_i \in [0,1], \tag{6.18}$$

which implies that $\begin{cases} |V'''(x_i, t_{j+1})| \le C(1+\varepsilon^{-1/2}), \\ |V^{(4)}(x_i, t_{j+1})| \le C(1+\varepsilon^{-1}). \end{cases}$

Since $x_{i+1}-x_{i-1} \le \frac{2}{N}$, (6.17) and (6.18) yield

$$|\mathcal{L}_\varepsilon^{N,M}(V_i^{j+1}-V^{j+1}(x_i))| \le \begin{cases} CN^{-1}\varepsilon(1+\varepsilon^{-\frac{1}{2}}), & x_i \in (\tau, 1-\tau), \\ CN^{-2}\varepsilon(1+\varepsilon^{-1}), & \text{otherwise.} \end{cases}$$

Taking the smaller order of ε gives

$$|\mathcal{L}_\varepsilon^{N,M}(V_i^{j+1}-V^{j+1}(x_i))| \le \begin{cases} CN^{-1}\varepsilon^{1/2}, & x_i \in (\tau, 1-\tau), \\ CN^{-2}, & \text{otherwise.} \end{cases}$$

Introduce barrier functions as

$$\psi(x_i) = CN^{-2} + CN^{-2}\frac{\tau}{\sqrt{\varepsilon}} \begin{cases} \frac{x_i}{\tau}, & 0 \le x_i \le \tau, \\ 1, & \tau \le x_i \le 1-\tau, \\ \frac{1-x_i}{\tau}, & 1-\tau \le x_i \le 1, \end{cases}$$

which provide $\psi(x_i) = CN^{-2} + CN^{-2}\frac{\tau}{\sqrt{\varepsilon}}(1)$, for $x_i \in (\tau, 1-\tau)$. Since $\tau = 2\sqrt{\frac{\varepsilon}{\lambda}}\ln N$, it leads to $\psi(x_i) \le CN^{-2}\ln N$. Consequently,

$$\mathcal{L}_\varepsilon^{N,M}\left(\psi(x_i) \pm (V_i^{j+1}-V^{j+1}(x_i))\right) \ge 0 \ \text{ and } \ \mathcal{L}_\varepsilon^{N,M}\psi(x_i) \ge \begin{cases} CN^{-1}\varepsilon^{1/2}, & x_i \in (\tau, 1-\tau), \\ CN^{-2}, & \text{otherwise.} \end{cases}$$

Application of the discrete maximum principle yields $|V_i^{j+1}-V^{j+1}(x_i)| \le \psi(x_i) \le CN^{-2}\ln N$. Following similar procedure for $i = \frac{N}{2}+1, \frac{N}{2}+2, ..., N-1$, one can obtain $|V_i^{j+1}-V^{j+1}(x_i)| \le \psi(x_i) \le CN^{-1}$, and as a result

$$|V_i^{j+1}-V^{j+1}(x_i)| \le CN^{-2}\ln N. \tag{6.19}$$

For the singular component, the error is estimated considering the transition parameter $\tau = \frac{1}{4}$ and $\tau = 2\sqrt{\frac{\varepsilon}{\lambda}}\ln N$ separately. That is, for the case $\tau = \frac{1}{4}$, the mesh is uniform and $2\sqrt{\frac{\varepsilon}{\lambda}}\ln N \geq \frac{1}{4}$, so that $\varepsilon^{-1/2} \leq C\ln N$. By the classical argument

$$|\mathcal{L}_{\varepsilon}^{N,M}(W_i^{j+1} - W^{j+1}(x_i))| \leq C\theta(x_i - x_{i-1})^2\varepsilon|W(x_i)|_4.$$

Since $|W^{j+1}(x_i)|_4 \leq C\varepsilon^{-2}$ and $x_i - x_{i-1} \leq N^{-1}$,

$$|\mathcal{L}_{\varepsilon}^{N,M}(W_i^{j+1} - W^{j+1}(x_i))| \leq C(N^{-1}\ln N)^2.$$

Consequently, applying the maximum principle gives

$$|(W_i^{j+1} - W^{j+1}(x_i))| \leq C(N^{-1}\ln N)^2, \ \forall x_i \in [0, \tau]. \tag{6.20}$$

By a similar argument on $(1-\tau, 1)$, the same estimate can obtained as in (6.20). For the case $\tau \leq \frac{1}{4}$, a piece-wise uniform meshes exist with $\frac{4(1-2\tau)}{N}$ mesh sizes in $[\tau, 1-\tau]$ and $\frac{8\tau}{N}$ mesh sizes in each of $[0,\tau]$ and $[1-\tau, 1]$. Thus, to estimate $|W_i^{j+1} - W^{j+1}(x_i)|$, different arguments can be considered depending on the mesh spacing. For x_i in the sub-intervals $[0,\tau]$ and $[1-\tau, 1]$ the classical argument gives

$$|\mathcal{L}_{\varepsilon}^{N,M}(W_i^{j+1} - W^{j+1}(x_i))| \leq C\varepsilon\theta(x_i - x_{i-1})^2|W^{j+1}(x_i)|_4.$$

Since $x_i - x_{i-1} = \frac{8\tau}{N}$ and $|W^{j+1}(x_i|_4 \leq C\varepsilon^{-2}$,

$$|\mathcal{L}_{\varepsilon}^{N,M}(W_i^{j+1} - W^{j+1}(x_i))| \leq C\varepsilon\theta\left(\frac{8\tau}{N}\right)^2 C\varepsilon^{-2} \leq CN^{-2}\tau^2\varepsilon^{-1}.$$

But $\tau = 2\sqrt{\frac{\varepsilon}{\lambda}}\ln N$ and hence $|\mathcal{L}_{\varepsilon}^{N,M}(W_i^{j+1} - W^{j+1}(x_i))| \leq CN^{-2}\tau^2\varepsilon^{-1} \leq C(N^{-1}\ln N)^2$. The maximum principle gives $|(W_i^{j+1} - W^{j+1}(x_i))| \leq C(N^{-1}\ln N)^2, \ \ x_i \in [0,\tau] \cup [1-\tau, 1]$. On the sub-interval $[\tau, 1-\tau]$, the local truncation error of the singular component is

$$|\mathcal{L}_{\varepsilon}^{N,M}(W_i^{j+1} - W^{j+1}(x_i))| \leq \varepsilon\theta|\left(D^+D^- - \frac{d^2}{dx^2}\right)W^{j+1}(x_i)|.$$

However, $|D^+D^-W^{j+1}(x_i)| \leq \max_{x\in[x_{i-1},\, x_{i+1}]}|W''(x_i, t_{j+1})|$, and as a result,

$$\begin{aligned}|\mathcal{L}_{\varepsilon}^{N,M}(W_i^{j+1} - W^{j+1}(x_i))| \leq & \varepsilon\theta|\left(D^+D^- - \frac{d^2}{dx^2}\right)W^{j+1}(x_i)| \\ \leq & \varepsilon\theta\left(|D^+D^-W^{j+1}(x_i)| + \left|\frac{d^2W^{j+1}(x_i)}{dx^2}\right|\right) \\ \leq & 2\varepsilon\theta\max_{x\in[x_{i-1},\, x_{i+1}]}|W''(x_i, t_{j+1})| \leq \ 2\varepsilon\theta|W^{j+1}(x_i)|_2.\end{aligned}$$

The estimate of $W''(x_i, t_{j+1})$ leads to

$$\begin{aligned}|\mathcal{L}_{\varepsilon}^{N,M}(W_i^{j+1} - W^{j+1}(x_i))| \leq\ & 2\varepsilon\theta|W^{j+1}(x_i)|_2 \leq 2\varepsilon\theta C\varepsilon^{-1}e^{-x_{i-1}\sqrt{\frac{\lambda}{\varepsilon}}}, \quad x_{i-1} > \tau \\ & \leq Ce^{-\sqrt{\frac{\lambda}{\varepsilon}}\tau} \\ & \leq CN^{-2},\ \tau = 2\sqrt{\frac{\varepsilon}{\lambda}}\ln N,\end{aligned}$$

which implies that $|\mathcal{L}_{\varepsilon}^{N,M}(W_i^{j+1} - W^{j+1}(x_i))| \leq CN^{-2} \leq C(N^{-1}\ln N)^2, \quad x_i \in (\tau, 1-\tau)$. So, the maximum principle leads to $|(W_i^{j+1} - W^{j+1}(x_i))| \leq C(N^{-1}\ln N)^2$ on $[\tau, 1-\tau]$.

Combining the aforementioned findings for singular components on $(0, 1]$ with analogous procedures and results on the interval $(1, 2)$, the singular component is estimated as

$$|W_i^{j+1} - W^{j+1}(x_i)| \leq C(N^{-1}\ln N)^2. \tag{6.21}$$

Thus, from the results in (6.19) and (6.21),

$$|U_i^{j+1} - U^{j+1}(x_i)| \leq C(N^{-1}\ln N)^2, \tag{6.22}$$

which is the error estimate in the spatial direction. ■

Theorem 6.3.2 *Let $u(x,t)$ be the solution of the continuous problem (6.1) and U_i^{j+1} be the solution of the discrete problem (6.16). Then, the uniform error estimate is*

$$\sup_{0<\varepsilon\leq 1}\|u(x_i, t_{j+1}) - U_i^{j+1}\| \leq \begin{cases} C(\Delta t + (N^{-1}\ln N)^2), & \frac{1}{2} < \theta \leq 1, \\ C((\Delta t)^2 + (N^{-1}\ln N)^2), & \theta = \frac{1}{2}. \end{cases}$$

Proof. From the triangular inequality,

$$|u(x_i, t_{j+1}) - U_i^{j+1}| \leq |u(x_i, t_{j+1}) - U^{j+1}(x_i)| + |U^{j+1}(x_i) - U_i^{j+1}|.$$

Then, combining Lemma 6.3.4 and Theorem 6.3.1 yields

$$\sup_{0<\varepsilon\leq 1}\|u(x_i, t_{j+1}) - U_i^{j+1}\| \leq \begin{cases} C(\Delta t + (N^{-1}\ln N)^2), & \frac{1}{2} < \theta \leq 1, \\ C((\Delta t)^2 + (N^{-1}\ln N)^2), & \theta = \frac{1}{2}, \end{cases}$$

which is the required uniform error estimate. ■

6.4 Numerical results and discussions

The numerical scheme proposed in this chapter is demonstrated by solving two examples of singularly perturbed parabolic differential equations involving large shift, which are taken from previous research works in the literature. Due to the presence of the perturbation parameter and delay term, it is difficult to solve the problems analytically. However, applying the proposed numerical method, the problems are treated easily. The maximum absolute error and corresponding rate of convergence are computed applying the double mesh principle of the form (4.44)-(4.47).

Example 6.4.1 *(Kumari & Kumar, 2020). Consider problem (6.1) with* $a(x) = 3$*,* $b(x) = -1$*,* $f(x) = 1$*,* $u_0(x) = 0$*,* $\phi(x,t) = 0$ *and* $\alpha(t) = 0$*.*

Example 6.4.2 *(Bansal & Sharma, 2018). Consider problem (6.1) with* $a(x) = 5$*,* $b(x) = -2$*,* $f(x) = 2$*,* $u_0(x) = \sin(\pi x)$*,* $\phi(x,t) = 0$ *and* $\alpha(t) = 0$*.*

The examples are solved applying the fitted mesh finite difference scheme formulated in this chapter. Since the exact solutions are not given, the double mesh principle is applied to compute the maximum absolute errors and rate of convergence, and the obtained results are given in tabular and graphical forms. The maximum absolute errors and corresponding rate of convergences are are computed as shown in Table 6.1 for Example 6.4.1 and in Table 6.2 for Example 6.4.2. From these tables, one can see that for a given ε, increasing the mesh numbers decreases the absolute point-wise error. And by fixing the mesh numbers and decreasing the value of the perturbation parameter results in stable and uniform maximum point-wise errors. This shows the ε-uniform convergence of the proposed numerical schemes. Table 6.3 shows the comparisons of the present method with other results published in the literature. As it is seen in the comparison table, the accuracy of the present method is better than that of the other methods.

The numerical solutions of 6.4.1 and 6.4.2 are simulated graphically as shown in Figures 6.1 and 6.2, respectively, at different time levels. From these graphs, one can visualize that for $\varepsilon = 2^0$, the figure shows the solution of unperturbed differential equation and decreasing the perturbation parameter decreases the width of the layers. Also, to depict the physical behaviors of the solutions, surface plots are shown in Figures 6.2 and 6.4 for Examples 6.4.1 and 6.4.2, respectively. From these figures, it is also observed that as ε approaches to zero, the widths of the boundary and the interior layers are are minimized.

Table 6.1: Maximum absolute errors and convergence rate for Example 6.4.1 taking $\beta = 1$ and $\theta = 0.5$.

ε $\vert N \rightarrow$	36	72	144	288	576
$\downarrow$ $\vert M \rightarrow$	36	72	144	288	576
2^0	3.4088e-03	1.6766e-03	8.4491e-04	4.2326e-04	2.1177e-04
	1.0224	0.9887	0.9973	0.9990	
2^{-2}	3.2042e-03	1.6160e-03	8.1425e-04	4.1563e-04	2.1031e-04
	0.9875	0.9889	0.9702	0.9829	
2^{-4}	1.4063e-03	1.1065e-03	7.5135e-04	4.0055e-04	2.0233e-04
	0.3459	0.5584	0.9075	0.9853	
2^{-6}	2.3392e-03	7.9088e-04	4.0311e-04	2.6921e-04	1.0661e-04
	1.5645	0.9723	0.5824	1.3364	
2^{-8}	5.9840e-03	2.7311e-03	7.9285e-04	2.0350e-04	5.1067e-05
	1.1316	1.7844	1.9620	1.9946	
2^{-10}	9.5374e-03	6.7288e-03	2.7339e-03	7.9334e-04	2.0359e-04
	0.5032	1.2994	1.7849	1.9623	
2^{-12}	9.5374e-03	7.2339e-03	3.6544e-03	1.5725e-03	5.0898e-04
	0.3988	0.9851	1.2166	1.6274	
2^{-14}	9.5374e-03	7.2339e-03	3.6544e-03	1.5725e-03	5.0898e-04
	0.3988	0.9851	1.2166	1.6274	
$e^{N,M}$	9.5374e-03	7.2339e-03	3.6544e-03	1.5725e-03	5.0898e-04
$r^{N,M}$	0.3988	0.9851	1.2166	1.6274	-

Table 6.2: Maximum absolute errors and convergence rate for Example 6.4.2, taking $\beta = 1.5$ and $\theta = 0.5$

ε $\|N \rightarrow$	64	128	256	512	1024
$\downarrow$ $\|M \rightarrow$	32	64	128	256	512
2^{-2}	8.6368e-03	3.8818e-03	1.9143e-03	9.5221e-04	4.7773e-04
	1.1538	1.0199	1.0075	0.9951	
2^{-4}	6.8183e-03	3.6671e-03	1.8082e-03	9.4268e-04	4.7524e-04
	0.8948	1.0201	0.9397	0.9881	
2^{-6}	4.8601e-03	2.3395e-03	1.6507e-03	9.0401e-04	4.4682e-04
	1.0548	0.5031	0.8687	1.0166	
2^{-8}	6.6227e-03	2.1333e-03	5.7181e-04	5.5287e-04	4.0721e-04
	1.6343	1.8995	0.0486	0.4417	
2^{-10}	1.1337e-02	6.2471e-03	2.1336e-03	5.7187e-04	1.4558e-04
	0.8598	1.5499	1.8995	1.9739	
2^{-12}	1.1337e-02	6.2470e-03	2.5144e-03	8.5861e-04	2.7178e-04
	0.8598	1.3129	1.5501	1.6596	
2^{-14}	1.1336e-02	6.2469e-03	2.5144e-03	8.5860e-04	2.7178e-04
	0.8597	1.3129	1.5502	1.6595	
2^{-16}	1.1336e-02	6.2468e-03	2.5144e-03	1.0525e-03	2.7178e-04
	0.8597	1.3129	1.2564	1.9533	
2^{-18}	1.1336e-02	6.2468e-03	2.5144e-03	1.1547e-03	2.8047e-04
	0.8597	1.3129	1.1227	2.0416	
2^{-20}	1.1336e-02	6.2468e-03	2.5144e-03	1.2045e-03	2.9409e-04
	0.8597	1.3129	1.0618	2.0341	
$e^{N,M}$	1.1337e-02	6.9304e-03	2.5144e-03	1.2045e-03	4.7875e-04
$r^{N,M}$	0.7100	1.4627	1.0618	1.3311	-

Table 6.3: Comparisons of the present method with other results in literature.

Example 6.4.1 with $\theta = 0.5$ and $T = 1$				
$N = M$:	36	72	144	288
Present method				
$e^{N,M}$	5.1103e-03	2.8812e-03	1.2004e-03	3.9571e-04
$r^{N,M}$	0.8267	1.2632	1.6010	
Kumari & Kumar (2020)				
$e^{N,M}$	7.0100e-03	2.9700e-03	1.1400e-03	4.0600e-04
$r^{N,M}$	1.2390	1.3814	1.4895	
Example 6.4.2 with $\theta = 0.5$ and $e^{2N,4M}$				
N/M :	$64/32$	$128/128$	$256/512$	5122048
Present method				
$r^{N,M}_{\varepsilon=2^{-20}}$	1.7710	1.8278	1.7093	1.6930
Bansal & Sharma (2018)				
$r^{N,M}_{\varepsilon=2^{-20}}$	1.7908	1.8354	1.5091	1.6257

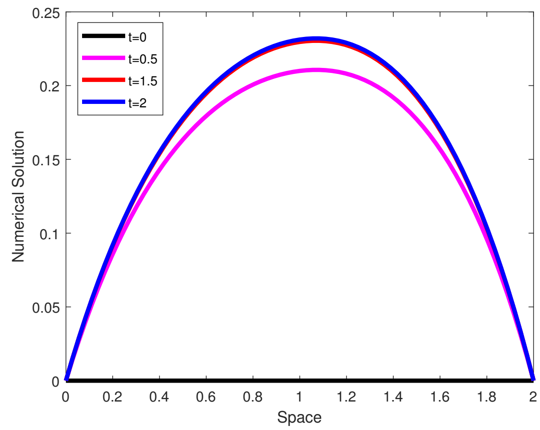

(a) $\varepsilon = 2^0$ (b) $\varepsilon = 2^{-14}$

Figure 6.1: Simulations of the numerical solution of Example 6.4.1, taking θ=0.5, β=1 and N=72 and M=72 at four different time levels (line plots).

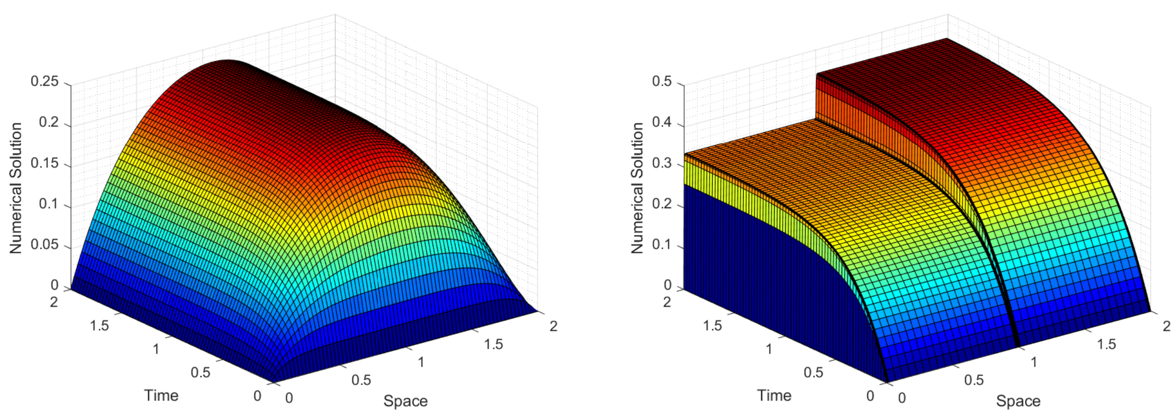

(a) $\varepsilon = 2^0$ (b) $\varepsilon = 2^{-14}$

Figure 6.2: Simulations of the numerical solution of Example 6.4.1, taking θ=0.5, β=1 and N=72 and M=72 at four different time levels (Surface plots).

6.5 Summary

In this chapter, a singularly perturbed differential equation with large negative shift is considered. Due to the influences of the perturbation parameter and the shifted term, the solution of the problem changes rapidly in the layers, which is a challenging factor to solve the problem analytically. Here the problem is solved by formulating a fitted mesh finite difference scheme. The scheme is derived using the θ-method on a uniform temporal mesh and using the central difference operator on a piece-wise uniform meshes. The stability estimate is established and

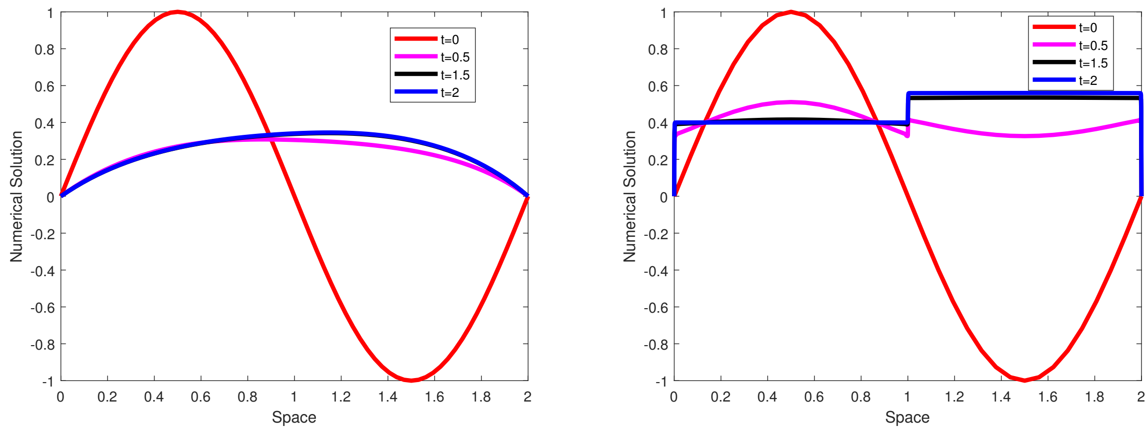

(a) $\varepsilon = 2^0$ (b) $\varepsilon = 2^{-14}$

Figure 6.3: Simulations of the numerical solution of Example 6.4.2, taking θ=0.5, β=1 and N=64 and M=32 at four different time levels (line plots).

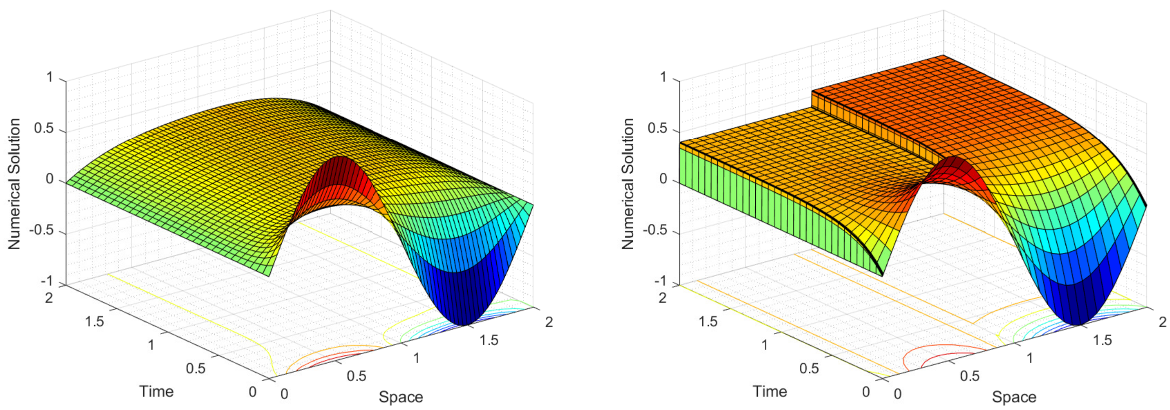

(a) $\varepsilon = 2^0$ (b) $\varepsilon = 2^{-14}$

Figure 6.4: Simulations of the numerical solution of Example 6.4.2, taking θ=0.5, β=1 and N=64 and M=32 at four different time levels (Surface plots).

uniform convergence analysis is investigated for the developed numerical method. The method is demonstrated by solving two model examples. From the theoretical and numerical results of the obtained scheme, it is observed that the obtained numerical scheme is uniformly convergent in time and space variables.

CHAPTER SEVEN

A NONSTANDARD FINITE DIFFERENCE METHOD FOR SINGULARLY PERTURBED PARTIAL DIFFERENTIAL EQUATIONS WITH LARGE NEGATIVE SHIFT

The chapter deals with the formulation and analysis of a nonstandard finite difference method for a singularly perturbed partial differential equations with large negative shift. Nonstandard finite difference methods are important to capture the instability of standard numerical methods and handle the abruptly varying behavior of the solution in the layers. To formulate the numerical scheme, the spatial and temporal domains are discretized uniformly. Then, a nonstandard finite difference method is proposed by deriving denominator functions for both the temporal and spatial discretization.

7.1 The governing problem

Consider a singularly perturbed partial differential equation on $\Omega = \Gamma \times \mathit{\Lambda} = (0,2) \times (0,T]$ as

$$\mathcal{L}_\varepsilon u(x,t) = u_t(x,t) - \varepsilon u_{xx}(x,t) + a(x)u(x,t) + b(x)u(x-1,t) = f(x,t), \tag{7.1}$$

subjected to the initial and interval-boundary conditions

$$u(x,0) = u_0(x),\ x \in \bar{\Gamma}, \tag{7.2a}$$

$$u(x,t) = \phi(x,t),\ (x,t) \in \Omega^-, \tag{7.2b}$$

$$u(2,t) = \alpha(t),\ (2,t) \in \Omega^+, \tag{7.2c}$$

where $0 < \varepsilon \ll 1$, $\Omega^- = \{(x,t) : x \in [-1,0]; t \in (0,T]\}$, $\Omega^+ = \{(2,t) : t \in (0,T]\}$ for a finite time T and the differential operator $\mathcal{L}_\varepsilon$ independent of ε.The functions involved in the governing equation are assumed to be sufficiently smooth. Moreover, for arbitrary positive constant λ, the coefficient functions are considered to satisfy

$$a(x) + b(x) \geq 2\lambda > 0 \text{ and } b(x) < 0,\ x \in \bar{\Gamma}. \tag{7.3}$$

Depending on the interval condition, (7.1) can be equivalently written as

$$\mathcal{L}_\varepsilon u(x,t) \equiv \begin{cases} u_t(x,t) - \varepsilon u_{xx}(x,t) + a(x)u(x,t) = f(x,t) - b(x)\phi(x-1.t),\ (x,t) \in (0,1] \times \Lambda, \\ u_t(x,t) - \varepsilon u_{xx}(x,t) + a(x)u(x,t) + b(x)u(x-1,t) = f(x,t),\ (x,t) \in (1,2) \times \Lambda. \end{cases} \tag{7.4}$$

with the conditions given as in (7.2a)-(7.2c). Setting $\varepsilon = 0$, (7.4) is reduced to

$$\mathcal{L}_\varepsilon u_0(x,t) \equiv \begin{cases} (u_0)_t + a(x)u_0(x,t) = f(x,t) - b(x)\phi(x-1.t), \ (x,t) \in (0,1] \times \Lambda, \\ (u_0)_t + a(x)u_0(x,t) + b(x)u_0(x-1,t) = f(x,t), \ (x,t) \in (1,2) \times \Lambda. \end{cases} \tag{7.5}$$

In the reduced problem (7.5), since $u_0(x,t)$ need not necessarily satisfy the conditions $u_0(0,t) = \phi(0,t)$, $u_0(2,t) = \alpha(t)$, $u_0(1^+,t) = u_0(1^-,t)$ and $(u_0)_x(1^+,t) = (u_0)_x(1^-,t)$, in general the solution $u(x,t)$ exhibits two strong boundary layers at the two ends of the domain and strong interior layer at $x = 1$ (Lange & Miura, 1982). Also, compatibility conditions are imposed as

$$\begin{cases} u_0(0,0) = \phi(0,0), \\ u_0(2,0) = \alpha(2,0). \end{cases} \tag{7.6}$$

and

$$\begin{cases} \phi_t(0,0) - \varepsilon(u_0)_{xx}(0) + a(0)u_0(0) = f(0,0) - b(0)\phi(-1.0), \\ \alpha_t(2,0) - \varepsilon(u_0)_{xx}(2) + a(2)u_0(2) + b(2)u_0(1,0) = f(2,0), \end{cases} \tag{7.7}$$

which show that the considered data hold at the two corner points $(0,0)$ and $(2,0)$. From the imposed compatibility conditions in (7.6) - (7.7), the existence of C independent ε is guaranteed and the problem has unique solution (Eloe et al., 2005). Thus, $(x,t) \in \bar{\Omega}$,

$$|u(x,t) - u(x,0)| \le Ct. \tag{7.8}$$

If ε small enough, the solution $u(x,t)$ of (7.1)-(7.2) closes to $u_0(x,t)$. Also, with out lose of generality assuming that all the data given in (7.2a)-(7.2c) are identically zero (Kadalbajoo & Awasthi, 2011), so that the following properties of $u(x,t)$ are true.

7.2 Properties of the continuous solution

Lemma 7.2.1 *(Roos et al., 2008). The solution $u(x,t)$ of (7.1)-(7.2) can be bounded as*

$$|u(x,t)| \le C, \ (x,t) \in \bar{\Omega}.$$

Proof. From (7.8), it follows that $|u(x,t)| - |u_0(x)| \le |u(x,t) - u_0(x)| \le Ct$, which gives $|u(x,t)| \le Ct + |u_0(x)|$, $\forall (x,t) \in \bar{\Omega}$. Thus, as $u_0(x)$ is bounded and $t \in (0,T]$, $|u(x,t)| \le C$ for all $(x,t) \in \bar{\Omega}$. ■

Lemma 7.2.2 *(Continuous maximum principle). Let $\omega(x,t)$ is any continuous function in $\bar{\Omega}$. If $\omega(x,t) \ge 0, \ (x,t) \in \partial\Omega$ and $\mathcal{L}_\varepsilon \omega(x,t) \ge 0, \ (x,t) \in \Omega$, then $\omega(x,t) \ge 0, (x,t) \in \bar{\Omega}$.*

Proof. Let $(\xi,\iota)\in\bar{\Omega}$ such that $\omega(\xi,\iota)=\min_{\bar{\Omega}}\omega(x,t)$ and let $\omega(\xi,\iota)<0$. By the given hypothesis, $(\xi,\iota)\notin\partial\Omega$ and by the extreme value theorem, $\omega_x(\xi,\iota)=0$, $\omega_t(\xi,\iota)=0$, $\omega_{xx}(\xi,\iota)\geq 0$.
Case 1: On $(0,1]$, $\mathcal{L}_{\varepsilon,1}\omega(\xi,\iota)=\frac{\partial\omega}{\partial t}(\xi,\iota)-\varepsilon\frac{\partial^2\omega}{\partial x^2}(\iota,\iota)+a(\xi)\omega(\xi,\iota)=(-\varepsilon\frac{\partial^2}{\partial x^2}+a(\xi))\omega(\xi,\iota)\leq 0$.
Case 2: On $(1,2)$, $\mathcal{L}_{\varepsilon,2}\omega(\xi,\iota)=\frac{\partial\omega}{\partial t}(\xi,\iota)-\varepsilon\frac{\partial^2\omega}{\partial x^2}(\xi,\iota)+a(\xi)\omega(\xi,\iota)+b(\xi)\omega(\xi-1,\iota)\leq\frac{\partial\omega}{\partial t}(\xi,\iota)-\varepsilon\frac{\partial^2\omega}{\partial x^2}(\xi,\iota)+a(\xi)\omega(\xi,\iota)+b(\xi)\omega(\xi,\iota)\leq 0$.
From the two cases, a contradiction to the hypothesis is occurred. Thus, the assumption fails and $\omega(\xi,\iota)\geq 0$, which implies that $\omega(x,t)\geq 0,\ (x,t)\in\bar{\Omega}$. ■

Lemma 7.2.3 *(Swaminathan et al., 2016). Let $u(x,t)$ be the solution of (7.1). Then, it can be bounded as*

$$|u(x,t)|\leq\max\left\{||u||_{\partial\Omega},\frac{1}{\lambda}||\mathcal{L}_\varepsilon u||\right\},$$

where $\|u\|_{\partial\Omega}=\{u(x,0)|,|u(0,t)|,|u(2,t)|\}$.

Proof. Define barrier functions as $\omega^{\pm}(x,t)=\max\left\{||u||_{\partial\Omega},\frac{1}{\lambda}||\mathcal{L}_\varepsilon u||\right\}\pm u(x,t)$. Then,

$$\text{For } t=0,\ \omega^{\pm}(x,0)=\max\left\{\|u\|_{\partial\Omega},\frac{1}{\lambda}\|\mathcal{L}_\varepsilon u\|\right\}\pm u(x,0)\geq\frac{1}{\lambda}\|\mathcal{L}_\varepsilon u\|\pm u(x,0)\geq 0.$$
$$\text{For } x=0,\ \omega^{\pm}(0,t)=\max\left\{\|u\|_{\partial\Omega},\frac{1}{\lambda}\|\mathcal{L}_\varepsilon u\|\right\}\pm u(0,t)\geq\frac{1}{\lambda}\|\mathcal{L}_\varepsilon u\|\pm u(0,t)\geq 0.$$
$$\text{For } x=2,\ \omega^{\pm}(2,t)=\max\left\{\|u\|_{\partial\Omega},\frac{1}{\lambda}\|\mathcal{L}_\varepsilon u\|\right\}\pm u(2,t)\geq\frac{1}{\lambda}\|\mathcal{L}_\varepsilon u\|\pm u(2,t)\geq 0.$$
$$\begin{aligned}\text{For } x\in(0,1],\ \mathcal{L}_\varepsilon\omega^{\pm}(x,t)&=\omega_t^{\pm}-\varepsilon\omega_{xx}^{\pm}+a(x)\omega^{\pm}(x,t)+b(x)\phi^{\pm}(x-1,t)\\&\geq a(x)\max\left\{\|u\|_{\partial\Omega},\frac{1}{\lambda}\|f\|\right\}\pm f(x,t)\geq 0.\\\text{For } x\in(1,2),\ \mathcal{L}_\varepsilon\omega^{\pm}(x,t)&=\omega_t^{\pm}-\varepsilon\omega_{xx}^{\pm}+a(x)\omega^{\pm}(x,t)+b(x)u^{\pm}(x-1,t)\\&\geq 2\lambda\max\left\{\|u\|_{\partial\Omega},\frac{1}{\lambda}\|f\|\right\}\pm f(x,t)\geq 0.\end{aligned}$$

Hence, applying Lemma 7.2.2 implies $\omega^{\pm}(x,t)\geq 0$ for all $(x,t)\in\bar{\Omega}$, which yields the required stability estimate. ■

Lemma 7.2.4 (Bound on the derivatives of the solution). The derivatives of the solution $u(x,t)$ of (7.1) can be bounded as

$$\left|\frac{\partial^{i+j}u(x,t)}{\partial x^i\partial t^j}\right|\leq\begin{cases}C\left[1+\varepsilon^{\frac{-i}{2}}\left(\exp(-\sqrt{\frac{\lambda}{\varepsilon}}x)+\exp(-\sqrt{\frac{\lambda}{\varepsilon}}(1-x))\right)\right],\ (x,t)\in(0,1]\times\Lambda,\\C\left[1+\varepsilon^{\frac{-i}{2}}\left(\exp(-\sqrt{\frac{\lambda}{\varepsilon}}(x-1))+\exp(-\sqrt{\frac{\lambda}{\varepsilon}}(2-x))\right)\right],\ (x,t)\in(1,2)\times\Lambda\end{cases}$$

for all non-negative integer i,j such that $i+2j\in[0,4]$.

Proof. To determine the bound of the derivatives of the solution of the continuous problem, we follow the procedures in Clavero & Gracia (2010) and Kellogg & Tsan (1978). For $(x,t) \in \bar{\Omega}$, consider the case when $i = 0$, which implies differentiating $u(x,t)$ with respect to time. For $j = 0$, it implies Lemma 7.2.1. For $j = 1$, rearranging (7.1) gives

$$u_t(x,t) = \varepsilon u_{xx}(x,t) - a(x)u(x,t) - b(x)u(x-1,t) + f(x,t). \tag{7.9}$$

With out lose of generality assuming that $u(x,0) = u_0 = 0$, $u(x,t) = \phi(x,t) = 0$, $u(2,t) = \gamma(t) = 0$, (7.9) becomes

$$u_t(x,0) = \varepsilon u_{xx}(x,0) - a(x)u(x,0) - b(x)u(x-1,0) + f(x,0). \tag{7.10}$$

Thus, along $x = 0$ and $x = 2$, $u(x,t) = 0$ which gives $u_t = 0$ and along $t = 0$, $u(x,0) = 0$, so that $u_{xx} = 0,\ t = 0$. On the interval $[0,1]$, $u(x-1,0) = \phi(x-1,0) = 0$ and on the interval $[1,2]$, $u(x-1,0) = u_0(x-1,0) = 0$. Combining these results give $u(x-1,0) = 0$, so that (7.10) becomes $u_t(x,0) = f(x,0)$ and since f is smooth function, $|u(x,0)| \le C$ on $\partial\Omega$, which implies that

$$|u_t(x,t)| \le C \quad \text{on } \bar{\Omega}. \tag{7.11}$$

In a similar way for $j = 2$, assuming that all the data given in (7.2a)-(7.2c) are identically zero and differentiating with respect to t gives $u_{tt}(x,t) - \varepsilon u_{xxt}(x,t) + a(x)u_t(x,t) + b(x)u_t(x-1,t) = f_t(x,t)$ and along $t = 0$, it becomes

$$u_{tt}(x,0) - \varepsilon u_{xxt}(x,0) + a(x)u_t(x,0) + b(x)u_t(x-1,0) = f_t(x,0). \tag{7.12}$$

But, from $u_t(x,0) = f(x,0)$, it follows that $u_{xxt}(x,0) = f_{xx}(x,0)$ and $u_t(x-1,0) = 0$, so that (7.12) becomes $u_{tt}(x,0) = \varepsilon f_{xx}(x,0) - a(x)f(x,0) + f_t(x,0)$. Therefore, $|u_{tt}(x,0)| \le C$ on $\partial\Omega$ and since f is smooth function, $|u_{tt}(x,t)| \le C$. Thus, for large value of C, $|u_{tt}(x,t)| \le C$, $(x,t) \in \bar{\Omega}$.

On the other hand, to obtain the bound of derivatives of the solution with respect to the spatial variable, consider for $i = 0,1,2,3,4$. For $i = 0$, it is an immediate result of Lemma 7.2.1. For $i = 1$, let $x \in \Gamma$ and consider a neighborhood $I = (\iota, \iota + \sqrt{\varepsilon})$, $\forall x \in I$. Then, for some d in $\bar{I}$ and fixed $t \in (0,T]$, by the mean value theorem,

$$|u_x(d,t)| = \left| \frac{u(\iota + \sqrt{\varepsilon}, t) - u(\iota, t)}{\sqrt{\varepsilon}} \right| = \frac{1}{\sqrt{\varepsilon}} |u(\iota + \sqrt{\varepsilon}, t) - u(\iota, t)| \le C\varepsilon^{\frac{-1}{2}} \|u\|. \tag{7.13}$$

For $x \in \bar{I}$, it is true that

$$u_x(x,t) = u_x(d,t) + \varepsilon^{-1} \int_d^x (u_t(s,t) + a(s)u(s,t) + b(s)u(s-1,t) - f(s,t))\, ds,$$

which implies that

$$|u_x(x,t)| \leq \; |u_x(d,t)| + C\varepsilon^{-1} \int_d^x \left(\|u\| + \|f\|\right) ds = \; |u_x(d,t)| + C\varepsilon^{-1} \left(\|u\| + \|f\|\right) \varepsilon^{\frac{1}{2}}.$$

Using (7.13) in the above result yields $|u_x(x,t)| \leq C\varepsilon^{\frac{-1}{2}}, \forall (x,t) \in \bar{\Omega}$. Rearranging the terms in (7.1) gives

$$u_{xx}(x,t) = \varepsilon^{-1} \left(u_t(x,t) + a(x)u(x,t) + b(x)u(x-1,t) - f(x,t)\right). \tag{7.14}$$

For a fixed t in $[0,T]$ and for $x \in [0,2]$, since $|u| \leq C$, $|u_t| \leq C$ and f is smooth function, it implies that $|u_{xx}(x,t)| \leq C\varepsilon^{-1}$. Differentiating both sides of (7.14) with respect to t gives

$$u_{xxt}(x,t) = \varepsilon^{-1} \left(u_{tt}(x,t) + a(x)u_t + b(x)u_t(x-1,t) - f_t(x,t)\right).$$

Since $|u_t(x,t)| \leq C$, $|u_{tt}(x,t)| \leq C$ and $|f_t(x,t)| \leq C$, it follows that $|u_{xxt}(x,t)| \leq C\varepsilon^{-1}$. By a similar procedure for the remaining values of i and j satisfying $0 \leq i+2j \leq 4$, the derivatives of the solution can be bounded. ■

7.3 The numerical method

In this section, the temporal domain is discretized into M uniform meshes, and a semi-discrete scheme is constructed. Then, the spatial domain $[0,2]$ is discretized into N uniform meshes, on which a fully discrete scheme is to be formulated.

7.3.1 Temporal discretization

Let $(0,T]$ be a given time domain for some finite time T, which can be sub-divided into M equal intervals forming uniform temporal mesh as $\Omega_t^M = \{t_j = j\Delta t, \;\; j = 0(1)M-1, \;\; T = M\Delta t\}$. From the rules upon which nonstandard schemes are based Ehrhardt & Mickens (2013), the time derivative in (7.1) takes the form $u_t \to \frac{U^{j+1}(x) - U^j(x)}{\mu(\Delta t)}$, where $\mu(\Delta t)$ is the denominator function satisfying $\mu(\Delta t) = \Delta t + O((\Delta t)^2)$. Thus, for the sub-equation $u_t(x,t) = -\lambda u(x,t)$, where $a(x) \geq \lambda > 0$, the standard forward difference approximation is $\frac{U^{j+1}(x) - U^j(x)}{\Delta t} = -\lambda U^j$, which can be written as

$$U^{j+1}(x) = \left(1 - \lambda\Delta t\right) U^j(x). \tag{7.15}$$

However, it is well known that (7.15) leads to instability if $\lambda\Delta t > 1$ Mickens (1994). Instead, from the fact that $1 - \lambda\Delta t = \exp(-\lambda\Delta t) + O((\lambda\Delta t)^2)$ for sufficiently small $\lambda\Delta t$ (i.e., $0 < \lambda\Delta t \ll 1$), it is possible to make the replacement $1 - \lambda\Delta t \approx \exp(-\lambda\Delta t)$, so that $\Delta t \approx \frac{1-\exp(-\lambda\Delta t)}{\lambda}$. Adapting this for the variable coefficient yields a denominator function as

$$\mu(\Delta t) = \frac{1 - \exp(-a(x)\Delta t)}{a(x)}. \tag{7.16}$$

Now, applying the Crank-Nicolson method in the temporal direction incorporating the denominator function (7.16), a semi-discrete scheme is obtained as

$$\begin{aligned}\mathcal{L}_{\varepsilon}^{M}U^{j+1}(x) \equiv &\frac{U^{j+1}(x)-U^{j}(x)}{\mu(\Delta t)} - \frac{\varepsilon}{2}\left(U_{xx}^{j+1}(x)+U_{xx}^{j}(x)\right) + \frac{a(x)}{2}\left(U^{j+1}(x)+U^{j}(x)\right)\\ &+\frac{b(x)}{2}\left(U^{j+1}(x-1)+U^{j}(x-1)\right) = \frac{1}{2}\left(f^{j+1}(x)+f^{j}(x)\right) \end{aligned} \tag{7.17}$$

and rearranging terms and simplifying on $[0,2]$ become

$$\mathcal{L}_{\varepsilon}^{M}U^{j+1}(x)=\begin{cases}-\varepsilon U_{xx}^{j+1}(x)+\left(\frac{2}{\mu(\Delta t)}+a(x)\right)U^{j+1}(x)=\varepsilon U_{xx}^{j}(x)+\left(\frac{2}{\mu(\Delta t)}-a(x)\right)U^{j}(x)\\ -2b(x)\phi^{j+1/2}(x-1)+2f^{j+1/2}(x),\ \text{for } x\in(0,1],\\ -\varepsilon U_{xx}(x)+\left(\frac{2}{\mu(\Delta t)}+a(x)\right)U^{j+1}(x)+2b(x)U^{j+1}(x-1)\\ =\varepsilon U_{xx}^{j}(x)+\left(\frac{2}{\mu(\Delta t)}-a(x)\right)U^{j}(x)+2f^{j+1/2}(x),\ \text{for } x\in(1,2),\end{cases} \tag{7.18}$$

subjected to $U^{j+1}(x,0)=U_0^{j+1}(x),\ x\in\Gamma$, $U^{j+1}(x)=\phi(x,t_{j+1})$ and $U^{j+1}(2)=\alpha(2,t_{j+1})$ for $j=0(1)M-1$, where $U^{j+1}(x)$ is the approximate of $U(x,t_{j+1})$ at $(j+1)^{th}$ level. Equation (7.18) can rewritten as

$$\left(\frac{2}{\mu(\Delta t)}+\mathcal{L}_{\varepsilon}^{M}\right)U^{j+1}(x)=\vartheta^{j+1}(x),\ x\in\Gamma, \tag{7.19}$$

where

$$\mathcal{L}_{\varepsilon}^{M}U^{j+1}(x)=\begin{cases}-\varepsilon U_{xx}^{j+1}(x)+a(x)U^{j+1}(x),\ x\in(0,1],\\ -\varepsilon U_{xx}^{j+1}(x)+a(x)U^{j+1}(x)+b(x)U^{j+1}(x-1),\ x\in(1,2)\end{cases}$$

and

$$\vartheta^{j+1}(x)=\begin{cases}\varepsilon U_{xx}^{j}(x)+\left(\frac{2}{\mu(\Delta t)}-a(x)\right)U^{j}(x)-2b(x)\phi^{j+1/2}(x-1)+2f^{j+1/2}(x),\ x\in(0,1],\\ \varepsilon U_{xx}^{j}(x)+\left(\frac{2}{\mu(\Delta t)}-a(x)\right)U^{j}(x)-b(x)U^{j}(x-1)+2f^{j+1/2}(x),\ x\in(1,2),\end{cases}$$

where $\phi^{j+1/2}(x-1)=\frac{1}{2}(\phi^{j+1}(x-1)+\phi^{j}(x-1))$ and $f^{j+1/2}(x)=\frac{1}{2}(f^{j+1}(x)+f^{j}(x))$.

Lemma 7.3.1 *(Semi-discrete maximum principle). For a sufficiently smooth function ω^{j+1} in $\bar{\Omega}$, if $\omega^{j+1}(0)\geq 0$, $\omega^{j+1}(2)\geq 0$ and $\mathcal{L}_{\varepsilon}\omega^{j+1}(x)\geq 0$ for all $x\in\Gamma$, then $\omega^{j+1}(x)\geq 0,\ x\in\bar{\Gamma}$.*

Proof. Let $r\in\bar{\Gamma}$ such that $\omega^{j+1}(r)=\min_{\bar{\Gamma}}\omega^{j+1}(x)$ and suppose $\omega^{j+1}(r)<0$. From the given conditions, $r\notin\partial\Gamma$ and by the extreme value theorem, $\omega_x^{j+1}(r)=0$, $\omega_{xx}^{j+1}(r)\geq 0$.
Case 1: For $r\in(0,1]$,

$$\mathcal{L}_{\varepsilon,1}^{M}\omega^{j+1}(r)=-\varepsilon\omega_{xx}^{j+1}(r)+\left(\frac{2}{\mu(\Delta t)}+a(r)\right)\omega^{j+1}(r)\leq 0.$$

Case 2: For $r \in (1,2)$,

$$\begin{aligned}\mathcal{L}^{M}_{\varepsilon,2}\omega^{j+1}(r) &= -\,\varepsilon\omega^{j+1}_{xx}(r) + \left(\frac{2}{\mu(\Delta t)} + a(r)\right)\omega^{j+1}(r) + b(r)\omega^{j+1}(r-1)\\ &\leq -\,\varepsilon\omega^{j+1}_{xx}(r) + \left(\frac{2}{\mu(\Delta t)} + a(r) + b(r)\right)\omega^{j+1}(r) \leq 0.\end{aligned}$$

From the two cases, one can observe that the given hypothesis is contradicted and hence the assumption fails, so that $\omega^{j+1}(x) \geq 0$, $\forall x \in \bar{\Gamma}$. Thus, the maximum principle is satisfied by the operator $\mathcal{L}^{M}_{\varepsilon}$, and hence

$$\left\|\left(\mathcal{L}^{M}_{\varepsilon,x}\right)^{-1}\right\| \leq \frac{1}{1+2\lambda\Delta t}, \tag{7.20}$$

which is used to estimate the truncation error in the semi-discrete scheme. ■

Lemma 7.3.2 *(Bansal & Sharma, 2017). Let the solution of (7.19) be $U^{j+1}(x)$. Then. it can be estimated as*

$$|U^{j+1}(x)| \leq \frac{\|\vartheta^{j+1}\|}{1+2\lambda\Delta t} + \max\left\{|U^{j+1}(0)|, |U^{j+1}(2)|\right\},\ \forall x \in \bar{\Gamma}.$$

Proof. Can be easily shown following similar procedure as Lemma 7.2.3. ■

Definition 7.3.1 At the $(j+1)^{th}$ time level, local truncation error is defined as the difference between the solution $U(x,t_{j+1})$ and the numerical solution $U^{j+1}(x)$ of the semi-discrete problem (7.19) and given $e^{j+1}(x) = U(x,t_{j+1}) - U^{j+1}(x)$ and the global error E^{j+1} as the contribution of local truncation error up to the $(j+1)^{th}$ time level.

Lemma 7.3.3 *(Estimate of the local truncation error). Suppose it is given that $\left|\frac{\partial^k U(x,t)}{\partial t^k}\right| \leq C$ for all $(x,t) \in \bar{\Omega}$ and $k = 0,1,2$. Then, at $(j+1)^{th}$ time level, $\|e^{j+1}\| \leq C(\Delta t)^3$.*

Proof. Let us choose the center point $(x, t_{j+1/2})$ of the temporal mesh as a convenient base point where the Taylor series is expanded. Then $U(x,t_{j+1})$ and $U(x,t_j)$ can be expanded as

$$U^{j+1}(x) = U^{j+1/2}(x) + \frac{\Delta t}{2}\frac{\partial U^{j+1/2}(x)}{\partial t} + \frac{(\Delta t)^2}{8}\frac{\partial U^{j+1/2}(x)}{\partial t^2} + O((\Delta t))^3, \tag{7.21a}$$

$$U^{j}(x) = U^{j+1/2}(x) - \frac{\Delta t}{2}\frac{\partial U^{j+1/2}(x)}{\partial t} + \frac{(\Delta t)^2}{8}\frac{\partial U^{j+1/2}(x)}{\partial t^2} + O((\Delta t))^3. \tag{7.21b}$$

Now, subtracting (7.21b) from (7.21a) gives

$$\frac{U^{j+1}(x) - U^{j}(x)}{\mu(\Delta t)} = \frac{\partial U^{j+1/2}(x)}{\partial t} + O((\Delta t))^3. \tag{7.22}$$

Using (7.1) into (7.22) at $(x, t_{j+1/2})$ gives

$$\begin{aligned}\frac{U^{j+1}(x)-U^j(x)}{\mu(\Delta t)} =&\varepsilon\frac{\partial^2 U^{j+1/2}(x)}{\partial x^2} - a(x)U^{j+1/2}(x) - b(x)U^{j+1/2}(x-1)\\ &+ f(x,t_{j+1/2}) + O((\Delta t))^3.\end{aligned} \tag{7.23}$$

Putting (7.23) into the time semi-discrete problem (7.19) gives

$$\begin{aligned}&\varepsilon\frac{\partial^2 U^{j+1/2}(x)}{\partial x^2} - a(x)U^{j+1/2}(x) - b(x)U^{j+1/2}(x-1) + f(x,t_{j+1/2}) + O(\Delta t)^3\\ &-\frac{\varepsilon}{2}\left(\frac{\partial^2 U^{j+1}}{\partial x^2}+\frac{\partial^2 U^{j}}{\partial x^2}\right)+\frac{a(x)}{2}\left(U^{j+1}(x)+U^j(x)\right)\\ &+\frac{b(x)}{2}\left(U^{j+1}(x-1)+U^j(x-1)\right)=\frac{1}{2}\left(f^{j+1}(x)+f^j(x)\right),\end{aligned}$$

which can be written equivalently as

$$\mathcal{L}^M_{\varepsilon,x}\left(U(x,t_{j+1})-U^{j+1}(x)\right)=O((\Delta t))^3. \tag{7.24}$$

Using (7.20) into (7.24), a boundary value problem of the type $\mathcal{L}^M e^{j+1}(x) = O(\Delta t)^3$ with $e^{j+1}(0,t_{j+1}) = 0$ and $e^{j+1}(2) = 0$. Applying Lemma 7.3.1, the local truncation error is estimated as $\|e^{j+1}\| \le C(\Delta t)^3$. ■

Lemma 7.3.4 *(Estimation of the global error). Assuming that Lemma 7.3.3 holds, the global error in the time direction can be estimated as* $\|E^{j+1}\| \le C(\Delta t)^2$, $\forall j$ *such that* $j\Delta t \le T$.

Proof. Using Lemma 7.3.3 up to the $(j+1)^{th}$ level,

$$\begin{aligned}||E^{j+1}|| =&\left\|\sum_{k=1}^{j} e^k\right\|,\ \ j\bigtriangleup t\le T\\ \le&\|e^1\|+...+\|e^j\|\\ \le& C(\bigtriangleup t)^2.\end{aligned}$$

Thus, $\|E^{j+1}\| \le C(\Delta t)^2$, where C is independent of ε and the mesh numbers. ■

Lemma 7.3.5 *(Bansal & Sharma, 2018). Let the solution of (7.19) be $U^{j+1}(x)$. Then its derivatives can be bounded as*

$$\left|\frac{d^n U^{j+1}(x)}{dx^n}\right| \le \begin{cases} C\left[1+\varepsilon^{-n/2}\left(\exp(-\sqrt{\frac{\lambda}{\varepsilon}}x)+\exp(-\sqrt{\frac{\lambda}{\varepsilon}}(1-x))\right)\right], & x\in\bar{\Gamma},\ n=0(1)4,\\ C\left[1+\varepsilon^{-n/2}\left(\exp(-\sqrt{\frac{\lambda}{\varepsilon}}(x-1))+\exp(-\sqrt{\frac{\lambda}{\varepsilon}}(2-x))\right)\right], & x\in\bar{\Gamma}, n=0(1)4.\end{cases}$$

Proof. See Lemma 6.3.5 of Chapter 6. ■

7.3.2 Spatial discretization

Suppose $[0,2]$ be sub-divided into N equal steps of length h and form a mesh $\Omega_x^N = \{0 = x_0, x_1, ..., x_{N/2} = 1, x_{N/2+1}, ..., x_N = 2,\ x_i = ih, i = 0(1)N,\ h = 2/N\}$. Applying the techniques and rules of Mickens (2005), construct a nonstandard finite difference method for (7.19). Let β_1 and β_2 be denominator functions for the discrete difference schemes corresponding to the constant coefficient sub-equations

$$-\varepsilon U_{xx}^{j+1}(x) + \lambda U^{j+1}(x) = 0, \tag{7.25a}$$

and

$$\varepsilon U_{xx}^{j}(x) - \lambda U^{j}(x) = 0, \tag{7.25b}$$

respectively, where $a(x) \geq \lambda > 0$. Each of the characteristic equations of (7.25) has two distinct roots $r_1 = \exp(\sqrt{\frac{\lambda}{\varepsilon}}x)$ and $r_2 = \exp(-\sqrt{\frac{\lambda}{\varepsilon}}x)$. Using the theory of finite differences methods for (7.25a) and (7.25b) respectively,

$$-\varepsilon\frac{U_{i-1}^{j+1} - 2U_i^{j+1} + U_{i+1}^{j+1}}{\beta_1^2} + \lambda U_i^{j+1} = 0, \tag{7.26a}$$

$$\varepsilon\frac{U_{i-1}^{j} - 2U_i^{j} + U_{i+1}^{j}}{\beta_2^2} - \lambda U_i^{j} = 0. \tag{7.26b}$$

Denoting U_i^{j+1} to be the approximation of (7.25a) at the grid point x_i, then it is given as $U_i^{j+1} = c_1 e^{\sqrt{\frac{\lambda}{\varepsilon}}x_i} + c_2 e^{-\sqrt{\frac{\lambda}{\varepsilon}}x_i}$. Following the approaches of Mickens (1994),

$$det\begin{pmatrix} U_{i-1}^{j+1} & e^{\sqrt{\frac{\lambda}{\varepsilon}}x_{i-1}} & e^{-\sqrt{\frac{\lambda}{\varepsilon}}x_{i-1}} \\ U_{i}^{j+1} & e^{\sqrt{\frac{\lambda}{\varepsilon}}x_{i}} & e^{-\sqrt{\frac{\lambda}{\varepsilon}}x_{i}} \\ U_{i+1}^{j+1} & e^{\sqrt{\frac{\lambda}{\varepsilon}}x_{i+1}} & e^{-\sqrt{\frac{\lambda}{\varepsilon}}x_{i+1}} \end{pmatrix} = 0.$$

Simplifying this equation gives

$$U_{i-1}^{j+1} - 2\cosh\left(\sqrt{\frac{\lambda}{\varepsilon}}h\right)U_i^{j+1} + U_{i+1}^{j+1} = 0. \tag{7.27}$$

By the hyperbolic identity $\sinh(d/2) = \pm\sqrt{(\cosh(d)-1)/2}$, it implies that

$$\cosh\left(\sqrt{\frac{\lambda}{\varepsilon}}h\right) = 2\sinh^2\left(\sqrt{\frac{\lambda}{\varepsilon}}\frac{h}{2}\right) + 1. \tag{7.28}$$

Putting (7.28) into (7.27) gives

$$U_{i-1}^{j+1} + \left[-4\sinh^2\left(\sqrt{\frac{\lambda}{\varepsilon}}\frac{h}{2}\right) - 2\right]U_i^{j+1} + U_{i+1}^{j+1} = 0. \tag{7.29}$$

Comparing the coefficients of (7.26a) and (7.29) yields the denominator function as $\beta_1^2 = \frac{4\varepsilon}{\lambda}\sinh^2\left(\sqrt{\frac{\lambda}{\varepsilon}}\frac{h}{2}\right)$. By a similar procedure, $\beta_2^2 = \frac{4\varepsilon}{\lambda}\sinh^2\left(\sqrt{\frac{\lambda}{\varepsilon}}\frac{h}{2}\right)$. Adapting these for the variable coefficient problem gives the denominator functions $\beta_1^2 = \frac{4\varepsilon}{a^{j+1}(x_i)}\sinh^2\left(\sqrt{\frac{a^{j+1}(x_i)}{\varepsilon}}\frac{h}{2}\right)$ and $\beta_2^2 = \frac{4\varepsilon}{a^{j}(x_i)}\sinh^2\left(\sqrt{\frac{a^{j}(x_i)}{\varepsilon}}\frac{h}{2}\right)$. Incorporating these denominator functions, the required finite difference scheme is obtained as

$$\left(\frac{2}{\mu(\Delta t)} + \mathcal{L}_\varepsilon^{N,M}\right)U_i^{j+1} = \vartheta_i^{j+1},\ j = 0,1,2,...,M-1, \tag{7.30}$$

where

$$\mathcal{L}_\varepsilon^{N,M}U_i^{j+1} = \begin{cases} -\varepsilon\frac{U_{i-1}^{j+1}-2U_i^{j+1}+U_{i+1}^{j+1}}{\beta_1^2} + a_iU_i^{j+1},\ i = 1,2,...,\frac{N}{2}, \\ -\varepsilon\frac{U_{i-1}^{j+1}-2U_i^{j+1}+U_{i+1}^{j+1}}{\beta_1^2} + a_iU_i^{j+1} + b_iU_{i-\frac{N}{2}}^{j+1},\ i = \frac{N}{2}+1, \frac{N}{2}+2, ..., N-1 \end{cases}$$

and

$$\vartheta_i^{j+1} = \begin{cases} \varepsilon\frac{U_{i-1}^{j}-2U_i^{j}+U_{i+1}^{j}}{\beta_2^2} + \left(\frac{2}{\mu(\Delta t)} - a_i\right)U_i^j - 2b_i\phi_{i-\frac{N}{2}}^{j+1/2} + 2f_i^{j+1/2},\ i = 1,2,...,\frac{N}{2}, \\ \varepsilon\frac{U_{i-1}^{j}-2U_i^{j}+U_{i+1}^{j}}{\beta_2^2} + \left(\frac{2}{\mu(\Delta t)} - a_i\right)U_i^j - b_iU_{i-\frac{N}{2}}^{j} + 2f_i^{j+1/2},\ i = \frac{N}{2}+1, \frac{N}{2}+2, ..., N-1 \end{cases}$$

with the discrete initial and boundary conditions $U_i^0 = U_0(x_i), i = 0,1,...,N$, $U_i^{j+1} = \phi_i^{j+1}, i = -\frac{N}{2}, -\frac{N}{2}+1, ..., 0, j = 0,1,...,M-1$ and $U_N^{j+1} = \beta_N^{j+1}, j = 0,1,...,M-1$. From (7.30), a system of equation is derived as

$$A_iU_{i-1}^{j+1} + B_iU_i^{j+1} + A_iU_{i+1}^{j+1} = D_iU_{i-1}^{j} + E_iU_i^j + D_iU_{i+1}^j + G_i^{j+1}, \tag{7.31}$$

where

$$A_i = \frac{-a_i}{4\sinh^2\left(\sqrt{\frac{a_i^{j+1}}{\varepsilon}}\frac{h}{2}\right)},\quad B_i = \frac{a_i}{2\sinh^2\left(\sqrt{\frac{a_i}{\varepsilon}}\frac{h}{2}\right)} + a_i + \frac{2a_i}{1-\exp(-a_i\Delta t)},$$

$$D_i = \frac{a_i}{4\sinh^2\left(\sqrt{\frac{a_i}{\varepsilon}}\frac{h}{2}\right)},\quad E_i = \frac{-a_i}{2\sinh^2\left(\sqrt{\frac{a_i}{\varepsilon}}\frac{h}{2}\right)} - a_i + \frac{2a_i}{1-\exp(-a_i\Delta t)},$$

$$G_i^{j+1} = \begin{cases} 2f_i^{j+1/2} - 2b_i\phi_{i-\frac{N}{2}}^{j+1/2},\ i = 1,2,...,\frac{N}{2},\ j = 0,1,...,M-1, \\ 2f_i^{j+1/2} - 2b_iU_{i-\frac{N}{2}}^{j+1/2},\ i = \frac{N}{2}+1,...,N-1,\ j = 0,1,...,M-1. \end{cases}$$

Lemma 7.3.6 *(Discrete maximum principle). Suppose ω_i^{j+1} be any mesh function. If $\omega_0^{j+1} \geq 0$, $\omega_N^{j+1} \geq 0$ and $\left(\frac{2}{\mu(\Delta t)} + \mathcal{L}_\varepsilon^{N,M}\right)\omega_i^{j+1} \geq 0$, $i = 1,2,...,N-1$, then $w_i^{j+1} \geq 0$, $i = 0,1,2,...,N$.*

Proof. Assume that there exist $\iota \in \{0,1,...,N\}$ such that $\omega_\iota^{j+1} = \min_{i\in[0,N]}\omega_i^{j+1} < 0$. From the hypothesis, one can see that $\iota \notin \{0, N\}$. Assuming that $\omega_{\iota+1}^{j+1} - \omega_\iota^{j+1} > 0$ and

$\omega_\iota^{j+1} - \omega_{\iota-1}^{j+1} < 0$,

Case 1: For $\iota = 1, 2, ..., \frac{N}{2}$,

$$\left(\frac{2}{\mu(\Delta t)} + \mathcal{L}_\varepsilon^{N,M}\right)\omega_\iota^{j+1} = \frac{2\omega_\iota^{j+1}}{\mu(\Delta t)} - \varepsilon\left(\frac{\omega_{\iota-1}^{j+1} - 2\omega_\iota^{j+1} + \omega_{j+1}^{j+1}}{\beta_1^2}\right) + a_\iota\omega_\iota^{j+1} < 0.$$

Case 2: For $\iota = \frac{N}{2}+1, \frac{N}{2}+2, ..., N-1$,

$$\begin{aligned}\left(\frac{2}{\mu(\Delta t)} + \mathcal{L}_\varepsilon^{N,M}\right)\omega_\iota^{j+1} =& \frac{2\omega_\iota^{j+1}}{\mu(\Delta t)} - \varepsilon\left(\frac{\omega_{\iota-1}^{j+1} - 2\omega_\iota^{j+1} + \omega_{j+1}^{j+1}}{\beta_1^2}\right) + a_\iota\omega_\iota^{j+1} + b_\iota\omega_{\iota-N/2}^{j+1}\\ \le& \frac{2\omega_\iota^{j+1}}{\mu(\Delta t)} - \varepsilon\left(\frac{\omega_{\iota-1}^{j+1} - 2\omega_\iota^{j+1} + \omega_{j+1}^{j+1}}{\beta_1^2}\right) + a_\iota\omega_\iota^{j+1} + b_\iota\omega_\iota^{j+1} < 0.\end{aligned}$$

By the above cases for $\iota = 1, 2, ..., N-1$, $\left(\frac{2}{\mu(\Delta t)} + \mathcal{L}_\varepsilon^{N,M}\right)\omega_\iota^{j+1} \le 0$, which is a contradiction to the hypothesis. Thus, the assumption $\omega_\iota^{j+1} < 0$ is wrong, which implies that $\omega_i^{j+1} \ge 0, i = 0, 1.2, ..., N$. ∎

Lemma 7.3.7 *(Bansal & Sharma, 2017). The numerical solution U_i^{j+1} of (7.30), $i = 0, 1, 2, ..., N$, $j+1 = 1, 2, ..., M$ is bounded as*

$$\left|U_i^{j+1}\right| \le \frac{\|\vartheta_i^{j+1}\|}{1+2\lambda\Delta t} + \max\{|U_0^{j+1}|, |U_N^{j+1}|\}.$$

Proof. Define barrier functions $\omega_{i,j+1}^{\pm} = \frac{\|\vartheta_i^{j+1}\|}{1+2\lambda\Delta t} + \max\{|U_0^{j+1}|, |U_N^{j+1}|\} \pm U_i^{j+1}$.
For $i = 0$, $\omega_{0,j+1}^{\pm} = \frac{\|\vartheta_0^{j+1}\|}{1+2\lambda\Delta t} + \max\{|U_0^{j+1}|, |U_N^{j+1}|\} \pm U_0^{j+1} \ge \frac{\|\vartheta_0^{j+1}\|}{1+2\lambda\Delta t} \ge 0$.
For $i = N$, $\omega_{N,j+1}^{\pm} = \frac{\|\vartheta_N^{j+1}\|}{1+2\lambda\Delta t} + \max\{|U_0^{j+1}|, |U_N^{j+1}|\} \pm U_N^{j+1} \ge \frac{\|\vartheta_N^{j+1}\|}{1+2\lambda\Delta t} \ge 0$.
For $i = 1, 2, ..., \frac{N}{2}$, we have

$$\begin{aligned}\left(\frac{2}{\mu(\Delta t)} + \mathcal{L}_\varepsilon^{N,M}\right)\omega_{i,j+1}^{\pm} =& \frac{-\varepsilon\omega_{i-1,j+1}^{\pm} + 2\varepsilon\omega_{i,j+1}^{\pm} - \varepsilon\omega_{i+1,j+1}^{\pm}}{\beta_1^2} + a_i\omega_{i,j+1}^{\pm}\\ \ge& a_i\max\{|U_0^{j+1}|, |U_N^{j+1}|\} \ge 0.\end{aligned}$$

For $i = \frac{N}{2}+1, \frac{N}{2}+2, ..., N-1$,

$$\begin{aligned}\left(\frac{2}{\mu(\Delta t)} + \mathcal{L}_\varepsilon^{N,M}\right)\omega_{i,j+1}^{\pm} =& \frac{-\varepsilon\omega_{i-1,j+1}^{\pm} + 2\varepsilon\omega_{i,j+1}^{\pm} - \varepsilon\omega_{i+1,j+1}^{\pm}}{\beta_1^2} + a_i\omega_{i,j+1}^{\pm} + b_i\omega_{i-\frac{N}{2},j+1}^{\pm}\\ \ge& (a_i + b_i)\max\{|U_0^{j+1}|, |U_N^{j+1}|\} \ge 0.\end{aligned}$$

Applying the discrete maximum principle gives $\omega_{i,j+1}^{\pm} \ge 0,\ i = 0, 2, ..., N$, which implies the discrete stability estimate. ∎

Theorem 7.3.1 *Let $U^{j+1}(x_i)$ be the solution of (7.19) and U_i^{j+1} be the solution of (7.30). Then, the truncation error is bounded as*

$$\left|\left(\frac{2}{\mu(\Delta t)}+\mathcal{L}_\varepsilon^{N,M}\right)\left(U^{j+1}(x_i)-U_i^{j+1}\right)\right| \le Ch^2 \begin{cases} \left[1+\sup\limits_{x_i\in(0,1]} d_1(x_i)\right], \\ \\ \left[1+\sup\limits_{x_i\in(1,2)} d_2(x_i)\right], \end{cases}$$

where $d_1(x_i)=\frac{\exp(-\sqrt{\frac{a(x_i)}{\varepsilon}}x_i)+\exp(-\sqrt{\frac{a(x_i)}{\varepsilon}}(1-x_i))}{\varepsilon^{k/2}}$, $d_2(x_i)=\frac{\exp(-\sqrt{\frac{a(x_i)}{\varepsilon}}(x_i-1))+\exp(-\sqrt{\frac{a(x_i)}{\varepsilon}}(2-x_i))}{\varepsilon^{k/2}}$ *and* $k=1,2,3,\ldots$

Proof. From the theory of finite differences, define the finite difference operators as $D^+U_i^{j+1}=\frac{U_{i+1}^{j+1}-U_i^{j+1}}{h}$, $D^-U_i^{j+1}=\frac{U_i^{j+1}-U_{i-1}^{j+1}}{h}$ and $D^+D^-U_i^{j+1}=\frac{(D^+-D^-)U_i^{j+1}}{h^2}$. Then, using the differential and difference operators,

$$\begin{aligned}\left|\left(\frac{2}{\mu(\Delta t)}+\mathcal{L}_\varepsilon^{N,M}\right)\left(U^{j+1}(x_i)-U_i^{j+1}\right)\right| &= \left|-\varepsilon\left(\frac{d^2U^{j+1}(x_i)}{dx^2}-h^2\frac{D^+D^-U_i^{j+1}}{\beta_\iota^2}\right)\right| \\ &\le \varepsilon\left|\frac{d^2U^{j+1}(x_i)}{dx^2}-D^+D^-U_i^{j+1}\right|+\varepsilon\left|\left(\frac{h^2}{\beta_\iota^2}-1\right)D^+D^-U_i^{j+1}\right| \\ &\le C\varepsilon h^2\left|\frac{d^4U^{j+1}(x_i)}{dx^4}\right|+\varepsilon\left|\left(\frac{h^2}{\beta_\iota^2}-1\right)D^+D^-U_i^{j+1}\right|.\end{aligned}$$

Here, claim that $\varepsilon\left|\frac{h^2}{\beta_\iota^2}-1\right|\le Ch^2$. For the denominator function $\beta_\iota^2=\frac{4\varepsilon}{a(x_i)}\sinh^2\left(\sqrt{\frac{a(x_i)}{\varepsilon}}\frac{h}{2}\right)$ from the nonstandard finite difference, let us define $\xi\in(0,\infty)$, such that $\xi=\frac{a(x_i)h^2}{\varepsilon}$. Then,

$$\beta_\iota^2=\frac{4h^2}{\xi}\sinh^2\left(\frac{\sqrt{\xi}}{2}\right)=\frac{h^2}{\xi}\left(e^{\sqrt{\xi}}-2+e^{-\sqrt{\xi}}\right).$$

Using this, one can obtain

$$\varepsilon\left|\frac{h^2}{\beta_\iota^2}-1\right|=\varepsilon\left|\frac{\xi}{e^{\sqrt{\xi}}-2+e^{-\sqrt{\xi}}}-1\right|=a(x_i)h^2\left|\frac{\xi+2-e^{\sqrt{\xi}}-e^{-\sqrt{\xi}}}{\xi(e^{\sqrt{\xi}}-2+e^{-\sqrt{\xi}})}\right|.$$

Let $Z(\xi)=\frac{\xi+2-e^{\sqrt{\xi}}-e^{-\sqrt{\xi}}}{\xi(e^{\sqrt{\xi}}-2+e^{-\sqrt{\xi}})}$. Then, using L'Hospital's rule repeatedly gives

$$\lim_{\xi\to 0}Z(\xi)=-\frac{1}{12}\quad\text{and}\quad\lim_{\xi\to\infty}Z(\xi)=0.$$

This implies that $|Z(\xi)|\le C$, so that $\varepsilon\left|\frac{h^2}{\beta_\iota^2}-1\right|\le Ca(x_i)h^2\le Ch^2$, which is the claim. Thus,

$$\left|\left(\frac{2}{\mu(\Delta t)}+\mathcal{L}_\varepsilon^{N,M}\right)\left(U^{j+1}(x_i)-U_i^{j+1}\right)\right|\le C\varepsilon h^2\left|\frac{d^4U^{j+1}(x_i)}{dx^4}\right|+Ch^2\left|\frac{d^2U^{j+1}(x_i)}{dx^2}\right|.$$

Using Lemma 7.3.5 yields

$$\left|\left(\frac{2}{\mu(\Delta t)}+\mathcal{L}_{\varepsilon}^{N,M}\right)\left(U^{j+1}(x_i)-U_i^{j+1}\right)\right|\leq C\left[1+\sup_{x_i\in(0,1]} d_1(x_i)\right]$$

By similar procedure, the required estimate can be obtained on $(1,2)$. ∎

Lemma 7.3.8 *(Tiruneh et al., 2023). For a given mesh N, assuming $\varepsilon\to 0$ gives*

$$\lim_{\varepsilon\to 0}\begin{cases}\max\limits_{x_i\in(0,1]}\frac{\exp(-\sqrt{\frac{a(x_i)}{\varepsilon}}x_i)+\exp(-\sqrt{\frac{a(x_i)}{\varepsilon}}(1-x_i))}{\varepsilon^{k/2}}=0,\\ \max\limits_{x_i\in(1,2)}\frac{\exp(-\sqrt{\frac{a(x_i)}{\varepsilon}}(x_i-1))+\exp(-\sqrt{\frac{a(x_i)}{\varepsilon}}(2-x_i))}{\varepsilon^{k/2}}=0,\end{cases}$$

for all $i=1,2,...,N-1$ and $k=1,2,3,...$.

Proof. For the interval $(0,1]$, consider $x_i=ih$, where $i=0,1,...,\frac{N}{2}$ and $h=\frac{2}{N}$. Since $x_i=h$ and $1-x_{N/2-1}=h$,

$$\max_{1\leq i\leq\frac{N}{2}-1}\frac{\exp(-\sqrt{\frac{a(x_i)}{\varepsilon}}x_i)}{\varepsilon^{k/2}}\leq\frac{\exp(-\sqrt{\frac{a(x_i)}{\varepsilon}}x_1)}{\varepsilon^{k/2}}=\frac{\exp(-\sqrt{\frac{a(x_i)}{\varepsilon}}h)}{\varepsilon^{k/2}}$$

and

$$\max_{1\leq i\leq\frac{N}{2}-1}\frac{\exp(-\sqrt{\frac{a(x_i)}{\varepsilon}}(1-x_i))}{\varepsilon^{k/2}}\leq\frac{\exp(-\sqrt{\frac{a(x_i)}{\varepsilon}}(1-x_{N/2-1}))}{\varepsilon^{k/2}}=\frac{\exp(-\sqrt{\frac{a(x_i)}{\varepsilon}}h)}{\varepsilon^{k/2}}$$

But, for $\varepsilon\to 0$,

$$\lim_{\varepsilon\to 0}\frac{\exp(-\sqrt{\frac{a(x_i)}{\varepsilon}}h)}{\varepsilon^{k/2}}=\lim_{\rho\to\infty}\frac{\rho^{k/2}}{(\sqrt{a(x_i)}h)^k\exp(\sqrt{\rho})}=\lim_{\rho\to\infty}\frac{k!}{(\sqrt{a(x_i)}h)^k\exp(\sqrt{\rho})}=0.$$

By a similar procedure, the required argument holds true on the interval $(1,2)$. ∎

Theorem 7.3.2 *If $u(x_i,t_{j+1})$ is the solution of (7.1) and U_i^{j+1} is the solution of (7.30), then the uniform error is given by*

$$\sup_{0<\varepsilon\leq 1}\|u(x_i,t_{j+1})-U_i^{j+1}\|\leq C\left((\Delta t)^2+N^{-2}\right)$$

Proof. Using Lemma 7.3.8 into Theorem 7.3.1 yields $\left|\left(\frac{2}{\mu(\Delta t)}+\mathcal{L}_{\varepsilon}^{N,M}\right)\left(U^{j+1}(x_i)-U_i^{j+1}\right)\right|\leq Ch^2$. Then, Lemma 7.3.6 gives

$$\left|U^{j+1}(x_i)-U_i^{j+1}\right|\leq Ch^2. \tag{7.32}$$

Since $\left|u(x_i,t_{j+1})-U_i^{j+1}\right|=\left|u(x_i,t_{j+1})-U^{j+1}(x_i)+U^{j+1}(x_i)-U_i^{j+1}\right|\leq|u(x_i,t_{j+1})-U^{j+1}(x_i)|+\left|U^{j+1}(x_i)-U_i^{j+1}\right|$, combining Lemma 7.3.4 and equation (7.32), the result follows. ∎

7.4 Numerical results and discussions

To demonstrate the validity and applicability of the formulated numerical method, three examples are solved. Since it is difficult to find the analytical solution, a variant of the double mesh principle (4.44)-(4.47) is applied to determine the maximum absolute errors and corresponding rate of convergences.

Example 7.4.1 *(Bansal & Sharma, 2018). Consider* $-u_t(x,t)+\varepsilon u_{xx}(x,t)-5u(x,t)+2u(x-1,t)=-2$, $u(x,0)=\sin(\pi x)$ *for* $x\in[0,2]$, $u(x,t)=0$ *for* $(x,t)\in\{(x,t):x\in[-1,0],\ \ 0\le t\le 2\}$ *and* $u(2,t)=0$ *for* $(2,t)\in\{(2,t):0\le t\le 2\}$.

Example 7.4.2 *(Kumari & Kumar, 2020). Consider* $-u_t(x,t)+\varepsilon u_{xx}(x,t)-(x+6)u(x,t)+(x^2+1)u(x-1,t)=-3$, $u(x,0)=0$ *for* $x\in[0,2]$, $u(x,t)=0$ *for* $(x,t)\in\{(x,t):x\in[-1,0],\ \ 0\le t\le 2\}$ *and* $y(2,t)=0$ *for* $(2,t)\in\{(2,t):0\le t\le 2\}$.

Example 7.4.3 *(Kumari & Kumar, 2020; Bansal & Sharma, 2018). Consider* $-u_t(x,t)+\varepsilon u_{xx}(x,t)-3u(x,t)+u(x-1,t)=-1$, $u(x,0)=0$ *for* $x\in[0,2]$, $u(x,t)=0$ *for* $(x,t)\in\{(x,t):x\in[-1,0],\ \ 0\le t\le 2\}$ *and* $u(2,t)=0$ *for* $(2,t)\in\{(2,t):0\le t\le 2\}$.

For each example, the maximum point-wise errors, rate of convergences and the numerical solutions are computed applying the numerical scheme formulated in this chapter. The maximum point-wise error and convergence rate at a point are obtained as shown in Tables 7.1-7.3. From these tables, one can see that increasing the mesh numbers decreases the truncation error and decreasing ε yields a uniform point-wise errors. This shows that the formulated numerical scheme is ε-uniformly convergent. In Table 7.4, the accuracy of the present method is compared with some other published results in the literature.

The numerical solutions for the model examples are simulated in Figures 7.1-7.4. Figures 7.1 and 7.3 show the line plots of the solutions at different time level, and to show the physical behaviors of the solutions, surface plots are simulated in Figures 7.2 and 7.4. From these figures, the effect of ε can be easily observed. That is, decreasing the value of ε decreases the width of the two boundary layers and the interior layer. This indicates that the errors in the layers have been handled. To visualize the solution behaviors, contour lines are also drawn with the surface plots. Figure 7.5 is log-log plots of the maximum point-wise errors versus N, which confirms the ε-uniform convergence of the developed scheme. From the log-log plots, one can observe that increasing the mesh number decreases the maximum absolute errors, and decreasing the value of the perturbation parameter yields stable and uniform point-wise errors.

Table 7.1: Maximum absolute error and rate of convergence for Example 7.4.1.

ε $\|N \rightarrow$	32	64	128	256	512
$\downarrow$ $\|M \rightarrow$	8	32	128	512	2048
2^{-4}	5.9335e-02	1.0399e-02	1.4848e-03	1.9482e-04	4.1549e-05
	2.5124	2.8081	2.9301	2.2293	
2^{-6}	7.9072e-02	1.4990e-02	2.3170e-03	3.1664e-04	4.1042e-05
	2.3992	2.6936	2.8713	2.9477	
2^{-8}	8.1385e-02	2.0199e-02	4.1768e-03	6.9064e-04	1.2562e-04
	2.0105	2.2738	2.5965	2.4589	
2^{-10}	8.1361e-02	2.0405e-02	6.2087e-03	1.8411e-03	4.6589e-04
	1.9954	1.7166	1.7536	1.9825	
2^{-12}	8.1240e-02	2.0054e-02	5.2325e-03	1.9563e-03	4.3560e-04
	2.0183	1.9383	1.4194	2.1671	
2^{-14}	8.1230e-02	2.0042e-02	4.7207e-03	1.7769e-03	5.1954e-04
	2.0190	2.0860	1.4096	1.7741	
2^{-16}	8.1229e-02	2.0041e-02	4.7136e-03	1.1282e-03	3.0203e-04
	2.0190	2.0881	2.0628	1.9013	
2^{-18}	8.1229e-02	2.0041e-02	4.7134e-03	1.1209e-03	2.7989e-04
	2.0190	2.0881	2.07221	2.0017	
2^{-20}	8.1228e-02	2.0041e-02	4.7134e-03	1.1209e-03	2.7197e-04
	2.0190	2.0881	2.0721	2.0431	
2^{-22}	8.1229e-02	2.0041e-02	4.7134e-03	1.1209e-03	2.7196e-04
	2.0190	2.0881	2.0721	2.0432	
2^{-24}	8.1229e-02	2.0041e-02	4.7134e-03	1.1209e-03	2.7196e-04
	2.0190	2.0881	2.0721	2.0432	
$e^{N,M}$	8.1385e-02	2.0405e-02	6.2087e-03	1.9563e-03	5.1954e-04
$r^{N,M}$	1.9958	1.7166	1.6662	1.9128	-

Table 7.2: Maximum absolute error and rate of convergence for Example 7.4.2.

ε $\vert N \rightarrow$	18	36	72	144	288
$\downarrow$ $\vert M \rightarrow$	18	72	288	1152	4608
2^{-4}	2.8392e-02	6.7928e-03	1.1932e-03	1.8358e-04	3.2692e-05
	2.0634	2.5092	2.7004	2.4894	
2^{-6}	3.0557e-02	9.9272e-03	2.7617e-03	6.2088e-04	1.4208e-04
	1.6220	1.8458	2.1532	2.0734	
2^{-8}	3.0410e-02	9.3899e-03	3.0633e-03	8.6458e-04	2.0542e-04
	1.6954	1.6160	1.8250	2.0734	
2^{-10}	3.0405e-02	9.1485e-03	2.8443e-03	7.2955e-04	1.8578e-04
	1.7327	1.6855	1.9630	1.9734	
2^{-12}	3.0404e-02	9.1460e-03	2.5253e-03	6.0965e-04	1.8431e-04
	1.7330	1.8567	2.0504	1.7258	
2^{-14}	3.0404e-02	9.1460e-03	2.5229e-03	6.9753e-04	1.9546e-04
	1.7330	1.8581	1.8548	1.8354	
2^{-16}	3.0404e-02	9.1460e-03	2.5229e-03	6.9489e-04	2.0669e-04
	1.7330	1.8581	1.8602	1.7493	
2^{-18}	3.0404e-02	9.1460e-03	2.5229e-03	6.9489e-04	2.0335e-04
	1.7330	1.8581	1.8602	1.7728	
2^{-20}	3.0404e-02	9.1460e-03	2.5229e-03	6.9489e-04	2.0335e-04
	1.7330	1.8581	1.8602	1.7728	
2^{-22}	3.0404e-02	9.1460e-03	2.5229e-03	6.9489e-04	2.0335e-04
	1.7330	1.8581	1.8602	1.7728	
$e^{N,M}$	3.0557e-02	9.9272e-03	3.0633e-03	8.6458e-04	2.0669e-04
$r^{N,M}$	1.6220	1.6963	1.8250	2.0645	-

Table 7.3: Maximum absolute error and rate of convergence for Example 7.4.3.

ε $\|N \rightarrow$	32	64	128	256	512
$\downarrow$ $\|M \rightarrow$	8	32	128	512	2048
2^{-4}	1.2490e-02	2.1437e-03	3.8863e-04	7.9803e-05	2.1163e-05
	2.5426	2.4636	2.2839	1.9149	
2^{-6}	2.1674e-02	4.0560e-03	6.0966e-04	8.2225e-05	1.2670e-05
	2.4178	2.7340	2.8904	2.6982	
2^{-8}	2.7470e-02	7.3034e-03	1.4872e-03	2.7381e-04	5.9638e-05
	1.9112	2.2960	2.4414	2.1989	
2^{-10}	2.7310e-02	8.3566e-03	1.9371e-03	4.8577e-04	1.1996e-04
	1.7084	2.1090	1.9956	2.0177	
2^{-12}	2.7287e-02	7.6132e-03	1.9513e-03	4.8654 e-04	1.1612e-04
	1.8416	1.9641	2.0038	2.0669	
2^{-14}	2.7287e-02	7.5769e-03	2.0051e-03	4.5717e-04	1.1799e-04
	1.8485	1.9179	2.1329	1.9541	
2^{-16}	2.7287e-02	7.5768e-03	1.9603e-03	5.4465e-04	1.2315e-04
	1.8486	1.9505	1.8477	2.1449	
2^{-18}	2.7287e-02	7.5768e-03	1.9602e-03	4.9447e-04	1.2319e-04
	1.8486	1.9505	1.9870	2.0050	
2^{-20}	2.7287e-02	7.5768e-03	1.9602e-03	4.9442e-04	1.2393 e-04
	1.8486	1.9505	1.9870	1.9962	
2^{-22}	2.7287e-02	7.5768e-03	1.9602e-03	4.9442e-04	1.2389e-04
	1.8486	1.9505	1.9870	1.9967	
2^{-24}	2.7287e-02	7.5768e-03	1.9602e-03	4.9442e-04	1.2389e-04
	1.8486	1.9505	1.9870	1.9967	
$e^{N,M}$	2.7470e-02	8.3566e-03	2.0051e-03	5.4465e-04	1.2393e-04
$r^{N,M}$	1.7169	2.0592	1.8803	2.1358	-

Table 7.4: Comparison of the proposed method with other published results in the literature.

Rates of convergence for Example 7.4.1				
$N:$	64	128	256	512
$M:$	32	128	512	2048
Present scheme				
$\varepsilon=2^{-16}$	2.0881	2.0628	1.9013	1.8972
$\varepsilon=2^{-18}$	2.0881	2.0721	2.0017	2.0036
$\varepsilon=2^{-20}$	2.0881	2.0721	2.0431	2.0032
Bansal & Sharma (2018)				
$\varepsilon=2^{-16}$	1.7908	1.8314	1.5121	1.6261
$\varepsilon=2^{-18}$	1.7908	1.8341	1.5101	1.6258
$\varepsilon=2^{-20}$	1.7908	1.8354	1.5091	1.6257
Maximum error and rate of convergence for Example 7.4.3				
Present scheme				
$\varepsilon=2^{-16}$	1.9505	1.8477	2.1449	1.8972
$\varepsilon=2^{-20}$	1.9505	1.9870	2.0050	1.8970
Bansal & Sharma (2018)				
$\varepsilon=2^{-16}$	1.3369	1.5402	1.6333	1.6722
$\varepsilon=2^{-20}$	1.3369	1.5402	1.6333	1.6722
Maximum error and rate of convergence for Example 7.4.2				
$N=M:$	18	36	72	144
Present scheme				
e^N	1.3081e-03	7.8288e-04	4.7719e-04	2.3539e-04
r^N	0.7406	0.7130	1.0207	0.9999
Kumari & Kumar (2020)				
$e^{N,M}$	1.3600e-02	1.0900e-02	5.5600e-03	2.2800e-03
$r^{N,M}$	0.3193	0.9712	1.2861	0.8787
Maximum error and rate of convergence for Example 7.4.3				
Present scheme				
e^N	9.7731e-03	4.5542e-03	1.9746e-03	6.7654e-04
r^N	1.1016	1.2056	1.5453	1.3814
Kumari & Kumar (2020)				
$e^{N,M}$	1.1200e-02	7.0100e-03	2.9700e-03	1.1400e-03
$r^{N,M}$	0.6760	1.2390	1.3814	1.4895

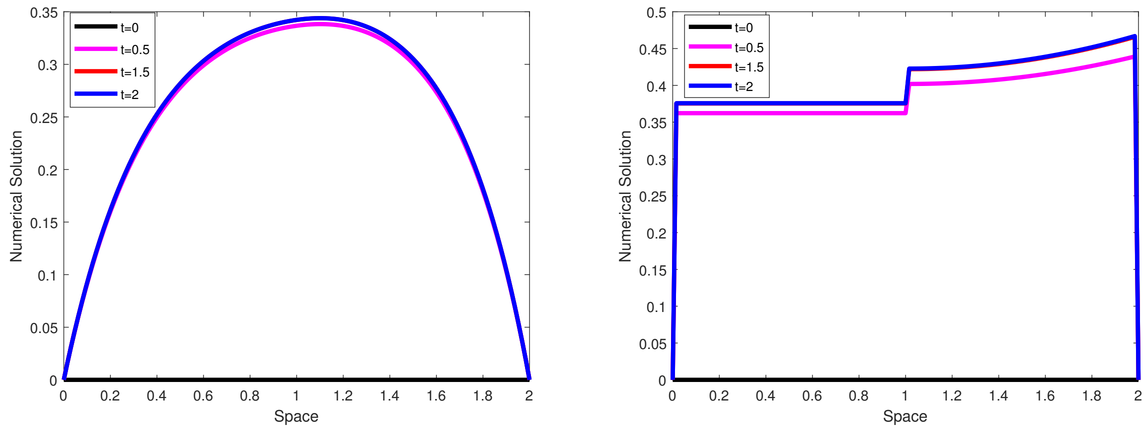

(a) $\varepsilon = 2^0$ (b) $\varepsilon = 2^{-14}$

Figure 7.1: Line plots for the numerical solution of Example 7.4.2 for $N = 72$ and $M = 72$ at different time levels.

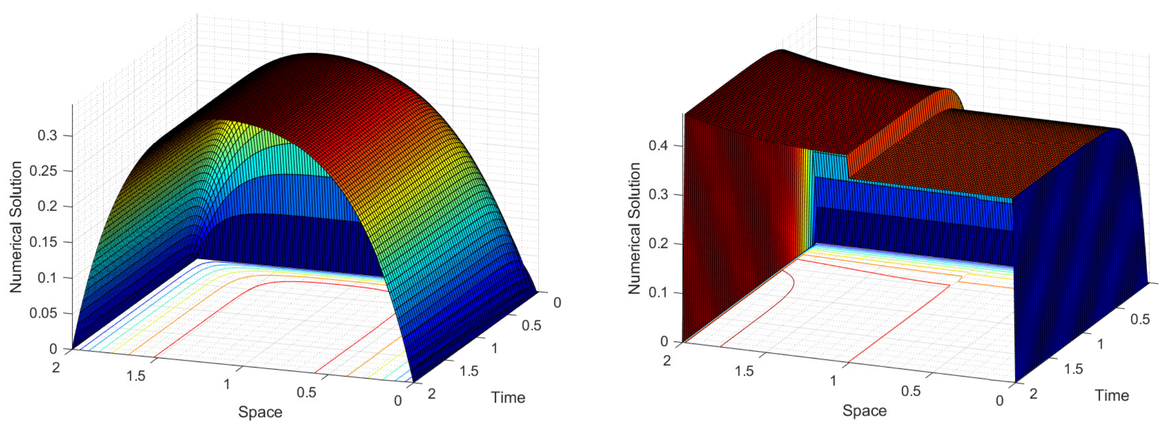

(a) $\varepsilon = 2^0$ (b) $\varepsilon = 2^{-14}$

Figure 7.2: Surface plots for the numerical solution of Example 7.4.2 for $N = 72$ and $M = 72$.

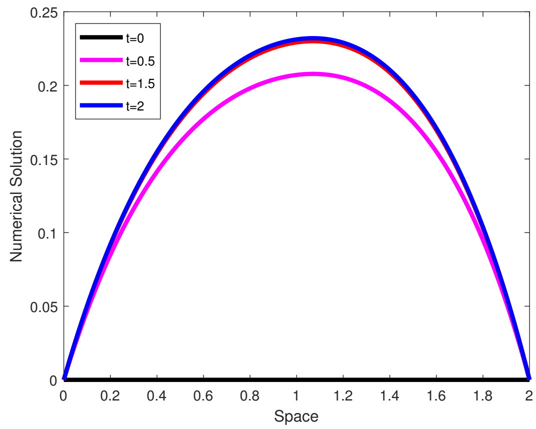

(a) $\varepsilon = 2^0$ (b) $\varepsilon = 2^{-14}$

Figure 7.3: Line plots for the numerical solution of Example 7.4.3 for $N = 128$ and $M = 64$.

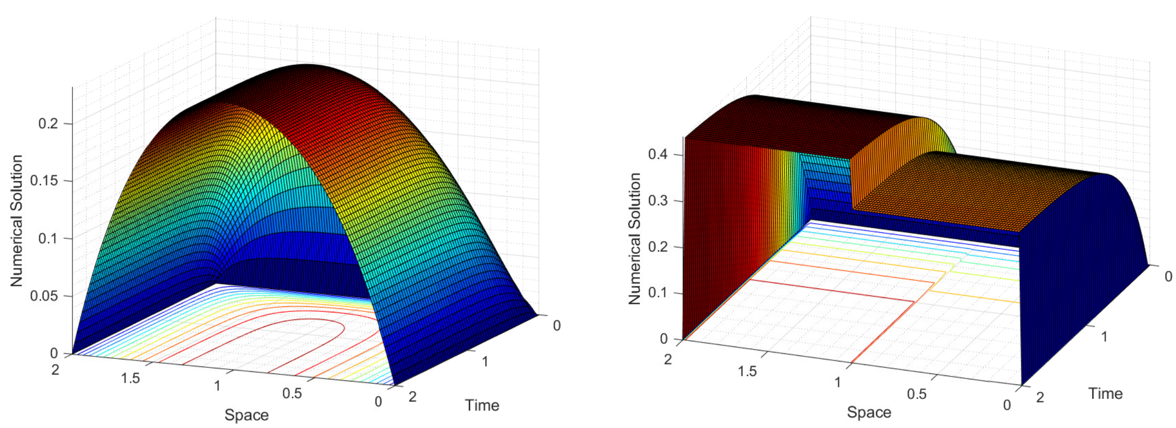

(a) $\varepsilon = 2^0$ (b) $\varepsilon = 2^{-14}$

Figure 7.4: Surface plots for the numerical solution of Example 7.4.3 for $N = 128$ and $M = 64$.

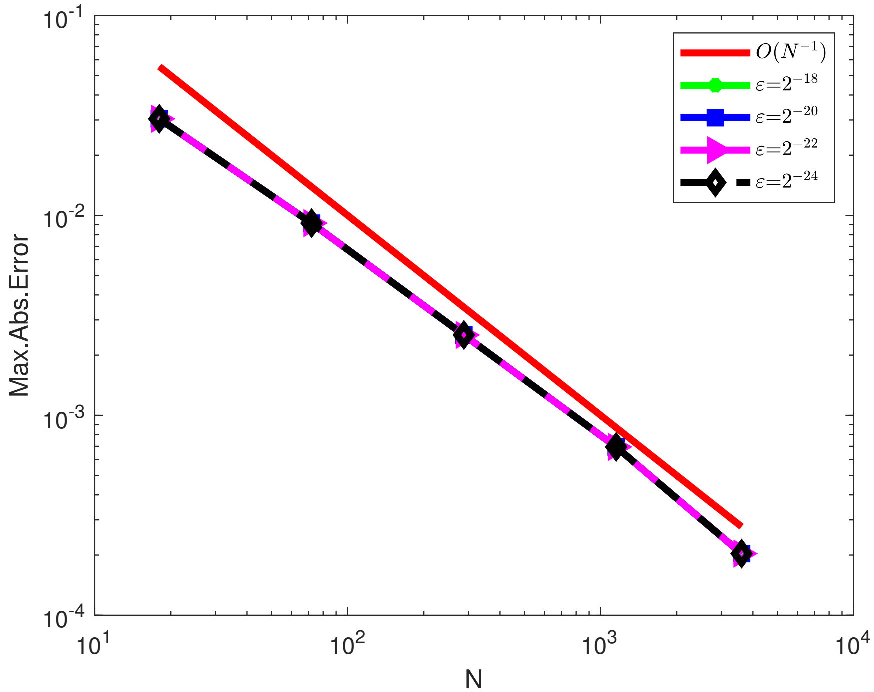

(a)

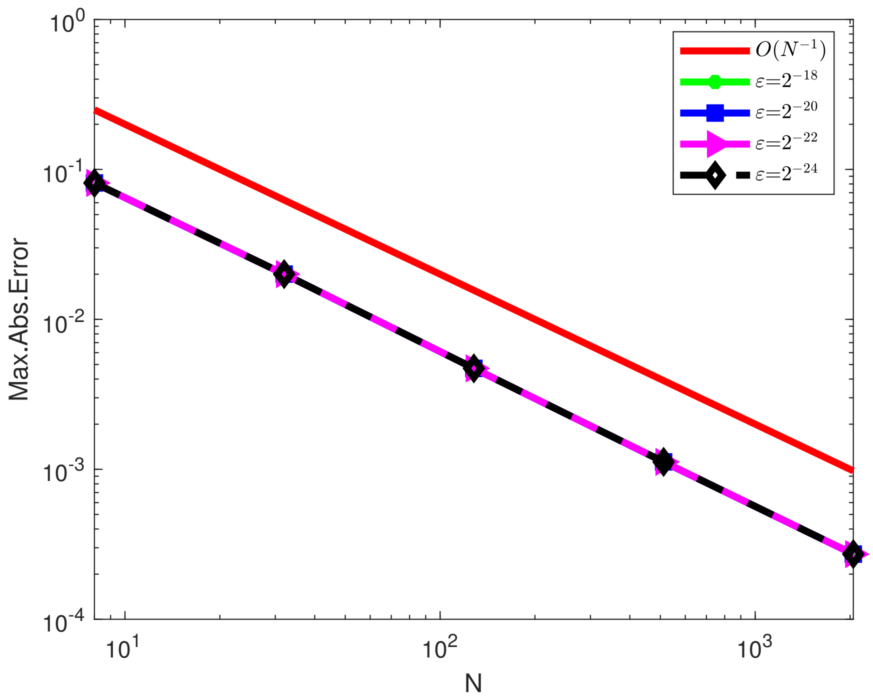

(b)

Figure 7.5: Log-log plots of maximum absolute error versus N for (a) Example 7.4.2 and (b) Example 7.4.3.

7.5 Summary

In this chapter, a nonstandard finite difference scheme is formulated and analyzed for a singularly perturbed partial differential equations with large negative shift. Due to the presence of ε, the solution involves two boundary layers and the large negative shift causes interior layer at $x = 1$. The original differential equation is transformed into a nonstandard finite difference scheme by using the Crank-Nicolson method and the central difference method in temporal and spatial direction, respectively. Stability and uniform convergence analysis are investigated and proved. To validate the theoretical findings, model numerical examples are considered. For each example, the numerical solution is computed and given in graphical form. Maximum point-wise errors and corresponding rate of convergences of the proposed method are displayed in tabular forms for each example. The main findings can be summarized as follow.

1. ε-uniformly convergent nonstandard finite difference scheme is formulated.
2. The stability estimate and uniform convergence of the developed numerical scheme are investigated and proved.
3. The validity and applicability of the developed scheme is validated using numerical experiments and obtained that it is an efficient method to treat the problem.
4. It is more accurate as compared to other results in the literature.

CHAPTER EIGHT

A TENSION SPLINE FITTED METHOD FOR SINGULARLY PERTURBED PARTIAL DIFFERENTIAL EQUATIONS WITH LARGE NEGATIVE SHIFT

In the present chapter, a numerical scheme is formulated and analyzed for a SPDDE. The numerical scheme is constructed by discretizing the temporal variable using the implicit Euler method, and then fitting a tension spline method on a uniform spatial meshes. In this technique the tension parameter controls the smoothness of the fitting curve and enhances the accuracy of the results. To handle the influence of the perturbation parameter, a fitting factor is introduced in the discrete scheme, and by this the formulated scheme is shown to be accurate and uniformly convergent.

8.1 The governing problem

A singularly perturbed delay differential equation is considered on $\Omega = \Gamma \times \Lambda = (0, 2) \times (0, T)$ as

$$\begin{aligned} &\mathcal{L}_\varepsilon u(x,t) = u_t(x,t) - \varepsilon u_{xx}(x,t) + a(x)u(x,t) + b(x)u(x-1,t) = f(x,t), \qquad (8.1)\\ &u(x,0) = u_0(x),\ x \in \bar{\Gamma},\\ &u(x,t) = \phi(x,t),\ (x,t) \in \Omega^-,\\ &u(2,t) = \alpha(t),\ (2,t) \in \Omega^+, \end{aligned}$$

where $0 < \varepsilon \ll 1$, $\Omega^- = \{(x,t) :\ x \in [-1,0];\ 0 \le t \le T\}$ and $\Omega^+ = \{(2,t) : 0 \le t \le T\}$ for finite time T. The functions $a(x)$, $b(x)$, $f(x,t)$, $u_0(x)$, $\phi(x)$ and $\alpha(t)$ are assumed to be sufficiently smooth, bounded and independent of ε. Moreover, for arbitrary positive constant λ, it is assumed that

$$a(x) + b(x) \ge 2\lambda > 0 \text{ and } b(x) < 0,\ x \in [0, 2]. \qquad (8.2)$$

Equation (8.1) can be equivalently written as

$$\mathcal{L}_\varepsilon u(x,t) = \begin{cases} u_t(x,t) - \varepsilon u_{xx}(x,t) + a(x)u(x,t) = f(x,t) - b(x)\phi(x-1.t),\ (x,t) \in (0,1] \times \Lambda,\\ u_t(x,t) - \varepsilon u_{xx}(x,t) + a(x)u(x,t) + b(x)u(x-1,t) = f(x,t),\ (x,t) \in (1,2) \times \Lambda, \end{cases} \qquad (8.3)$$

subjected to

$$\begin{cases} u(x,0) = u_0(x), \ \forall x \in [0,2], \\ u(x,t) = \phi(x,t), \ (x,t) \in \Omega^-, \\ u(2,t) = \alpha(t), \ (2,t) \in \Omega^+. \end{cases} \tag{8.4}$$

setting $\varepsilon = 0$, the governing problem is reduced to

$$\mathcal{L}_\varepsilon u_0(x,t) = \begin{cases} (u_0)_t + a(x)u_0(x,t) = f(x,t) - b(x)\phi(x-1.t), \ (x,t) \in (0,1] \times \Lambda, \\ (u_0)_t + a(x)u_0(x,t) + b(x)u_0(x-1,t) = f(x,t), \ (x,t) \in (1,2) \times \Lambda \end{cases} \tag{8.5}$$

with the conditions

$$\begin{cases} u_0(x,0) = u_0(x), \ x \in [0,2], \\ u_0(x,t) = \phi(x,t), \ (x,t) \in \Omega^-, \\ u_0(2,t) = \alpha(t), \ (2,t) \in \Omega^+. \end{cases} \tag{8.6}$$

From the reduced problem (8.5), it can be seen that $u_0(x,t)$ needs not necessarily satisfy the conditions $u_0(0,t) = \phi(0,t)$, $u_0(2,t) = \alpha(t)$, $u_0(1^+,t) = u_0(1^-,t)$ and $(u_0)_x(1^+,t) = (u_0)_x(1^-,t)$ and hence, the solution $u(x,t)$ involves two boundary layers at the two ends of $[0,2]$ and interfacing layers at $x = 1$ (Roos et al., 2008). Moreover, the initial and boundary data are assumed to satisfy Holder continuity and impose the compatibility conditions as

$$\begin{cases} u_0(0,0) = \phi(0,0), \\ u_0(2,0) = \alpha(2,0), \end{cases} \tag{8.7}$$

$$\begin{cases} \phi_t(0,0) - \varepsilon(u_0)_{xx} + a(0)u_0(0) = f(0,0) - b(0)\phi(-1.0), \\ \alpha_t(2,0) - \varepsilon(u_0)_{xx}(2) + a(2)u_0(2) + b(2)u_0(1,0) = f(2,0). \end{cases} \tag{8.8}$$

From the above assumptions and conditions, the existence and uniqueness of the solution are guaranteed (Kumari & Kumar, 2020). And by the approaches of Kadalbajoo & Awasthi (2011), it follows that

$$|u(x,t) - u_0(x)| \leq Ct, \ (x,t) \in \bar{\Omega}. \tag{8.9}$$

The solution of (8.1) approaches to $u_0(x,t)$ for small values of ε. As it is described by Clavero & Gracia (2010), it is assumed that all the considered data values in (8.1) are identically zero, so that the following properties hold.

8.2 Properties of the continuous solution

Lemma 8.2.1 *(Roos et al., 2008). The solution $u(x,t)$ of the continuous problem (8.1) is bounded as*

$$|u(x,t)| \leq C, \ (x,t) \in \bar{\Omega}.$$

Proof. From (8.9), it follows that $|u(x,t)| - |u_0(x)| \leq Ct$, which implies $|u(x,t)| \leq Ct + |u_0(x)|$, $(x,t) \in \bar{\Omega}$. Since $u_0(x)$ is bounded, fixing t in $(0,T]$, gives $|u(x,t)| \leq C$, $(x,t) \in \bar{\Omega}$. ■

Lemma 8.2.2 *(Maximum principle). Let $z(x,t)$ be a continuous function in $\bar{\Omega}$. If $z(x,t) \geq 0$, $(x,t) \in \partial\Omega$ and $\mathcal{L}_\varepsilon z(x,t) \geq 0$, $(x,t) \in \Omega$, then $z(x,t) \geq 0$, $(x,t) \in \bar{\Omega}$.*

Proof. Let $(\hat{x},\hat{t}) \in \bar{\Omega}$ and $z(\hat{x},\hat{t}) = \min_{\bar{\Omega}} z(x,t)$. Assume that $z(\hat{x},\hat{t}) < 0$. By the considered hypothesis, $(\hat{x},\hat{t}) \notin \partial\Omega$ and by the extreme value theorem, $z_x(\hat{x},\hat{t}) = 0$, $z_{xx}(\hat{x},\hat{t}) \geq 0$.
Case 1: For $0 < \hat{x} \leq 1$,

$$\mathcal{L}_{\varepsilon,1} z(\hat{x},\hat{t}) = z_t(\hat{x},\hat{t}) - \varepsilon z_{xx}(\hat{x},\hat{t}) + a(\hat{x})z(\hat{x},\hat{t}) = -\varepsilon z_{xx}(\hat{x},\hat{t}) + a(\hat{x})z(\hat{x},\hat{t}) < 0$$

Case 2: For $1 < \hat{x} < 2$,

$$\begin{aligned}
\mathcal{L}_{\varepsilon,2} z(\hat{x},\hat{t}) =& z_t(\hat{x},\hat{t}) - \varepsilon z_{xx}(\hat{x},\hat{t}) + a(\hat{x})z(\hat{x},\hat{t}) + b(\hat{x})z(\hat{x}-1,\hat{t}) \\
=& z_t(\hat{x},\hat{t}) - \varepsilon z_{xx}(x,t) + [a(\hat{x}) + b(\hat{x})]\, z(\hat{x},\hat{t}) + m(\hat{x}) \left[z(\hat{x}-1,\hat{x}) - z(\hat{x},\hat{t})\right] \\
=& -\varepsilon z_{xx}(\hat{x},\hat{t}) + [a(\hat{x}) + b(\hat{x})]\, z(\hat{x},\hat{t}) + b(\hat{x}) \left[z(\hat{x}-1,\hat{t}) - z(\hat{x},\hat{t})\right] < 0
\end{aligned}$$

The two cases contradict the hypothesis, so that the assumption fails and $z(\hat{x},\hat{t}) \geq 0$, which implies $z(x,t) \geq 0$, $(x,t) \in \bar{\Omega}$. ■

Lemma 8.2.3 *(Sathya & Rao, 2020). The solution of the continuous problem (8.1) is estimated as*

$$|u(x,t)| \leq \lambda^{-1}\|f\| + \max\left\{|u_0(x)|, |\phi(0,t)|, |\alpha(2,t)|\right\}.$$

Proof. Let's define barrier functions as

$$\pi^{\pm}(x,t) = \lambda^{-1}\|f\| + \max\left\{|u_0(x)|, |\phi(0,t)|, |\alpha(2,t)|\right\} \pm u(x,t).$$

Then,

$$\begin{aligned}
\pi^{\pm}(x,0) &= \lambda^{-1}\|f\| + \max\left\{|u_0(x)|, |\phi(0,t)|, |\alpha(2,t)|\right\} \pm u_0(x) \geq 0, \\
\pi^{\pm}(0,t) &= \lambda^{-1}\|f\| + \max\left\{|u_0(x)|, |\phi(0,t)|, |\alpha(2,t)|\right\} \pm \phi(0,t) \geq 0, \\
\pi^{\pm}(2,t) &= \lambda^{-1}\|f\| + \max\left\{|u_0(x)|, |\phi(0,t)|, |\alpha(2,t)|\right\} \pm \alpha(t) \geq 0.
\end{aligned}$$

For $(x,t) \in (0,1] \times [0,T]$, it follows that

$$\mathcal{L}_{\varepsilon,1}\pi^{\pm}(x,t) = \pi^{\pm}_t(x,t) - \varepsilon\pi^{\pm}_{xx}(x,t) + a(x)\pi^{\pm}(x,t) \geq a(x)\max\{|u_0(x)|, |\phi(0,t)|, |\alpha(2,t)|\} \geq 0.$$

For $(x,t) \in (1,2) \times [0,T]$, it follows that

$$\mathcal{L}_{\varepsilon,2}\pi^{\pm}(x,t) = \pi^{\pm}_t(x,t) - \varepsilon\pi^{\pm}_{xx}(x,t) + a(x)\pi^{\pm}(x,t) + b(x)\pi^{\pm}(x-1,t) \geq 2\lambda\max\{|u_0(x)|, |\phi(0,t)|, |\alpha(2,t)|\} \geq$$

Therefore, by Lemma 8.2.2, the stability estimate holds true. ■

Lemma 8.2.4 *The derivatives of the solution $u(x,t)$ of the continuous problem (8.1) is bounded as*

$$\left|\frac{\partial^{k+j}u(x,t)}{\partial x^k \partial t^j}\right| \leq \begin{cases} C(1+\varepsilon^{\frac{-k}{2}}\delta_1(x)), \ 0 < x \leq 1, \ 0 < t \leq T], \\ C(1+\varepsilon^{\frac{-k}{2}}\delta_2(x)), \ 1 < x < 2, \ 0 < t \leq T] \end{cases}$$

for the non-negative integers k and j such that $0 \leq k+2j \leq 4$, where $\delta_1(x) = \exp(-\sqrt{\frac{\lambda}{\varepsilon}}x) + \exp(-\sqrt{\frac{\lambda}{\varepsilon}}(1-x))$ and $\delta_2(x) = \exp(-\sqrt{\frac{\lambda}{\varepsilon}}(x-1)) + \exp(-\sqrt{\frac{\lambda}{\varepsilon}}(2-x))$.

Proof. Refer Lemma 7.2.4 of Chapter 7. ■

8.3 The numerical method

A temporal semi-discrete scheme is obtained on M uniformly discretized temporal mesh, and using a tension spline fitted method a finite difference scheme is constructed on N uniformly discretized mesh.

8.3.1 Temporal semi-discretization

Let's divide $(0,T]$ into equally spaced intervals and form a uniform temporal mesh as $\Omega_t^M = \{t_j = j\Delta t, \ j = 0,1,...,M, \ T = M\Delta t\}$. Then, using the implicit Euler method for the time derivative, the semi-discrete scheme is given by

$$\frac{U^{j+1}(x) - U^j(x)}{\Delta t} - \varepsilon U^{j+1}_{xx}(x) + a(x)U^{j+1}(x) + b(x)U^{j+1}(x-1) = f(x,t_{j+1}).$$

On rearrangement and simplification, it becomes

$$\mathcal{L}^M_\varepsilon U^{j+1}(x) = \vartheta^{j+1}(x), \ j+1 = 1,2,...,M \tag{8.10}$$

where

$$\mathcal{L}^M_\varepsilon U^{j+1}(x) = \begin{cases} -\varepsilon\Delta t U^{j+1}_{xx}(x) + p(x)U^{j+1}(x), \ x \in (0,1], \\ -\varepsilon\Delta t U^{j+1}_{xx}(x) + p(x)U^{j+1}(x) + q(x)U^{j+1}(x-1), \ x \in (1,2) \end{cases}$$

and

$$\vartheta^{j+1}(x)=\begin{cases}\Delta t f(x,t_{j+1})+U^j(x)-q(x)\alpha(x-1,t_{j+1}),\ x\in(0,1],\\ \Delta t f(x,t_{j+1})+U^j(x),\ x\in(1,2)\end{cases}$$

subject to $U^{j+1}(x)=U_0(x)$, $x\in\bar{\Gamma}$, $U^{j+1}(x)=\phi(x,t_{j+1})$, $x\in(0,1]$, $U^{j+1}(2)=\alpha(2,t_{j+1})$, $x\in(1,2)$, and for $p(x)=1+\Delta t a(x)$ and $q(x)=\Delta t b(x)$.

Lemma 8.3.1 *Let $\psi^{j+1}(x)$ be a continuous function on $\bar{\Gamma}$. If $\psi^{j+1}(0)\geq 0$, $\psi^{j+1}(2)\geq 0$ and $\mathcal{L}_\varepsilon\psi^{j+1}(x)\geq 0$, $x\in\Gamma$, then $\psi^{j+1}(x)\geq 0$, $x\in\bar{\Gamma}$.*

Proof. For some $\nu\in[0,2]$, let $\psi^{j+1}(\nu)=\min_{\bar{\Gamma}}\psi^{j+1}(x)$ and assume that $\psi^{j+1}(\nu)<0$. From the given conditions, $\nu\notin\partial\Gamma$ and from the extreme value theorem $\psi_x^{j+1}(\nu)=0$, $\psi_{xx}^{j+1}(\nu)\geq 0$. And

Case 1: For $\nu\in(0,1]$, one can obtain

$$\mathcal{L}_{\varepsilon,1}^M\psi^{j+1}(\nu)=-\varepsilon\psi_{xx}^{j+1}(\nu)+p(x)\psi^{j+1}(\nu)<0.$$

Case 2: For $\nu\in(1,2)$, one can obtain

$$\begin{aligned}\mathcal{L}_{\varepsilon,2}^M\psi^{j+1}(\nu)=&-\varepsilon\psi_{xx}^{j+1}(\nu)+p(x)\psi^{j+1}(\nu)+q(\nu)\psi^{j+1}(\nu-1)\\ \leq&-\varepsilon\psi_{xx}^{j+1}(\nu)+(p(\nu)+q(\nu))\psi^{j+1}(\nu)<0.\end{aligned}$$

By these two cases, the given condition is contradicted, which implies that our assumption does not holds and hence $\psi^{j+1}(x)\geq 0$, $x\in\bar{\Omega}_x$. Thus, the maximum principle is satisfied by $\mathcal{L}_{\varepsilon,x}^M$, and

$$\left\|\left(\mathcal{L}_{\varepsilon,x}^M\right)^{-1}\right\|\leq(1+\lambda\Delta t)^{-1}, \tag{8.11}$$

which is used in estimating the truncation error of the semi-discrete scheme. ■

Lemma 8.3.2 *(Bansal & Sharma, 2018). The solution $U^{j+1}(x)$ of the semi-discrete problem (8.10) can be estimated as*

$$|U^{j+1}(x)|\leq\frac{\|\vartheta\|}{1+\lambda\Delta t}+\max\left\{|U^{j+1}(0)|,|U^{j+1}(2)|\right\},\ x\in\bar{\Gamma}.$$

Proof. Define barrier functions as

$$\pi_\pm^{j+1}(x)=\frac{\|\vartheta\|}{1+\lambda\Delta t}+\max\left\{|U^{j+1}(0)|,|U^{j+1}(2)|\right\}\pm U^{j+1}(x).$$

At $x=0$, $\pi_\pm^{j+1}(0)=\frac{\|\vartheta\|}{1+\lambda\Delta t}+\max\{|U^{j+1}(0)|,|U^{j+1}(2)|\}\pm U^{j+1}(0)\geq\frac{\|\vartheta\|}{1+\lambda\Delta t}\geq 0.$
At $x=2$, $\pi_\pm^{j+1}(2)=\frac{\|\vartheta\|}{1+\lambda\Delta t}+\max\{|U^{j+1}(0)|,|U^{j+1}(2)|\}\pm U^{j+1}(2)\geq\frac{\|\vartheta\|}{1+\lambda\Delta t}\geq 0.$

For $x \in (0,1]$,

$$\begin{aligned}\mathcal{L}^M_{\varepsilon,1}\pi^{j+1}_{\pm}(x) =& -\varepsilon(\pi_{\pm})^{j+1}_{xx}(x) + p(x)\pi^{j+1}_{\pm}(x)\\ =& \pm\vartheta^{j+1}(x) + p(x)\frac{\|\vartheta\|}{1+\lambda\Delta t} + p(x)\max\left\{|U^{j+1}(0)|, |U^{j+1}(2)|\right\}\\ \geq& \mu\left(\max\left\{|U^{j+1}(0)|, |U^{j+1}(2)|\right\}\right) \geq \ 0.\end{aligned}$$

For $x \in (1,2)$,

$$\begin{aligned}\mathcal{L}^M_{\varepsilon,2}\pi^{j+1}_{\pm}(x) =& -\varepsilon(\pi_{\pm})^{j+1}_{xx}(x) + p(x)\pi^{j+1}_{\pm}(x) + q(x)\pi^{j+1}_{\pm}(x-1)\\ =& \pm\vartheta^{j+1}(x) + [p(x)+q(x)]\frac{\|\vartheta\|}{1+\lambda\Delta t} + [p(x)\\ &+ q(x)]\max\left\{|U^{j+1}(0)|, |U^{j+1}(2)|\right\}\\ \geq& \lambda\left(\max\left\{|U^{j+1}(0)|, |U^{j+1}(2)|\right\}\right) \geq \ 0.\end{aligned}$$

Thus, it is obtained that $\mathcal{L}^M_{\varepsilon}\pi^{j+1}_{\pm}(x) \geq 0$ for all $x \in [0,2]$. Hence, by the semi-discrete maximum principle, the required estimation of $U^{j+1}(x)$ is attained. ■

At the $(j+1)^{th}$ time level, the local truncation error e^{j+1} is defined as the difference between the exact solution $U(x,t_{j+1})$ and the approximate solution $U^{j+1}(x)$ of (8.10), and the global error estimate E^{j+1} as the contribution of local truncation error up to the $(j+1)^{th}$ time level.

Lemma 8.3.3 *(Local truncation error estimate). Suppose that* $\left|U^{(k)}(x,t)\right| \leq C$, $(x,t) \in \bar{\Omega}$, $k = 0,1,2$. *Then at the* $(j+1)^{th}$ *time level, the local truncation error is given as* $\|e^{j+1}\| \leq C(\Delta t)^2$.

Proof. See Lemma 6.3.3 of Chapter 6. ■

Lemma 8.3.4 *(Estimation of the global error). Suppose that Lemma 8.3.3 holds. Then the global truncation error is estimated as* $\|E^{j+1}\| \leq C(\Delta t)$, $j = 0,1,2,...,M-1$.

Proof. Considering the local truncation error in Lemma 8.3.3 up to the $(j+1)^{th}$ time level,

$$\begin{aligned}\|E^{j+1}\| =& \left\|\sum_{\iota=1}^{j} e^{\iota}\right\|, \quad j \leq T/\Delta t\\ =& \|e^1 + e^2 + ... + e^j\|\\ \leq& \|e^1\| + \|e^2\| + ... + \|e^j\|\\ \leq& C(\Delta t), \ j = 0,1,2,...,M-1.\end{aligned}$$

Thus, the semi-discrete scheme is convergent of order one in time. ■

Lemma 8.3.5 *The derivatives of the solution $U^{j+1}(x),\ j=0,1,2,...,M-1$ of (8.10) can be bounded as*

$$\left|\frac{d^kU^{j+1}(x)}{dx^k}\right| \le \begin{cases} C\left[1+\varepsilon^{-k/2}\left(\exp(-\sqrt{\frac{\lambda}{\varepsilon}}x)+\exp(-\sqrt{\frac{\lambda}{\varepsilon}}(1-x))\right)\right], \\ \quad x\in(0,1],\ k=0.1,2,3,4, \\ C\left[1+\varepsilon^{-k/2}\left(\exp(-\sqrt{\frac{\lambda}{\varepsilon}}(x-1))+\exp(-\sqrt{\frac{\lambda}{\varepsilon}}(2-x))\right)\right], \\ \quad x\in(1,2), k=0,1,2,3,4. \end{cases}$$

Proof. See the proof of Lemma 6.3.5 of Chapter 6. ∎

8.3.2 Spatial discretization

Suppose that the domain $[0,2]$ be subdivided into N equal intervals of step size h and form a uniform mesh as $\bar{\Gamma}_x^N=\{0=x_0,x_1,...,x_{\frac{N}{2}}=1,x_{\frac{N}{2}+1},...,x_N=2,\ x_i=ih, i=0,1,..,N,\ h=\frac{2}{N}\}$.

On a uniform mesh, a function $S(x,\gamma)$ of class $C^2[0,2]$ that interpolates $U^{j+1}(x)$ at x_i depends on the compression parameter γ and reduced to a cubic spline on the interval $[0,2]$ for γ approaching to zero is known as parametric cubic spline function Chakravarthy et al. (2017b). In any interval $[x_i,x_{i+1}]\subset[0,2]$, the spline function $S(x,\gamma)=S(x)$, which satisfies the linear second order differential equation

$$\begin{aligned} S_{xx}(x,t_{j+1})-\gamma S(x,t_{j+1}) =&[S_{xx}(x_i,t_{j+1})-\gamma S(x_i,t_{j+1})]\left(\frac{x_{i+1}-x}{h}\right) \\ &+[S_{xx}(x_{i+1},t_{j+1}-\gamma S(x_{i+1},t_{j+1})]\left(\frac{x-x_i}{h}\right), \end{aligned} \tag{8.12}$$

where $S(x_i,t_{j+1})=U_i^{j+1}$ for $\gamma>0$ is called cubic spline in compression. Solving the homogeneous part (8.12) and setting $\sqrt{\gamma}=\frac{\mu}{h}$ gives

$$S_1(x,t_{j+1})=A\exp(\frac{\mu}{h}(x-x_i))+B\exp(\frac{\mu}{h}(x_{i+1}-x)), \tag{8.13}$$

where A and B are arbitrary constants. And let

$$S_2(x,t_{j+1})=k\left\{[S_{xx}(x_i,t_{j+1})-\gamma S(x_i,t_{j+1})]\frac{x_{i+1}-x}{h}+[S_{xx}(x_{i+1},t_{j+1})-\gamma S(x_{i+1},t_{j+1})]\frac{x-x_i}{h}\right\}$$

be the solution of the non-homogeneous part of (8.12). From this $k=-1/\gamma$, so that

$$S_2(x,t_{j+1})=-\left(\frac{h}{\mu}\right)^2[M_i-\left(\frac{\mu}{h}\right)^2U_i^{j+1}]\left(\frac{x_{i+1}-x}{h}\right)-\left(\frac{h}{\mu}\right)^2[M_{i+1}-\left(\frac{\mu}{h}\right)^2U_{i+1}^{j+1}]\left(\frac{x-x_i}{h}\right), \tag{8.14}$$

where $M_i = S_{xx}(x_i, t_{j+1})$ and $M_{i+1} = S_{xx}(x_{i+1}, t_{j+1})$. From (8.13) and (8.14),

$$\begin{aligned} S(x,t_{j+1}) =& A\exp(\frac{\mu}{h}(x-x_i)) + B\exp(\frac{\mu}{h}(x_{i+1}-x)) - \left(\frac{h}{\mu}\right)^2 [M_i - \left(\frac{\mu}{h}\right)^2 U_i^{j+1}] \left(\frac{x_{i+1}-x}{h}\right) \\ & - \left(\frac{h}{\mu}\right)^2 [M_{i+1} - \left(\frac{\mu}{h}\right)^2 U_{i+1}^{j+1}] \left(\frac{x-x_i}{h}\right). \end{aligned} \tag{8.15}$$

The values of the constants A and B can be determined by the interpolation conditions. That is, in $[x_i, x_{i+1}]$ equation (8.15) gives

$$S(x_i, t_{j+1}) = A + B\exp(\mu) - \left(\frac{h}{\mu}\right)^2 (M_i - \left(\frac{\mu}{h}\right)^2 U_i^{j+1}) \tag{8.16}$$

and

$$S(x_{i+1}, t_{j+1}) = A\exp(\mu) + B - \left(\frac{h}{\mu}\right)^2 (M_{i+1} - \left(\frac{\mu}{h}\right)^2 U_{i+1}^{j+1}). \tag{8.17}$$

From (8.16) and (8.17), one can find obtain that $A = \frac{h^2}{2\mu^2\sinh(\mu)}[M_{i+1} - e^{\mu}M_i]$ and $B = \frac{h^2}{2\mu^2\sinh(\mu)}[M_i - e^{\mu}M_{i+1}]$. Thus, (8.15) becomes

$$\begin{aligned} S(x,t_{j+1}) =& \frac{h^2}{2\mu^2\sinh(\mu)}\left[M_{i+1}\sinh\left(\frac{\mu(x-x_i)}{h}\right) + M_i\sinh\left(\frac{\mu(x_{i+1}-x)}{h}\right)\right] \\ & - \left[\frac{h}{\mu^2}M_i - \frac{1}{h}U_i^{j+1}\right](x_{i+1}-x) - \left[\frac{h}{\mu^2}M_{i+1} - \frac{1}{h}U_{i+1}^{j+1}\right](x-x_i), \end{aligned} \tag{8.18}$$

which is the cubic spline in compression on $[x_i, x_{i+1}]$, where $M_i = S_{xx}(x_i, t_{j+1})$. The derivative of (8.18) at (x_i^+, t_{j+1}) is

$$S_x(x_i^+, t_{j+1}) = \frac{U_{j+1}^{i+1} - U_i^{j+1}}{h} - \frac{hM_{i+1}}{\mu^2}\left(1 - \frac{\mu}{\sinh(\mu)}\right) - \frac{hM_i}{\mu^2}\left(\mu\coth(\mu) - 1\right). \tag{8.19}$$

On the other hand, for $x \in [x_{i-1}, x_i]$, a linear second order differential equation is defined as

$$\begin{aligned} S_{xx}(x,t_{j+1}) - \left(\frac{\mu}{h}\right)^2 S(x,t_{j+1}) =& \left[S_{xx}(x_{i-1},t_{j+1}) - \left(\frac{\mu}{h}\right)^2 S(x_{i-1},t_{j+1})\right]\left(\frac{x_i-x}{h}\right) \\ & + \left[S_{xx}(x_i,t_{j+1}) - \left(\frac{\mu}{h}\right)^2 S(x_i,t_{j+1})\right]\left(\frac{x-x_{i-1}}{h}\right), \end{aligned} \tag{8.20}$$

where $S^{j+1}(x_{i-1}) = U_{i-1}^{j+1}$, $S_{xx}(x_{i-1}, t_{j+1}) = M_{i-1}$. Solving (8.20) gives

$$\begin{aligned} S(x,t_{j+1}) =& E\exp(\frac{\mu}{h}(x-x_{i-1})) + F\exp(\frac{\mu(x_i-x)}{h}) - \left[\frac{h}{\mu^2}M_{i-1} - \frac{1}{h}U_{i-1}^{j+1}\right](x-x_{i-1}) \\ & - \left[\frac{h}{\mu^2}M_i - \frac{1}{h}U_i^{j+1}\right](x_i-x), \end{aligned} \tag{8.21}$$

where the constants E and F are given by

$$E = \frac{h^2}{2\mu^2 \sinh(\mu)} \left(M_i - \exp(-\mu M_{i-1})\right)$$

and

$$F = \frac{h^2}{2\mu^2 \sinh(\mu)} \left(M_{i-1} - \exp(-\mu M_i)\right).$$

So, (8.21) becomes

$$\begin{aligned} S(x, t_{j+1}) = &\frac{h^2}{2\mu^2 \sinh(\mu)} \left[M_i \sinh\left(\frac{\mu(x - x_{i-1})}{h}\right) + M_{i-1} \sinh\left(\frac{\mu(x_i - x)}{h}\right)\right] \\ &- [\frac{h}{\mu^2} M_i - \frac{1}{h} U_i^{j+1}](x - x_{i-1}) - [\frac{h}{\mu^2} M_{i-1} - \frac{1}{h} U_{i-1}^{j+1}](x_i - x). \end{aligned} \tag{8.22}$$

Differentiating (8.22) and evaluating for x approaching to x_i^- gives

$$S_x(x_i^-, t_{j+1}) = \frac{U_i^{j+1} - U_{i-1}^{j+1}}{h} + \frac{hM_i\left(\mu \coth(\mu) - 1\right)}{\mu^2} + \frac{hM_{i-1}}{\mu^2}\left(1 - \frac{\mu}{\sinh(\mu)}\right). \tag{8.23}$$

At the mesh point x_i, equations (8.19) and (8.23) give

$$h^2\left(\mu_1 M_{i-1} + 2\mu_2 M_i + \mu_1 M_{i+1}\right) = U_{i-1}^{j+1} - 2U_i^{j+1} + U_{i+1}^{j+1}, \tag{8.24}$$

where $\mu_1 = \frac{1}{\mu^2}\left(1 - \frac{\mu}{\sinh(\mu)}\right)$ and $\mu_2 = \frac{1}{\mu^2}(\mu \coth(\mu) - 1)$. The consistency condition in (8.24) guarantees the continuity of the first derivative of the spline function at the interior points. The developed scheme is used to solve the considered problem if it is consistent, which holds for $\mu_1 + \mu_2 = 1/2$ (Chakravarthy et al., 2017b). Now, from the time semi-discrete problem (8.16),

$$\varepsilon \Delta t M_i = p_i U_i^{j+1} + q_i U_{i-\frac{N}{2}}^{j+1} - \Delta t f_i^{j+1} - U_i^j, \tag{8.25a}$$

$$\varepsilon \Delta t M_{i\pm1} = p_{i\pm1} U_{i\pm1}^{j+1} + q_{i\pm1} w_{i\pm1-\frac{N}{2}}^{j+1} - \Delta t f_i^{j+1} - U_{i\pm1}^j, \tag{8.25b}$$

where $p_i = 1 + \Delta t a(x_i)$ and $q_i = \Delta t b(x_i)$. Inserting (8.25) into (8.24) gives

$$\begin{aligned} \varepsilon \Delta t(U_{i-1}^{j+1} - 2U_i^{j+1} + U_{i+1}^{j+1}) = &h^2\mu_1[p_{i-1}U_{i-1}^{j+1} + q_{i-1}U_{i-1-\frac{N}{2}}^{j+1} - \Delta t f_{i-1}^{j+1} - U_{i-1}^j] + 2h^2\mu_2[p_i U_i^{j+1} \\ &+ q_i U_{i-\frac{N}{2}}^{j+1} - \Delta t f_i^{j+1} - U_i^j] + h^2\mu_1[p_{i+1}U_{i+1}^{j+1} + q_{i+1}U_{i+1-\frac{N}{2}}^{j+1} \\ &- \Delta t f_{i+1}^{j+1} - U_{i+1}^j],\ i = 1, 2, ..., N-1, j = 0, 1, 2, ..., M-1. \end{aligned} \tag{8.26}$$

On rearrangement of terms, (8.26) can be rewritten as

$$
\begin{aligned}
&(-\varepsilon\Delta t+\mu_1h^2p_{i-1})U_{i-1}^{j+1}+(2\varepsilon\Delta t+2\mu_2h^2p_i)U_i^{j+1}+(-\varepsilon\Delta t+\mu_1h^2p_{i+1})U_{i+1}^{j+1}\\
&=\mu_1h^2U_{i-1}^j+2\mu_2h^2U_i^j+\mu_1h^2U_{i+1}^j-\mu_1h^2q_{i-1}U^{j+1}(x_{i-1}-1)-2\mu_2h^2q_iU^{j+1}(x_i-1)\\
&-\mu_1h^2q_{i+1}U^{j+1}(x_{i+1}-1)+\mu_1h^2\Delta tf_{i-1}^{j+1}+2\mu_2h^2\Delta tf_i^{j+1}+\mu_1h^2\Delta tf_{i+1}^{j+1},\\
&\qquad i=0,1,...,N,\ j=0,1,2,...,M-1.
\end{aligned}
\tag{8.27}
$$

Exponential fitting factor

To control the influence of ε in the layers, an exponential fitting factor is introduced. Using analogous procedures of Chakravarthy et al. (2017a), the analytical solution of (8.10) is written as

$$
\begin{aligned}
U^{j+1}(x)=&\eta_1\exp\left(\sqrt{\frac{p_i}{\varepsilon\Delta t}}(x-x_i)\right)+\eta_2\exp-\left(\sqrt{\frac{p_i}{\varepsilon\Delta t}}(x-x_i)\right)-\frac{1}{p_i}(q_iU^{j+1}(x_i-1)\\
&-\Delta tf(x_i,t_{j+1})-U^j(x_i)),\ x\in(x_{i-1},x_{i+1}),
\end{aligned}
\tag{8.28}
$$

where the arbitrary constants η_1 and η_2 are determined using the conditions $U^{j+1}(x_{i\pm1})=U_{i\pm1}^{j+1}$ and $U^{j+1}(x_i)=U_i^{j+1}$ as

$$
\eta_1=\frac{U_{i-1}^{j+1}-2U_i^{j+1}+U_{i+1}^{j+1}}{8\sinh^2(\frac{\rho}{2}\sqrt{\frac{p_i}{\Delta t}})}+\frac{U_{i-1}^{j+1}-U_{i+1}^{j+1}}{2\cosh(\rho\sqrt{\frac{p_i}{\Delta t}})},\tag{8.29}
$$

$$
\eta_1=\frac{U_{i-1}^{j+1}-2U_i^{j+1}+U_{i+1}^{j+1}}{8\sinh^2(\frac{\rho}{2}\sqrt{\frac{p_i}{\Delta t}})}-\frac{U_{i-1}^{j+1}-U_{i+1}^{j+1}}{2\cosh(\rho\sqrt{\frac{p_i}{\Delta t}})}.\tag{8.30}
$$

Then, introducing a fitting factor σ_1 on $(0,1]$ yields

$$
\begin{aligned}
&\frac{\varepsilon\Delta t\sigma_1}{h^2}(U_{i+1}^{j+1}-2U_i^{j+1}+U_{i-1}^{j+1})-p_i[\eta_1\exp\left(\sqrt{\frac{p_i}{\varepsilon\Delta t}}(x-x_i)\right)+\eta_2\exp-\left(\sqrt{\frac{p_i}{\varepsilon\Delta t}}(x-x_i)\right)\\
&-\frac{1}{p_i}\left(q_iU^{j+1}(x_i-1)-\Delta tf^{j+1}(x_i)-U^j(x_i)\right)]-q_iU^{j+1}(x_i-1)=\Delta tf^{j+1}(x_i)-U_i^j
\end{aligned}
\tag{8.31}
$$

On simplification of (8.31) for $i=1,2,...,\frac{N}{2}$, the fitting factor is

$$
\sigma_1=\left(\frac{\rho/2\sqrt{p(0)/\Delta t}}{\sinh(\rho/2\sqrt{p(0)/\Delta t})}\right)^2,\tag{8.32}
$$

where $p(0)=1+\Delta ta(0)$ and $\rho=h/\sqrt{\varepsilon}$. By a similar procedure $i=\frac{N}{2}+1,\frac{N}{2}+2,...,N$, the fitting factor is given as

$$
\sigma_2=\left(\frac{\rho/2\sqrt{p(2)/\Delta t}}{\sinh(\rho/2\sqrt{p(2)/\Delta t})}\right)^2,\tag{8.33}
$$

Thus, with the fitting factor σ_1 and σ_2 in (8.27), the fully-discrete numerical scheme is

$$\mathcal{L}_{\varepsilon}^{N,M}U_i^{j+1}=\vartheta_i^{j+1},\ j=0,1,2,...,M-1, \tag{8.34}$$

where

$$\mathcal{L}_{\varepsilon}^{N,M}U_i^{j+1}=\begin{cases}(-\varepsilon\sigma_1\Delta t+\mu_1h^2p_{i-1})U_{i-1}^{j+1}+(2\varepsilon\sigma_1\Delta t+2\mu_2h^2p_i)U_i^{j+1}+(-\varepsilon\sigma_1\Delta t+\mu_1h^2p_{i+1})U_{i+1}^{j+1},\\ \qquad i=1,2,...,\frac{N}{2},\\ (-\varepsilon\sigma_2\Delta t+\mu_1h^2p_{i-1})U_{i-1}^{j+1}+(2\varepsilon\sigma_2\Delta t+2\mu_2h^2p_i)U_i^{j+1}(-\varepsilon\sigma_2\Delta t+\mu_1h^2p_{i+1})U_{i+1}^{j+1}\\ +\mu_1h^2q_{i-1}U_{i-1-\frac{N}{2}}^{j+1}+2\mu_2h^2q_iU_{i-\frac{N}{2}}^{j+1}+\mu_1h^2q_{i+1}U_{i+1-\frac{N}{2}}^{j+1},\\ \qquad i=\frac{N}{2}+1,\frac{N}{2}+2,...,N\end{cases}$$

and

$$\vartheta_i^{j+1}=\begin{cases}\mu_1h^2U_{i-1}^j+2\mu_2h^2U_i^j+\mu_1h^2U_{i+1}^j-\mu_1h^2q_{i-1}\alpha_{i-1-\frac{N}{2}}^{j+1}-2\mu_2h^2q_i\alpha_{i-\frac{N}{2}}^{j+1}\\ -\mu_1h^2q_{i+1}\alpha_{i+1-\frac{N}{2}}^{j+1}+\mu_1h^2\Delta tf_{i-1}^{j+1}+2\mu_2h^2\Delta tf_i^{j+1}+\mu_1h^2\Delta tf_{i+1}^{j+1},\ i=1,2,...,\frac{N}{2},\\ \mu_1h^2U_{i-1}^j+2\mu_2h^2U_i^j+\mu_1h^2U_{i+1}^j+\mu_1h^2\Delta tf_{i-1}^{j+1}+2\mu_2h^2\Delta tf_i^{j+1}+\mu_1h^2\Delta tf_{i+1}^{j+1},\\ \quad i=\frac{N}{2}+1,\frac{N}{2}+2,...,N.\end{cases}$$

From (8.34), a system of equation is derived as

$$\gamma_1^-U_{i-1}^{j+1}+\gamma_1^0U_i^{j+1}+\gamma_1^+U_{i+1}^{j+1}=G_{i,j},\ j=0,1,2,...,M-1 \tag{8.35}$$

with $U_0^{j+1}=U^{j+1}(0)$ and $U_N^{j+1}=U^{j+1}(x_N)$, where

$$\begin{aligned}\gamma_1^-=&-\varepsilon\sigma_\iota\Delta t+\mu_1h^2p_{i-1},\\ \gamma_1^0=&2\varepsilon\sigma_\iota\Delta t+2\mu_2h^2p_i,\\ \gamma_1^+=&-\varepsilon\sigma_\iota\Delta t+\mu_1h^2p_{i+1},\end{aligned}$$

$$G_{i,j}=\begin{cases}\mu_1h^2U_{i-1}^j+2\mu_2h^2U_i^j+\mu_1h^2U_{i+1}^j-\mu_1h^2q_{i-1}\phi_{i-1-\frac{N}{2}}^{j+1}-2\mu_2h^2q_i\phi_{i-\frac{N}{2}}^{j+1}\\ -\mu_1h^2q_{i+1}\alpha_{i+1-\frac{N}{2}}^{j+1}+\mu_1h^2\Delta tf_{i-1}^{j+1}+2\mu_2h^2\Delta tf_i^{j+1}+\mu_1h^2\Delta tf_{i+1}^{j+1},\ i=1,2,...,\frac{N}{2},\\ \mu_1h^2U_{i-1}^j+2\mu_2h^2U_i^j+\mu_1h^2U_{i+1}^j-\mu_1h^2q_{i-1}U_{i-1-\frac{N}{2}}^{j+1}-2\mu_2h^2q_iU_{i-\frac{N}{2}}^{j+1}\\ -\mu_1h^2q_{i+1}U_{i+1-\frac{N}{2}}^{j+1}+\mu_1h^2\Delta tf_{i-1}^{j+1}+2\mu_2h^2\Delta tf_i^{j+1}+\mu_1h^2\Delta tf_{i+1}^{j+1},\ i=\frac{N}{2}+1,...,N,\end{cases}$$

where $\sigma_\iota=\sigma_1$ for $i=1,2,...,\frac{N}{2}$ and $\sigma_\iota=\sigma_2$ for $i=\frac{N}{2}+1,\frac{N}{2}+2,...,N$. The systems in (8.35) is solved easily using suitable solver of system of equations.

Lemma 8.3.6 *For a mesh function ψ_i^{j+1} if $\psi_0^{j+1}\geq 0$, $\psi_N^{j+1}\geq 0$ and $\mathcal{L}_{\varepsilon}^{N,M}\psi_{\varsigma}^{j+1}\geq 0$, $\varsigma=1,2,...,N-1$, then $\psi_i^{j+1}\geq 0$, $i=0,1,...,N$.*

Proof. For $\varsigma = 0, 1, ..., N$, let $\psi_{\varsigma}^{j+1} = \min_{\bar{\Omega}^{N,M}} \psi_i^{j+1}$ and suppose that $\psi_{\varsigma}^{j+1} < 0$. From the given condition, it is clear that $\varsigma \neq \{0, N\}$.
Case 1 : For $\varsigma = 1, 2, ..., \frac{N}{2}$, it becomes

$$\mathcal{L}_{\varepsilon,1}^{N,M}\psi_{\varsigma}^{j+1} = (-\varepsilon\sigma_1\Delta t+\mu_1 h^2 p_{\varsigma-1})\psi_{\varsigma-1}^{j+1}+(2\varepsilon\sigma_1\Delta t+2\mu_2 h^2 p_{\varsigma})\psi_{\varsigma}^{j+1}+(-\varepsilon\sigma_1\Delta t+\mu_1 h^2 p_{\varsigma+1})\psi_{\varsigma+1}^{j+1} < 0.$$

Case 2 : When $\varsigma = \frac{N}{2}+1, \frac{N}{2}+2, ..., N-1$, it becomes

$$\begin{aligned}\mathcal{L}_{\varepsilon,2}^{N,M}\psi_{\varsigma}^{j+1} =&(-\varepsilon\sigma_2\Delta t + \mu_1 h^2 p_{\varsigma-1})\psi_{\varsigma-1}^{j+1} + (2\varepsilon\sigma_2\Delta t + 2\mu_2 h^2 p_{\varsigma})\psi_{\varsigma}^{j+1}(-\varepsilon\sigma_2\Delta t + \mu_1 h^2 p_{\varsigma+1})\psi_{\varsigma+1}^{j+1}\\ &+ \mu_1 h^2 q_{\varsigma-1}\psi_{\varsigma-1-N/2}^{j+1} + 2\mu_2 h^2 q_{\varsigma} u_{\varsigma-N/2}^{j+1} + \mu_1 h^2 q_{\varsigma+1}\psi_{\varsigma+1-N/2}^{j+1}\\ \leq&(-\varepsilon\sigma_2\Delta t + \mu_1 h^2 p_{\varsigma-1})\psi_{\varsigma-1}^{j+1} + (2\varepsilon\sigma_2\Delta t + 2\mu_2 h^2 p_{\varsigma})\psi_{\varsigma}^{j+1}(-\varepsilon\sigma_2\Delta t + \mu_1 h^2 p_{\varsigma+1})\psi_{\varsigma+1}^{j+1}\\ &+ \mu_1 h^2 q_{\varsigma-1}\psi_{\varsigma-1}^{j+1} + 2\mu_2 h^2 q_{\varsigma} u_{\varsigma}^{j+1} + \mu_1 h^2 q_{\varsigma+1}\psi_{\varsigma+1}^{j+1} \leq 0.\end{aligned}$$

From the two cases, $\mathcal{L}_{\varepsilon}^{N,M}\psi_{\varsigma}^{j+1} \leq 0$, which contradicts the given hypothesis. Thus, the assumption is not hold, and hence $\psi_i^{j+1} \geq 0, i = 0, 1, ..., N$. ■

Lemma 8.3.7 *(Bansal & Sharma, 2018). The solution U_i^{j+1} of the difference scheme (8.34) is estimated as*

$$|U_i^{j+1}| \leq (1+\lambda\Delta t)^{-1}\|\vartheta\| + \max\left\{|U_0^{j+1}|, |U_N^{j+1}|\right\},\ i = 0, 1, ..., N.$$

Proof. Let $\pi_{i,\pm}^{j+1}$ be the barrier functions defined by

$$\pi_{i,\pm}^{j+1} = (1+\lambda\Delta t)^{-1}\|\vartheta\| + \max\left\{|U_0^{j+1}|, |U_N^{j+1}|\right\} \pm U_i^{j+1}.$$

Then, by these functions when $i = 0$,

$$\pi_{0,\pm}^{j+1} = (1+\lambda\Delta t)^{-1}\|\vartheta\| + \max\left\{|U_0^{j+1}|, |U_N^{j+1}|\right\} \pm U_0^{j+1} \geq (1+\lambda\Delta t)^{-1}\|\vartheta\| \geq\ 0.$$

When $i = N$,

$$\pi_{N,\pm}^{j+1} = (1+\lambda\Delta t)^{-1}\|\vartheta\| + \max\left\{|U_0^{j+1}|, |U_N^{j+1}|\right\} \pm U_N^{j+1} \geq (1+\lambda\Delta t)^{-1}\|\vartheta\| \geq\ 0.$$

Now , let $\omega = (1+\lambda\Delta t)^{-1}\|\vartheta\| + \max\left\{|U_0^{j+1}|, |U_N^{j+1}|\right\}$. Then, when $i = 1, 2, ..., \frac{N}{2}$,

$$\begin{aligned}\mathcal{L}_{\varepsilon,1}^{N,M}\pi_{i,\pm}^{j+1} =&(-\varepsilon\sigma_1\Delta t + \mu_1 h^2 p_{i-1})(\omega \pm U_{i-1}^{j+1}) + (2\varepsilon\sigma_1\Delta t + 2\mu_2 h^2 p_i)(\omega \pm U_i^{j+1})\\ &+ (-\varepsilon\sigma_1\Delta t + \mu_1 h^2 p_{i+1})(\omega \pm U_{i+1}^{j+1})\\ =&h^2(\mu_1(p_{i-1}+p_{i+1}) + 2\mu_2 p_i)\left[(1+\mu\Delta t)^{-1}\|\vartheta\| + \max\{|U_0^{j+1}|, |U_N^{j+1}|\}\right] \pm \vartheta(x_i, t_j)\\ \geq&(\mu_1 h^2 p_{i-1} + 2\mu_2 h^2 p_i + \mu_1 h^2 p_{i+1})\left[\max\{|U_0^{j+1}|, |U_N^{j+1}|\}\right] \geq 0.\end{aligned}$$

And for $i = \frac{N}{2}+1, \frac{N}{2}+2, ..., N-1$,

$$\begin{aligned}
\mathcal{L}_{\varepsilon,2}^{N,M}\pi_{i,\pm}^{j+1} =&(-\varepsilon\sigma_2\Delta t + \mu_1 h^2 p_{i-1})(\omega \pm U_{i-1}^{j+1}) + (2\varepsilon\sigma_2\Delta t + 2\mu_2 h^2 p_i)(\omega \pm U_i^{j+1})\\
&+ (-\varepsilon\sigma_2\Delta t + \mu_1 h^2 p_{i+1})(\omega \pm U_{i+1}^{j+1}) + \mu_1 h^2 q_{i-1}(\omega + U_{i-1-\frac{N}{2}}^{j+1})\\
&+ 2\mu_2 h^2 q_i(\omega \pm U_{i-\frac{N}{2}}^{j+1}) + \mu_1 h^2 q_{i+1}(\omega \pm U_{i+1-\frac{N}{2}}^{j+1})\\
=&h^2(\mu_1 p_{i-1} + 2\mu_2 p_i + \mu_1 p_{i+1} + \mu_1 q_{i-1} + 2\mu_1 q_i + \mu_1 q_{i+1})\\
&\big[(1+\lambda\Delta t)^{-1}\|\vartheta\| + \max\{|U_0^{j+1}|, |U_N^{j+1}|\}\big] \pm \vartheta(x_i, t_j)\\
\geq& h^2[\mu_1(p_{i-1} + p_{i+1} + q_{i-1} + q_{i+1}) + 2\mu_2(p_i + q_i)]\,\big[\max\{|U_0^{j+1}|, |U_N^{j+1}|\}\big] \geq 0.
\end{aligned}$$

Therefore, $\mathcal{L}_\varepsilon^M \pi_{i,\pm}^{j+1} \geq 0$, $i = 0, 1, 2, ..., N$, and applying Lemma 8.3.6 yields the required stability estimate. ■

Theorem 8.3.1 *Let $U^{j+1}(x_i)$ and U_i^{j+1} be the solutions of the schemes (8.10) and (8.34), respectively. Then, the error estimate in the spatial discretization is given by*

$$|U^{j+1}(x_i) - U_i^{j+1}| \leq CN^{-2},\ i = 0, 1, 2, ..., N.$$

Proof. For $i - 1, 2, ..., \frac{N}{2}$, the truncation error is

$$\begin{aligned}
|\mathcal{L}_\varepsilon^M u^{j+1}(x_i) - \mathcal{L}_\varepsilon^{N,M} U_i^{j+1}| =&| -\varepsilon\Delta t U_{xx}^{j+1} + p(x_i)U^{j+1}(x_i) + \varepsilon\sigma_1\Delta t\delta_x^2 U_i^{j+1}\\
&- \mu_1 p_{i+1}U_{i+1}^{j+1} - 2\mu_2 p_i U_i^{j+1} - \mu_1 p_{i-1}U_{i-1}^{j+1}|\\
=&| -\varepsilon\Delta t U_{xx}^{j+1} + p(x_i)U^{j+1}(x_i) + \frac{\varepsilon\sigma_1\Delta t}{h^2}(U_{i+1}^{j+1} - 2U_i^{j+1} + U_{i-1}^{j+1})\\
&- \mu_1 p_{i+1}U_{i+1}^{j+1} - 2\mu_2 p_i U_i^{j+1} - \mu_1 p_{i-1}U_{i-1}^{j+1}|
\end{aligned}$$

Using Taylor's series expansion for $U_{i\pm1}^{j+1}$ leads to

$$\begin{aligned}
|\mathcal{L}_\varepsilon^M U^{j+1}(x_i) - \mathcal{L}_\varepsilon^{N,M} U_i^{j+1}| =&| -\varepsilon\Delta t U_{xx}^{j+1}(x_i) + p(x_i)U^{j+1}(x_i) + \varepsilon\sigma_1\Delta t(U_{xx}^{j+1}(x_i) + \frac{h^2}{12}U_{xxxx}^{j+1}(\xi)\\
&+ \frac{h^4}{360}U_{xxxxxx}^{j+1}(\xi) + O(h^6)) - \mu_1 p_{i+1}(U_i^{j+1} + hU_x^{j+1}(x_i) + \frac{h^2}{2}U_{xx}^{j+1}(x_i)\\
&+ \frac{h^3}{6}U_{xxx}^{j+1}(\xi) + \frac{h^4}{24}U_{xxxx}^{j+1}(\xi) + \frac{h^5}{120}U_{xxxxx}^{j+1}(\xi) + O(h^6)) - 2\mu_2 p_i U_i^{j+1}\\
&-\mu_1 p_{i-1}(U_i^{j+1} - hU_x^{j+1}(x_i) + \frac{h^2}{2}U_{xx}^{j+1}(x_i) - \frac{h^3}{6}U_{xxx}^{j+1}(\xi) + \frac{h^4}{24}U_{xxxx}^{j+1}(\xi)\\
&- \frac{h^5}{120}U_{xxxxx}^{j+1}(\xi) + O(h^6))|,\ \xi \in (x_{i-1}, x_{i+1}). \qquad (8.36)
\end{aligned}$$

For a μ_1 and μ_2 satisfying $2\mu_2 = 1 - 2\mu_1$, using the Taylor's series expansion on $p_{i\pm1}$ and on the fitting factor σ_1, (8.36) became

$$\begin{aligned}
|\mathcal{L}_\varepsilon^M U^{j+1}(x_i)-\mathcal{L}_\varepsilon^{N,M}U_i^{j+1}| =&|(\frac{\varepsilon\Delta t}{12}U_{xxxx}^{j+1}(\xi)-\mu_1 p_i U_{xx}^{j+1}(\xi))h^2+(\frac{\varepsilon\Delta t}{360}U_{xxxxxx}^{j+1}(\xi)-\frac{\Delta t p_i}{144}U_{xxxx}^{j+1}(\xi)\\
&-\frac{\mu_1 p_i}{24}U_{xxxx}^{j+1}(\xi))h^4+O(h^6)|\\
\leq&|\frac{\varepsilon\Delta t}{12}U_{xxxx}^{j+1}(\xi)-\mu_1 p_i U_{xx}^{j+1}(x_i)|h^2+|\frac{\varepsilon\Delta t}{360}U_{xxxxxx}^{j+1}(\xi)-\frac{\Delta t p_i}{144}U_{xxxx}^{j+1}(\xi)\\
&-\frac{\mu_1 p_i}{24}U_{xxxx}^{j+1}(\xi)|h^4+O(h^6)\leq Ch^2.
\end{aligned}$$

Now, invoking Lemma 8.3.6 yields

$$|U^{j+1}(x_i)-U_i^{j+1}|\leq Ch^2,\ i=0,1,2,...,\frac{N}{2}. \tag{8.37}$$

For $i=\frac{N}{2}+1,\frac{N}{2}+2,...,N$,

$$\begin{aligned}
|\mathcal{L}_\varepsilon^M U^{j+1}(x_i)-\mathcal{L}_\varepsilon^{N,M}U_i^{j+1}| =&|-\varepsilon\Delta t U_{xx}^{j+1}+p(x_i)U^{j+1}(x_i)+q(x_i)U^{j+1}(x_{i-\frac{N}{2}})+\varepsilon\sigma_2\Delta t\delta_x^2U_i^{j+1}\\
&-\mu_1 p_{i+1}U_{i+1}^{j+1}-2\mu_2 p_i U_i^{j+1}-\mu_1 p_{i-1}uU_{i-1}^{j+1}-\mu_1 q_{i-1}U_{i-1-\frac{N}{2}}^{j+1}\\
&-2\mu_2 q_i U_{i-\frac{N}{2}}^{j+1}-\mu_1 q_{i+1}U_{i+1-\frac{N}{2}}^{j+1}|.
\end{aligned}\tag{8.38}$$

Using Taylor's series expansion on $U_{i\pm1}^{j+1}$, $p_{i\pm1}$, $q_{i\pm1-\frac{N}{2}}$ and σ_2 in equation (8.38) gives

$$\begin{aligned}
|\mathcal{L}_\varepsilon^M U^{j+1}(x_i)-\mathcal{L}_\varepsilon^{N,M}U_i^{j+1}| =&|(\frac{\varepsilon\Delta t}{12}U_{xxxx}^{j+1}(\xi)-\mu_1(p_iU_{xx}^{j+1}(x_i)+q_iU_{xx}^{j+1}(x_{i-\frac{N}{2}})+2q_i'U_x^{j+1}(x_{i-\frac{N}{2}}))\\
&-\mu_1 q_i''U^{j+1}(x_{i-\frac{N}{2}}))h^2+(\frac{\varepsilon\Delta t}{360}U_{xxxxxx}^{j+1}(\xi)-\frac{\Delta t p_i}{144}U_{xxxx}^{j+1}(\xi)\\
&-\frac{\mu_1 p_i}{24}U_{xxxx}^{j+1}(\xi)-\frac{\mu_1 q_i'}{3}U_{xxx}^{j+1}(x_{i-\frac{N}{2}})-\frac{\mu_1 q_i}{12}U_{xxxx}^{j+1}(x_{i-\frac{N}{2}}))h^4+O(h^6)|\\
\leq&|\frac{\varepsilon\Delta t}{12}U_{xxxx}^{j+1}(\xi)-\mu_1(p_iU_{xx}^{j+1}(x_i)+q_iU_{xx}^{j+1}(x_{i-\frac{N}{2}})+2q_i'U_x^{j+1}(x_{i-\frac{N}{2}}))\\
&-\mu_1 q_i''U^{j+1}(x_{i-\frac{N}{2}})|h^2+|\frac{\varepsilon\Delta t}{360}U_{xxxxxx}^{j+1}(\xi)-\frac{\Delta t p_i}{144}U_{xxxx}^{j+1}(\xi)\\
&-\frac{\mu_1 p_i}{24}U_{xxxx}^{j+1}(\xi)-\frac{\mu_1 q_i'}{3}U_{xxx}^{j+1}(x_{i-\frac{N}{2}})-\frac{\mu_1 q_i}{12}u_{xxxx}^{j+1}(x_{i-\frac{N}{2}})|h^4+O(h^6)\\
\leq& Ch^2.
\end{aligned}$$

Invoking Lemma 8.3.6 gives

$$|U^{j+1}(x_i)-U_i^{j+1}|\leq Ch^2,\ i=\frac{N}{2}+1,\frac{N}{2}+2,...,N. \tag{8.39}$$

For $h=\frac{2}{N}$, combining (8.37) and (8.39) gives the required error estimate. Hence, the proposed scheme is uniformly convergent of order two in space. ∎

Theorem 8.3.2 *Let $u(x,t)$ be the solution of (8.1) and U_i^{j+1} be the solution of (8.34). Then, the uniform error is estimated as*

$$\sup_{0<\varepsilon\leq 1} \|u(x_i,t_{j+1}) - U_i^{j+1}\| \leq C(\Delta t + N^{-2})$$

Proof. Combining the proofs of Lemma 8.3.4 and Theorem 8.3.1, yields the required uniform error estimate. ■

8.4 Numerical results and discussions

In this section, to illustrate the applicability of the proposed numerical scheme, two numerical examples are solved. Since the exact solutions of the problems are not known, the double mesh principles of the form (4.44)–(4.47) are used to determine the maximum absolute errors and corresponding rate of convergences.

Example 8.4.1 *(Bansal & Sharma, 2018). Consider* $-\frac{\partial u(x,t)}{dt} + \varepsilon\frac{\partial^2 u(x,t)}{\partial x^2} - 5u(x,t) + 2u(x-1,t) = -2$, $u(x,0) = \sin(\pi x)$ *for* $(x,0) \in [0,2]$, $u(x,t) = 0$ *for* $(x,t) \in \{(x,t) : x \in [-1,0]$ and $t \in [0,2]\}$ *and* $u(2,t) = 0$ *for* $(2,t) \in \{(2,t) : 0 \leq t \leq 2\}$.

Example 8.4.2 *(Kumari & Kumar, 2020). Consider* $-\frac{\partial u(x,t)}{dt} + \varepsilon\frac{\partial^2 u(x,t)}{\partial x^2} - 3u(x,t) + u(x-1,t) = -1$, $u(x,0) = 0$, $(x,0) \in [0,2]$, $u(x,t) = 0$, $(x,t) \in \{(x,t) : x \in [-1,0];\quad t \in [0,2]\}$ *and* $u(2,t) = 0$ *for* $(2,t) \in \{(2,t) : t \in [0,2]\}$.

The numerical solutions and error analysis of both examples are computed applying the scheme formulated in this chapter taking $\lambda_1 = 1/24$ and $\lambda_1 = 11/24$. The maximum nodal error and corresponding convergence rate of both examples are computed as shown in Table 8.1 and Table 8.2. From these tables, one can observe that by increasing the number of meshes, the maximum absolute error decreases, and for a given mesh numbers, decreasing ε gives stable and uniform maximum errors. This confirms the uniform convergence of the formulated numerical scheme for all values of ε. Table 8.3 shows the accuracy of the scheme as compared to other results in literature. That is, for the same mesh sizes,value of perturbation parameter and data values, the maximum absolute error committed in the present method is less than the errors committed in the other schemes.

The numerical solutions of the examples are simulated graphically as shown in Figures 8.1-8.4. From the line plots given in Figure 8.1 and Figure 8.3, one can observe the behaviors of the solutions at different time levels. Also, physical behavior of the solutions and changes in the layers' width for different values of the perturbation parameter can be observed from Figures 8.2

and 8.4. Figure 8.5 shows log-log plots of the maximum error versus the number of meshes for the examples, which indicate that the formulated numerical method is convergent independent of the perturbation parameter.

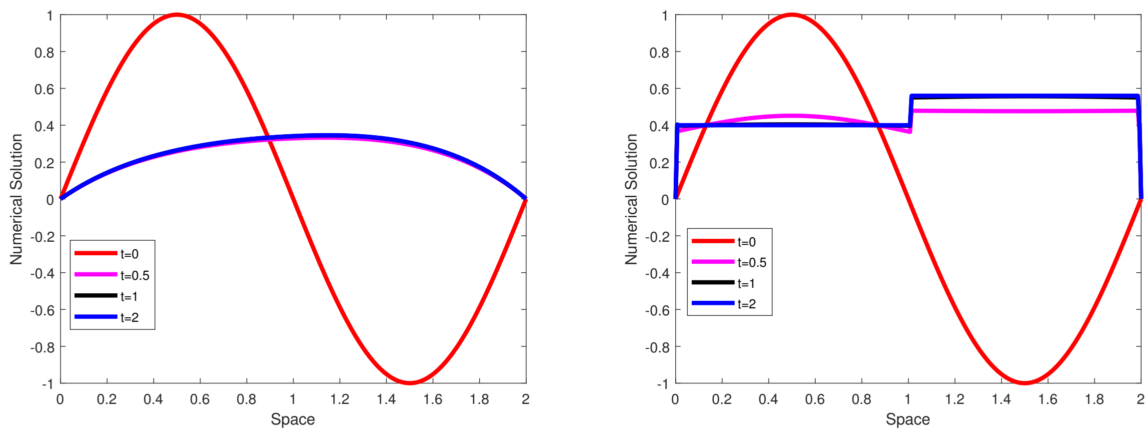

(a) $\varepsilon = 2^{0}$ (b) $\varepsilon = 2^{-16}$

Figure 8.1: Line plots for the solution of Example 8.4.1 for $N = 128$ at different time levels.

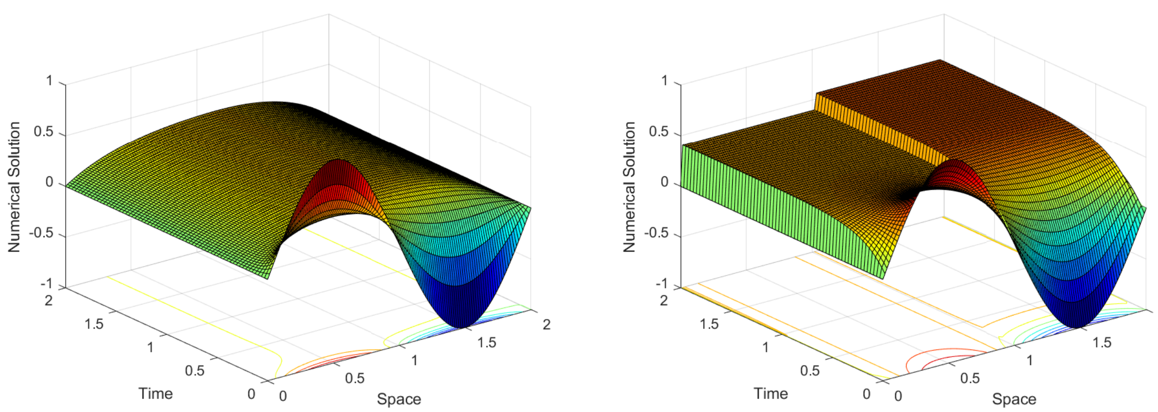

(a) $\varepsilon = 2^{0}$ (b) $\varepsilon = 2^{-16}$

Figure 8.2: Surface plots for the solution of Example 8.4.1 for $N = 128$ and $M = 64$.

Table 8.4 shows the comparisons of the fitted mesh method, nonstandard finite difference method and a tension spline fitted method proposed in this dissertation. From the table it is shown that for the same mesh size, a tension spline fitted method has more convergence order than the nonstandard finite difference method, and the nonstandard finite difference method has more

Table 8.1: Maximum errors and corresponding convergence rate of Example 8.4.1.

ε | $N \rightarrow$ $\downarrow$ | $M \rightarrow$	16 32	32 64	64 128	128 256	256 512
2^{0}	5.2038e-02	1.7483e-02	4.9785e-03	1.3260e-03	3.4229e-04
	1.5736	1.8122	1.9086	1.9538	
2^{-2}	4.7981e-02	1.5766e-02	4.3204e-03	1.1229e-03	2.8612e-04
	1.6056	1.8676	1.9439	1.9725	
2^{-4}	4.5798e-02	1.8492e-02	5.3904e-03	1.4174e-03	3.6547e-04
	1.3084	1.7784	1.9271	1.9554	
2^{-6}	3.5906e-02	1.8311e-02	6.1997e-03	1.3990e-03	4.5341e-04
	0.9715	1.5624	2.1478	1.6255	
2^{-8}	3.3221e-02	1.2981e-02	6.1191e-03	2.7049e-03	1.0428e-03
	1.3557	1.0850	1.1777	1.3751	
2^{-10}	3.3117e-02	1.2380e-02	4.8776e-03	2.0203e-03	1.0245e-03
	1.4196	1.3438	1.2716	0.9796	
2^{-12}	3.3117e-02	1.2376e-02	4.7903e-03	2.0772e-03	1.0013e-03
	1.4200	1.3694	1.2055	1.0528	
2^{-14}	3.3117e-02	1.2376e-02	4.7902e-03	2.0709e-03	1.0076e-03
	1.4200	1.3694	1.2098	1.0393	
2^{-16}	3.3117e-02	1.2376e-02	4.7902e-03	2.0709e-03	1.0075e-03
	1.4200	1.3694	1.2098	1.0395	
2^{-18}	3.3117e-02	1.2376e-02	4.7902e-03	2.0709e-03	1.0075e-03
	1.4200	1.3694	1.2098	1.0395	
$e^{N,M}$	5.2038e-02	1.8492e-02	6.1997e-03	2.7049e-03	1.0428e-03
$r^{N,M}$	1.4927	1.5766	1.1966	1.3751	

Table 8.2: Maximum errors and corresponding convergence rates of Example 8.4.2.

ε | $N \rightarrow$	18	36	72	144	288
$\downarrow$ | $M \rightarrow$	18	36	72	144	288
2^{0}	4.9315e-03	1.6091e-03	5.5532e-04	1.9610e-03	3.9612e-05
	1.6158	1.5349	1.5017	1.4942	
2^{-2}	8.3785e-03	2.7112e-03	9.6535e-04	3.6187e-04	1.3305e-04
	1.6278	1.4898	1.4156	1.4435	
2^{-4}	1.2009e-02	4.7851e-03	1.5672e-03	5.6198e-04	2.2895e-04
	1.3275	1.6104	1.4796	1.2955	
2^{-6}	1.2133e-02	6.2859e-03	1.9900e-03	7.4889e-04	3.2170e-04
	0.9487	1.6594	1.4099	1.2190	
2^{-8}	9.5475e-03	6.7757e-03	2.8381e-03	1.5221e-03	7.7066e-04
	0.4948	1.2554	0.8989	0.9809	
2^{-10}	9.3401e-03	5.0933e-03	3.4973e-03	1.6184e-03	7.2280e-04
	0.8748	0.5424	1.1117	1.1629	
2^{-12}	9.3397e-03	5.0529e-03	2.6405e-03	1.5946e-03	7.2447e-04
	0.8863	0.9363	0.7276	1.1382	
2^{-14}	9.3397e-03	5.0529e-03	2.6371e-03	1.3578e-03	7.1757e-04
	0.8863	0.9382	0.9577	0.9201	
2^{-16}	9.3397e-03	5.0529e-03	2.6371e-03	1.3577e-03	6.9879e-04
	0.8863	0.9382	0.9578	0.9582	
2^{-18}	9.3397e-03	5.0529e-03	2.6371e-03	1.3577e-03	6.9879e-04
	0.8863	0.9382	0.9578	0.9582	
$e^{N,M}$	1.2133e-02	6.7757e-03	3.4973e-03	1.5946e-03	7.7066e-04
$r^{N,M}$	0.8405	0.9541	1.1330	1.0490	

Table 8.3: Comparison of the proposed scheme and other results in literature.

$r_\varepsilon^{2N,4M}$ of Example 8.4.1					
$N:$	64	128	256	512	
$M:$	32	128	512	2048	
Present method					
$\varepsilon = 2^{-16}$	1.8871	2.1168	2.0830	1.9190	
$\varepsilon = 2^{-18}$	1.8871	2.1168	2.0830	1.9190	
$\varepsilon = 2^{-20}$	1.8871	2.1168	2.0830	1.9190	
Bansal & Sharma (2018)					
$\varepsilon = 2^{-16}$	1.7908	1.8314	1.5121	1.6261	
$\varepsilon = 2^{-18}$	1.7908	1.8354	1.5091	1.6257	
$\varepsilon = 2^{-20}$	1.7908	1.8354	1.5091	1.6257	
$e^{N,M}$ and $r^{N,M}$ of Example 8.4.2 for $T = 1$					
$N = M:$	18	36	72	144	288
Present method					
e^N	6.7757e-03	3.4973e-03	1.5994e-03	7.1757e-04	3.6436e-04
r^N	0.9541	1.1287	1.1563	0.9778	
Kumari & Kumar (2020)					
$e^{N,M}$	1.1200e-02	7.0100-03	2.9700e-03	1.1400e-03	4.0600e-04
$r^{N,M}$	0.6760	1.2390	1.3814	1.4895	

Table 8.4: Comparison of the proposed fitted mesh, nonstandard finite difference and tension spline fitted methods .

Consider $a(x) = 3,\ b(x) = -1,\ f(x) = 1,\ u_0(x) = 0,\ \phi(x,t) = 0,\ \alpha(t) = 0.$				
N/M :	$64/32$	$128/128$	$256/512$	$512/2048$
Fitted mesh finite difference method				
$e^{N,M}$	7.8529e-03	4.1975e-03	1.8672e-03	6.2063e-04
$r^{N,M}$	0.9037	1.1687	1.5891	1.6912
Nonstandard finite difference method				
$e^{N,M}$	7.5768e-03	1.9602e-03	4.9447e-04	1.3119e-04
$r^{N,M}$	1.9506	1.9870	1.9142	1.9312
Tension spline fitted method				
$e^{N,M}$	5.6299e-03	1.5204e-03	4.3406e-04	1.2224e-04
$r^{N,M}$	1.8887	1.9037	1.8282	1.8957
Consider $a(x) = 5,\ b(x) = -2,\ f(x) = 2,\ u_0(x) = \sin(\pi x),\ \phi(x,t) = 0,\ \alpha(t) = 0.$				
Fitted mesh finite difference method				
$e^{N,M}$	1.2881e-02	8.4743e-03	3.7744e-03	1.3445e-03
$r^{N,M}$	0.6041	1.1668	1.4892	1.6107
Nonstandard finite difference method				
$e^{N,M}$	2.0044e-02	4.7134e-03	1.1209e-03	2.7989e-04
$r^{N,M}$	2.0881	2.0721	2.0017	2.0011
Tension spline fitted method				
$e^{N,M}$	1.6679e-02	3.8454e-03	9.0761e-04	2.4000e-04
$r^{N,M}$	2.1168	2.0830	1.9190	1.9502
Consider $a(x) = x + 6,\ b(x) = -(x^2 + 1),\ f(x) = 3,\ u_0(x) = 0,\ \phi(x,t) = 0,\ \alpha(t) = 0.$				
Fitted mesh finite difference method				
$e^{N,M}$	1.0936e-02	8.4424e-03	4.0736e-03	1.6157e-03
$r^{N,M}$	0.3734	1.0513	1.3341	1.5788
Nonstandard finite difference method				
$e^{N,M}$	1.9394e-02	5.3597e-03	1.4084e-03	3.6982e-04
$r^{N,M}$	1.8554	1.9281	1.9302	1.9753
Tension spline fitted method				
$e^{N,M}$	1.4386e-02	4.3089e-03	1.1765e-03	3.3406e-04
$r^{N,M}$	1.7393	1.8728	1.8163	1.8824

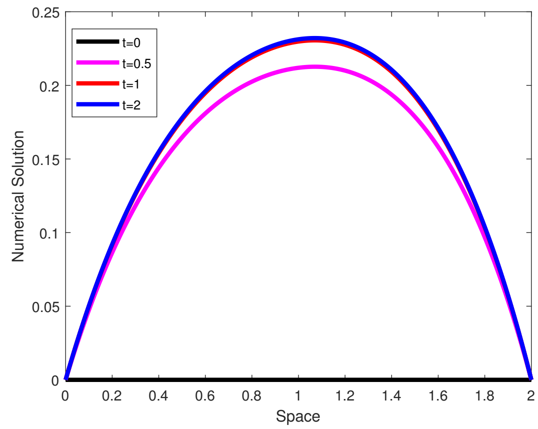

(a) $\varepsilon = 2^0$

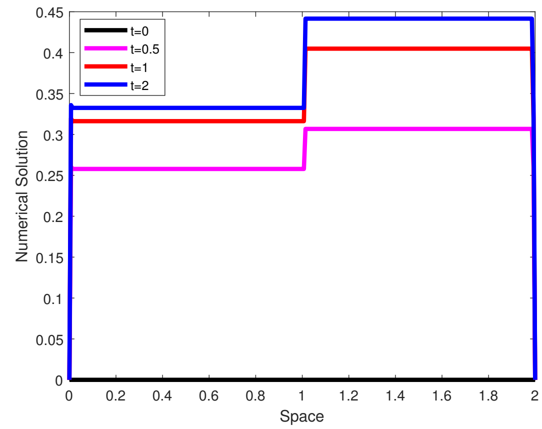

(b) $\varepsilon = 2^{-14}$

Figure 8.3: Line plots for the solution of Example 8.4.2 taking $N = 288$ at different time levels.

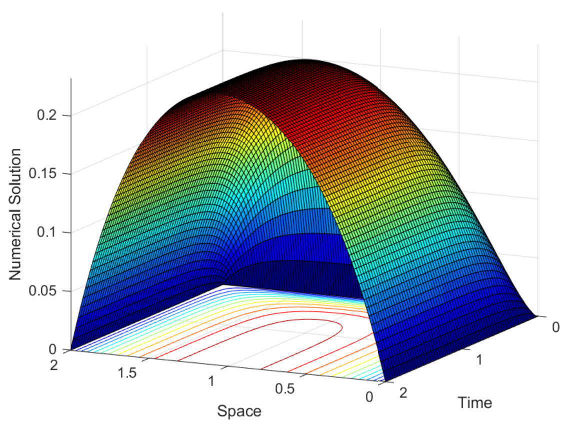

(a) $\varepsilon = 2^0$

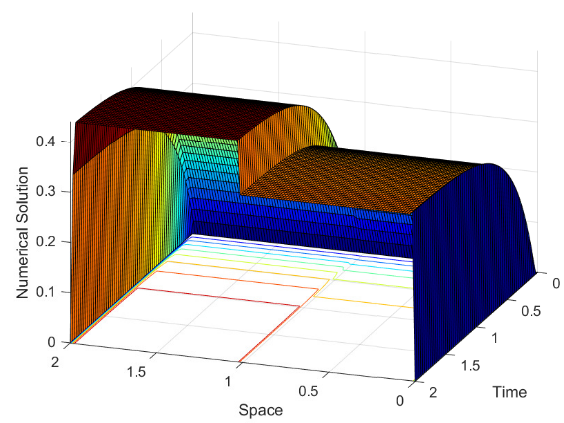

(b) $\varepsilon = 2^{-14}$

Figure 8.4: Surface plots for the solution of Example 8.4.2 taking $N = 72$ and $M = 72$.

convergence order than the fitted mesh method. The fitted operator methods (the nonstandard finite difference method and a tension spline fitted method) have more convergence rate than the fitted mesh method.

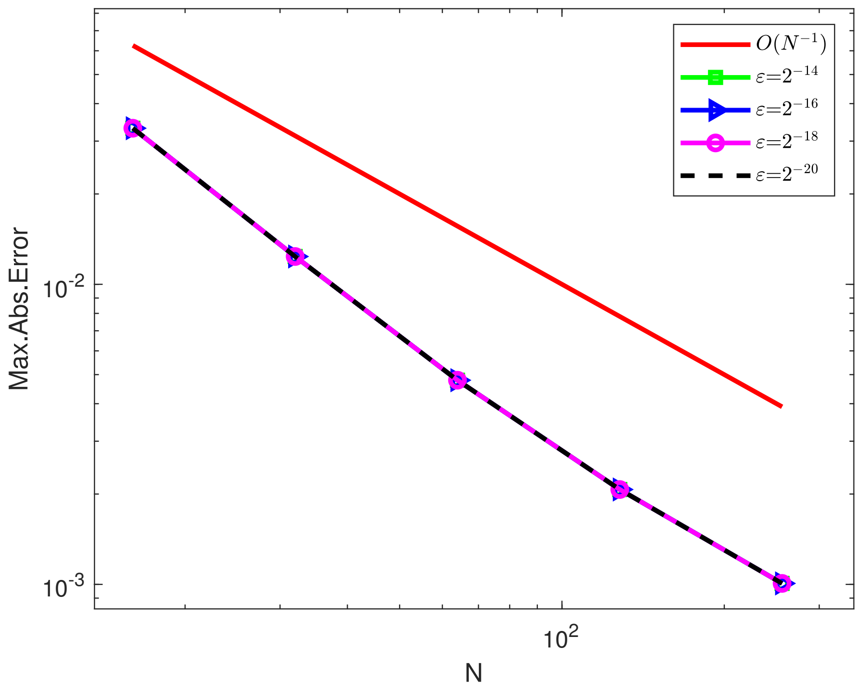

(a)

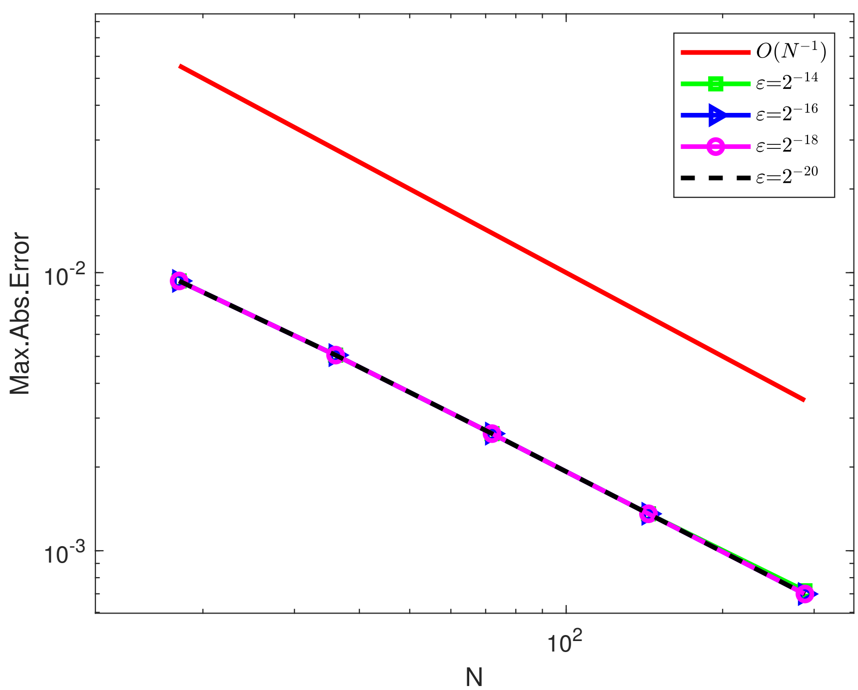

(b)

Figure 8.5: The log-log graphs of the maximum absolute errors versus mesh numbers for Example 8.4.1 in (a) and for Example 8.4.2 in (b).

8.5 Summary

In this chapter, singularly perturbed reaction-diffusion problem involving large negative shift is considered. The problem is treated by formulating a numerical scheme applying the implicit Euler method in the temporal variable and a tension spline fitted method in the spatial variable on a uniform meshes. The stability estimate of the discrete solution is established, and its uniform convergence is investigated and proved. To validate the theoretical findings, two numerical examples are solved. From the theoretical and numerical findings, it is shown that the formulated numerical scheme is uniformly convergent of order one in time and order two in space. The main results of this chapter can be summarized as follow.

1. The developed numerical scheme is stable and convergent independent of ε.
2. In the solution, decreasing the mesh sizes decreases the maximum absolute error.
3. In the solution, decreasing the value of ε yields stable and uniform maximum absolute errors.
4. The accuracy of the present method is better than that of other previous results in the literature.
5. The accuracy of the method is enhanced by taking the values of μ_1 and μ_2 satisfying $\mu_1 + \mu_2 = \frac{1}{2}$, so that μ_1 is approaching to zero and μ_2 is approaching to $\frac{1}{2}$.

CHAPTER NINE

A NONSTANDARD FINITE DIFFERENCE SCHEME FOR SINGULARLY PERTURBED PARTIAL DIFFERENTIAL EQUATIONS WITH SPATIO-TEMPORAL DELAYS

The chapter focuses on treating a singularly perturbed differential equations involving spatial and temporal delays. The effects of the perturbation parameter, spatial delay, and temporal delay make the problem more difficult to solve analytically. So, to solve such problem, it needs constructing a parameter independent numerical method. In this chapter, a fitted numerical scheme is developed using the implicit Euler method in the temporal direction and the non-standard finite difference approach in the spatial direction on a uniform meshes. The temporal delay is handled by using the Taylor's series approximation and the spatial delay is handled by choosing special meshes, in such a way that the term with the spatial delay coincides with the mesh point $x_i = 1$. Stability estimate of the proposed method is established, and its convergence result is investigated and proved.

9.1 The governing problem

Considered a singularly perturbed delay parabolic differential equation of the form

$$\begin{cases} \mathcal{L}_\varepsilon u(x,t) = (u_t(x,t) - \varepsilon u_{xx}(x,t) + a(x)u(x,t)) = f(x,t) - b(x)u(x-1,t-\tau),\ (x,t) \in \Omega, \\ u(x,t) = u_0(x,t),\ (x,t) \in \Omega^0 = \{(x,t) : x \in [0,2], t \in [-\tau, 0]\}, \\ u(u,t) = \phi(u,t),\ (x,t) \in \Omega^- = \{(x,t) : x \in [-1,0],\ t \in [0,T]\}, \\ u(2,t) = \alpha(t),\ (2,t) \in \Omega^+ = \{(2,t),\ t \in [0,T]\}, \end{cases} \tag{9.1}$$

where $\bar{\Omega} = [0,2] \times [0,T]$, $0 < \varepsilon \ll 1$, τ is a temporal shift of $o(\varepsilon)$ and T is a finite time. It is assumed that the functions $a(x)$, $b(x)$, $f(x,t)$, $u_0(x,t)$, $\phi(x,t)$ and $\alpha(2,t)$ are smooth enough and bounded on the considered domain. Moreover, to avoid oscillation in the solution, the coefficient functions $a(x)$ and $b(x)$ satisfy the conditions

$$a(x) + b(x) \geq 2\lambda > 0 \text{ and } b(x) < 0,\ x \in [0,2], \tag{9.2}$$

for arbitrary positive constant λ (Bansal & Sharma, 2018).

Setting $\varepsilon = 0$, the associated reduced problem is given by

$$\mathcal{L}_0 u(x,t) = \begin{cases} \left(\frac{\partial}{\partial t} + a(x)\right) u_0(u,t) = f(x,t) = b(x)\phi_0(x-1, t-\tau), \; x \in (0,1], \\ \left(\frac{\partial}{\partial t} + a(x)\right) u_0(x,t) = f(x,t) = b(x)u_0(x-1, t-\tau), \; x \in (1,2). \end{cases}$$

Since u_0 need not satisfy the conditions $u_0(0, t-\tau) = \phi(0, t-\tau)$, $u_0(0, t-\tau) = \phi(0,0)$, $u_0(2, t-\tau) = \alpha(2,t)$, $u_0(1^-, t) = u_0(1^+, t)$ and $(u_0)_x(1^-, t) = (u_0)_x(1^+, t)$, the solution exhibits two boundary layers and an interior layer at $x = 1$ (Kadalbajoo & Gupta, 2010). The functions involved in the continuous problem (9.1) should satisfy Holder continuity and compatibility conditions are imposed at the corner points as

$$\begin{cases} u_0(0,0) = \phi(0,0), \\ u_0(2,0) = \alpha(2,0) \end{cases} \tag{9.3}$$

and

$$\begin{cases} \frac{\partial\phi(0,0)}{\partial t} - \varepsilon\frac{\partial^2 u_0(0,0)}{\partial x^2} + a(0)u_0(0,0) + b(0)u_0(-1,-\tau) = f(0,0), \\ \frac{\partial\alpha(2,0)}{\partial t} - \varepsilon\frac{\partial^2 u_0(2,0)}{\partial x^2} + a(2)u_0(2,0) + b(2)u_0(1,-\tau) = f(2,0). \end{cases} \tag{9.4}$$

From the above assumptions and conditions, one can observe that the solution involves layers and there exists a constant C independent of ε (Roos et al., 2008). So for $(x,t) \in \bar{\Omega}$, $|u(x,t) - u_0(x,0)| = |u(x,t) - u_0(x)| \leq Ct$. Applying Taylor's series expansion,

$$u(x-1, t-\tau) = u(x-1,t) - \tau u_t(x-1,t) + O(\tau^2) \tag{9.5}$$

Inserting (9.5) into (9.1) gives

$$\mathcal{L}_\varepsilon u(x,t) = \vartheta(x,t), \; (x,t) \in \bar{\Omega} \tag{9.6}$$

subject to

$$\begin{cases} u(x,t) = u_0(x), \; x \in [0,2] \\ u(x,t) = \phi(x,t), \; (x,t) \in \Omega^- = \{(x,t) : x \in [-1,0], \; t \in [0,T]\} \\ u(2,t) = \alpha(2,t), \; (2,t) \in \Omega^+ = \{(2,t), \; t \in [0,T]\}, \end{cases} \tag{9.7}$$

where

$$\mathcal{L}_\varepsilon u(x,t) = u_t(x,t) - \varepsilon u_{xx}(x,t) + a(x)u(x,t)$$

$$\vartheta(x,t) = \begin{cases} f(x,t) - b(x)\phi(x-1,t) + \tau b(x)\phi_t(x-1, \; t), \; (x,t) \in (0,1] \times (0,T] \\ f(x,t) - b(x)u(x-1,t) + \tau b(x)u_t(x-1, \; t), \; (x,t) \in (1,2) \times (0,T]. \end{cases}$$

9.2 Properties of the continuous solution

Lemma 9.2.1 *Suppose $z(x,t)$ be a smooth function in $\bar{\Omega}$. If $z(x,t) \geq 0$, $(x,t) \in \partial\Omega$ and $\mathcal{L}_\varepsilon z(x,t) \geq 0$, $(x,t) \in \Omega$, then $\mathcal{L}_\varepsilon z(x,t) \geq 0$, $(x,t) \in \bar{\Omega}$.*

Proof. For $(\hat{x},\hat{t}) \in \bar{\Omega}$, suppose that $z(\hat{x},\hat{t}) = \min_{\bar{\Omega}} z(x,t) < 0$. From the considered hypothesis $(\hat{x},\hat{t}) \notin \partial\Omega$. By extreme value theorem, $z_t(\hat{x},\hat{t}) = 0,\ z_x(\hat{x},\hat{t}) = 0$ and $z_{xx}(\hat{x},\hat{t}) > 0$. Then,
Case 1: For $x \in (0,1]$,

$$\mathcal{L}_\varepsilon z(\hat{x},\hat{t}) = z_t(\hat{x},\hat{t}) - \varepsilon z_{xx}(\hat{x},\hat{t}) + a(\hat{x},\hat{t}) < 0.$$

Case 2: For $x \in (1,2)$,

$$\begin{aligned}
\mathcal{L}_\varepsilon z(\hat{x},\hat{t}) =& z_t(\hat{x},\hat{t}) - \varepsilon z_{xx}(\hat{x},\hat{t}) + a(\hat{x}) + b(\hat{x})z(\hat{x}-1,\hat{t}) - \tau b(\hat{x}) z_t(\hat{x}-1,\hat{t}) \\
\leq& z_t(\hat{x},\hat{t}) - \varepsilon z_{xx}(\hat{x},\hat{t}) + [a(\hat{x}) + b(\hat{x})]z(\hat{x},\hat{t}) - \tau b(\hat{x}) z_t(\hat{x},\hat{t}) < 0.
\end{aligned}$$

Thus, $\mathcal{L}_\varepsilon z(\hat{x},\hat{t}) < 0$, which contradicts the given condition. Therefore, the supposition fails, so that $z(\hat{x},\hat{t}) \geq 0$, which implies that $z(x,t) \geq 0$, $(x,t) \in \bar{\Omega}$. ■

Lemma 9.2.2 *(Swaminathan et al., 2016). The solution of the continuous problem (9.6)-(9.7) is estimated as*

$$|u(x,t)| \leq \frac{\|\vartheta\|}{\lambda} + \max\{|\partial\Omega|\},$$

where $|\partial\Omega| = \{|u(x,0)|, |u(0,t)|, |u(2,t)|\}$

Proof. Let's define $z^{\pm}(x,t) = \frac{\|\vartheta\|}{\lambda} + \max\{|\partial\Omega|\} \pm u(x,t)$. Then, $z^{\pm}(x,0) \geq 0$, $z^{\pm}(0,t) \geq 0$ and $z^{\pm}(2,t) \geq 0$.
For $x \in (0,1],\ t \in [0,T]$, it becomes

$$\mathcal{L}_\varepsilon z^{\pm}(x,t) = \left(\frac{\partial}{\partial t} - \varepsilon\frac{\partial}{\partial x^2} + a(x)\right) z^{\pm}(x,t) = a(x)\left(\frac{\|\vartheta\|}{\lambda} + \max\{|\partial\Omega|\}\right) \pm \vartheta(x,t) \geq 0.$$

For $x \in (1,2),\ t \in [0,T]$, it becomes

$$\begin{aligned}
\mathcal{L}_\varepsilon z^{\pm}(x,t) =& \left(\frac{\partial}{\partial t} - \varepsilon\frac{\partial}{\partial x^2} + a(x)\right) z^{\pm}(x,t) + b(x)z^{\pm}(x-1,t) - \tau b(x)\frac{\partial z^{\pm}(x-1,t)}{\partial t} \\
\geq& [a(x) + b(x)]\max\{|\partial\Omega|\} \geq 0.
\end{aligned}$$

Thus, $\mathcal{L}_\varepsilon z^{\pm}(x,t) \geq 0$ and by Lemma 9.2.1, we have $z^{\pm}(x,t) \geq 0$, $(x,t) \in \bar{\Omega}$, which yields the stability estimate. ■

Lemma 9.2.3 *(Kumari & Kumar, 2020). The derivatives of the solution $u(x,t)$ of (9.6)-(9.7) are bounded as*

$$\left|\frac{\partial^{k+l}u(x,t)}{\partial x^k\partial t^l}\right| \leq \begin{cases} C\left(1+\varepsilon^{-k/2}\left[e^{-x\sqrt{\frac{\lambda}{\varepsilon}}}+e^{-(1-x)\sqrt{\frac{\lambda}{\varepsilon}}}\right]\right), & (x,t)\in(0,1]\times(0,T], \\ C\left(1+\varepsilon^{-k/2}\left[e^{-(x-1)\sqrt{\frac{\lambda}{\varepsilon}}}+e^{-(2-x)\sqrt{\frac{\lambda}{\varepsilon}}}\right]\right), & (x,t)\in(1,2)\times(0,T] \end{cases}$$

for all non-negative integer k, l such that $0 \leq k+2l \leq 4$.

Proof. For $k = 0$ and $l = 0$, it is to show the bound of the solution $u(x,t)$, which is Lemma 9.2.2. For $k = 0, l \neq 0$, it is to show the bound of derivatives of $u(x,t)$ with respect to t. For $k \neq 0, l = 0$, it is to show the bound of derivatives of the solution $u(x,t)$ with respect to x and for the cases when $(k,l) \neq 0$, it is to determine the bound of its derivatives of the solution $u(x,t)$ with respect to x and t. Let $q_{\varepsilon,1}(x) = e^{-x\sqrt{\frac{\lambda}{\varepsilon}}}+e^{-(1-x)\sqrt{\frac{\lambda}{\varepsilon}}}$, $x \in (0,1]$ and $q_{\varepsilon,2}(x) = e^{-(x-1)\sqrt{\frac{\lambda}{\varepsilon}}}+e^{-(2-x)\sqrt{\frac{\lambda}{\varepsilon}}}$, $x \in (1,2)$. For a fixed value of λ, following the approaches of Kellogg & Tsan (1978), it is possible to get $|q_{\varepsilon,\iota}(x)| \leq c$, for constant c and $\iota = 1, 2$. For the case $k = 0$, equation (9.6) becomes

$$\frac{\partial u(x,t)}{\partial t} = \varepsilon\frac{\partial^2 u(x,t)}{\partial x^2} - a(x)u(x,t) + \begin{cases} f(x,t) - b(x)\phi(x-1,t) + \tau b(x)\frac{\partial\phi(x-1,\,t)}{\partial t}, & x\in(0,1] \\ f(x,t) - b(x)u(x-1,t) + \tau b(x)\frac{\partial u(x-1,\,t)}{\partial t}, & x\in(1,2). \end{cases} \tag{9.8}$$

Along the sides $t = 0$, $u = 0$, which implies that $\frac{\partial^2 u(x,t)}{\partial x^2} = 0$. Then, (9.8) becomes,

$$\frac{\partial u(x,0)}{\partial t} = \varepsilon\frac{\partial^2 u(x,0)}{\partial x^2} - a(x)u(x,0) + \begin{cases} f(x,0) - b(x)\phi(x-1,0) + \tau b(x)\frac{\partial\phi(x-1,\,0)}{\partial t}, & x\in(0,1] \\ f(x,0) - b(x)u(x-1,0) + \tau b(x)\frac{\partial u(x-1,\,0)}{\partial t}, & x\in(1,2). \end{cases} \tag{9.9}$$

With out loss of generality, assuming that all the values considered in (9.7) are zero, it follows that $u(x-1,0) = \phi(x-1,0) = 0,\ x \in [0,1]$ and $u(x-1,0) = u_0(x-1,0) = 0,\ x \in (1,2]$. Then, (9.9) becomes $\frac{\partial u(x,0)}{\partial t} = f(x,0)$. Since f is smooth function, it implies $\left|\frac{\partial u(x,t)}{\partial t}\right| \leq C$, for sufficiently chosen C on $\partial\Omega$. Applying the the operator $\mathcal{L}_\varepsilon$ given in (9.6) on $\frac{\partial u(x,t)}{\partial t}$ gives $|\mathcal{L}_\varepsilon u_t(x,t)| = |\vartheta_t(x,t)| \leq C$ on Ω. Thus, applying Lemma 9.2.1 gives $\left|\frac{\partial u(x,t)}{\partial t}\right| \leq C$ on $\bar{\Omega}$. For $l = 2$, differentiating (9.8) with respect to t gives

$$\frac{\partial^2 u(x,t)}{\partial t^2} = \varepsilon\frac{\partial^3 u(x,t)}{\partial x^2\partial t} - a(x)\frac{\partial u(x,t)}{\partial t} + \begin{cases} \frac{\partial f(x,t)}{\partial t} - b(x)\frac{\partial\phi(x-1,t)}{\partial t} + \tau b(x)\frac{\partial^2\phi(x-1,t)}{\partial t^2}, & x\in(0,1] \\ \frac{\partial f(x,t)}{\partial t} - b(x)\frac{\partial u(x-1,t)}{\partial t} + \tau b(x)\frac{\partial^2 u(x-1,\,t)}{\partial t^2}, & x\in(1,2). \end{cases} \tag{9.10}$$

Along $x = 0$ and $x = 2$, $\frac{\partial^2 u(x,t)}{\partial t^2} = 0$ and along t=0, $u = 0$ and $\frac{\partial^2 u(x,0)}{\partial x^2} = 0$. From $\frac{\partial u(x,0)}{\partial t} = f(x,0)$, $\frac{\partial^3 u(x,0)}{\partial x^2\partial t} = \frac{\partial^2 f(x,0)}{\partial x^2}$. Assuming that the initial and boundary conditions are identically zero, $u_t(x-1,0)=\phi_t(x-1,0)=0$, $x\in(0,1]$ and $u_t(x-1,0)=u_{0t}(x-1,0)=0$, $x\in(1,2]$. Then, equation (9.10) becomes

$$\frac{\partial^2 u(s,0)}{\partial t^2}=\varepsilon\frac{\partial^2 f(s,0)}{\partial u^2}-a(x)\frac{\partial f(x,0)}{\partial t}+\begin{cases}\frac{\partial\gamma(x,0)}{\partial t}, \in(0,1]\\ \frac{\partial f(x,0)}{\partial t}+\tau b(x)\frac{\partial^2 u(x-1,0)}{\partial t^2},\ x\in(1,2).\end{cases}\tag{9.11}$$

From (9.11), along $t=0$ $\left|\frac{\partial^2 u(x,0)}{\partial t^2}\right|\leq 0$ on $\partial\Omega$ and the operator $\mathcal{L}_\varepsilon$ implies $|\mathcal{L}_\varepsilon\frac{\partial^2 u(x,t)}{\partial t^2}|=|\frac{\partial^2\vartheta(x,t)}{\partial t^2}|\leq C$ on Ω and applying Lemma 9.2.1 yields $\left|\frac{\partial^2 u(x,t)}{\partial t^2}\right|\leq C$ on $\bar{\Omega}$. The bound of derivatives of the solution $u(x,t)$ for the cases $k\neq 0$ can be determined by similar procedures as above. For the case $k=1$, let $x\in\Omega$ and consider a neighborhood $R=(e,e+\sqrt{\varepsilon})$, $\forall x\in R$. For some $\xi\in\bar{R}$ and $t\in(0,T]$, the mean value theorem gives

$$\left|\frac{\partial u(\xi,t)}{\partial x}\right|=\varepsilon^{\frac{-1}{2}}|u(e+\sqrt{\varepsilon},t)-u(e,t)|\leq C\varepsilon^{\frac{-1}{2}}\|u\|.\tag{9.12}$$

For $x\in\bar{R}$,

$$\begin{aligned}\frac{\partial u(x,t)}{\partial x}=&\frac{\partial u(\xi,t)}{\partial x}+\frac{\partial u(x,t)}{\partial x}-\frac{\partial u(\xi,t)}{\partial x}=\frac{\partial u(\xi,t)}{\partial x}+\int_\xi^x\frac{\partial w(s,t)}{\partial s}ds\\ =&\ \frac{\partial u(\xi,t)}{\partial x}+\varepsilon^{-1}\int_\xi^x\left(\frac{\partial u(s,t)}{\partial s}+a(s)u(s,t)+b(s)u(s-1,t)-f(s,t)\right)ds.\end{aligned}$$

$$\Rightarrow\ \left|\frac{\partial u(x,t)}{\partial x}\right|\leq\left|\frac{\partial u(\xi,t)}{\partial x}\right|+C\varepsilon^{-1}\int_\xi^x(\|u\|+\|f\|)\,ds=\left|\frac{\partial u(\xi,t)}{\partial x}\right|+C\varepsilon^{-1}(\|u\|+\|f\|)\,\varepsilon^{\frac{1}{2}}.$$

Putting (9.12) into the above result gives $\left|\frac{\partial u(x,t)}{\partial x}\right|\leq C(1+\varepsilon^{\frac{-1}{2}}q_{\varepsilon,\iota})$, $(x,t)\in\bar{\Omega}$ for sufficiently large chosen C. For $k=2$, by rearranging (9.1) leads to

$$\frac{\partial^2 u(x,t)}{\partial x^2}=\varepsilon^{-1}\left[\frac{\partial u(x,t)}{\partial t}+a(x)u(x,t)+b(x)u(x-1,t)-f(x,t)\right].\tag{9.13}$$

For a fixed time $t\in[0,T]$ and for $x\in[0,2]$, since $|u|\leq C$, $\left|\frac{\partial u(x,t)}{\partial t}\right|\leq C$ and f is smooth function, $|\frac{\partial^2 u(x,t)}{\partial x^2}|\leq C(1+\varepsilon^{-1}q_{\varepsilon,\iota})$. The derivative of (9.13) with respect to t gives

$$\frac{\partial^3 u(x,t)}{\partial x^2\partial t}=\varepsilon^{-1}\left(\frac{\partial^2 u(x,t)}{\partial t^2}+a(x)\frac{\partial u(x,t)}{\partial t}+b(x)\frac{\partial u(x-1,t)}{\partial t}-\frac{\partial f(x,t)}{\partial t}\right).$$

Since $\left|\frac{\partial u(x,t)}{\partial t}\right|\leq C$, $\left|\frac{\partial^2 u(x,t)}{\partial t^2}\right|\leq C$ and $|ft(x,t)|\leq C$, we get $|\frac{\partial^3 u(x,t)}{\partial x^2\partial t}|\leq C(1+\varepsilon^{-1}q_{\varepsilon,\iota})$. In a similar procedure, the bounds on the derivatives of the solution can be easily determined for the remaining values of k and l with $0\leq k+2l\leq 4$. ■

9.3 The numerical method

In this section, first the temporal domain is discretized into M uniform meshes, and the problem is semi-discretized using implicit Euler method. Then, nonstandard finite difference method is constructed on a uniform spatial mesh, which yields a fully discrete scheme.

9.3.1 Temporal discretization

Let M be a uniform mesh number on $[0,T]$ with step size Δt. Then, the uniform temporal discretization is given as $\bar{\Lambda}_t^M = \{t_j = j\Delta t,\ \Delta t = T/M,\ j = 0,1,...,M\}$. Using the implicit Euler method, a semi-discrete scheme is obtained as

$$\mathcal{L}_\varepsilon^M U^{j+1}(x) = \vartheta^{j+1}(x),\ j = 0,1,2,...,M-1, \tag{9.14}$$

where

$$\mathcal{L}_\varepsilon^M U^{j+1}(x) = \begin{cases} -\varepsilon U_{xx}^{j+1}(x) + (\frac{1}{\Delta t} + a(x))U^{j+1}(x),\ 0 < x \leq 1, \\ -\varepsilon U_{xx}^{j+1}(x) + (\frac{1}{\Delta t} + a(x))U^{j+1}(x) + (1 - \frac{\tau}{\Delta t})b(x)U^{j+1}(x-1),\ 1 < x < 2 \end{cases}$$

and

$$\vartheta^{j+1}(x) = \begin{cases} f^{j+1}(x) + \frac{U^j(x)}{\Delta t} - (1 - \frac{\tau}{\Delta t})b(x)\phi^{j+1}(x-1) - \frac{\tau b(x)}{\Delta t}\phi^j(x-1),\ x \in (0,1], \\ f^{j+1}(x) + \frac{U^j(x)}{\Delta t} - \frac{\tau b(x)}{\Delta t}U^j(x-1),\ x \in (1,2) \end{cases}$$

with the initial and boundary conditions

$$\begin{cases} U^0(x) = u_0(x),\ x \in [0,2], \\ U^{j+1}(x) = \phi^{j+1}(x),\ x \in (0,1], \\ U^{j+1}(2) = \alpha^{j+1}(2),\ x \in (1,2). \end{cases} \tag{9.15}$$

Lemma 9.3.1 *For a smooth function $z^{j+1}(x)$, if $z^{j+1}(x) \geq 0$, $x \in \partial\Gamma$ and $\mathcal{L}_\varepsilon^M z^{j+1}(x) \geq 0$, $x \in \Gamma$, then $z^{j+1}(x) \geq 0$, $x \in \bar{\Gamma}$.*

Proof. Let $x^* \in \bar{\Gamma}$ and suppose that $z^{j+1}(x^*) = \min_{\bar{\Gamma}} z^{j+1}(x) < 0$. By the considered hypothesis, $x^* \notin \partial\Gamma$ and by the extreme value theorem, $z_x^{j+1}(x^*) = 0$ and $z_{xx}^{j+1}(x^*) \geq 0$.
Case 1: For $x^* \in (0,1]$, it become

$$\mathcal{L}_\varepsilon^M z^{j+1}(x^*) = -\varepsilon z_{xx}^{j+1}(x^*) + (\frac{1}{\Delta t} + a(x^*))z^{j+1}(x^*) < 0.$$

Case 2: For $x^* \in (1,2)$, it becomes

$$\begin{aligned} \mathcal{L}_\varepsilon^M z^{j+1}(x^*) =& -\varepsilon z_{xx}^{j+1}(x^*) + (\frac{1}{\Delta t} + a(x^*))z^{j+1}(x^*) + (1 - \frac{\tau}{\Delta t})b(x^*)z^{j+1}(x^*-1) \\ \leq& -\varepsilon z_{xx}^{j+1}(x^*) + (\frac{1}{\Delta t} + a(x^*) + (1 - \frac{\tau}{\Delta t})b(x^*))z^{j+1}(x^*) < 0. \end{aligned}$$

The two cases contradict the given hypothesis. So, the given assumption is wrong, which implies that $z^{j+1}(x) \geq 0$, $x \in \bar{\Omega}$. Moreover, the operator $\mathcal{L}_\varepsilon^M$ satisfies

$$\left\|(\mathcal{L}_\varepsilon^M)^{-1}\right\| \leq (1 + \lambda\Delta t)^{-1}, \tag{9.16}$$

which is used in estimating the truncation error. ■

Lemma 9.3.2 *(Semi-discrete stability estimate). The solution $U^{j+1}(x)$, $j = 0, 1, 2, ..., M-1$ of (9.14)-(9.15) can be estimated as*

$$|U^{j+1}(x)| \leq \frac{\|\mathcal{L}_\varepsilon^M U\|}{1+\lambda\Delta t} + \max\{|\partial\Omega^M|\},\ x \in [0,2],$$

where $\{|\partial\Omega^M|\} = \{|U^{j+1}(0)|, |U^{j+1}(2)|\}$.

Proof. Define two barrier functions as $Z_\pm^{j+1}(x) = \frac{\|\mathcal{L}_\varepsilon^M U\|}{1+\lambda\Delta t} + \max\{|\partial\Omega^M|\} \pm U^{j+1}(x)$, which give $Z_\pm^{j+1}(0) \geq 0$ and $Z_\pm^{j+1}(2) \geq 0$.

Case 1: For $0 < x \leq 1$, one can obtain

$$\begin{aligned}
\mathcal{L}_\varepsilon^m Z_\pm^{j+1}(x) &= -\,\varepsilon Z_{xx,\pm}^{j+1}(x) + \left(\frac{1}{\Delta t} + a(x)\right) Z_\pm^{j+1}(x) \\
&= \pm\,\vartheta^{j+1}(x) + \left(\frac{1}{\Delta t} + a(x)\right)\left[\frac{\|\mathcal{L}_\varepsilon^M U\|}{1+\lambda\Delta t} + \max\{|\partial\Omega^M|\}\right] \\
&\geq \left(\frac{1}{\Delta t} + a(x)\right)\left[\max\{|\partial\Omega^M|\}\right] \geq 0.
\end{aligned}$$

Case 2: For $1 < x < 2$, one can obtain

$$\begin{aligned}
\mathcal{L}_\varepsilon^M Z_\pm^{j+1}(x) &= -\,\varepsilon Z_{xx,\pm}^{j+1}(x) + \left(\frac{1}{\Delta t} + a(x)\right) Z_\pm^{j+1}(x) + (1 - \frac{\tau}{\Delta t})b(x)Z_\pm^{j+1}(x-1) \\
&\geq -\,\varepsilon Z_{xx,\pm}^{j+1}(x) + \left(\frac{1}{\Delta t} + a(x)\right) Z_\pm^{j+1}(x) + (1 - \frac{\tau}{\Delta t})b(x)Z_\pm^{j+1}(x) \\
&= \pm\,\vartheta^{j+1}(x) + \left(\frac{1}{\Delta t} + a(x) + (1 - \frac{\tau}{\Delta t})b(x)\right)[\frac{\|\mathcal{L}_\varepsilon^M U\|}{1+\lambda\Delta t} + \max\{|\partial\Omega^M|\}] \\
&\geq \left(\frac{1}{\Delta t} + a(x) + (1 - \frac{\tau}{\Delta t})b(x)\right)[\max\{|\partial\Omega^M|\}] \geq 0.
\end{aligned}$$

Thus, applying Lemma 9.3.1 yields $Z_\pm^{j+1}(x) \geq 0$, $x \in [0,2]$, which implies the required estimation. ■

Lemma 9.3.3 *Suppose that $|\frac{\partial^k U(x,t)}{\partial t^k}| \leq C$, $(x,t) \in \bar{\Omega}$, $k = 0, 1, 2$. The local error is estimated as $\|e_{j+1}\| \leq C(\Delta t)^2$, and with this condition, the global error is estimated as $\|E_{j+1}\| \leq C(\Delta t)$, $j = 0, 1, 2, ..., M-1$.*

Proof. From the Taylor series expansion, we have $U^{j+1}(x) = U^j(x) + \Delta t U_t^j(x) + O((\Delta t)^2)$ and this leads to

$$\frac{U^{j+1}(x) - U^j(x)}{\Delta t} = U_t^j(x) + O(\Delta t). \tag{9.17}$$

Using (9.17) into (9.6) gives

$$\mathcal{L}_{\varepsilon}^{M}U^{j+1}(x)+O((\Delta t)^2)=\vartheta^{j+1}(x) \tag{9.18}$$

From (9.14) and (9.18), one can find the boundary value problem of the form

$$\mathcal{L}_{\varepsilon}^{M}e^{j+1}(x)=O((\Delta t)^2),\ e^{j+1}(0)=0=e^{j+1}(2) \tag{9.19}$$

Using ((9.16)) into (9.19) yields $\|e^{j+1}\|\leq C(\Delta t)^2$.

Assuming the estimation of e^{j+1} holds true, one can have

$$\begin{aligned}\|E^{j+1}\|=&\left\|\sum_{\xi=1}^{j}e^{\xi}\right\|,\ \ j(\Delta t)\leq T\\ =&\|e^1+e^2+...+e^j\|\\ \leq&\|e^1\|+\|e^2\|+...+\|e^j\|\\ \leq&C'T(\Delta t)\leq C(\Delta t),\ j=0,1,2,...,M-1.\end{aligned}$$

Thus, the semi-discrete scheme is convergent of order one in time. ■

Lemma 9.3.4 *(Kumari & Kumar, 2020). Let the solution of (9.14) be $U^{j+1}(x)$. Then its derivatives can be bounded as*

$$\left|\frac{d^kU^{j+1}(x)}{dx^k}\right|\leq\begin{cases}C\left[1+\varepsilon^{\frac{-k}{2}}\left(\exp(-\sqrt{\frac{\lambda}{\varepsilon}}x)+\exp(-\sqrt{\frac{\lambda}{\varepsilon}}(1-x))\right)\right],\ x\in[0,1],\\ C\left[1+\varepsilon^{\frac{-k}{2}}\left(\exp(-\sqrt{\frac{\lambda}{\varepsilon}}(x-1))+\exp(-\sqrt{\frac{\lambda}{\varepsilon}}(2-x))\right)\right],\ x\in(1,2],\end{cases}$$

where $k=0,1,2,3$.

Proof. Similar procedures of Lemma 6.3.5 of Chapter 6. ■

9.3.2 Spatial discretization

Let's sub-divide the domain $[0,2]$ into N uniform meshes of size h, such that $\Gamma_x^N=\{0=x_0,x_1,...,x_{\frac{N}{2}}=1,x_{\frac{N}{2}+1},...,x_N=2,\ x_i=x_0+ih,i=0,1,...,N,\ h=\frac{2}{N}\}$. Following the procedures of Ehrhardt & Mickens (2013), consider a constant coefficient sub-equation from (9.14) as

$$-\varepsilon U_{xx}^{j+1}(x)+\lambda U^{j+1}(x)=0, \tag{9.20}$$

where $\frac{1}{\Delta t}+a(x)\geq\lambda>0$. The characteristic equation of (9.20) has two distinct roots $r_1=e^{\sqrt{\frac{\lambda}{\varepsilon}}x}$ and $r_2=e^{-\sqrt{\frac{\lambda}{\varepsilon}}x}$. Denoting U_i^{j+1} as the approximation of $U^{j+1}(x)$ at the grid point x_i, it is given by $U_i^{j+1} = c_1 e^{\sqrt{\frac{\lambda}{\varepsilon}}x_i} + c_2 e^{-\sqrt{\frac{\lambda}{\varepsilon}}x_i}$. Using the theory of difference equations in (Mickens, 1994),

$$\begin{vmatrix} U_{i-1}^{j+1} & e^{\sqrt{\frac{\lambda}{\varepsilon}}x_{i-1}} & e^{-\sqrt{\frac{\lambda}{\varepsilon}}x_{i-1}} \\ U_i^{j+1} & e^{\sqrt{\frac{\lambda}{\varepsilon}}x_i} & e^{-\sqrt{\frac{\lambda}{\varepsilon}}x_i} \\ U_{i+1}^{j+1} & e^{\sqrt{\frac{\lambda}{\varepsilon}}x_{i+1}} & e^{-\sqrt{\frac{\lambda}{\varepsilon}}x_{i+1}} \end{vmatrix} = 0.$$

After certain manipulation, it is simplified to

$$U_{i-1}^{j+1} - 2\cosh\left(\sqrt{\frac{\lambda}{\varepsilon}}h\right)U_i^{j+1} + U_{i+1}^{j+1} = 0. \tag{9.21}$$

The finite difference approximation of (9.20) is given as

$$-\varepsilon\frac{U_{i-1}^{j+1} - 2U_i^{j+1} + U_{i+1}^{j+1}}{\beta_i^2} + \lambda U_i^{j+1} = 0, \tag{9.22}$$

where β_i is a denominator function. From (9.21) and (9.22), the denominator function for the variable coefficients is given as

$$\beta_i = \frac{2}{\omega_i}\sinh\left(\frac{\omega_i h}{2}\right), \text{ where } \omega_i = \sqrt{\frac{1+\Delta t a_i}{\varepsilon\Delta t}}. \tag{9.23}$$

Incorporating the denominator function (9.23), a fully discrete scheme obtained as

$$\mathcal{L}_\varepsilon^{N,M}U_i^{j+1} = \vartheta_i^{j+1},\ j = 0,1,2,...,M-1, \tag{9.24}$$

where

$$\mathcal{L}_\varepsilon U_i^{j+1} = \begin{cases} -\varepsilon\delta^2 U_i^{j+1} + (\frac{1}{\Delta t} + a_i)U_i^{j+1},\ i = 1,2,...,\frac{N}{2}, \\ -\varepsilon\delta^2 U_i^{j+1} + (\frac{1}{\Delta t} + a_i)U_i^{j+1} + (1-\frac{\tau}{\Delta t})b_i U_{i-\frac{N}{2}}^{j+1},\ i = \frac{N}{2}+1, \frac{N}{2}+2, ..., N-1 \end{cases}$$

and

$$\vartheta_i^{j+1} = \begin{cases} f_i^{j+1} + \frac{U_i^j}{\Delta t} - (1-\frac{\tau}{\Delta t})b_i\phi_{i-\frac{N}{2}}^{j+1} - \frac{\tau}{\Delta t}b_i\phi_{i-\frac{N}{2}}^j,\ i = 1,2,...,\frac{N}{2}, \\ f_i^{j+1} + \frac{U_i^j}{\Delta t} - \frac{\tau}{\Delta t}b_i U_{i-\frac{N}{2}}^j,\ i = \frac{N}{2}+1, \frac{N}{2}+2, ..., N-1, \end{cases}$$

with $\delta^2 U_i^{j+1} = \frac{U_{i+1}^{j+1} - 2U_i^{j+1} + U_{i-1}^{j+1}}{\beta_i^2}$ and the discrete initial and boundary conditions $U^0(x_i) = U_0(x_i),\ x_i \in [0,2],\ U^{j+1}(x_i) = \phi^{j+1}(x_i),\ x_i \in \Omega^-,\ U^{j+1}(2) = \alpha(2,t_{j+1}),\ (2,t_{j+1}) \in \Omega^+$.

Lemma 9.3.5 *Let Z_i^{j+1} be a given mesh function satisfying $Z_0^{j+1} \geq 0$ and $Z_N^{j+1} \geq 0$. If $\mathcal{L}_\varepsilon^{N,M}Z_i^{j+1} \geq 0$ for $i = 1,2,...,N-1$, then $Z_i^{j+1} \geq 0$ for $i = 0,1,...,N$.*

Proof. For some $k \in \{1, ..., N-1\}$, suppose that $Z_k^{j+1} = \min_{i=1,\dots,n-1} Z_i^{j+1} < 0$.
Case 1: For $k = 1, 2, ..., \frac{N}{2}$, one can obtain

$$\mathcal{L}_{\varepsilon,1}^{N} Z_k^{j+1} = -\varepsilon\delta^2 Z_k^{j+1} + (\frac{1}{\Delta t} + a_k) Z_k^{j+1} < 0$$

Case 2: For $k = \frac{N}{2}+1, \frac{N}{2}+2, ..., N-1$, one can obtain

$$\begin{aligned}\mathcal{L}_{\varepsilon,2}^{N,M} Z_k^{j+1} &= -\varepsilon\delta^2 Z_k^{j+1} + (\frac{1}{\Delta t} + a_k) Z_k^{j+1} + (1 - \frac{\tau}{\Delta t}) b_k Z_{k-\frac{N}{2}}^{j+1} \\ &\leq -\varepsilon\delta^2 Z_k^{j+1} + (\frac{1}{\Delta t} + a_k) Z_k^{j+1} + (1 - \frac{\tau}{\Delta t}) b_k Z_k < 0.\end{aligned}$$

From the two cases, it can be seen that the given hypothesis is contradicted, and hence the assumption fails. Thus, $Z_k^{j+1} \geq 0$, $k = 0, 1, ..., N$. ■

Lemma 9.3.6 *The solution U_i^{j+1} of the fully discrete scheme (9.24) is estimated as*

$$|U_i^{j+1}| \leq \frac{\Delta t \|\vartheta\|}{1 + \lambda \Delta t} + \max\{|\partial\Omega^{N,M}|\}, \; i = 0, 1, ..., N,$$

where $\{|\partial\Omega^{N,M}|\} = \{|U_0^{j+1}|, |U_N^{j+1}|\}$.

Proof. Let's define $\pi_{\pm,i}^{j+1} = \frac{\Delta t\|\vartheta\|}{1+\lambda\Delta t} + \max\{|\partial\Omega^{N,M}|\} \pm U_i^{j+1}$. Then,

$$\begin{aligned}\pi_{0,j+1}^{\pm} &= \frac{\Delta t\|\vartheta\|}{1 + \lambda\Delta t} + \max\{|\partial\Omega^{N,M}|\} \pm U_0^{j+1} \geq \frac{\Delta t\|\vartheta\|}{1+\lambda\Delta t} \geq 0 \\ \pi_{N,j+1}^{\pm} &= \frac{\Delta t\|\vartheta\|}{1 + \lambda\Delta t} + \max\{|\partial\Omega^{N,M}\|\} \pm U_N^{j+1} \geq \frac{\Delta t\|\vartheta\|}{1+\lambda\Delta t} \geq 0\end{aligned}$$

When $i = 1, 2, ..., \frac{1}{N}$,

$$\begin{aligned}\mathcal{L}_{\varepsilon,1}^{N,M} \pi_{\pm,i}^{j+1} &= -\varepsilon\delta^2 \pi_{\pm,i}^{j+1} + \left(\frac{1}{\Delta t} + a_i\right) \pi_{\pm,i}^{j+1} \\ &= \left(\frac{1}{\Delta t} + a_i\right)\left(\frac{\Delta t\|\vartheta\|}{1+\lambda\Delta t} + \max\{|\partial\Omega^{N,M}|\}\right) \pm \vartheta_i^{j+1} \geq \left(\frac{1}{\Delta t} + a_i\right)\left(\max\{|\partial\Omega^{N,M}|\}\right) \geq 0\end{aligned}$$

When $i = \frac{N}{2}+1, \frac{N}{2}+2, ..., N-1$,

$$\begin{aligned}\mathcal{L}_{\varepsilon,2}^{N,M} \pi_{\pm,i}^{j+1} &= -\varepsilon\delta^2 \pi_{\pm,i}^{j+1} + \left(\frac{1}{\Delta t} + a_i\right) \pi_{\pm,i}^{j+1} + (1 - \frac{\tau}{\Delta t}) b_i \phi_{i-\frac{N}{2},j+1}^{\pm} \\ &= \left(\frac{1}{\Delta t} + a_i + (1 - \frac{\tau}{\Delta t}) b_i\right)\left(\frac{\Delta t\|\vartheta\|}{1+\lambda\Delta t} + \max\{|\partial\Omega^{N,M}|\}\right) \pm \vartheta_i^{j+1} \\ &\geq \left(1 + \Delta t a_i + (1 - \frac{\tau}{\Delta t}) b_i\right)\left(\max\{|\partial\Omega^{N,M}|\}\right) \geq 0\end{aligned}$$

Thus, applying Lemma 9.3.5, we have $\pi_{\pm,i}^{j+1} \geq 0$, $i = 0, 1, ..., N$, which yields the stability estimate. ■

Lemma 9.3.7 *(Tiruneh et al., 2023). For a given fixed mesh number N, the following holds true.*

$$\lim_{\varepsilon\to 0}\begin{cases}\max\limits_{x_i\in(0,1]}\dfrac{\exp(-\sqrt{\frac{a(x_i)}{\varepsilon}}x_i)+\exp(-\sqrt{\frac{a(x_i)}{\varepsilon}}(1-x_i))}{\varepsilon^{k/2}}=0,\\ \max\limits_{x_i\in(1,2)}\dfrac{\exp(-\sqrt{\frac{a(x_i)}{\varepsilon}}(x_i-1))+\exp(-\sqrt{\frac{a(x_i)}{\varepsilon}}(2-x_i))}{\varepsilon^{k/2}}=0\end{cases}$$

for all $i=1,2,...,N-1$ and $k=1,2,3,....$

Proof. See the proof of Lemma 7.3.8 of Chapter 7. ∎

Theorem 9.3.1 *Let the solution of (9.14) be $U(x,t_{j+1})$ and the solution of (9.24) be U_i^{j+1}. Then,*

$$|U_i^{j+1}-U(x_i,t_{j+1})|\leq CN^{-2}.$$

Proof. From the differential and difference equations, the truncation error for $i=0,1,2,...,\frac{N}{2}$ is

$$\begin{aligned}\left|\mathcal{L}_\varepsilon^{N,M}\left(U^{j+1}(x_i)-U_i^{j+1}\right)\right| &= \left|-\varepsilon\frac{d^2U^{j+1}(x_i)}{dx^2}+\varepsilon\delta^2U_i^{j+1}\right|\\ &=\left|-\varepsilon\frac{d^2U^{j+1}(x_i)}{dx^2}+\frac{\varepsilon}{\sigma_i^2}\left(U_{i+1}^{j+1}-2U_i^{j+1}+U_{i-1}^{j+1}\right)\right| \end{aligned}\tag{9.25}$$

By the Taylor series expansion of U_{i+1}^{j+1}, U_{i-1}^{j+1} and $\frac{1}{\sigma_i}$ truncated up to order five,

$$\begin{aligned}U_{i+1}^{j+1}&=U_i^{j+1}+h\frac{dU^{j+1}}{dx}+\frac{h^2}{2!}\frac{d^2U^{j+1}}{dx^2}+\frac{h^3}{3!}\frac{d^3U^{j+1}}{dx^3}+\frac{h^4}{4!}\frac{d^4U^{j+1}(\zeta_i)}{dx^4},\ \zeta_i\in(x_{i-1},x_{i+1}),\\ U_{i-1}^{j+1}&=U_i^{j+1}-h\frac{dU^{j+1}}{dx}+\frac{h^2}{2!}\frac{d^2U^{j+1}}{dx^2}-\frac{h^3}{3!}\frac{d^3U^{j+1}}{dx^3}+\frac{h^4}{4!}\frac{d^4U^{j+1}(\zeta_i)}{dx^4},\ \zeta_i\in(x_{i-1},x_{i+1}),\\ \frac{1}{\sigma_i^2}&=\frac{\omega_i^2}{4\sinh^2(\omega_ih/2)}=\frac{\omega_i^2}{4}\left(\frac{4}{(\omega_ih)^2}-\frac{1}{3}+\frac{(\omega_ih)^2}{60}\right).\end{aligned}$$

Putting these expansions in (9.25) yields

$$\begin{aligned}|\mathcal{L}_\varepsilon^{N,M}\left(U^{j+1}(x_i)-U_i^{j+1}\right)| =&| -\varepsilon\frac{d^2U_i^{j+1}}{dx^2}+\varepsilon\frac{d^2U_i^{j+1}}{dx^2}+\left(\frac{\varepsilon}{12}\frac{d^4U^{j+1}(\zeta_i)}{dx^4}-\frac{\varepsilon\omega_i^2}{12}\frac{d^2U_i^{j+1}}{dx^2}\right)h^2\\ &+\left(\frac{\varepsilon\omega_i^4}{240}\frac{d^2U_i^{j+1}}{dx^2}-\frac{\varepsilon\omega_i^2}{144}\frac{d^4U^{j+1}(\zeta_i)}{dx^4}\right)h^4+\frac{\varepsilon\omega_i^4}{2880}\frac{d^4U^{j+1}(\zeta_i)}{dx^4}h^6|.\end{aligned}$$

Applying the bound of derivatives in Lemma 9.3.4 and then using Lemma 9.3.7 yields

$$\left|\mathcal{L}_\varepsilon^{N,M}\left(U^{j+1}(x_i)-U_i^{j+1}\right)\right|\leq C_1h^2+C_2h^4+C_3h^6\leq Ch^2.\tag{9.26}$$

Invoking Lemma 9.3.5 gives $|U_i^{j+1}-U(x_i,t_{j+1})|\leq CN^{-2}$, as $h=2N^{-1}$. ∎

Theorem 9.3.2 *For the solutions $u(x,t)$ of (9.6) and U_i^{j+1} of (9.24), the uniform error is estimated as*

$$\sup_{0<\varepsilon\leq 1} \|u(x_i,t_{j+1}) - U_i^{j+1}\| \leq C\left(\Delta t + N^{-2}\right).$$

Proof. By the triangular inequality, we can obtain that

$$\begin{aligned}\left|u(x_i,t_{j+1}) - U_i^{j+1}\right| &= \left|u(x_i,t_{j+1}) - U^{j+1}(x_i) + U^{j+1}(x_i) - U_i^{j+1}\right| \\ &\leq \left|u(x_i,t_{j+1}) - U^{j+1}(x_i)\right| + \left|U^{j+1}(x_i) - U_i^{j+1}\right|.\end{aligned}$$

Then, combination of Lemma 9.3.3 and Theorem 9.3.1 yields the uniform error estimate. ■

9.4 Numerical results and discussions

In this section, three numerical examples are considered to demonstrate the validity and applicability of the proposed numerical scheme. Since it is tedious to find the exact solution, a variant of the double mesh principle in (4.44)–(4.47) is used to determine the maximum absolute errors and corresponding convergence rates. As it is surveyed in literature, the model problem considered in this chapter is not solved by other researchers. And hence, there is no numerical results to be compared with the present method. The examples solved below are taken considering the basic assumptions and properties of the functions involved in the problem, and the continuous solution.

Example 9.4.1 *Consider $u_t(x,t) - \varepsilon u_{xx}(x,t) + 6u(x,t) - 2u(x-1,t-\tau) = 1$, subjected to $u_0(x) = 0$, $u(x,t) = 0$ and $u(2,t) = 0$.*

Example 9.4.2 *Consider $u_t(x,t) - \varepsilon u_{xx}(x,t) + (x+4)u(x,t) - (x^2+1)u(x-1,t-\tau) = 2$, subjected to $u_0(x) = 0$, $u(x,t) = 0$ and $u(2,t) = 0$.*

Example 9.4.3 *Consider $u_t(x,t) - \varepsilon u_{xx}(x,t) + 5u(x,t) - 2u(x-1,t-\tau) = 2$, subjected to $u_0(x) = \sin(\pi x)$, $u(x,t) = 0$ and $u(2,t) = 0$.*

The three model examples are treated applying the proposed numerical method. Since the exact solutions of the examples are not given or difficult to find, the absolute errors and rate of convergence are computed using a variant of the double mesh principle. The obtained results are displayed in tables and graphs. For each examples, the maximum point-wise error and the convergence rates are computed as shown in Tables 9.1-9.3, respectively. From these tables, one can observe that for a fixed value of ε, increasing the mesh numbers, minimizes the maximum absolute error. On the other hand, for fixed number of meshes, decreasing ε yields stable and

Table 9.1: Maximum absolute errors and convergence rates for Example 9.4.1, taking $\tau = \frac{\varepsilon}{4}$.

ε $\mid N \rightarrow$	40	80	160	320	640
$\downarrow$ $\mid M \rightarrow$	20	80	320	1280	5120
2^{-4}	9.0018e-03	2.1164e-03	4.7823e-04	1.1625e-04	5.4060e-05
	2.0886	2.1458	2.0405	1.1046	
2^{-6}	1.1641e-02	3.2085e-03	1.0967e-03	2.1814e-04	6.0927e-05
	1.8592	1.5487	2.3298	1.8401	
2^{-8}	1.1803e-02	3.9262e-03	1.0893e-03	2.4892e-04	6.6173e-05
	1.5879	1.8497	2.1296	1.9114	
2^{-10}	1.1806e-02	4.2510e-03	1.1623e-03	2.6394e-04	6.7668e-05
	1.4736	1.8708	2.1387	1.9637	
2^{-12}	1.1811e-02	4.2735e-03	1.1605e-03	2.8472e-04	7.6245e-05
	1.4667	1.8807	2.0271	1.9008	
2^{-14}	1.1812e-02	4.2737e-03	1.1797e-03	3.0293e-04	7.6249e-05
	1.4667	1.8571	1.9614	1.9902	
2^{-16}	1.1812e-02	4.2737e-03	1.1798e-03	3.0293e-04	7.6250e-05
	1.4667	1.8569	1.9615	1.9902	
$\vdots$	$\vdots$	$\vdots$	$\vdots$	$\vdots$	$\vdots$
2^{-40}	1.1812e-02	4.2737e-03	1.1798e-03	3.0293e-04	7.6250e-05
	1.4667	1.8569	1.9615	1.9902	
$e^{N,M}$	1.1812e-02	4.2737e-03	1.1798e-03	3.0293e-04	7.6250e-05
$r^{N,M}$	1.4667	1.8569	1.9615	1.9902	-

uniform maximum point-wise errors after certain changes of the values of ε. This shows that the developed numerical scheme is ε-uniformly convergent.

The numerical solution profiles of the considered examples are simulated by figures. In Figure 9.1, the effect of the perturbation parameter in layer resolving is shown for Examples 9.4.2 and 9.4.3. To show the physical behaviors of the solutions, surface plots and contour lines are simulated in Figures 9.2 and9.3 for Examples 9.4.2 and 9.4.3, respectively. From each figure, one can observe the effect of ε. That is, if the value of ε approaches to zero, the width of the layers decreases. The uniform convergence of the developed scheme is illustrated by plotting log-log figures as shown in Figure 9.4.

Table 9.2: Maximum absolute errors and convergence rates for Example 9.4.2 taking $\tau = \frac{\varepsilon}{4}$.

ε $\mid N \rightarrow$	40	80	160	320	640
$\downarrow$ $\mid M \rightarrow$	20	80	320	1280	5120
2^{-4}	1.7988e-02	4.2929e-03	9.5899e-04	2.9234e-04	1.0276e-04
	2.0670	2.1623	1.7139	1.5084	
2^{-6}	2.3252e-02	6.5120e-03	2.0897e-03	4.3974e-04	1.5494e-04
	1.8362	1.6398	2.2486	1.5049	
2^{-8}	2.3609e-02	7.9555e-03	2.3536e-03	6.2910e-04	1.6514e-04
	1.5693	1.7571	1.9035	1.9296	
2^{-10}	2.3343e-02	8.7007e-03	2.3793e-03	6.2889e-04	1.6533e-04
	1.4238	1.8706	1.9197	1.9275	
2^{-12}	2.3344e-02	8.6447e-03	2.4462e-03	6.1828e-04	1.6385e-04
	1.4332	1.8213	1.9842	1.9159	
2^{-14}	2.3345e-02	8.6449e-03	2.4443e-03	6.5550e-04	1.6880e-04
	1.4332	1.8224	1.8988	1.9573	
2^{-16}	2.3346e-02	8.6450e-03	2.4446e-03	6.5050e-04	1.7486e-04
	1.4332	1.8223	1.9100	1.8953	
2^{-18}	2.3346e-02	8.6450e-03	2.4446e-03	6.5551e-04	1.7898e-04
	1.4332	1.8223	1.8989	1.8728	
2^{-20}	2.3346e-02	8.6451e-03	2.4446e-03	6.5551e-04	1.7900e-04
	1.4332	1.8223	1.8989	1.8727	
$\vdots$	$\vdots$	$\vdots$	$\vdots$	$\vdots$	$\vdots$
2^{-40}	2.3346e-02	8.6451e-03	2.4446e-03	6.5551e-04	1.7900e-04
	1.4332	1.8223	1.8989	1.8727	
$e^{N,M}$	2.3609e-02	8.7007e-03	2.4462e-03	6.5551e-04	1.7900e-04
$r^{N,M}$	1.4401	1.8306	1.8999	1.8727	-

Table 9.3: Maximum absolute errors and convergence rates for Example 9.4.3 taking $\tau = \frac{\varepsilon}{4}$.

ε $\mid N \rightarrow$	40	80	160	320	640
$\downarrow$ $\mid M \rightarrow$	20	80	320	1280	5120
2^{-4}	3.3141e-02	8.4683e-03	2.1599e-03	4.3730e-04	1.2568e-04
	1.9685	1.9711	2.3043	1.7989	
2^{-6}	4.7466e-02	1.1454e-02	2.6426e-03	5.6940e-04	1.5517e-04
	2.0510	2.1158	2.2144	1.8756	
2^{-8}	4.7176e-02	1.2003e-02	2.2515e-03	5.7746e-04	1.5432e-04
	1.9747	2.4144	1.9631	1.9038	
2^{-10}	4.6634e-02	1.2830e-02	2.3415e-03	5.8625e-04	1.5541e-04
	1.8619	2.4540	1.9978	1.9154	
2^{-12}	4.6595e-02	1.2728e-02	2.9457e-03	6.6726e-04	1.5984e-04
	1.8722	2.1113	2.1423	2.0616	
2^{-14}	4.6594e-02	1.2727e-02	2.9430e-03	6.8613e-04	1.6442e-04
	1.8723	2.1125	2.1007	2.0611	
2^{-16}	4.6594e-02	1.2727e-02	2.9431e-03	6.8614e-04	1.6442e-04
	1.8723	2.1125	2.1007	2.0630	
$\vdots$	$\vdots$	$\vdots$	$\vdots$	$\vdots$	$\vdots$
2^{-40}	4.6594e-02	1.2727e-02	2.9431e-03	6.8614e-04	1.6442e-04
	1.8723	2.1125	2.1007	2.0630	
$e^{N,M}$	4.7466e-02	1.2830e-02	2.9457e-03	6.8614e-04	1.6442e-04
$r^{N,M}$	1.8874	2.1228	2.1020	2.0611	-

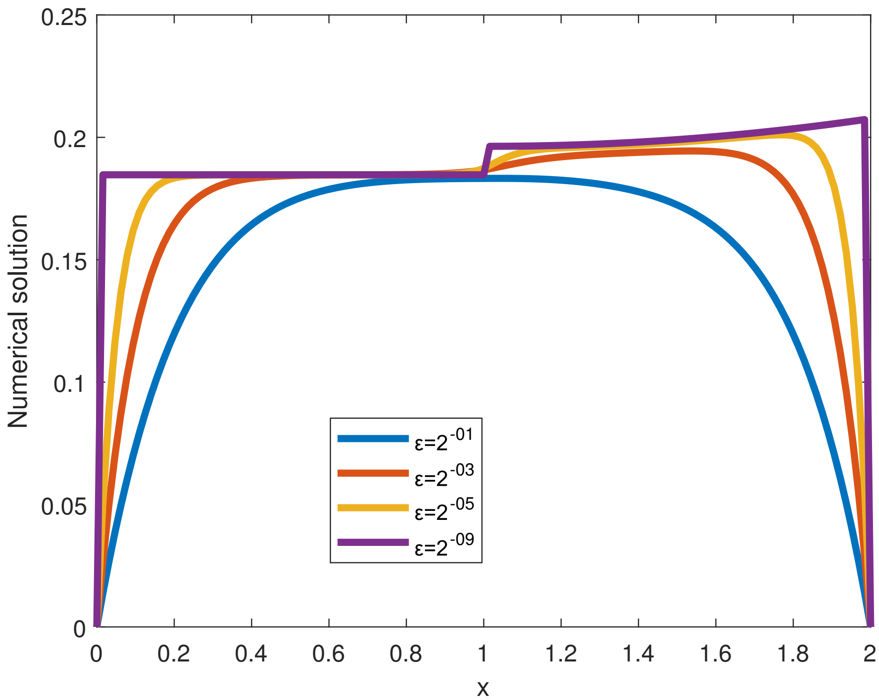

(a)

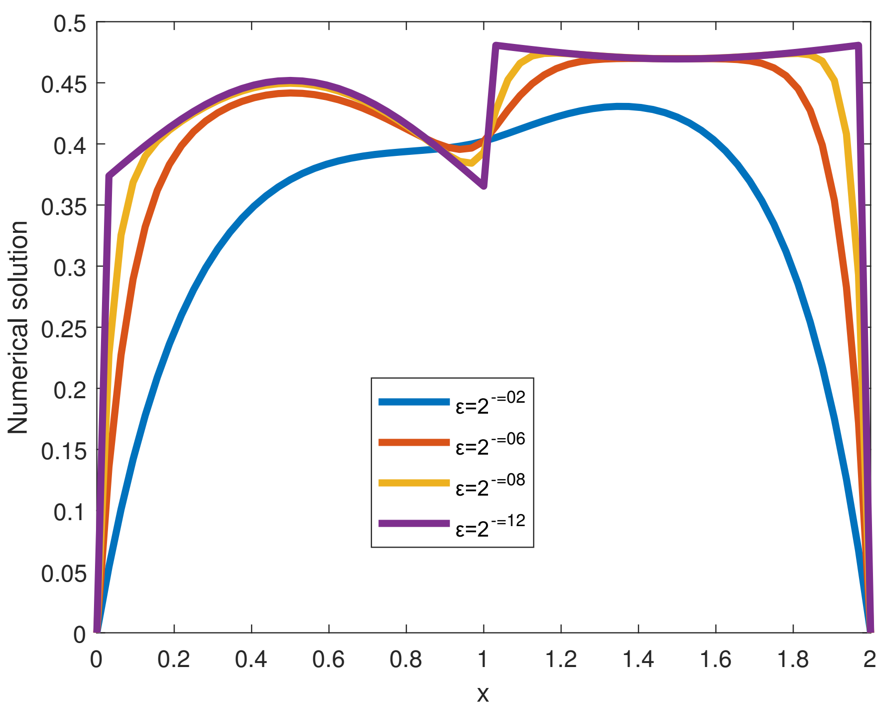

(b)

Figure 9.1: Effect of the perturbation parameter in boundary layers resolving for (a) Example 9.4.2 and (b) Example 9.4.3 when $\tau = \frac{\varepsilon}{4}$.

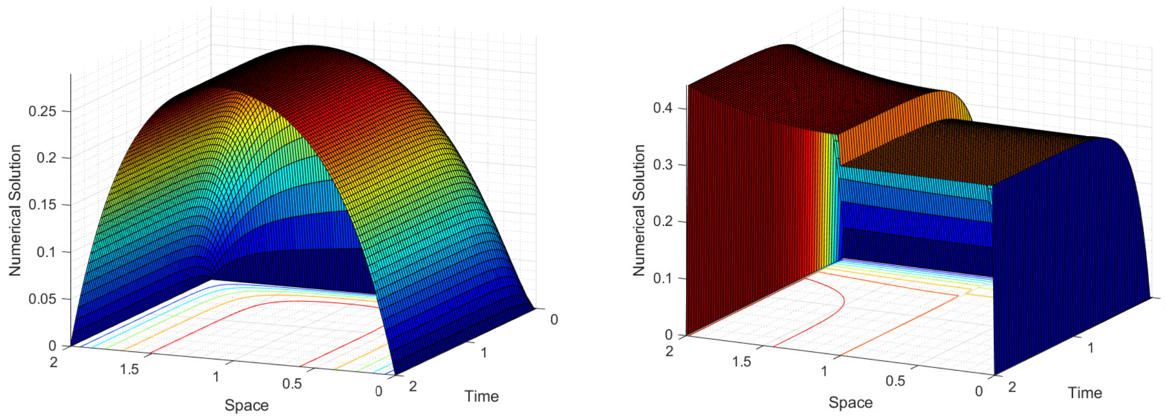

(a) $\varepsilon = 2^0$ (b) $\varepsilon = 2^{-16}$

Figure 9.2: Surface plot simulations of Example 9.4.2, for various values of ε at $\tau = \frac{\varepsilon}{4}$.

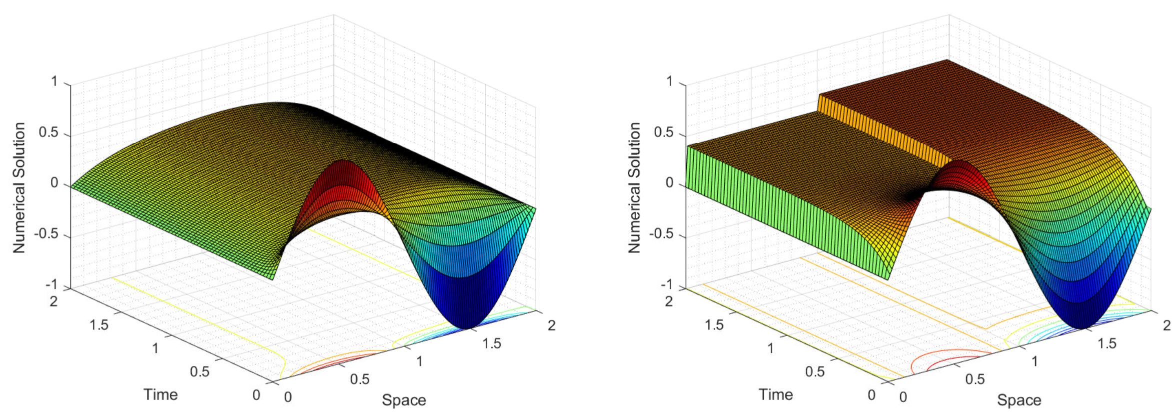

(a) $\varepsilon = 2^0$ (b) $\varepsilon = 2^{-16}$

Figure 9.3: Surface plot simulations of Example 9.4.3, for various values of ε at $\tau = \frac{\varepsilon}{4}$.

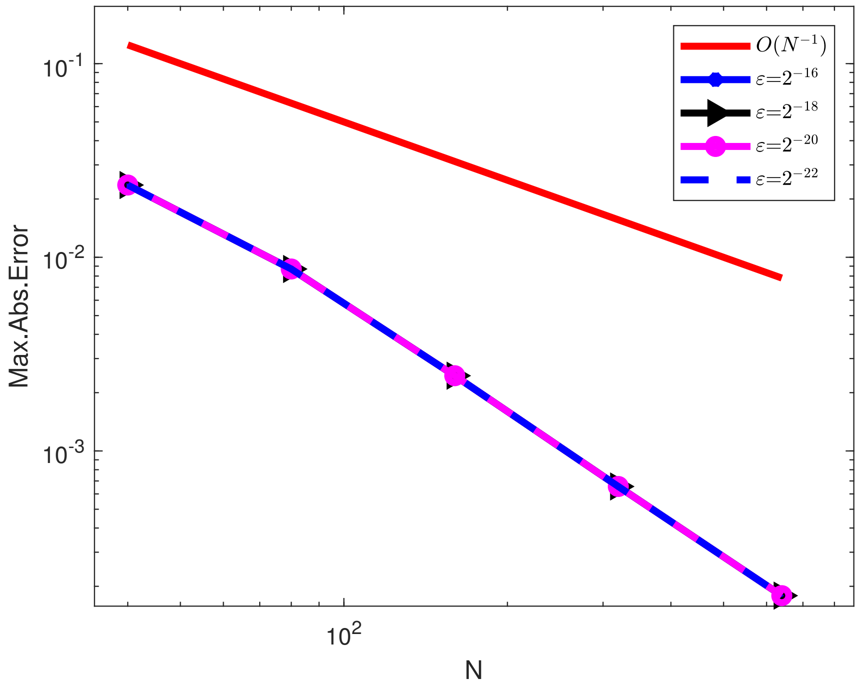

(a)

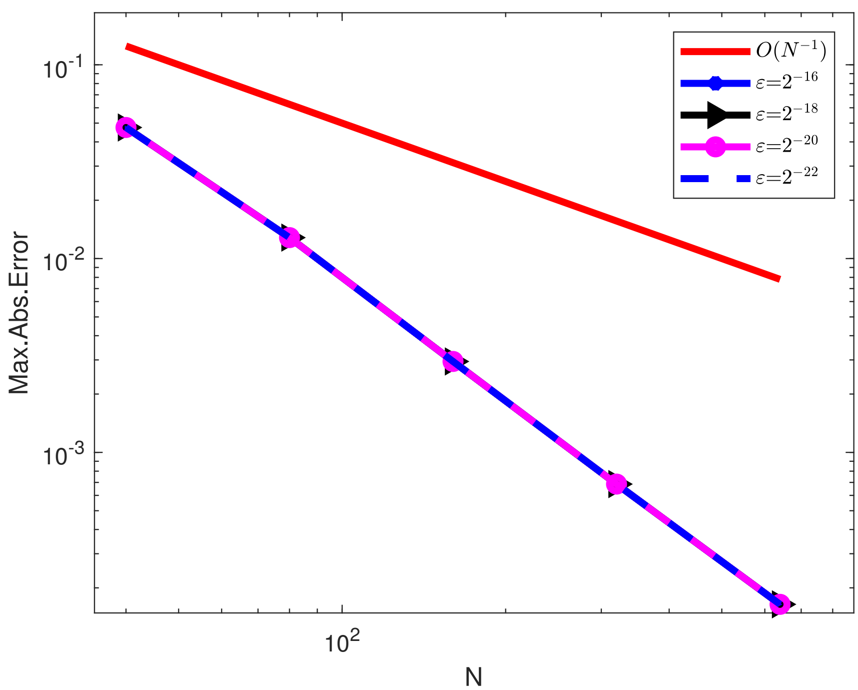

(b)

Figure 9.4: The log-log plots of maximum absolute errors versus N for (a) Example 9.4.2 and (b) Example 9.4.3.

9.5 Summary

In this chapter, singularly perturbed differential equation involving the spatial and temporal delays in the reaction term is treated. The presence of the perturbation parameter exhibits boundary layers in the solution, and the large negative shift causes interior layer. As a result, the solution varies abruptly in the layer regions. The rapidly changing behavior of the layers makes it difficult to find an exact solution. To solve the problem, a numerical scheme is developed by using the implicit Euler method in the temporal variable and using the nonstandard finite difference method in the spatial variable on a uniform discretizations. The effect of the temporal delay is handled applying Taylor's series approximation and the negative shift is handled by choosing a special mesh, so that the shifted term lies on the mesh point $x_i = 1$. The stability of the method is established and proved. Its uniform convergence is also investigated and proved. Three numerical examples are considered and solved applying the developed method to test its validity and applicability. The solutions and error analysis of the examples are shown in graphical and tabular forms. From the theoretical and numerical findings discussed in this chapter, the proposed numerical scheme is obtained to be uniformly convergent. The main findings of this chapter are summarized as follows.

1. A robust and uniformly convergent nonstandard finite difference scheme is developed for singularly perturbed differential equations with spatio-temporal delays.
2. In applying the developed numerical scheme, decreasing the grid sizes decreases the maximum absolute errors. and decreasing the value of the ε yields stable and uniform maximum absolute errors.
3. The convergence rate of the obtained method is shown to be of order one in the temporal direction and order two in the spatial direction.

CONCLUSIONS AND RECOMMENDATIONS

Conclusion

This dissertation focuses on formulating and analyzing fitted numerical schemes for a class of singularly perturbed differential-difference equations. Due to the presence of the perturbation parameter and negative shift argument, the solutions of these problems involve layers, which make it difficult to solve the problems analytically. To treat these problems, there is a need of formulating parameter independent numerical methods. This dissertation has contributed six uniformly convergent numerical schemes, wich are summarized as follows.

For singularly perturbed ordinary differential equations with large negative shift, an exponentially fitted finite difference scheme is formulated by decomposing the domain into its inner and outer regions. The stability estimate and convergence analysis of the formulated scheme are investigated and shown that the scheme is accurate and uniformly convergent of order two.

For singularly perturbed partial differential equations involving a shift argument $\delta \in (0, 1)$, a fitted mesh finite difference method is formulated on a piece-wise uniform Shishkin's meshes. The stability estimate is established and its uniform convergence is investigated and shown that the method is uniformly convergent of order two in the time variable and almost of second order in the spatial variable.

For singularly perturbed partial differential equation with large negative shift, three fitted numerical schemes are formulated. One of these schemes is a fitted mesh finite difference method on a piece-wise uniform Shishkin-type meshes. The stability estimate and convergence analysis are investigated for this method and shown that it is uniformly convergent of almost order two in the spatial direction and order one or two in the temporal direction depending on the θ value used for the time discretization. The second scheme formulated is a nonstandard finite difference method on a uniform meshes. It is proved that this method is stable and uniformly convergent of order two in the temporal and spatial directions. The third scheme formulated for such problem is a tension spline fitted method. The stability estimate and the uniform convergence investigation of this method is shown that the method is uniformly convergent of order one in time and order two in the spatial variable.

For a singularly perturbed partial differential equation with large negative shift and small delay, a nonstandard finite difference scheme is formulated on a uniform meshes. It is proved that the scheme is stable and its uniform convergence is investigated that the method is uniformly convergent of order one in the temporal direction and second order in the spatial direction.

Recommendations

The numerical schemes formulated in this dissertation are accurate and uniformly convergent for solving a class of singularly perturbed differential-difference equations. Based on the schemes formulated, several recommendations can be made to enhance the applicability of the developed numerical schemes and provide a direction for future research works. These recommendations include the following.

1) One can extend these methods to solve two and three dimensional singularly perturbed differential-difference equations.
2) The methods can be extended to singularly perturbed integro-differential equations.
3) The methods can be extended to singularly perturbed system of differential-difference equations.
4) One can extend the methods to solve singularly perturbed non-linear differential equations and fractional-order derivative problems.
5) One can further modify the methods on a non-uniform (graded) meshes like Bakhvalov's meshes, and on a Harmonic meshes.

REFERENCES

Adilaxmi, M., Bhargavi, D., & Reddy, Y. (2019). An initial value technique using exponentially fitted non standard finite difference method for singularly perturbed differential-difference equations. *Applications and Applied Mathematics: An International Journal (AAM)*, *14*(1), 16.

Allen, D. G. D., & Southwell, R. (1955). Relaxation methods applied to determine the motion, in two dimensions, of a viscous fluid past a fixed cylinder. *The Quarterly Journal of Mechanics and Applied Mathematics*, *8*(2), 129–145.

Angasu, M. A., Duressa, G. F., & Woldaregay, M. M. (2021). Exponentiall fitted numerical scheme for singularly perturbed differential equations involving small delays. *Journal of applied mathematics & informatics*, *39*(3_4), 419–435.

Ayele, M. A., Tiruneh, A. A., & Derese, G. A. (2022). Uniformly convergent scheme for singularly perturbed space delay parabolic differential equation with discontinuous convection coefficient and source term. *Journal of Mathematics*, *2022*.

Babu, G., Prithvi, M., Sharma, K. K., & Ramesh, V. (2022). A robust numerical algorithm on harmonic mesh for parabolic singularly perturbed convection-diffusion problems with time delay. *Numerical Algorithms*, 1–20.

Bakhvalov, N. S. (1969). On the optimization of the methods for solving boundary value problems in the presence of a boundary layer. *Zhurnal Vychislitel'noi Matematiki i Matematicheskoi Fiziki*, *9*(4), 841–859.

Bansal, K., & Sharma, K. K. (2017). Parameter uniform numerical scheme for time dependent singularly perturbed convection-diffusion-reaction problems with general shift arguments. *Numerical Algorithms*, *75*, 113–145.

Bansal, K., & Sharma, K. K. (2018). Parameter-robust numerical scheme for time-dependent singularly perturbed reaction–diffusion problem with large delay. *Numerical Functional Analysis and Optimization*, *39*(2), 127–154.

Brdar, M., Franz, S., Ludwig, L., & Roos, H.-G. (2023). A balanced norm error estimation for the time-dependent reaction-diffusion problem with shift in space. *Applied Mathematics and Computation*, *437*, 127507.

Campillo, F., & Lobry, C. (2012). Effect of population size in a predator–prey model. *Ecological Modelling*, *246*, 1–10.

Chakravarthy, P. P., & Kumar, K. (2018). An adaptive mesh method for time dependent singularly perturbed differential-difference equations. *Nonlinear Engineering*, *8*(1), 328–339.

Chakravarthy, P. P., & Kumar, K. (2021). A novel method for singularly perturbed delay differential equations of reaction-diffusion type. *Differential Equations and Dynamical Systems*, *29*(3), 723–734.

Chakravarthy, P. P., Kumar, S. D., & Rao, R. N. (2017a). An exponentially fitted finite difference scheme for a class of singularly perturbed delay differential equations with large delays. *Ain Shams Engineering Journal*, *8*(4), 663–671.

Chakravarthy, P. P., Kumar, S. D., & Rao, R. N. (2017b). Numerical solution of second order singularly perturbed delay differential equations via cubic spline in tension. *International Journal of Applied and Computational Mathematics*, *3*, 1703–1717.

Chen, F., Janjić, Z., & Mitchell, K. (1997). Impact of atmospheric surface-layer parameterizations in the new land-surface scheme of the ncep mesoscale eta model. *Boundary-Layer Meteorology*, *85*(3), 391–421.

Clavero, C., & Gracia, J. L. (2010). On the uniform convergence of a finite difference scheme for time dependent singularly perturbed reaction-diffusion problems. *Applied mathematics and computation*, *216*(5), 1478–1488.

Coombes, S. (2008). Neuronal networks with gap junctions: A study of piecewise linear planar neuron models. *SIAM Journal on Applied Dynamical Systems*, *7*(3), 1101–1129.

Culshaw, R. V., & Ruan, S. (2000). A delay-differential equation model of hiv infection of cd4+ t-cells. *Mathematical biosciences*, *165*(1), 27–39.

Daba, I. T., & Duressa, G. F. (2022). Computational method for singularly perturbed parabolic differential equations with discontinuous coefficients and large delay. *Heliyon*, *8*(9), e10742.

Das, P., & Natesan, S. (2013). A uniformly convergent hybrid scheme for singularly perturbed system of reaction-diffusion robin type boundary-value problems. *Journal of Applied Mathematics and Computing*, *41*, 447–471.

Debela, H. G., & Duressa, G. F. (2020). Accelerated fitted operator finite difference method for singularly perturbed delay differential equations with non-local boundary condition. *Journal of the Egyptian Mathematical Society*, *28*, 1–16.

Debela, H. G., Kejela, S. B., & Negassa, A. D. (2020). Exponentially fitted numerical method for singularly perturbed differential-difference equations. *International Journal of Differential Equations*, *2020*.

Derstine, M., Gibbs, H., Hopf, F., & Kaplan, D. (1982). Bifurcation gap in a hybrid optically bistable system. *Physical Review A*, *26*(6), 3720.

Devendra, K. (2018). A collocation method for singularly perturbed differential-difference turning point problems exhibiting boundary/interior layers. *Journal of Difference Equations and Applications*, *24*(12), 1847–1870.

Dinesh, S. K., Rao, R. N., & Chakravarthy, P. P. (2017). A numerical scheme for singularly perturbed reaction-diffusion problems with a negative shift via numerov method. In *Iop conference series: Materials science and engineering* (Vol. 263, p. 042110).

Doolan, E. P., Miller, J. J., & Schilders, W. H. (1980). *Uniform numerical methods for problems with initial and boundary layers*. Boole Press.

Duan, L., Choudhari, M. M., Li, F., & Wu, M. (2013). Direct numerical simulation of transition in a swept wing boundary layer. In *43rd aiaa fluid dynamics conference* (p. 2617).

Duressa, G. F. (2021). Novel approach to solve singularly perturbed boundary value problems with negative shift parameter. *Heliyon*, *7*(7), e07497.

Duressa, G. F., & Bullo, T. A. (2021). Higher-order numerical method for singularly perturbed delay reaction-diffusion problems. *Pure and Applied Mathematics Journal*, *10*(3), 68.

Duressa, G. F., Daba, I. T., & Deressa, C. T. (2023). A systematic review on the solution methodology of singularly perturbed differential difference equations. *Mathematics*, *11*(5), 1108.

Ehrhardt, M., & Mickens, R. E. (2013). A nonstandard finite difference scheme for convection–diffusion equations having constant coefficients. *Applied Mathematics and Computation*, *219*(12), 6591–6604.

Elango, S. (2023). Second order singularly perturbed delay differential equations with non-local boundary condition. *Journal of Computational and Applied Mathematics*, *417*, 114498.

Elango, S., Tamilselvan, A., Vadivel, R., Gunasekaran, N., Zhu, H., Cao, J., & Li, X. (2021). Finite difference scheme for singularly perturbed reaction diffusion problem of partial delay differential equation with nonlocal boundary condition. *Advances in Difference Equations*, *2021*(1), 1–20.

Elango, S., & Unyong, B. (2023). Numerical scheme for singularly perturbed mixed delay differential equation on shishkin type meshes. *Fractal and Fractional*, *7*(1), 43.

Eloe, P. W., Raffoul, Y. N., & Tisdell, C. C. (2005). Existence, uniqueness and constructive results for delay differential equations. *Electronic Journal of Differential Equations (EJDE)[electronic only]*, *2005*, Paper–No.

Erfani, A., Rezaei, S., Pourseifi, M., & Derili, H. (2018). Optimal control in teleoperation systems with time delay: A singular perturbation approach. *Journal of Computational and Applied Mathematics*, *338*, 168–184.

Farrell, A. (1987). Sufficient conditions for uniform convergence of a class of difference schemes for a singularly perturbed problem. *IMA journal of numerical analysis*, *7*(4), 459–472.

Farrell, A., Miller, J. M., O'Riordan, E., & Shishkin, G. I. (2000). *Robust computational techniques for boundary layers*. Chapman and hall/CRC.

Friedrichs, K., & Wasow, W. (1946). Singular perturbations of non-linear oscillations. *Duke Mathematical Journal*, *13*(3), 367–381.

Gartland, E. C. (1988). Graded-mesh difference schemes for singularly perturbed two-point boundary value problems. *Mathematics of Computation*, *51*(184), 631–657.

Gartland Jr, E. C. (1989). Strong uniform stability and exact discretizations of a model singular perturbation problem and its finite-difference approximations. *Applied Mathematics and Computation*, *31*, 473–485.

Glizer, V. (2003). Asymptotic analysis and solution of a finite-horizon control problem for singularly-perturbed linear systems with small state delay. *Journal of Optimization Theory and Applications*, *117*(2), 295–325.

Gobena, W. T., & Duressa, G. F. (2022). An optimal fitted numerical scheme for solving singularly perturbed parabolic problems with large negative shift and integral boundary condition. *Results in Control and Optimization*, *9*, 100172.

Govindarao, L., & Mohapatra, J. (2018). A second order numerical method for singularly perturbed delay parabolic partial differential equation. *Engineering Computations*, *36*(2), 420–444.

Guglielmi, N., Iacomini, E., & Viguerie, A. (2022). Delay differential equations for the spatially resolved simulation of epidemics with specific application to covid-19. *Mathematical Methods in the Applied Sciences*.

Hailu, W. S., & Duressa, G. F. (2023). Accelerated parameter-uniform numerical method for singularly perturbed parabolic convection-diffusion problems with a large negative shift and integral boundary condition. *Results in Applied Mathematics*, *18*, 100364.

Holmes, M. H. (2007). *Introduction to numerical methods in differential equations*. Springer.

Hunter, J. K. (2004). Asymptotic analysis and singular perturbation theory. *Department of Mathematics, University of California at Davis*, 1–3.

Il'in, A. M. (1969). Differencing scheme for a differential equation with a small parameter affecting the highest derivative. *Mathematical Notes of the Academy of Sciences of the USSR*, *6*(2), 596–602.

Kadalbajoo, M. K., & Awasthi, A. (2011). The midpoint upwind finite difference scheme for time-dependent singularly perturbed convection-diffusion equations on non-uniform mesh. *International Journal for Computational Methods in Engineering Science and Mechanics*, *12*(3), 150–159.

Kadalbajoo, M. K., & Gupta, V. (2010). A brief survey on numerical methods for solving singularly perturbed problems. *Applied mathematics and computation*, *217*(8), 3641–3716.

Kadalbajoo, M. K., & Reddy, Y. (1989). Asymptotic and numerical analysis of singular perturbation problems: a survey. *Applied Mathematics and computation*, *30*(3), 223–259.

Kellogg, R. B., & Tsan, A. (1978). Analysis of some difference approximations for a singular perturbation problem without turning points. *Mathematics of computation*, *32*(144), 1025–1039.

Kokotović, P., Khalil, H. K., & O'reilly, J. (1999). *Singular perturbation methods in control: analysis and design*. SIAM.

Kumar, M., et al. (2011). Methods for solving singular perturbation problems arising in science and engineering. *Mathematical and Computer Modelling*, *54*(1-2), 556–575.

Kumar, M., Singh, P., & Mishra, H. K. (2007). A recent survey on computational techniques for solving singularly perturbed boundary value problems. *International Journal of Computer Mathematics*, *84*(10), 1439–1463.

Kumari, P., & Kumar, D. (2020). Parameter-uniform numerical treatment of singularly perturbed initial-boundary value problems with large delay. *Applied Numerical Mathematics*.

Kurina, G., Dmitriev, M., & Naidu, D. (2017). Discrete singularly perturbed control problems (a survey). *Dyn. Contin. Discrete Impuls. Syst. Ser. B Appl. Algorithms*, *24*(5), 335–370.

Landau, L. D., & Lifshitz, E. M. (2013). *Fluid mechanics: Landau and lifshitz: Course of theoretical physics, volume 6* (Vol. 6). Elsevier.

Lange, C. G., & Miura, R. M. (1982). Singular perturbation analysis of boundary value problems for differential-difference equations. *SIAM Journal on Applied Mathematics*, *42*(3), 502–531.

Linß, T. (2009). *Layer-adapted meshes for reaction-convection-diffusion problems*. Springer.

Liseıkin, V. (1983). On the numerical solution of a two-dimensional elliptic equation with a small parameter in the highest derivatives. *Num. Meth. Mech. Cont. Media*, *14*, 110–115.

Longtin, A., & Milton, J. G. (1989). Modelling autonomous oscillations in the human pupil light reflex using non-linear delay-differential equations. *Bulletin of Mathematical Biology*, *51*(5), 605–624.

Lubuma, J. M.-S., & Patidar, K. C. (2007). Non-standard methods for singularly perturbed problems possessing oscillatory/layer solutions. *Applied Mathematics and Computation*, *187*(2), 1147–1160.

Majumdar, A., & Natesan, S. (2019). An epsilon-uniform hybrid numerical scheme for a singularly perturbed degenerate parabolic convection–diffusion problem. *International Journal of Computer Mathematics*, *96*(7), 1313–1334.

Manikandan, M., Shivaranjani, N., Miller, J., & Valarmathi, S. (2014). A parameter-uniform numerical method for a boundary value problem for a singularly perturbed delay differential equation. In *Advances in applied mathematics* (pp. 71–88). Springer.

Mbroh, N. A., Noutchie, S. C. O., & Massoukou, R. Y. M. (2020). A robust method of lines solution for singularly perturbed delay parabolic problem. *Alexandria Engineering Journal*, *59*(4), 2543–2554.

Melesse, W. G., Tiruneh, A. A., & Derese, G. A. (2020). Fitted mesh method for singularly perturbed delay differential turning point problems exhibiting twin boundary layers. *Journal of applied mathematics & informatics*, *38*(1_2), 113–132.

Mickens, R. E. (1994). *Nonstandard finite difference models of differential equations*. world scientific.

Mickens, R. E. (2005). *Advances in the applications of nonstandard finite difference schemes*. World Scientific.

Miller, J. J., O'riordan, E., & Shishkin, G. I. (2012). *Fitted numerical methods for singular perturbation problems: error estimates in the maximum norm for linear problems in one and two dimensions*. World scientific.

Mohapatra, J., & Natesan, S. (2011). Parameter-uniform numerical methods for singularly perturbed mixed boundary value problems using grid equidistribution. *Journal of Applied Mathematics and Computing*, *37*, 247–265.

Musharary, J. M., S.R. Sahu. (2020). A parameter uniform numerical scheme for singularly perturbed differential-difference equations with mixed shifts. *Journal of Applied and Computational Mechanics*.

Naidu, D. (2002). Singular perturbations and time scales in control theory and applications: an overview. *Dynamics of Continuous Discrete and Impulsive Systems Series B*, *9*, 233–278.

Natesan, S., & Bawa, R. K. (2007). Second-order numerical scheme for singularly perturbed reaction-diffusion robin problems. *J. Numer. Anal. Ind. Appl. Math*, *2*(3-4), 177–192.

Nayfeh, A. H. (2008). *Perturbation methods*. John Wiley & Sons.

Nicaise, S., & Xenophontos, C. (2013). Robust approximation of singularly perturbed delay differential equations by the hp finite element method. *Computational Methods in Applied Mathematics*, *13*(1), 21–37.

Novikov, A., Papanicolaou, G., & Ryzhik, L. (2005). Boundary layers for cellular flows at high péclet numbers. *Communications on pure and applied mathematics*, *58*(7), 867–922.

O'Malley, R. E. (1991). *Singular perturbation methods for ordinary differential equations* (Vol. 89). Springer.

O'Malley, R. E. (2014). *Historical developments in singular perturbations*. Springer.

Prasad, E. S., Omkar, R., & Phaneendra, K. (2022). Fitted parameter exponential spline method for singularly perturbed delay differential equations with a large delay. *Computational and Mathematical Methods*, *2022*.

Rao, R. N., & Chakravarthy, P. P. (2014). A fitted numerov method for singularly perturbed parabolic partial differential equation with a small negative shift arising in control theory. *Numerical Mathematics: Theory, Methods and Applications*, *7*(1), 23–40.

Rihan, F. A. (2021). *Delay differential equations and applications to biology*. Springer.

Roos, H.-G. (2012). Robust numerical methods for singularly perturbed differential equations: a survey covering 2008–2012. *International Scholarly Research Notices*, *2012*.

Roos, H.-G., Stynes, M., & Tobiska, L. (2008). *Robust numerical methods for singularly perturbed differential equations: convection-diffusion-reaction and flow problems* (Vol. 24). Springer Science & Business Media.

Sahihi, H., Abbasbandy, S., & Allahviranloo, T. (2019). Computational method based on reproducing kernel for solving singularly perturbed differential-difference equations with a delay. *Applied Mathematics and Computation*, *361*, 583–598.

Sathya, K. N., & Rao, R. N. (2020). A second order stabilized central difference method for singularly perturbed differential equations with a large negative shift. *Differential Equations and Dynamical Systems*, 1–18.

Sekar, E., & Tamilselvan, A. (2019). Singularly perturbed delay differential equations of convection–diffusion type with integral boundary condition. *Journal of Applied Mathematics and Computing*, *59*, 701–722.

Selvi, P. A., & Ramanujam, N. (2016). An iterative numerical method for singularly perturbed reaction–diffusion equations with negative shift. *Journal of Computational and Applied Mathematics*, *296*, 10–23.

Sharma, K. K., Rai, P., & Patidar, K. C. (2013). A review on singularly perturbed differential equations with turning points and interior layers. *Applied Mathematics and computation*, *219*(22), 10575–10609.

Shayak, B., Sharma, M. M., Rand, R. H., Singh, A., & Misra, A. (2020). A delay differential equation model for the spread of covid-19. *International Journal of Engineering Research and Applications*, *10*(10/3), 1–13.

Shishkin, G. I. (1988). A difference scheme for a singularly perturbed equation of parabolic type with a discontinuous initial condition. In *Doklady akademii nauk* (Vol. 300, pp. 1066–1070).

Shishkin, G. I., & Shishkina, L. P. (2008). *Difference methods for singular perturbation problems*. Chapman and Hall/CRC.

Sirisha, C., & Reddy, Y. (2017a). Numerical integration of singularly perturbed delay differential equations using exponential integrating factor. *Mathematical Communications*, *22*(2), 251–264.

Sirisha, C., & Reddy, Y. (2017b). Solution of singularly perturbed delay differential equations with dual-layer behavior using numerical integration. *Transactions on Mathematics, e-ISSN*, 2224–2880.

Smith, G. D., Smith, G. D., & Smith, G. D. S. (1985). *Numerical solution of partial differential equations: finite difference methods*. Oxford university press.

Stein, R. B. (1965). A theoretical analysis of neuronal variability. *Biophysical Journal*, *5*(2), 173–194.

Subburayan, V. (2016). An hybrid initial value method for singularly perturbed delay differential equations with interior layers and weak boundary layer. *Ain Shams Engineering Journal*, *9*(4), 727–733.

Subburayan, V., & Ramanujam, N. (2013). An initial value technique for singularly perturbed reaction-diffusion problems with a negative shift. *Novi Sad J. Math*, *43*(2), 67–80.

Swaminathan, P., Sigamani, V., & Victor, F. (2016). Numerical method for a singularly perturbed boundary value problem for a linear parabolic second order delay differential equation. In *Differential equations and numerical analysis: Tiruchirappalli, india, january 2015* (pp. 117–133).

Swamy, D. K., Phaneendra, K., Babu, A. B., & Reddy, Y. (2015). Computational method for singularly perturbed delay differential equations with twin layers or oscillatory behaviour. *Ain Shams Engineering Journal*, *6*(1), 391–398.

Tirfesa, B. B., Duressa, G. F., & Debela, H. G. (2022). Non-polynomial cubic spline method for solving singularly perturbed delay reaction-diusion equations. *Thai Journal of Mathematics*, *20*(2), 679–692.

Tiruneh, A. A., Derese, G. A., & Ayele, M. A. (2023). Singularly perturbed reaction diffusion problem with large spatial delay via non-standard fitted operator method. *Research in Mathematics*, *10*(1), 2171698.

Tiruneh, A. A., & Reddy, Y. (2007). An exponentially fitted special second-order finite difference method for solving singular perturbation problems. *Applied Mathematics and Computation*, *190*(2), 1767–1782.

Van Dyke, M. (1975). Perturbation methods in fluid mechanics/annotated edition. *NASA STI/Recon Technical Report A*, *75*, 46926.

Venkata, A. S. R. K., & Palli, M. M. K. (2017). A numerical approach for solving singularly perturbed convection delay problems via exponentially fitted spline method. *Calcolo*, *54*, 943–961.

Vulanovic, R. (1986). Mesh construction for discretization of singularly perturbed boundary value problems. *Doctoral Dissertatation, Faculty of Sciences, University of Novi Sad*.

Woldaregay, M. M., & Duressa, G. F. (2019). Parameter uniform numerical method for singularly perturbed parabolic differential difference equations. *Journal of the Nigerian Mathematical Society*, *38*(2), 223–245.

Woldaregay, M. M., & Duressa, G. F. (2020). Higher-order uniformly convergent numerical scheme for singularly perturbed differential difference equations with mixed small shifts. *International Journal of Differential Equations*, *2020*, 1–15.

Woldaregay, M. M., & Duressa, G. F. (2021). Robust numerical scheme for solving singularly perturbed differential equations involving small delays. *Applied Mathematics E-Notes*, *21*, 622–633.

Zhang, Y., Naidu, D. S., Cai, C., & Zou, Y. (2014). Singular perturbations and time scales in control theories and applications: An overview 2002–2012. *Int. J. Inf. Syst. Sci*, *9*(1), 1–36.

Zhao, P., & Lam, S. (2019). Toward computational singular perturbation (csp) without eigendecomposition. *Combustion and Flame*, *209*, 63–73.

APPENDIX A

LIST OF PUBLISHED AND SUBMITTED PAPERS

The following papers are parts of this dissertation contributed to peer-reviewed international journals.

1. A.H. Ejere, G.F. Duressa, M.M. Woldaregay and T.G. Dinka, An exponentially fitted numerical scheme via domain decomposition for solving singularly perturbed differential equations with large negative shift, *Journal of Mathematics*, vol. 2022, Article ID 7974134, 13 pages 2022. https://doi.org/10.1155/2022/7974134.

2. A.H. Ejere, G.F. Duressa, M.M. Woldaregay and T.G. Dinka, A uniformly convergent numerical scheme for solving singularly perturbed differential equations with large spatial delay, *SN Applied Sciences*, vol. 4, no. 12, pp.324–415, 2022. https://doi.org/10.1007/s42452-022-05203-9.

3. A.H. Ejere, G.F. Duressa, M.M. Woldaregay and T.G. Dinka, A parameter-uniform numerical scheme for solving singularly perturbed parabolic reaction-diffusion problems with delay in the spatial variable, *International Journal of Mathematics and Mathematical Sciences*, vol. 2023, Article ID 7215106, 17 pages, 2023. https://doi.org/10.1155/2023/7215106.

4. A.H. Ejere, G.F. Duressa, M.M. Woldaregay and T.G. Dinka, A robust numerical scheme for singularly perturbed differential equations with spatio-temporal delays, *Front. Appl. Math. Stat. - Numerical Analysis and Scientific Computation*, vol. 9, Article ID 1125347, 12 pages, 2023. https://doi.org/10.3389/fams.2023.1125347.

5 A.H. Ejere, G.F. Duressa, M.M. Woldaregay and T.G. Dinka, A tension spline fitted numerical scheme for singularly perturbed reaction-diffusion problem with negative shift, *BMC Research Note*, vol. 112(16), 2023. https://doi.org/10.1186/s13104-023-06361-8.

6. A.H. Ejere, G.F. Duressa, M.M. Woldaregay and T.G. Dinka, Fitted mesh finite difference scheme for solving singularly perturbed parabolic differential equations with negative shift, (Under review).

APPENDIX B

MATLAB PROGRAMS

The matlab programs used for solving the examples are obtained on the google drive as shared below.

1) Matlab program for Examples 4.4.1–4.4.3 of Chapter 4.
   https://drive.google.com/file/d/1bqtEqfEyUmGh1Qh7WXEvK8vorvCuV2ZZ/view?usp=sharing.
2) Matlab program for Examples 5.4.1–5.4.3 of Chapter 5.
   https://drive.google.com/file/d/11S0sjMObAEwY3auhgtoj9-s6PFnXBMNc/view?usp=sharing.
3) Matlab program for Examples 6.4.1–6.4.2 of Chapter 6.
   https://drive.google.com/file/d/1uSgxH_uTTXPuZN4v40x4FDKruvfTqX8D/view?usp=sharing.
4) Matlab program for Examples 7.4.1–7.4.3 of Chapter 7.
   https://drive.google.com/file/d/1qWeh4kwAVPz_R8zOfglk_cNkvlR3xJrO/view?usp=sharing.
5) Matlab program for Examples 8.4.1–8.4.2 of Chapter 8.
   https://drive.google.com/file/d/1WpJzr2RO4b4pEMFUis5_ZbMlZICQd0ze/view?usp=sharing.
6) Matlab program for Examples 9.4.1–9.4.3 of Chapter 9.
   https://drive.google.com/file/d/1e_5ZA_kRx4447fniCVt4xZr2wq-Yp2GR/view?usp=sharing.